Framework for Evaluation of Active Solar Collection Systems

Marwa M. Hassan
Yvan Beliveau, Chairman

(ABSTRACT)

A framework that presents a new methodology for design-evaluation of active solar collection systems was developed. Although this methodology emphasizes the importance of detailed modeling for accurate prediction of building performance, it also presents a process through which the detailed modeling results can be reused in a simplified iterative procedure allowing the designer the flexibility of revising and improving the preliminary design. For demonstration purposes, the framework was used to design and evaluate two case studies located in Blacksburg (VA) and Minneapolis (MN). These locations were selected because they both represent a cold weather region; presenting a need for using solar energy for heating and hot water requirements. Moreover, the cold weather in Blacksburg is not as severe as in Minneapolis. Therefore, the two cases will result in different thermal loading structures enabling the framework validation process. The solar collection system supplying both case studies consisted of a low temperature flat plate solar collector and storage system.

Thermal performance of the case study located in Blacksburg was conducted using detailed modeling evaluation techniques; while thermal performance of the case study located in Minneapolis was conducted using a simplified modeling evaluation technique. In the first case study, hourly evaluation of the thermal performance of the solar collection system was accomplished using finite element (FE) analysis, while hourly evaluation of the building thermal performance was made using Energy Plus software. The results of the finite element analysis were used to develop a statistical predictive design equation. The energy consumption for the second case study was

calculated using the heating design day method and the energy collection for that case study was calculated using the predictive design equation developed from the first case study results. Results showed that, in the case of the building located in Blacksburg, the solar collection system can supply an average of 85% of the building's heating and hot water requirements through out the year. In the case of the building located in Minneapolis, the solar collection system can supply an average of 56% of the building's heating and hot water requirements through out the year given no night time window insulation and using similar insulation thicknesses for both cases.

To my Mom & Dad
Nadia & Mohamed, and
to Mostafa, Sara, and
Noha

Acknowledgements

I would like to acknowledge my advisor, Dr. Yvan Beliveau; you have been my mentor, and my friend. You always had the patience and wisdom to guide me in every step of the way. You always took the time to listen to my problems, and advice me in every aspect of my life. I would like also to express my appreciation to my committee members: Dr. Imad L. Al-Qadi, Dr. James Thomas, Dr. Jim Jones, and Dr. Ron Wakefield; you always had time for me. You were there when I needed you with support and guidance. Thank you all very much.

Thanks to my husband, Mostafa, who was always by my side during every up and down of this long process. Thank you Mostafa for your caring and unconditional love. Thanks to my sisters Noha and Sara for your help and ceaseless support; you will always have a special place in my heart.

Finally, all the thanks in the world to my beloved mother and father. You endured so much to see this day, and the happiness it will bring to your heart is invaluable. I will always be in debt to you for all your sacrifice and love.

Table of Contents

1 INTRODUCTION 1

1.1 INTRODUCTION 1
1.2 PROBLEM STATEMENT 3
1.3 OBJECTIVES 4
1.4 SCOPE OF WORK 4
1.5 ASSUMPTIONS OF THE STUDY 4
1.6 CONTRIBUTION TO THE BODY OF KNOWLEDGE 5
1.7 LIMITATIONS OF THIS STUDY 5
1.8 ORGANIZATION OF THE DISSERTATION 6

2 LITERATURE REVIEW 9

2.1 METHODS FOR PERFORMANCE EVALUATION OF ACTIVE SOLAR SYSTEMS 9
2.1.1 Experimental Evaluation Techniques 10
2.1.2 Modeling and Simulation Evaluation Techniques 11
2.1.3 Design Methods 13
2.2 ENERGY COLLECTION 16
2.2.1 Solar Energy 16
2.2.2 Types of Solar Collectors 19
2.2.3 Theory of Flat Plate Collectors 20
2.2.3.1 Analytical Method 20
2.2.3.2 Numerical Methods 24
2.3 ENERGY STORAGE 29
2.4 ENERGY CONSUMPTION 34
2.4.1 Simplified Methods for Hot Water and Space Heating Thermal Load Calculations 34
2.4.2 Detailed methods for calculation of building system loads 35
2.4.2.1 TRANSYS 35
2.4.2.2 DOE, DOEPLUS and VISUAL DOE 37
2.4.2.3 Energy Plus 39
2.4.2.4 Other Simulation Tools 41
2.5 THERMAL COMFORT 44
2.5.1 Recent Researches in Thermal Comfort 49

3 FRAMEWORK AND DEMONSTRATION DESCRIPTION 54

3.1 INTRODUCTION 54
3.2 FRAMEWORK DESCRIPTION 54
3.2.1 Stage I: Preliminary Design Stage 56
3.2.2 Stage II: Solar Supply Evaluation Stage 60
3.2.3 Stage III: Building Demand Evaluation Stage 64
3.2.4 Stage IV: Storage Design and Sizing Stage 66
3.2.5 Stage V: Control System Design Stage 70
3.2.6 Stage VI: Overall System Energy Savings 70
3.3 STAGE I - DESCRIPTION OF CASE STUDIES USED FOR CONCEPT DEMONSTRATION 71
3.3.1 Building description 73
3.3.2 Mechanical system 76

4 FRAMEWORK WEATHER DATA PREPARATION 79

4.1 INTRODUCTION 79
4.2 SANDIA METHOD DESCRIPTION AND MODIFICATIONS 80
4.3 BLACKSBURG TMY2 82
4.4 GOODNESS OF FIT TEST 85
4.5 RELIABILITY OF TMY2 FILES 87
4.6 RESULTS AND DISCUSSION 88

4.6.1 Solution A ... *89*
4.6.2 Solution B ... *90*
4.6.3 Solution C ... *94*

5 STAGE II - ENERGY COLLECTION MODEL – FINITE ELEMENT AND STATISTICAL ANALYSIS ... 96

5.1 INTRODUCTION ... 96
5.2 BACKGROUND - PERFORMANCE EVALUATION ... 96
5.3 ENERGY COLLECTION MODEL ... 98
5.3.1 Finite Element Formulation ... *98*
5.3.1.1 Model Dimension and Geometry ... 99
5.3.1.2 Model Constraints ... 101
5.3.2 Heat Gain Calculations ... *103*
5.3.3 Model Verification ... *103*
5.3.4 Variation of Design, Environmental, and Operational Variables ... *109*
5.4 STATISTICAL ANALYSIS ... 110
5.4.1 Correlation and Trends ... *110*
5.4.2 Model Development ... *115*
5.4.2.1 Model Selection Criteria ... 115
5.4.2.2 Analysis of Variance ... 116
5.4.2.3 Model Transformation ... 117
5.4.2.4 Model Formulation ... 119
5.4.2.5 Sensitivity Analysis ... 120
5.4.2.6 Appropriateness of the Model ... 122
5.4.2.7 Model Validation ... 124
5.4.2.8 Energy Estimation from the proposed model ... 125
5.4.3 Design Example ... *126*

6 STAGE III - BUILDING AN ENERGY CONSUMPTION MODEL – ENERGY PLUS ... 129

6.1 INTRODUCTION ... 129
6.2 MODEL FORMULATION ... 132
6.2.1 Simulation Parameters ... *132*
6.2.2 Location and Weather Data ... *133*
6.2.3 Geometry and Construction Material ... *134*
6.2.4 Thermal Comfort Calculations ... *138*
6.2.5 Airflow ... *139*
6.2.6 Mechanical System Simulation ... *139*
6.2.6.1 Plant Loop ... 140
6.2.6.2 Condenser Loop ... 142
6.2.6.3 Air Loop ... 142
6.2.6.4 Zone Equipment ... 143
6.2.7 Design and Sizing Parameters ... *144*
6.2.8 Energy Plus Output ... *144*

7 STAGE IV - ENERGY STORAGE MODELS – FINITE ELEMENT ANALYSIS ... 146

7.1 INTRODUCTION ... 146
7.2 FINITE ELEMENT FORMULATION ... 148
7.2.1 Model Dimension and Geometry ... *149*
7.2.2 Model Constraints ... *150*
7.2.3 Sizing of the Storage Tank ... *150*

8 STAGE V - CONTROL STRATEGY ... 152

8.1 INTRODUCTION ... 152
8.2 CONTROL SYSTEM DESCRIPTION ... 154
8.3 CONTROL SYSTEM ALGORITHM ... 158
8.4 DEVIATIONS FROM THE ALGORITHM ... 161
8.5 CONTROL SYSTEM COMPONENTS ... 162

9 BLACKSBURG CASE STUDY RESULTS AND ANALYSIS 167

9.1 STAGE II - ENERGY SUPPLY 167
9.2 STAGE III - ENERGY CONSUMPTION 176
9.3 STAGE IV - ENERGY STORAGE 182
9.4 OVERALL ENERGY SAVING ANALYSIS 187
9.4.1 Effect of Weather Data Variation on Energy Gain 191

10 FURTHER DESIGN EVALUATION FRAMEWORK VALIDATION: MINNAPOLIS, MINNESOTA 194

10.1 INTRODUCTION 194
10.2 STAGE II - SOLAR SUPPLY EVALUATION STAGE 194
10.3 STAGE III – BUILDING DEMAND EVALUATION STAGE 195
10.4 STAGE IV – STORAGE DESIGN AND SIZING STAGE 196
10.5 STAGE V – CONTROL SYSTEM DESIGN 198
10.6 STAGE VI – OVERALL SYSTEM ENERGY SAVING STAGE 199
10.7 DECISION MAKING MODULE 200

11 FINDINGS, CONCLUSIONS, AND RECOMMENDATIONS 203

11.1 FINDINGS 204
11.1.1 Case Study Findings 204
11.1.2 General Findings 206
11.2 CONCLUSIONS 207
11.3 RECOMMENDATIONS AND FUTURE WORK 208

REFERENCES 211

List of Figures

Figure 2-1. Absorption, Reflection and Transmission through Covers 18
Figure 2-2. Flat Plate Collector Components 20
Figure 2-3. Resistances through a Flat Plate Collector 23
Figure 2-4. One-Dimensional Linear Function 28
Figure 2-5. Energy Plus Program Interface (After Energy Plus 2002) 41
Figure 2-6. Factors Influencing Human Comfort 45
Figure 3-1. Framework Steps 55
Figure 3-2. Factors Formulating the Preliminary Design Concept 56
Figure 3-3. Preliminary Design Stage 58
Figure 3-4. Factors Influencing Solar Energy Collection 61
Figure 3-5. Summary of the Solar Collection Evaluation Process 63
Figure 3-6. Factors Affecting Building Energy Consumption 65
Figure 3-7. Summary of the Building Energy Consumption Evaluation Process 66
Figure 3-8. Storage System Design Stage 67
Figure 3-9. Summary of the Storage Design and Sizing Stage 69
Figure 3-10. Stage I of the design evaluation framework 72
Figure 3-11. Proposed Building Preliminary Design 73
Figure 3-12. Cross section of the Building Shell Panels except for the South Roof 74
Figure 3-13. Cross Section of South Roof Panels: (a) First Design and (b) Final Design 75
Figure 3-14. Heat Distribution 77
Figure 3-15. Building Floor Slab 77
Figure 4-1. Observed versus Expected Frequency for an Hour in January 86
Figure 4-2. Reliability of the 12.00th Hour in (a) January and (b) June 89
Figure 4-3. Likelihood of Occurrence of Each Solar Radiation Interval 91
Figure 4-4. Cumulative Solar Radiation 92
Figure 4-5. Problem with Monte Carlo Analysis 93
Figure 4-6. Dry Bulb Hourly Temperature Variation during January 95
Figure 5-1. Stage II of the design evaluation framework 97
Figure 5-2. Solar Panel Cross Section for Integrated Solar Collector 98
Figure 5-3. Shape of the Mesh used for Finite element analysis of the design shown in Figure 5-1. a) 3D view; b) Complete Model Meshing; c) Cross section through the Fluid and Pipe 101
Figure 5-4. Modes of Heat Transfer Present in the Panel 102
Figure 5-5. Analytical versus Finite element Solution for a Day in January at a Mass Flow Rate of 0.0005 m^3/hr 107
Figure 5-6. Analytical versus Finite element solution for a Day in July at a Mass Flow Rate of 0.0005 m^3/hr 107
Figure 5-7. Analytical versus Finite Element Solution for a Day in July at a Mass Flow Rate of 0.01 m^3/hr 108
Figure 5-8. Analytical versus Finite Element Solution for a Day in January at a Mass Flow Rate of 0.01 m^3/hr 108
Figure 5-9. Variation of Fluid Outlet Temperature with Solar Radiation 112

Figure 5-10. Variation of Fluid Outlet Temperature with Ambient Temperature 112
Figure 5-11. Variation of Fluid Outlet Temperature with Inlet Fluid Temperature 113
Figure 5-12. Variation of Fluid Outlet Temperature with Convection Coefficient 114
Figure 5-13. Variation of Fluid Outlet Temperature with Mass Flow Rate 115
Figure 5-14. Plot of the Residual against the Predicted Values 122
Figure 5-15. Normality Probability Plot 124
Figure 5-16. Comparison between Results from the Finite Element and the Predictive Model 125
Figure 6-1. Stage III of the design evaluation framework 130
Figure 6-2. Energy Plus Modules Interaction (Energy Plus 2002) 131
Figure 6-3. Energy Plus Design Day Daily Range Multiplier (Energy Plus 2002) 134
Figure 6-4. Window Construction 135
Figure 6-5. Isometric of the Energy Plus Model (Energy Plus 2002) 136
Figure 6-6. Thermal Zones – First and Second Floor 137
Figure 6-7. Thermal Zones – Basement and Loft 138
Figure 6-8. Heating Plant Loop 141
Figure 6-9. Simulated Air Loop 143
Figure 7-1. Stage IV of the design evaluation framework 147
Figure 7-2. Storage Tank 148
Figure 7-3. Section A Enlarged 148
Figure 7-4. General Layout of the Finite Element Used in the Heat Storage Model 149
Figure 7-5. Modes of Heat Transfer in the Heat Storage Model 151
Figure 8-1. Stage V of the design evaluation framework 153
Figure 8-2. Combined Space Heating and Hot Water Configuration 155
Figure 8-3. Alternative Energy Supply Passages 156
Figure 8-4. A Typical Feedback Control Loop 163
Figure 9-1. Temperature Distribution in the (a) Fluid and (b) Solar Collector during noon in May (600W/m^2) 168
Figure 9-2. Temperature Distribution in the (a) Fluid and (b) Solar Collector during noon in January (540W/m^2) 169
Figure 9-3. Temperature Distribution in the (a) Fluid and (b) Solar Collector during noon in July (850W/m^2) 170
Figure 9-4. Performance of the Solar Collector under Winter and Summer Conditions 171
Figure 9-5. Variation of Fluid Nodal Temperature across the Pipe Diameter at a Solar Intensity of 800W/m^2 172
Figure 9-6. Variation of Maximum Fluid Temperature with respect to Mass Flow Rate at a Solar Intensity of 700W/m^2 173
Figure 9-7. Monthly Building Energy Collection using a collection area of 150m^2 174
Figure 9-8. Monthly Building Energy Collection using a collection area of 1.75m^2 174
Figure 9-9. Monthly Building Energy Collection using a collection area of 17500m^2 . 175
Figure 9-10. Monthly Building Energy Collection per Square Meter 175
Figure 9-11. Monthly Building Energy Consumption for an Area of 13.57m^2 176
Figure 9-12. Monthly Building Energy Consumption for an Area of 1357m^2 177
Figure 9-13. Monthly Building Energy Consumption for an Area of 135700m^2 177
Figure 9-14. Monthly Building Energy Consumption for the Three Cases 178

Figure 9-15. Fanger PMV Index Variation in the Zones during the Winter (Area Case I) 179
Figure 9-16. Fanger PMV Variation in the Zones during the Summer (Area case I).... 180
Figure 9-17. Minimum, Maximum, and Average Mean Radiant Temperature inside the Thermal Zones during the Year 181
Figure 9-18. Minimum, Maximum, and Average Mean Air Temperature inside the Thermal Zones during the Year 181
Figure 9-19. Temperature Distribution in the PCM Storage Model with an Inlet Fluid Temperature of 70°C 182
Figure 9-20. Temperature Distribution in the PCM Storage Model with an Inlet Fluid Temperature of 70°C – Beginning Enlarged 183
Figure 9-21. Decision Making Module of the design evaluation framework..... 185
Figure 9-22. Stage VI of the design evaluation framework..... 188
Figure 9-23. Monthly Building Energy Collection versus Consumption for Area Case I 189
Figure 9-24. Monthly Building Energy Collection versus Consumption for Area Case II 190
Figure 9-25. Monthly Building Energy Collection versus Consumption for Area Case III 190
Figure 9-26. Energy Collection under 5%, TMY2, and 95% for a Collection Area of 150m^2 192
Figure 10-1. Monthly Building Energy Collection for a Building Located in Minneapolis (MN) with a Collection Area of 150m^2 195
Figure 10-2. Monthly Building Energy Consumption for a Building Located in Minneapolis (MN) with an Area of 1357m^2 196
Figure 10-3. Collection versus Consumption for a year period..... 199
Figure 10-4. Monthly Building Energy Consumption – (after increasing insulation from 3 to 6 inches)..... 201
Figure 10-5. Monthly Building Energy Consumption – (after increasing window R-factor from 2 ^oF ft^2 h to 5 ^oF ft^2 h) 202
Figure 10-6. Monthly Building Energy Consumption – (after increasing window R-factor from 2 ^oF ft^2 h to 11 ^oF ft^2 h)..... 202

List of Tables

Table 2-1. Commercially Available PCMs (Guyer 1989) 33
Table 2-2. Equations for Predicting Thermal Sensation (Howell et. al. 1998) 47
Table 3-1. Properties of heating phase change material (Material Data Sheet and Bejan 1995) 78
Table 4-1. TMY Weighting Values 82
Table 4-2. Samples of the Blacksburg Data for 1964 84
Table 4-3. Samples of the Blacksburg TMY2 Created File – radiation data in W/m^2 85
Table 4-4. Proposed Run Schedule 95
Table 5-1. Material Properties Used in the Models 99
Table 5-2. Analysis of Variance for the Outlet Fluid Temperature 117
Table 5-3. Multiple Regression Analysis Results 120
Table 5-4. Correlation Matrix 123
Table 5-5. Weather Data used in the Design Example 126
Table 5-6. Design Example Output 127
Table 5-7. Design Example Output – Effect of Changing the Pipe Diameter 128
Table 6-1. Summer and Winter Design Days 133
Table 6-2. Proposed Area Variation 137
Table 6-3. Simulated Air Loop Mass Flow Rates for the Three Area Cases 142
Table 7-1. Phase Change Material Properties 149
Table 9-1. Storage Tank Sizes 184
Table 9-2. Percentage of Building Energy Supplied by the Solar Collection System 191
Table 9-3. Percentage of Building energy supplied by the solar collection system for case I under TMY2, 5%, and 95% weather conditions 193
Table 10-1. Storage Tank Sizes 198
Table 10-2. Percentage of Building Energy Supplied by the Solar Collection System. 200

1 INTRODUCTION

1.1 INTRODUCTION

Residential construction represents a $39 billion per year industry, accounting for approximately 60% of the overall construction expenditures in the United States (FMI 2003). The increase in consumption of different resources—including materials, energy, and labor—associated with this industry significantly impacts both the nation's economy and its environment. For the viability of the national, state, and local economies, the US housing industry must operate efficiently.

One of the major challenges currently facing the housing industry is that traditional sources of energy are becoming scarce, which results in increased utility costs. Until the early 1970s, natural gas and domestic coal costs were low, as was the interest in non-renewable sources of energy. After the 1973 oil embargo and the jump in prices of traditional energy sources, it became clear that as a nation we could no longer rely so heavily upon oil from foreign sources. In 1997, the average residential energy consumption was 130,000MJ (123 Million Btu) per building, corresponding to an annual energy expenditure of $1,632 per building (Department of Energy 2001). The residential energy consumption represents approximately 40% of the annual nation's energy utilization among the different sectors.

In the past 20 years, interest has been growing in the development of alternative methodologies that more effectively utilize renewable sources of energy. Supported by federal and private funds, that growing interest has yielded a variety of possibilities, with differing degrees of promise. In recent years, solar energy has received considerable attention as a viable source of energy supply. It possesses several characteristics that make it highly attractive as a primary energy source: it can be integrated effectively into local and regional power supplies, and it represents a sustainable environmentally friendly source of energy that can reduce users' energy bills (Lundsager 1996). However, due to the current up-front costs of solar collection systems compared to traditional conventional systems, the cost-effectiveness of solar energy is still in doubt (Rockwell 1999). This has led to a certain amount of uncertainty among agencies as to the true long-term benefits of such systems.

Most American and European governments and their sponsored research organizations, like the Department of Energy (DOE), have been supporting research development and promotion of solar energy since the early 1970s. Most of the research efforts of these organizations have been directed towards passive and active solar design and evaluation through experimental testing and/or validation.

Although the experimental approach yields accurate results, it is highly time consuming and cost prohibitive, as well as design dependent. Therefore, it cannot be used on a day-to-day basis. Therefore, simulation techniques have attracted special interest because they provide a general methodology that can be used to predict system performance. Two general simulation approaches are currently used: simplified methods and detailed methods. The simplified methods approach uses integrated weather representations, like degree days or degree hours, to predict the building's response to the exterior environment. Due to their weather dependency, these techniques cannot accurately predict energy impacts of features that have large hourly fluctuations— e.g., the amount of solar heat gain through windows with unique shading characteristics. They are also unable to predict accurately the impact of a building's operating schedule on its energy needs. On the other hand, detailed modeling performs a whole-building heat loss/heat gain calculation every hour of the year. On an hourly basis, it accounts for exact sun angles, cloud cover, wind, temperature and humidity (Beckman 1993). Therefore, detailed simulation techniques were utilized in the development of many energy simulation tools, including DOE2 and Energy Plus.

Although these methods provided a milestone for establishing a general design tool for predicting solar system performance, they require a high degree of expertise and time and include simplifications that may not fully account for all significant energy terms encountered. In addition, only a few tools allow for integrated evaluation of several or all of the relevant parameters, and the ones that combine all the different parameters use approximations and assumptions that result in little resemblance between the simulated model output and reality.

To address the aforementioned shortcomings, an accurate evaluation framework that can combine the different parameters and simulate reality with a high degree of

reliability is needed to fully utilize active and passive energy efficiency techniques in today's structures. That framework should address the following concerns:

- Quantify the energy savings in solar buildings in comparison to conventional buildings.
- Quantify the savings in the use of conventional sources of energy.
- Resolve the conflicts between traditional construction practices and the implementation of energy saving techniques in order to reduce the upfront costs of the system.

1.2 PROBLEM STATEMENT

To accurately predict the performance of integrated solar collection systems, a design-evaluation framework is needed. This design evaluation framework should be able to quantify the overall energy use for heating, and hot water requirements in any type of building. In addition, the design-evaluation procedure should be able to allow the designer to iteratively evaluate the effectiveness of the developed preliminary design and compare the effect of using different design alternatives to reach a final design. This design-evaluation framework can then be developed into an integrated evaluation predictive simulation tool.

This framework is needed for several reasons. First, after proper calibration and validation, the framework can predict adequate solar performance without the need for full scale experiments. Second, in order to construct active energy efficient facilities with integrated systems, the framework can be used to evaluate alternative designs. Third, the framework can be utilized by the building designer in the early stages of design to give the designer primary control over the building's energy consumption. Finally, since system component performance has advanced well beyond that of overall performance—so much so that the individual parts are used in such related applications as heating, ventilation, and air-conditioning (HVAC) systems—the framework will recommend an overall performance evaluation of the building systems.

1.3 OBJECTIVES

To address the aforementioned problem statement, the main objective of this study is to develop a design-evaluation framework that combines solar energy technology with energy-efficient construction techniques to create a new generation of cost-effective buildings with minimal need for non-renewable energy. This framework quantifies the overall energy use for heating, and hot water requirements in any type of building as well as allows the designer the flexibility of iterative evaluation of the effectiveness of the preliminary design. The framework also compares the effect of using different design alternatives to reach a final design while studying the building as a unified system. To achieve this general objective, the following tasks were undertaken:

1. Develop the design evaluation framework.
2. Validate the developed design evaluation framework using two case studies one located in Blacksburg, Virginia and the other located in Minneapolis, Minnesota.

1.4 SCOPE OF WORK

This study will present a design-evaluation framework that can be used for design and evaluation of active solar systems to improve the system's thermal performance. This framework will evaluate multiple system components in detail, as well as predict overall system performance.

This framework will be used to predict the overall energy savings for an integrated system design in two demonstrative cases located in Blacksburg, Virginia and Minneapolis, Minnesota. This integrated system design will include a control strategy tailored for effective energy collection, storage, and consumption.

1.5 ASSUMPTIONS OF THE STUDY

The following assumptions were made in this study:

- The energy storage model will be based on a 2D finite element analysis.
- The solar flux will be changed every hour according to the available weather data.

- Although the collector's tilt angle can be varied as a user input in the finite element model, it was assumed equal to the angle that maximizes the solar gain for the considered location (i.e., 37^{o} for the case of Virginia – Blacksburg that is equal to the latitude and 44.9 for the case of Minnesota – Minneapolis).
- Electrical energy is supplied to the building from the grid whenever the collector heats the fluid to a temperature below 50^{o}C (the Energy Plus software supply temperature).

1.6 CONTRIBUTION TO THE BODY OF KNOWLEDGE

The contribution of this study to the body of knowledge is the development and validation of a design-evaluation framework that quantifies the energy supply and demand for heating and hot water consumption in buildings. This framework identifies the necessary steps for iteratively evaluating the preliminary design to reach an energy efficient final design. In addition, this framework recommends an overall performance evaluation of the building as a unified system. Moreover, the development of this tool will result in less dependence on experimental data.

1.7 LIMITATIONS OF THIS STUDY

To generalize the proposed framework in this study, more case studies need to be conducted using the developed framework. Only then can a complete database be created that can be used by a designer. Therefore, this study will focus on creating the needed framework, demonstrating, and validating the methodology. The following future work is beyond the scope of this study but is needed before full implementation:

- Create a general database that includes the results of this study as well as other studies for different locations, assembly systems, storage systems, and types of collectors.
- Predict the cost effectiveness of the different assemblies.
- Provide the user-interface and programming, which interacts with the generalized database.

1.8 ORGANIZATION OF THE DISSERTATION

This dissertation consists of 11 chapters. The organization of this dissertation is as follows:

Chapter One: Introduction

Chapter 1 provides background information leading to the problem statement of this study, and defines the research's objectives, methodology, scope of work, and major assumptions and limitations. In addition, this chapter defines the research's contribution to the body of knowledge.

Chapter Two: Literature Review

Chapter 2 starts by reviewing the basic methods for performance evaluation of buildings. Chapter 2 also describes the different building consumption evaluation techniques using both experimental and simulation. In addition, this chapter gives an overview of the energy collection and storage technology, and then summarizes the basic concepts of thermal comfort.

Chapter Three: Framework and Demonstration Description

Chapter 3 presents the design evaluation framework. The presented framework consists of six stages linked together using a decision making module that gives the designer the flexibility of iterating the design or proceeding to the following steps. Chapter 3 also describes the design that was used in the two demonstration and validation case studies located in Blacksburg, Virginia and Minneapolis, Minnesota. That design represents the outcome of Stage I (the preliminary design stage) of the design evaluation framework.

Chapter Four: Weather Data Preparation

Chapter 4 describes the research effort conducted to improve the accuracy of the climatic data used in the simulation of Blacksburg, Va, case study. This improved weather data is used as inputs to the collection evaluation model and building consumption model represented as Stages II and III of the design evaluation framework presented in Chapter 3. The reason for this analysis is that the output of the simulation is highly dependant on the weather conditions.

Chapter Five: Stage II - Energy Collection Models–Finite Element Analysis

Chapter 5 describes the energy collection model that was developed for Blacksburg, Va, case study using the finite element method. This chapter describes the model dimensions, geometry, and constraints, as well as the heat gain calculation methodology. Chapter 5 also describes the verification procedure used to validate the finite element model and its results. In addition, Chapter 5 presents the development of the statistical predictive design equation that was developed based on the input and output of the finite element model. This design equation can be used instead of the finite element analysis to reduce time and effort.

Chapter Six: Stage III - Building an Energy Consumption Model

Chapter 6 describes the building energy consumption model developed for the Blacksburg, Va, case study using Energy Plus simulator with respect to the simulation parameters, the location, the design and sizing parameters, the geometry and construction materials, the airflow, and the mechanical systems. This chapter also describes the different outputs that can be generated by Energy Plus.

Chapter Seven: Stage IV - Energy storage Model–Finite Element Analysis

Chapter 7 describes the energy storage model that was developed for the Blacksburg, Va, case study using the finite element method. This chapter describes the model dimensions, geometry, and constraints, as well as the storage sizing tank calculations.

Chapter Eight: Stage V - Control strategy

Chapter 8 presents the building energy collection, storage and supply control strategy developed for the Blacksburg, Va, case study. The presented control strategy ensures efficient operation of the building energy system. This control strategy was used to link the three simulation models (collection, storage, and consumption) representing Stages II, III and IV of the design evaluation framework and presented in Chapters 5, 6, and 7 as well as provide the building with thermal comfort at all times.

Chapter Nine: Blacksburg Case Study Results and Analysis

Chapter 9 presents the results of the energy consumption model, the energy collection model and the energy storage model for the Blacksburg, Va, case study, representing Stages II, III and IV of the design evaluation framework, as well as the

overall energy savings, representing Stage VI of the design evaluation framework, that can be achieved using the proposed system.

Chapter Ten: Further Design Evaluation Framework Validation

Chapter 10 presents the second case study Minneapolis, Minnesota used for further validation of the developed design evaluation framework. This chapter describes the six stages of the design evaluation of the case study as presented in the design evaluation framework. Simplified evaluation methods (e.g., Heating degree day (HDD)) were used to simulate the energy consumption (Stage III of the framework), while the design equation presented in Chapter 5 was used to estimate the amount of collected energy (Stage II of the design evaluation framework). Furthermore, chapter 10 compares the results of the two validation case studies Blacksburg, Virginia and Minneapolis, Minnesota.

Chapter Eleven: Findings, Conclusions, and Recommendations

Chapter 11 summarizes the research's findings, results, conclusions and recommendations for future work.

2 LITERATURE REVIEW

The major objective of this research is the development of a design-evaluation framework for active solar systems. This framework proposes using modeling techniques for design and evaluation of active solar systems. Therefore, this chapter will summarize the current evaluation techniques of building simulation, energy collection, and energy storage. In addition, since solar energy is considered the main renewable energy supply source in this study, this chapter also provides an overview of current solar collection and storage technology. Moreover, since it is essential to ensure the simulated building system is capable of providing the occupants with a comfortable environment; this chapter also presents the available thermal comfort evaluation tools.

2.1 METHODS FOR PERFORMANCE EVALUATION OF ACTIVE SOLAR SYSTEMS

Traditionally, performance evaluation of buildings is performed in one of two ways: experimental investigation or modeling and simulation. Performance of the solar system is tested experimentally by measuring one or more of four factors (Smith 1993):

- *Collection efficiency*, which applies to the performance of the solar energy collection subsystem. It equals the energy collected divided by the incident radiation.
- *System efficiency*, which equals the solar heat delivered to the loads divided by the incident radiation.
- *Solar fraction*, that element of the total heat requirement met by solar energy. It relates the output of the solar system to the size of the load.
- *Electrical coefficient of performance*, the solar heat delivered to the load divided by the electrical energy used to operate the system.

Modeling involves development of a theoretical basis for performance calculation, while simulation involves using said theory to predict system performance. Solar collection has certain characteristics that increase modeling difficulty (Duffie 1993):

- It is transient in nature because of its time-dependant forcing functions and loads.
- It is driven by weather functions that are partially random in nature.
- It responds nonlinearly to solar radiation.

Because of these characteristics, mathematical solutions for the equations that describe the systems are difficult and impractical. Therefore, numerical solutions are used instead. There are two commonly used approaches or methods for energy modeling, *simplified* and *detailed*. Simplified methods use integrated weather representations, like degree days or degree hours, to predict a building's response to the exterior environment. However, they are unable to accurately predict the energy impacts of features that have large hourly fluctuations— e.g., the amount of solar heat gain through windows with unique shading characteristics. They are also unable to accurately predict the impact on energy of variations in a building's operating schedule. On the other hand, detailed modeling performs a whole building heat loss/heat gain calculation. On an hourly basis, it accounts for exact sun angles, cloud cover, wind, temperature and humidity; therefore, it accurately measures the effects of thermal time lag and thermal storage within the building.

2.1.1 Experimental Evaluation Techniques

Experimental system design evaluation has taken place principally at universities and scientific laboratories. For example, the Colorado State University solar houses are representative of this group. Domestic solar systems provide heating in the winter, cooling in the summer, and hot water throughout the year. The first system began operation in 1974. Since then, more than 100 different systems have been developed worldwide, including air-based and liquid-based active systems and passive systems.

In 1980, the Department of Energy (DOE) sponsored studies to increase the understanding of solar systems. One of these studies used paraffin oil to collect fluid in a single glazed collector with a nonselective absorber coating and water tanks with internal heat exchangers for heat storage. Another utilized reflective pyramidal optical focusing collection (concentrating techniques). A third study was performed at Colorado State University using liquid systems (solar house I and III), as well as air systems (solar house

II). Between 1977 and 1983, a series of different solar systems were installed and tested in the Colorado solar houses to investigate different performance aspects. Results showed substantial month-to-month variation in system efficiency, with an average of 32-44% in the case of one type flat plate collector, and an average of 49-50% in the case of evacuated tubes. The system efficiencies were highest in mid-winter when the system was fully utilized. The experiments also showed that the efficiency of the solar collector was higher than that of the overall system due to heat losses from the collector, the storage tank, and the piping loops, as well as heat that was discharged to avoid overheating the system. A study showed that 38% of the incidental solar radiation was collected and, of that number, only 50% was actually delivered to the space heating system (Smith 1993).

A study by Karaki et. al. (1984) evaluated system performance by measuring the effects of the solar system capacity on that fraction of the load provided by solar energy experimentally. They tested $54m^2$ and $27m^2$ of high efficiency evacuated tube collector systems. The former collector system supplied 100% of the load during winter conditions, while the latter supplied only 58% of the building's thermal load.

The performance of a passive cooling system was evaluated experimentally using two full-scale test cells with identical walls but different roof configurations. One roof was highly insulated, while the other consisted of a solar passive cooling system (SPCS) made of water (thermal mass). Results showed that by using the SPCS passive system, building cooling loads could be reduced by 41-66% (Rincon J. et. al. 2000).

As previously mentioned, there are four experimental measures of solar system performance: collection efficiency, system efficiency, solar fraction, and electrical coefficient performance. The main disadvantage with measuring the collection efficiency is that subsystem efficiency could be twice as efficient as that of the overall system. In that sense, the other three performance measures are superior, because they compare the energy delivered to the amount of energy needed or supplied, which represents a healthy measurement of overall system performance.

2.1.2 Modeling and Simulation Evaluation Techniques

The most highly effective modeling evaluation procedure includes two major steps:

- Step 1: formulation of component models and verification of these models against experimental measurements. This verification lends confidence to the conception that the model adequately simulates the performance of the system.
- Step 2: the development of a means for simultaneous solution of the component models, as with the TRNSYS program, or for algebraically combining the component models into system models for particular system configurations and then solving the system models. In both cases, the solutions to the models are obtained by using hourly meteorological data and hour-by-hour system loads.

A number of computer programs are available for analyzing and evaluation active and passive solar systems, ranging from full-building energy analysis programs with passive solar capabilities to programs for active solar energy systems that include some passive or hybrid capabilities. In general, building energy analysis programs are more appropriate for passive and/or hybrid solar applications, in which are required details of energy transfer between walls and rooms, or for multi-zone applications in which HVAC system simulation is important. For active solar system studies, or for passive applications for which non-passive elements are relatively unimportant, solar simulation programs like TRNSYS are more appropriate (ASHRAE 1993).

In general, the main disadvantage of building analysis simulation programs is that while they indeed provide a detailed picture of thermal energy flow and of the interaction between the heating and cooling loads and equipment, they include simplifications that may not fully account for all significant energy terms. The solar analysis component models —for flat plate collectors and evacuated tubes—are based on the analysis derived in the 1970s by Hottel, Whillier and Bliss (Beckman 1993). Another disadvantage of such programs is the large amount of input information they require to simulate a simple passive structure. The level of complexity encountered usually requires an analyst with training or experience in computer simulation. For this reason, such programs are not normally used as design tools. Instead, the F-chart developed in the early 70s is normally used in place of extensive simulation.

In spite of great accomplishments in the field of both simplified and detailed modeling techniques, currently only a few tools allow for integrated evaluation of several

or all of the relevant parameters, and the ones that do combine the different parameters use approximations and assumptions that result in little resemblance between the simulated output and reality. Thus, an accurate evaluation framework that can combine the different parameters and simulate reality with a high degree of reliability is needed to fully utilize active and passive energy efficiency techniques in today's structures.

2.1.3 Design Methods

As previously mentioned, a design method is needed that can prove superior to the aforementioned simulation programs, with their high levels of required expertise and their varying degrees of complexity. This design method should provide the means for estimating the long-term average performance of a specific system, while requiring relatively little calculation effort and utilizing readily available input data (Klein 1993). Design methods for active solar systems have been classified as correlations, simplified simulations, or utilizability-based methods:

- *Correlations methods* are the most widely used since they are easy to apply, easy to understand, and amenable to hand calculations. Their main disadvantages are that they are highly empirical and unreliable for systems that differ in any respect from those for which the method was derived.
- *Simplified simulation methods* are at an early state of development. Although they require fewer calculations than do simulation methods, the calculations still prove too involved to be accomplished by hand. Unfortunately, reducing the calculations induces large errors. An example of a simplified simulation method is SOLCOST (Connolly et. al. 1976). The main advantage of simplified simulation methods is that they are very flexible, and with the vast growth of computers, they could in the near future become the primary method of design.
- *Utilizability-based methods* require more computation than correlation methods but less than simplified simulation ones. These methods consist of a statistic of solar weather that provides a correlation between the radiation and its effect on solar collectors. Since these methods provide a means of accounting for the dependence of system performance on locations and weather conditions through the utilizability

factor, they tend to provide more accurate results than correlation methods. This factor is based on long-term average conditions.

The major disadvantages of these methods are their dependence on average solar radiation data, which could cause error in output, and their limited suitability to specific applications.

The most widely used correlation design method for active solar systems is the F-chart, developed by Klein, Beckman and Duffie (1979) to provide a means for easily determining the thermal performance of an active solar space heating system. The conditions of the simulations were varied over the ranges anticipated in practical system designs. The resulting correlations give *f*, the fraction of the monthly heating load (for space heating and hot water) supplied by solar energy, as a function of two dimensionless variables (X and Y) involving collector characteristics, heating loads, and weather conditions. The weather data used for the F-chart method are monthly average daily radiation and temperatures.

The system modeled by the F-chart method uses water or an antifreeze solution as the collection fluid. If the collector fluid is not water, a heat exchanger is used between the collector and the storage tank. The F-chart correlation for solar domestic water heating was developed for a two-tank system, in which energy from the collector loop is transferred to preheat the storage tank either directly or via a heat exchanger. A typical use profile developed by Mutch (1974) was assumed in the development of the correlation.

Initially, energy could be stored only as "sensible storage" in a water tank or pebble bed. Then researchers used the results of work performed by Jurinak and Abdel-Khalik (1979) to devise a correction factor to the F-chart for a pebble bed so that it becomes applicable to systems having phase change energy storage. The correction factor exists in the form of an effective thermal capacitance for phase change storage units in terms of the melting temperature, latent heat of fusion, and specific heats of solid and liquid phases of the material. To calculate the X dimensionless parameters used in the F-chart method, this effective capacitance is used in place of the thermal capacitance of the pebble bed. The main disadvantages of the F-chart method are (Klein 1993):

- Limited applications, since it can be used only for systems similar to that which it was designed to simulate; otherwise the output will not be accurate.
- Inaccuracy in predicting system performance. It estimates only the thermal performance of the system. Other energy appliances such as fans are not accounted for.
- It takes only monthly solar radiation and ambient temperature as input weather data. Other special local effects, like mountains, fog, and clouds, cannot be accounted for.

A number of other correlation design methods were developed based on the F-chart, such as Ward's Correlation, the Relative Area Method, the W-chart Method, and the GFL Method. These correlations inherently contain all of the restrictions of the F-chart method and more. Their main advantage is that they provide a means of designing solar energy systems with less computational effort than required by the F-chart method (Klein 1993).

Sherdian et al. (1967) was the first to simulate a solar process, solar water heating systems, using an analog computer. Although this research team investigated short-term dynamics, they made no long-term performance predictions due to the difficulties of using real data in analog simulations. The weather data used in this study were represented by analytic functions, and due to the high costs involved; only a few days of actual operation were simulated. In their effort to model a solar house heating system, Buchberg and Roulet (1968) used a digital computer and a full year of weather data. To find the optimum design for their particular house and climate, they used a pattern search technique.

It was not until the early 1970s that the National Science Foundation (NSF) offered a national plan for solar energy utilization which led researchers in a coherent direction. It was then that Lof and Tybout (1973) performed the first general solar system studies to look at a number of climates, buildings, and collector costs. Their simulation represented the first *what if* study to consider the potentially widespread use of solar energy. Their study was followed by that of Butz, Beckman, and Duffie (1974), which provided a general simulation of a solar heating and cooling system. Although the study was limited to the climate of Albuquerque, New Mexico, it clearly demonstrated

the potential advantages of combining heating, domestic hot water, and cooling. However, the computer code used in this study was not intended for general use.

The following sections will examine in detail each of the three components of the solar system simulator: the collection module, the storage module and the consumption module.

2.2 ENERGY COLLECTION

Any solar energy collection system follows climate. When comfortable conditions exist outside the building, the need for a heating system is non-existent. But when it gets cold outside, the collection of solar energy can be very crucial. In many locations in the United States, the application of solar design to houses could be both beneficial and cost effective. Solar collection systems fall into two categories, passive and active. Passive solar collection systems use only natural processes to collect, store and distribute heat. Active solar systems are assemblies of collectors, storage units, fluid transport devices (i.e. pipes, ducts, pumps, etc.), heat exchangers, auxiliary heating systems, and controllers. The collector absorbs solar energy during daylight hours and transports it through the absorber's (air or water) transport device to satisfy the thermal loads of the building or, if it is not immediately needed, to be collected in storage units. The storage units supply the building's thermal energy needs during night hours or low collection periods. Decisions governing when to supply, when to collect, and when to store— choices that ensure a high level of thermal performance throughout the building— are managed by a control system.

2.2.1 Solar Energy

Solar energy has many characteristics that make it a very attractive primary energy source. It is supplied through a continuously renewable source, the sun. It has minimal impact on the environment and it is free of any political control. Finally, present technology makes it possible to collect, convert, and store solar energy efficiently.

In spite of its advantages, solar energy does possess some disadvantages: it can be collected only during daylight and the quantity of its collection is affected by climatic

changes (daily cycle) and varies throughout the year (yearly cycle). These factors lead to an inconsistent supply of energy. To overcome such disadvantages, excess solar energy should be collected and stored. There is also the potential to store energy both for cooling and heating to mitigate the yearly cycle. The major current applications for solar energy are domestic hot water heating, swimming pool heating, space heating and cooling, industrial process heat, and agriculture process heat. Solar energy costs are calculated in terms of the solar collector's construction and installation cost, its operating efficiency and expected service life, and the amount of energy it can collect per year (Ametek 1983).

To understand how solar energy can be estimated and collected, radiation must be studied. There are two types of radiation, solar (also known as short wave) and long wave. The former originates from the sun in the wavelength range of 0.3-3.0 μm and is divided into beam radiation and diffuse radiation. Long wave radiation originates from sources at or near ambient temperature and contains wavelengths over 3 μm.

The geometric relationship between a plane of any orientation and the incoming beam of solar radiation depends upon several angles, namely, the latitude ϕ, declination δ, Slope β, surface azimuth angle γ, the hour angle ω, and the angle of incidence θ. The angle of incidence is related to the rest of the angles by (Duffie & Beckman 1980):

$$\begin{aligned} \cos\theta = {} & \sin\delta \sin\varphi \sin\beta - \sin\delta\cos\varphi \sin\beta \cos\gamma \\ & + \cos\delta\cos\varphi \cos\beta \cos\gamma \\ & + \cos\delta\sin\varphi \sin\beta \cos\gamma \cos\omega \\ & + \cos\delta\sin\beta \sin\gamma \sin\omega \end{aligned} \qquad (2\text{-}1)$$

Different methods estimate the average solar radiation by measuring the effect of atmospheric attenuation and cloud conditions (Duffie & Beckman 1980). Being able to calculate the amount of solar radiation a collector can absorb depends on the amount of reflection, transmission, and absorption passing through its covers, as shown in Figure 2-1. Fresnel derived expressions for the refraction of unpolarized radiation as it passes between two different mediums with refractive indices n_1 & n_2 as follows:

$$r_1 = \frac{\sin^2(\theta_2 - \theta_1)}{\sin^2(\theta_2 + \theta_1)} \quad , \quad r_2 = \frac{\tan^2(\theta_2 - \theta_1)}{\tan^2(\theta_2 + \theta_1)} \quad \text{and} \quad r = \frac{1}{2}[r_1 + r_2] \tag{2-2}$$

where, θ1 and θ2 = the angles of incidences and refraction and are related by Snell's law:

$$\frac{n_1}{n_2} = \frac{\mathrm{Sin}\theta_2}{\mathrm{Sin}\theta_1} \tag{2-3}$$

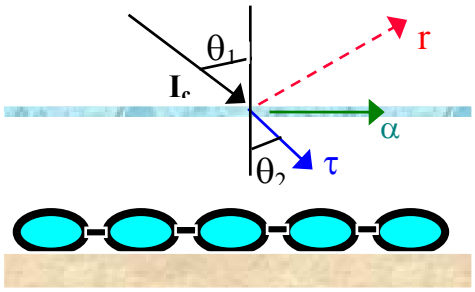

Figure 2-1. Absorption, Reflection and Transmission through Covers

The transmission τ can be calculated in terms of r_1 & r_2 as:

$$\tau_r = \frac{1}{2}\left[\frac{1 - r_1}{1 + r_1} + \frac{1 - r_{2t}}{1 + r_2}\right] \quad , \quad \tau_a = e^{-KL/\cos\theta_2} \quad \text{and} \quad \tau \cong \tau_a \tau_r \tag{2-4}$$

The absorption α is given by

$$\alpha \cong 1 - \tau_a \tag{2-5}$$

While the reflection is given by

$$\rho \equiv \iota_a - \iota \tag{2-6}$$

Since some of the reflected radiation is absorbed within the cover and emitted back to the absorber, it is important to evaluate the product of the transmittance-absorption (τα). It is approximately equal to 1.01 τα. The above analysis should be applied to the beam

component of solar radiation. In the case of diffuse radiation, an equivalent angle should be defined for beam radiation that gives the same transmittance as for diffuse radiation. For practical purposes, this angle can be taken as 60° (Duffie & Beckman 1980).

2.2.2 Types of Solar Collectors

There are many types of solar collectors, ranging from air and liquid cooled, non-concentrating, flat plate collectors to compound curvature, continuously tracking ones. Solar collectors are classified mainly as passive or active. The combination of passive solar techniques, based on architectural design and building situation, with active systems can result in a highly effective energy conservation system.

Passive solar collection consists of incorporating the sun into the architecture of the building. The architect tries to capture two basic seasonal variations: a) cold weather, when the goal is to maximize solar gain and retain it in storage within the building; and B) hot weather, when the goal is to minimize solar gain into the building and dissipate it by natural or forced ventilation. These objectives are achieved through proper utilization of the building structure's external and internal components, including roof angle and thermal insulation, as well as proper positioning of the building on site. Each component plays a valuable role in reducing the building's energy demand.

Active solar collection techniques include flat plate collection, concentrating collection, and Photovoltaic (PV) collection. Each type possesses its own distinct advantages and disadvantages that must be considered before it is chosen for a particular application:

Flat plate solar collectors represent the most economical, active method of solar energy collection (Duffie and Beckman 1980). They consist of an assembly of transparent covers over an absorber plate backed with thermal insulation, as shown in Figure 2-2. The cover serves three functions: preventing convection losses, reducing thermal radiation losses, and protecting the absorber plate against environmental hazards. While the absorber is a coated plate upon which the sun's energy is converted to heat, the insulation prevents back losses. Flat plate collectors use the absorber to heat air or water, which can then be used or stored for later use. They are usually used for applications requiring moderate heat gain (i.e. 100^{o}C above ambient temperature) (ASHRAE 1999).

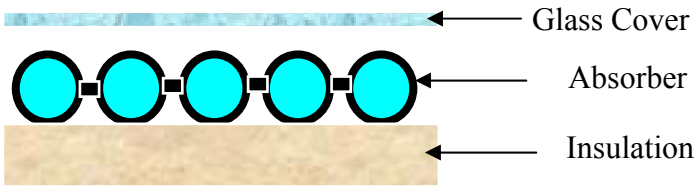

Figure 2-2. Flat Plate Collector Components

Concentrating collectors are essentially evacuated tubular collectors that eliminate convection losses. They deflect sunlight from a large area into a smaller region where the concentration of light can be used to yield temperatures higher than those obtainable from flat plates. Focusing mirrors or lenses are used for concentration but for greater efficiency, they must be aligned precisely toward the sun. This often requires a tracking system which, in combination with the evacuation, increases cost.

Photovoltaic collectors convert sunlight directly into electricity through the action of the sun on a semiconductor junction: this produces an electrical voltage that supplies current through conducting wires. These collectors can be incorporated into flat plate collectors or concentrating collectors, but the cost is currently higher than associated with regular non-renewable energy sources (Goswami 1999).

Due to their ability to supply the needed solar energy at a low cost and the ease with which they can be integrated within the structural members of a building, flat plate collectors were selected for use in this research.

2.2.3 Theory of Flat Plate Collectors

The performance of a solar plate collector can be predicted using two methods: analytical or numerical. The following sections provide an overview of each evaluation technique.

2.2.3.1 Analytical Method

The analytical method is based on a classical energy balance approach stating that *useful energy* is the difference between absorbed solar radiation and thermal losses:

$$Q_u = A_c[S - U_L(T_{p,m} - T_a)] \quad (2\text{-}7)$$

where

A_c = the collection area of the collector (m^2);

S = solar flux (W/m^2);

T_a = the ambient temperature (^oC);

U_L = the heat transfer coefficient ($W/m^{2o}C$) between plate and ambient; and

$T_{p,m}$ = the mean plate temperature (^oC).

Since this equation is given in terms of the mean plate temperature and heat transfer coefficient, which are unknown, research was conducted to define these components in terms of the inlet fluid temperature ($T_{f,i}$) and a quantity that relates the actual useful energy gain of the collector to the useful gain if the whole collector surface was at the fluid inlet temperature. This leads to the equation (Duffie and Beckman 1980):

$$Q_U = A_c F_R[S - U_L(T_{f,in} - T_a)] \quad (2\text{-}8)$$

where

A_c = the collection area of the collector (m^2);

S = solar flux (W/m^2);

T_a = the ambient temperature (^oC);

U_L = the heat transfer coefficient (W/m^2C);

$T_{f,in}$ = inlet fluid temperature (^oC); and

F_r = the collector's heat removal factor and is given by (Duffie and Beckman 1980):

$$F_R = \frac{\dot{m}C_p}{A_c U_L}[1 - e^{-(A_c U_L F'/\dot{m}C_p)}] \quad (2\text{-}9)$$

where

$\dot{m}$ = the fluid mass flow rate;

C_p = the specific heat; and

F’ = the collector efficiency factor, which represents the ratio of actual useful energy gain to the useful energy that would result if the collector absorbing surface had been at the local fluid temperature (Duffie and Beckman 1980). F’ is given by:

$$F' = \frac{\frac{1}{U_L}}{W\left[\frac{1}{U_L\left[D+(W-D)F\right]} + \frac{1}{C_B} + \frac{1}{\pi D_i h_{f,i}}\right]} \qquad (2\text{-}10)$$

where

W = the distance between the tubes in the collector;

D = the tube diameter;

$h_{f,i}$ = the heat transfer coefficient inside the tube, which ranges from 100 W/m^{2o}C in case of laminar flow to 1000W/m^{2} ^{o}C in case of turbulent flow, and

F is the standard fin efficiency for straight fins with rectangular profile (Duffie and Beckman 1980).

Beginning in 1942, Hottel and Woertz conducted a series of experiments on flat plate collectors and developed a correlation for thermal losses based on the mean plate temperature (Hottel and Woertz 1942). In 1958, Tabor modified their work to allow for accurate determination of loss coefficient for collectors with selective surfaces (Tabor 1958).

Whillier and Hottel suggested that the heat transfer coefficient U_L can be determined if the flat plate was considered as a series of resistances, as shown in Figure 2-3. Based on this assumption, the heat transfer coefficient U_L was divided into three components: top loss coefficient (U_t), which is a combination of the resistance to the surroundings (R_1) and the resistance through the cover (R_2); the back loss coefficient (U_b) which should be a combination of the resistance through the insulation (R_3) and the resistance to the inner space of the thermal zones (R_4) (R_4 is assumed to be small and is ignored); and the edge loss coefficient (U_e). Research recommends that the edge of the collector be insulated at the back to minimize the edge loss coefficient (Duffie & Beckman 1980).

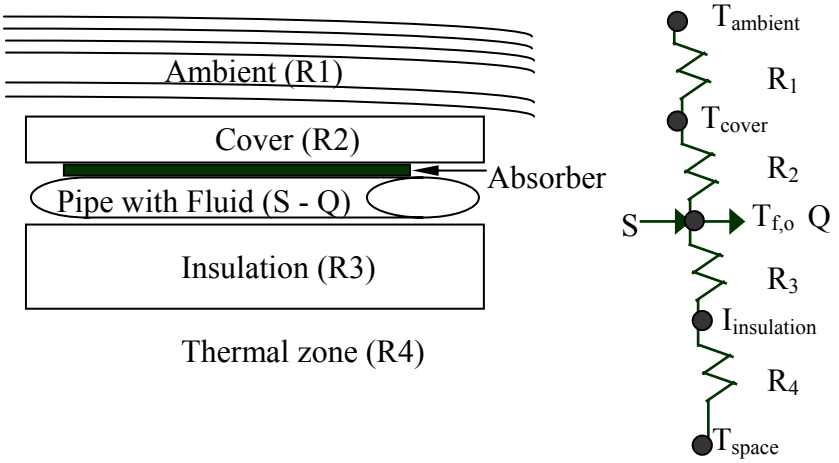

Figure 2-3. Resistances through a Flat Plate Collector

Resistances (R_1-R_4) are calculated from the convection, conduction, and radiation coefficients. Hottel, Whillier and Bliss expressed the efficiency of the collector η as (Goswami 1999):

$$\eta_c = \frac{Q_u}{I_c A_c} = F_R[S - U_L(T_{f,in} - T_A)/I_c] \text{ where, } I_c = S/\tau\alpha \qquad (2\text{-}11)$$

The above formulations are based on steady state conditions. Unfortunately, the very nature of solar radiation requires taking transient conditions into consideration. Equations do exist that can account for the transient nature of the problem, but although they produce accurate results in the case of a one- cover plate collector, their accuracy is reduced by 15% in cases involving two or more (Duffie and Beckman 1980).

The approach described above was used to formulate the basis for the F-chart software, which will be explained in detail in a later section. F-chart software analyzes active and passive solar systems, and is based on the F-chart method which provides a means for estimating the fraction of the total heating load that will be supplied to a given heating system by solar energy. The primary design variable is the collector area. Secondary variables are collector type, storage capacity, fluid flow rates, and load and collector heat exchanger sizes. The method correlates the results of several thermal performance simulations involving solar heating systems. The conditions of the

simulations were varied over appropriate ranges of parameters. The resulting correlations give "F", the fraction of the monthly heating load (for space heating and hot water) supplied by solar energy as a function of two dimensionless parameters, one related to the ratio of collector losses with heating loads and the other related to the ratio of absorbed solar radiation with heating loads (Beckman 1977). The two dimensionless variables are the collector's loss X and the collector's gain Y based on the collector's heat removal rate (F_r), the heat transfer coefficients (U_L), the absorbance (α) and the transmittance (τ) (ASHRAE 1999). The output of the program is a monthly thermal gain. The following assumptions were made in the development of the F-chart software:

- Meteorological data can be in error by 5-10%.
- Average data are used in the calculations.
- The accuracy of estimating the building thermal loads varies.
- Systems must be engineered and constructed with minimal heat losses, leakages etc.
- The storage systems used are all sensible (air or water) and have fixed storage capacity per square meter of collector
- There are differences between the f-chart correlation and the individual data points.
- All liquid storage tanks were assumed to be fully mixed, which means the collector's inlet temperatures are overestimated.
- All days are considered symmetrical around solar noon, which overestimates the system's output.
- The energy in the water above the set temperature is not useful.
- No leaks occur in the system.

2.2.3.2 Numerical Methods

There are two different numerical methods that can be used to evaluate solar collector efficiency, the finite difference method (FDM) and the finite element method (FEM), the second of which is considered to be more accurate. Numerical methods are used whenever there are geometrical complexities or when multidimensional analysis is required. They can be used for both transient and steady state conditions and simplify the

complexity by coupling the three modes of heat transfer. Their main drawback is that truncation errors can be significant (Arpaci 1966). Both methods can be used to approximate the derivatives of the heat conduction equation:

$$\frac{\partial^2 \varphi}{\partial x^2} + \frac{\partial^2 \varphi}{\partial y^2} + \frac{\partial^2 \varphi}{\partial z^2} = \frac{1}{\alpha}\left(\frac{\partial \varphi}{\partial \iota}\right) \qquad (2\text{-}12)$$

where

θ = temperature;

x, y, and z = the spatial coordinates;

α = thermal diffusivity, and

ι = time.

The finite difference method (FDM) approximates the derivatives of a scalar quantity with respect to space using three nodal points through Taylor series expansions. The Taylor series expansion around $\varphi(x)$ is:

$$\varphi(x+\Delta x) = \varphi(x) + \Delta x \frac{\partial \varphi(x)}{\partial x} + \frac{(\Delta x)^2}{2!}\left(\frac{\partial^2 \varphi(x)}{\partial x^2}\right) + \frac{(\Delta x)^3}{3!}\left(\frac{\partial^3 \varphi(x)}{\partial x^3}\right) + \ldots\ldots\ldots \qquad (2\text{-}13)$$

This approximation results in an erroneous order involving the leading term of the remainder, i.e. in $\frac{\partial \varphi}{\partial X} = \frac{\varphi_{i+1} - \varphi_{i-1}}{2\Delta X} + \text{Reminder}$, where the reminder of the approximation is of the order (ΔX) and so on. A list of the most common approximations and their leading truncation errors is given in Pepper and Baker (1988).

FDM also can be used to approximate the time derivative. This time differencing technique is used in both the finite difference and finite element methods. It can be used to approximate the time derivative in equation 2-13 using any one of the three methods; Explicit, also known as backward Euler technique:

$$\frac{\varphi_i^{n+1} - \varphi_i^n}{\Delta t} + \frac{\varphi_{i+1}^n - \varphi_{i-1}^n}{2\Delta x} - \frac{\varphi_{i+1}^n - 2\varphi_i^n + \varphi_{i-1}^n}{(\Delta x)^2} = 0 \qquad (2\text{-}14)$$

where

φ_i^n = is the value at a known (previous) time step, and

φ_i^{n+1} = is the value at an unknown (new) time step.

Implicit:

$$\frac{\varphi_i^{n+1}-\varphi_i^n}{\Delta t}+\frac{\varphi_{i+1}^{n+1}-\varphi_{i-1}^{n+1}}{2\Delta x}-\frac{\varphi_{i+1}^{n+1}-2\varphi_i^{n+1}+\varphi_{i-1}^{n+1}}{(\Delta x)^2}=0 \tag{2-15}$$

or Crank-Nicolson:

$$\frac{\varphi_i^{n+1}-\varphi_i^n}{\Delta t}+\frac{1}{2}\left(\frac{\varphi_{i+1}^{n+1}-\varphi_{i-1}^{n+1}}{2\Delta x}+\frac{\varphi_{i+1}^{n}-\varphi_{i-1}^{n}}{2\Delta x}\right)-\frac{1}{2}\left(\frac{\varphi_{i+1}^{n+1}-2\varphi_i^{n+1}+\varphi_{i-1}^{n+1}}{(\Delta x)^2}+\frac{\varphi_{i+1}^{n}-2\varphi_i^{n}+\varphi_{i-1}^{n}}{(\Delta x)^2}\right)=0 \tag{2-16}$$

In the explicit method only one unknown appears in the relation at each time step; thus, the solution is straightforward. Unfortunately, the time step Δt must be restricted to ensure numerical stability, and even with that restriction the method has an error of the Δt order. The implicit method, on the other hand, is unconditionally stable, but the accuracy of the method is still of the Δt order. Crank-Nicolson solves the problems associated with the previous two methods by averaging new and old values in time. There are three unknowns in that method, but the averaging of the implicit values with the previously calculated explicit values yields an unconditionally stable solution with an accuracy of order (Δt^2). The equations are then written in matrix form and solved for the unknown parameters. All three methods can be written in a single expression

$$\left(\theta[K]+\frac{[M]}{\Delta t}\right)\{\varphi\}^{n+1}=\left(\frac{[M]}{\Delta t}-(1-\theta)[K]\right)\{\varphi\}^n+\{F\} \tag{2-17}$$

If $\theta = 0$, the expression becomes explicit; if it equals 1, the expression is implicit; and if it equals one-half, the expression results in the Crank-Nicolson. In most cases, numerical instability results from improper spatial step specification. Refining the step size usually

alleviates the instability. The ratio of the time step to the spatial step is also very important.

There are several higher order schemes that can be used when second order spatial differences are not enough. These schemes require more nodal points—for example, a fourth order difference requires five nodal points. Some of these schemes, known as *compact schemes*, represent competition to the standard finite difference method.

The finite element method (FEM) consists of approximating the function in small domain portions called finite elements. These elements can be one-, two-, or three-dimensional (quadrilateral, triangular etc.). The unknown function is approximated in every element by continuously interpolating a polynomial with a continuous derivative of a certain order. The resulting approximations in each element are then assembled to give the solution for the global domain.

FEM is based on the series expansion of the functions, where a finite number of basis functions (sines, cosines etc.) that are "local" in nature (non zero over a small segment of the domain) are employed. The resulting coefficient matrices vary from node to node. The partial differential equations are then reduced to a finite system of ordinary differential equations using either the Rayleigh-Ritz method or the method of weighted residuals (MWR). The method of weighted residuals is more common since it allows a functional form of the dependent variables to be obtained for any transport equation regardless of complexity, while the Rayleigh-Ritz method needs a describing mathematical relation that is not always available in cases of most practical problems. MWR can be based on several variations, of which the Galerkin is the most popular. It is given by:

$$\varphi(x,t) = \sum_{i=1}^{N} N_i(x)\varphi_i(t) \tag{2-18}$$

where

N = the shape function and it differs according to the type of element used.

The most commonly used functions are the simplest; for example, one-dimensional linear approximation is given by $\varphi(x) = a + bx$, while higher order polynomials may be used to improve the accuracy. Figure 2-5 shows a one-dimensional linear function.

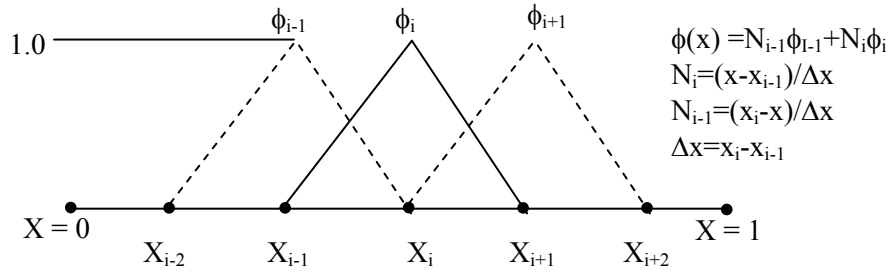

Figure 2-4. One-Dimensional Linear Function

To minimize the total error, the residual error resulting from inserting $\varphi(x,t)$ into the governing equations is made orthogonal to each member of the set. Likewise, to minimize the errors in the approximate solution, N equations are generated for N unknowns:

$$\int_A \left[L\left(\sum_{i=1}^{N} N_i(x)\varphi_i(t) \right) - f \right] N_i(x)\,dA = 0 \qquad (2\text{-}19)$$

where

L = differential operator (linear or non linear), and

f = a known function or constant.

Solving transient differential equations uses the same approach used by the FDM, i.e. implicit, explicit, or Crank-Nicolson.

Although the full capability of the finite element method for determining flat plate collector efficiency has not been reported in the literature, it was previously used to study thermal coupled conduction, convection, and long wave radiation within special building envelope components under transient conditions using 2D modeling. They established

the rate of heat transfer due to the difference between internal and external temperatures. A two-pane glazing system, an open cavity, and an opaque wall panel were used. Finally, the system efficiency was determined as a function of the climatic data (Agnoletti 1995).

2.3 ENERGY STORAGE

Whenever there is a mismatch between available energy and demand, the need for energy storage arises. Storage also eliminates one of the major disadvantages of solar energy, inconsistent levels of supply. Thermal energy can be stored as latent heat, sensible heat, or thermochemical energy. Sensible heat, Q, is stored in a material of mass m and specific heat c_p by raising the temperature of the storage material from T_1 to T_2 (Garg 1985).

$$Q = \int_{T_1}^{T_2} mc_p dT = \int_{T_1}^{T_2} \rho V c_p dT \tag{2-20}$$

where

m = the material mass;

ρ = the material density; and

V = the volume of the storage material.

Common storage media for sensible heat storage in buildings include water, soil, molten salts, rock, brick, ceramics, and concrete. Since it is cheap and abundant, the most common of these media is water. Since some of these materials can be integrated within the structure's walls and slabs, the building structure itself also can be used as a storage medium. The main objective for building mass storage is to limit the rise in temperature that occurs over a normal working day; by making use of the material's thermal inertia, a thermal lag is created (Ahuja 1997).

The need for thermal lag results from the difference between the time when solar heat peaks and the time when maximum internal heat is needed. Utilizing a material with a high thermal inertia allows a significant delay in the heat transfer, creating this thermal lag (Stein 2000). The effective use of building structural mass for thermal energy storage depends on:

- The physical characteristics of the structure,

- The dynamic nature of the building loads, and
- The strategies for charging and discharging the stored thermal energy.

The rate thermal energy is transferred to or from the thermal mass slab and is available for use within the space equals (ASHRAE 1999):

$$\dot{q} = \rho c_p V \frac{dt_s}{d\tau} = h_0 A(t_s - t) \qquad (2\text{-}21)$$

where

q_s = rate of heat flow from slab;

ρ = density of the material;

c_p = specific heat;

V = slab volume;

τ = time;

h_0 = heat transfer coefficient;

t_s = slab temperature, and;

t = space temperature

The total capacity of the thermal mass member (Q_{th}) is given by (ASHRAE 1999):

$$Q_{th} = \rho c_p V \Delta\theta \qquad (2\text{-}22)$$

Thermochemical energy can be stored as heat of reaction in reversible chemical reactions. In that mode of heat storage the reaction in the forward direction is endothermic (stores heat), while the reverse reaction is exothermic (releases heat). The amount of heat stored in a chemical reaction depends upon the heat of reaction and the extent of conversion as:

$$Q = a_r m \Delta H \qquad (2\text{-}23)$$

where

a_r = fraction of the material that has reacted;

m = mass; and

ΔH = heat of reaction per unit mass.

The greatest advantage of this type of energy storage is that it can be stored at room temperature with no need for insulation. Unfortunately, there is no single successful system for a complete storage cycle based on high temperature reversible thermo-chemical reaction (Garg 1985).

The use of latent or phase change material (PCM) is based on the heat absorbed or released when a material passes through a reversible phase transition, usually from a solid to a liquid state that cycles back and forth. The thermal energy Q stored in a mass m of the material is given by:

$$Q = \int_{T_1}^{T_m} mc_{p,s}\,dt + m\lambda + \int_{T_m}^{T_2} mc_{p,l}\,dt \qquad (2\text{-}24)$$

where

T_m = phase change temperature;

m = mass;

c_p = specific heat of the solid and liquid phases; and

λ = energy of phase transformation.

Compared to sensible heat storage systems, such as rock beds or water tanks, PCM have a greater storage capacity per unit volume or weight, less control complexity, and greater system efficiency. In addition, PCMs utilize sensible heat storage systems above and below the melting point. The most important criteria for choosing a PCM are (Lane 1983):

1. Thermal properties
    a. Suitable phase transition temperature
    b. High latent heat of fusion
    c. Good heat transfer
2. Physical properties
    a. Favorable phase equilibrium behavior
    b. Low vapor pressure
    c. Small volume changes
3. High density

    a. Kinetic properties
    b. No super cooling
    c. Sufficient crystallization rate
4. Chemical properties
    a. Long term chemical stability
    b. No toxicity
    c. No fire hazard
    d. No nuisance factor
5. Economics
    a. Abundance
    b. Availability
    c. Cost-effectiveness

The most important of these factors are:

1. *Supercooling*, which is a natural phenomenon in most materials, where the cooling process occurs too quickly preventing proper crystallization of the material. This results in no heat withdrawal from the material. Thus supercooling should be reduced to a minimum when using the material as a heat storage system.
2. *Favorable phase equilibrium behavior*, which means that it exhibits no segregation during phase change (i.e. from solid to liquid or vice versa). It should be classified as either congruent[1] or eutectic[2].
3. *Constructability*; and
4. *Encapsulation technology*.

In selecting a PCM for any application, the operating temperature of the heating system must be matched to the transition temperature of the storage material. In matching the system operating temperature with the PCM transition temperature, the PCM melting point must be chosen at a temperature interval above the operating temperature. This interval must be large enough to provide a sufficient temperature gradient for a satisfactory heat withdrawal rate, but not excessive, since the losses will increase and

[1] Congruent mixing mixtures are those which when melting or freezing at equilibrium have exactly the same composition in the liquid and solid phases so has no chemical or physical segregation. This is a candidate for off-peak electric heating system and also for laundry or dishwashing applications.

[2] A eutectic is a minimum melting composition of two or more components each of which melts and freezes congruently forming a mixture of component crystals during crystallization. Nearly always melts and freezes without segregation. This is an excellent heat storage material for hydronic heating and domestic hot water systems.

system efficiency will decrease. An interval of about 5-10^{o}C has been employed for many systems.

Another important factor in selecting the PCM is density, since high density is desirable for smaller-size storage containers. It is important in heat storage systems to reduce super cooling to a minimum since it interferes with the ability to withdraw stored heat. Most PCMs contain additives that minimize super cooling by acting as initiation sites for crystallization. Super cooling tends to be lessened as the container size increases. Table 2-1 lists some commercially available suitable PCMs.

Table 2-1. Commercially Available PCMs (Guyer 1989)

PCM	Melting point ^{o}C	Heat of fusion cal/g	Density liquid g/cm^3
Water	0-4	20	1.0
Glauber salt[3] stabilized with gelled hydrogel $Na_2So_4.10H_2O.NH_4Cl.KCl$	8	29	1.49 gel
Polyethylene Glycol	11	24	1.12
$CaCl_2.CaBr_2.6H_2O.KBr$	12	32	1.78 gel
$Cacl_2.6H_2O$ – Congruent (most widely used for passive solar houses.	27	46	1.56
Magnesium chloride hexahydrate - magnesium nitrate hexahydrate $MgCl_2.Mg(NO_3)_2.6H_2O$ Eutectics	58	32	1.52
Sodium acetate trihydrate $NaCO_2CH_3.3H_2O$ Incongruent	58	54	1.28
Sodium pyrophosphate decahydrate $Na_4P_2O_7.10H_2O$ Incongruent	70	44	1.80 gel
Magnesium nitrate hexahydrate $Mg(NO_3)_2.6H_2O$ Congruent mixture	89	39	1.55
Ammonium alum $NH_4Al(SO_4)_2.12H_2O$ Congruent	95	64	1.65 solid

Phase Change Materials, which melt at a somewhat higher temperature than ice (5-15 ^{o}C), also can be used for cooling and dehumidification. They are more expensive than ice but they operate at higher temperatures, which give them a distinct advantage. Materials

[3] Exhibits incongruent melting so needs to be stabilized.

providing storage at about 5-8 ^{o}C provide cooling and dehumidification while those melting at about 8-15 ^{o}C provide only cooling. Unfortunately, the choice of coolness storage PCMs is rather limited. Some commercially available PCMs for cooling are listed in Table 2-1. This study will utilize a combination of sensible heat storage within the building mass (walls and floors) and, for the remaining energy, latent heat storage system.

2.4 ENERGY CONSUMPTION

There are four main types of thermal loads ((Reddy 1987) :

- Loads dependent on weather data which do not require energy conversion, i.e. space heating loads;
- Loads independent of weather data which do not require energy conversion, i.e. hot water loads;
- Loads dependent on weather data which do not require energy conversion, i.e. space cooling by absorption cycles; and
- Loads independent of weather data but which require energy conversion, i.e. thermodynamic cycles and electricity production.

This research is concerned only with the first two types of thermal loads.

There are many methods of varying complexities for calculating these loads as was mentioned earlier. This section provides a brief overview of some of these methods.

2.4.1 Simplified Methods for Hot Water and Space Heating Thermal Load Calculations

Space heating and cooling thermal loads can be calculated using the Degree Day (DD) Method. The monthly space heating or cooling load (Q_L) is:

$$Q_L = (UA)_B \times DD \tag{2-25}$$

where

UA_B = the building overall loss gain per unit temperature; and

DD = the number of degree days in a month calculated using:

$$DD = \sum_{d=1}^{N} \left(18.3 - T_{a,d}\right) \quad (2\text{-}26)$$

where

N = the number of days in the month, and;

$T_{a,d}$ = average daily temperature (^{o}C)

The degree-day (DD) can either be positive or negative. A positive value represents a heating degree day (HDD), while a negative value represents a cooling degree day (CDD). The monthly hot water heating requirements (Q_h) can be calculated using:

$$Q_h = G \times C_p \times \Delta\theta \times D_M \quad (2\text{-}27)$$

where

$D_{a,d}$ = number of days in the month;

$\Delta\theta$ = increase in hot water temperature;

Cp = specific capacity of water; and

G = daily household hot water requirement (estimated at 10-20 gallons per person).

2.4.2 Detailed methods for calculation of building system loads

Detailed simulation methods that accurately predict the thermal loads as well as the performance of the system include TRANSYS, DOE2, DOEPlus, and Energy Plus, among others. This section will introduce each of these methods. Some of these simulators contain an integrated solar collection and storage module, but the calculations of these modules are based on the approach developed by Duffie and Beckman in 1980.

2.4.2.1 TRANSYS

In 1975, the University of Wisconsin Solar Energy Laboratory proposed to the NSF the development of a modular solar simulation computer program, and as a result the first version of TRNSYS (Transient systems) was developed. The TRNSYS was originally conceived as a general purpose, public domain program and has been continuously

updated since its creation (Klein, et. al. 1976). The program is written in ANSI standard Fortran. The latest version uses Fortran 77.

TRNSYS possesses a library of 50 subroutines, including utility components (like time-dependent forcing functions and psychometrics), solar collector data (like linear thermal efficiency data, theoretical flat plate[4] and theoretical CPC[1]), thermal storage data (like stratified liquid storage [based on a finite difference analysis], algebraic tank and rock bed), equipment (like conditioning equipment, heat exchangers), utility subroutines (as in matrix conversion), building loads and structures (like degree hour house, thermal storage wall, and windows), hydronic (like pump, fan and pipes), user contributed components (like storage battery, and electrical subsystems), combined subsystems (like liquid collector-storage system, air-collector storage system and domestic hot water system), controllers, and output.

Dorer and Weber integrated a multi-zone airflow and contaminant transport computer simulation program with TRANSYS to allow for the integral determination of the heat fluxes due to conduction, radiation, and convection, as well as to study interactions between building mass, equipment and air flow (Dorer and Weber 1999).

The models in TRNSYS are described by either algebraic or differential equations. The TRNSYS executive program is designed to solve simultaneously the set of equations describing the system. Under the TRNSYS system, the design engineer does not have to worry about analysis or details of modeling; instead, he simply connects the various components to form a system model, assigns sizes, and interprets the results.

The main disadvantage of this tool is that the building load calculations are less sophisticated than those of comprehensive building energy analysis programs (ASHRAE 1993). The solar analysis component models for flat plate collectors and evacuated tubes are based on the analysis derived in the 1970s by Hottel, Whillier, and Bliss (Beckman 1993).

The main advantages of TRANSYS are its flexibility for modeling a variety of energy systems with differing levels of complexity and its user friendliness. It also provides users with a web-based library of additional components and frequent

[4] See Duffie and Beckman "Solar Engineering of Thermal Processes" for details on the theoretical analysis procedure.

downloadable updates. TRNSYS also interfaces with various other simulation packages such as GenOpt, for doing system optimization studies, and SimCad, whose CAD representation of buildings can be read directly into TRNSYS as the basis of a thermal model.

2.4.2.2 DOE, DOEPLUS and VISUAL DOE

To simulate large, multi-zone buildings and their HVAC systems, DOE and DOE-2 provide useful examples of detailed building energy analysis programs. They can be used also for active and passive hybrid solar energy analysis. The large, public domain building analysis program DOE-2 (York and Tucker 1980) contains solar simulation capabilities in its Component Based Simulator section (CBS). Component Based Simulator is similar to TRNSYS in that its individual components are modeled in separate subroutines, and the user connects the components to build system models. However, all CBS models are algebraic; the differential equations are solved either analytically or numerically within the component model. The common systems are also available as pre-assembled subroutines.

A new version of DOE (VisualDOE) is currently available that provides a Windows interface to the DOE-2.1E energy simulation program. With the graphical interface, users construct a model of the building's geometry using standard block shapes or a built-in drawing tool. Building systems are defined through a point-and-click interface. A library of constructions, systems, and operating schedules is included, and the user can add custom elements as well. VisualDOE is especially useful for studies of envelope and HVAC design alternatives. Up to 20 alternatives can be defined for a single project. Summary reports and graphs can be printed directly from the program, and hourly reports of building parameters also can be viewed.

The main advantages of DOE, DOE-2 and VisualDOE are that they allow rapid development of energy simulations. They have been shown to be accurate simulation tools; they also implement day-lighting calculations and can import CAD data to define thermal zones. They also allow editing of equipment performance curves as well as simple management of up to 20 design alternatives (Pasqualetto et. al. 1997).

The main disadvantages of DOE, DOE-2 and VisualDOE are that passive solar models may not be accurate. Natural ventilation modeling is limited to specified air changes per hour (ACH) that may be scheduled on or off. Underground buildings must be modeled with exterior walls, although custom constructions can be entered to represent the mass of the earth. Under-floor air distribution systems can provide benefits that cannot be directly modeled in DOE-2. For instance, DOE-2 does not account for thermal stratification in a space. Some versions of VisualDOE do not support modeling of skylights (DOE 2001). Last, but not least, DOE programs are based on sequential simulation techniques that allow no feedback from one module to the other, which results in inaccurate predictions of space temperatures (Crawley 2000). That fact, among others, resulted in the development of Energy Plus

DOE programs attempt to find the heat flux at the inside and outside surfaces of the building using the response factors method, where a one-dimensional heat flow is assumed and the heat conduction equation is solved for a simple case, then the solutions for the more complicated cases are reached by superimposing on them the solutions of the simple cases. The solution of the simple function (the excitation) is assumed to be a combination of two simple functions, the outside temperature, $g(t) = 0$ and the inside temperature, $f(t)$ = a step function. The general solution would then be a weighted sum of the solution of the simpler cases.

Since the temperature information in building energy analysis is not known for $g(t)$ and $f(t)$ in the form of a continuous function but rather the outside temperature $g(t)$ is given at hourly intervals, rectangular or triangular pulses instead of a delta function can be used to represent the excitation. Overlapping triangular pulses are recommended since they can be more easily approximated into a smooth function. A series of response factors is then obtained by sampling the response function to a triangular excitation at equal (hourly) time intervals. Laplace transformation is used to solve the resulting equations, the solution is expressed as a transfer function, which relates the input (the excitation) to the output (response).

The weighted sum of the simple solutions is calculated using the weighting factor method developed by Mitalas and Stephenson (DOE-2 Engineers Manual 1982). This method presents a compromise between simplified and detailed methods, in that it

performs an hourly thermal load calculation based on the physical description of the building and the hour's ambient weather conditions. This method incorporates two general assumptions:

- It assumes the process modeled can be represented by linear differential equations.
- The system properties that influence the weighting factors are constant.

In DOE-2 the weighting factor calculations are performed in two steps:

- Assume the air temperature is fixed and calculate the instantaneous heat gains or losses for the given space. A cooling load for a space is defined as the rate at which energy must be removed from the room to maintain its reference air temperature. Weighting factors are used to calculate the cooling loads from the instantaneous heat gain by determining how much of the energy that enters the room is stored and how fast it is released during the coming hours. The cooling loads from various heat gains are then summed to give the total cooling loads.
- The total cooling load for the space, along with the data about the HVAC system used and a set of air temperatures weighting factors, are used to calculate the actual heat extraction rate and air temperature. The air temperature weighting factors relate the net cooling loads to the deviation of the air temperature from its reference value.

2.4.2.3 Energy Plus

Energy Plus is a new building performance simulation program recently developed by the Department of Energy to bridge the gap between advances in analytical methods and computational power and existing simulation methods that originated in the early 1960s, with particular attention paid to increased difficulty, time consumption, and high costs of modifying the existing tools (Crawley 2000). Energy Plus, which is written in Fortran 90, combines features from existing simulation programs like DOE-2 with new capabilities. Currently, it has no formal user interface but it can be linked to other programs.

The main advantage of the Energy Plus simulator over DOE-2 is that it uses an integrated simulation technique versus the traditional sequential technique. The new

technique calculates loads at a user specified time-step (15 minute default) and passes them to the building system simulation module during the same time step. The building system simulation module possesses a variable time step that could be mere seconds. It calculates heating and cooling, as well as plant and electrical system responses. Feedback from the building system simulation module on loads not met is reflected in the next time step of the load calculations (Crawley 2000). That technique results in a more accurate space temperature prediction.

Another major benefit of the program is that its code is much more object-oriented and modular in nature than those of DOE and BLAST. This benefit simplifies the addition of modules and of program upgrading.

In addition, Energy Plus is user friendly. It can import and export DXF files, allowing designers to utilize a CAD Interface to create, alter, or view the simulated building. It saves its output in the form of CSV files so that they can be easily viewed on Excel, reads weather data in the form of TMY and CSV, and interfaces with other simulation programs for detailed calculations of a specific variable (i.e. calculating air flow using COSMIS, etc), as shown in Figure 2-5.

Energy Plus uses a heat balance-based solution technique that simultaneously calculates conductive, convective, and radiative effects at every element (Energy Plus 2002). It can also create thermal comfort reports based on Fanger PMV, developed by P.O. Fanger; Pierce two node model, developed by J.B. Pierce; and Kansas State University's two node model.

Energy Plus also boasts a weather data converter that changes weather files prepared by the Department of Energy TMY2 to a format viewable by Excel (CSV) or readable by Energy Plus (EPW). Since there is no weather file available for Blacksburg from the DOE, a Blacksburg file was created, as described in Chapter 4. Although Energy Plus has excellent energy simulation capabilities, it does not simulate active solar collection systems but can be used to maximize the savings from passive solar system designs. It is also quite difficult to use without graphical interfaces.

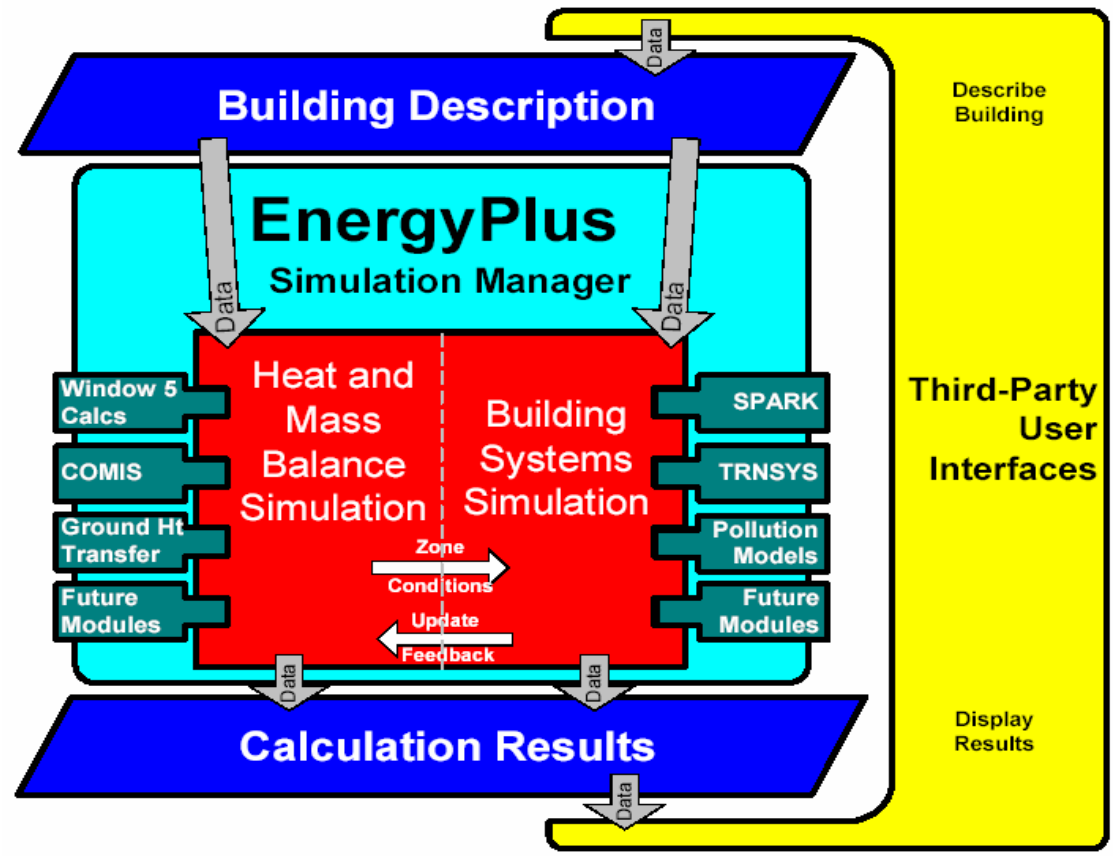

Figure 2-5. Energy Plus Program Interface (After Energy Plus 2002)

2.4.2.4 Other Simulation Tools

There are many other simulation tools that can calculate a building's thermal loads, including BLAST, PASSPORT, ENER-WIN, Solar5, and Hot2000. Building Loads Analysis and System Thermodynamics, better known as BLAST, is a building energy simulator that uses FORTRAN programming language to perform hourly simulations of buildings, air handling systems, and central plant equipment in order to provide mechanical, energy, and architectural engineers with accurate estimates of energy needs. The zone models of BLAST are based on the fundamental heat balance method. It does not analyze active solar systems. BLAST output may be utilized in conjunction with the Life Cycle Cost in Design (LCCID) program to perform an economic analysis of the building/system/plant design. It can be utilized for passive system evaluations and energy efficiency calculations (Rabghi et. al. 2001).

BLAST's main advantages are that it has a Windows interface, as well as a structured text interface which makes it user friendly. It contains detailed heat balance algorithms that allow for analysis of thermal comfort, passive solar structures; high and low intensity radiant heat, moisture, and variable heat transfer coefficients. Its main disadvantage is that it requires a high level of expertise to develop custom system and plant models (Rabghi et. al. 2001).

PASSPORT is a correlation-based evaluation tool that enables assessing of heating needs in residential buildings. It has been developed in the framework of the PASSYS project of the European Commission DG XII. The PASSPORT tool has close links to a preliminary European Standard for calculating energy requirements in residential buildings, but additional choice is offered to the user of PASSPORT: either to follow strictly the European Standard or to call upon features intended to improve the accuracy of the results, especially in the case of passive solar buildings (Belarbi et. al. 1997).

The calculation method is based on a steady-state energy balance for the building zone, with an allowance for external temperature variations and a utilization factor which takes into account the dynamic effect of internal and solar gains. The gain utilization factor is given as a function of the gain-to-load ratio (GLR) and an inertia parameter *t* (time constant of the building or of the zone). The method treats separately two phenomena associated with intermittent heating: decreased losses due to lower inside temperatures and reduction in utilized gains to take into account periods when the building is not heated. Two intermittency factors are obtained from formulae based on the heating pattern and the time constant of the building. To deal with multi-zone passive solar buildings, uniform temperature zones are defined; then the calculation method is applied to each zone. To take account interaction between the zones, an interactive procedure is used to solve the heat balance for all zones (Belarbi et. al. 1997).

Though it is easy to use, PASSPORT requires a DOS-based interface. Its main disadvantage is that it is based on correlations, which may mean that some configurations could not be accurately simulated.

ENER-WIN is a passive energy simulation program that calculates monthly energy loads, predicts utility bills, performs a peak load analysis, and evaluates demand

changes, as well as life cycle costs. It has a user-friendly interface that is written in Visual Basic and can easily be operated under Windows. It helps the designer with *what if* scenarios by allowing for iterative inputs, result examination, and design changes. As a result, design decisions can be made very early, even while little detailed information is available.

ENER-WIN provides fast access to databases and a short run time. It consists of an interface module, a weather data filing module, a sketching module, and an energy simulation module. The weather generator module and the energy simulation program were written in Fortran-77, while the weather file and retriever were written in Quick Basic. The sketching module was written in C, in Fortran 77. As for the databases and reports, they were written in ASCII text format.

The program's input data are the building type, its location, and its geometry. The weather data generation is performed hourly, producing the dry-bulb temperature, the dew point temperature, the wind speed, the sun angles, the cloud cover fraction, the direct insulation, and the diffuse insulation. The building can be described either by sketches or by using a zone processor. The load calculations, the system simulations, and the energy summations are performed simultaneously every hour for a year period. Heat transfer through walls and roofs is performed using a transient heat balance technique based on solar-air temperature, time lag, and a decrement factor (Degelman 1995).

The main advantage of this tool is that it can function as an energy advisor during the initial stages of design. Unfortunately, it cannot be used for active systems.

SOLAR5 is a visual FORTRAN tool that displays 3-D plots of hourly energy performance for the whole building, as well as heat flow into/out of thermal mass, and indoor air temperature, day lighting, output of the HVAC system, cost of electricity and heating fuel, and the corresponding amount of air pollution. SOLAR5 uses hourly weather data, and contains both an expert system to design an initial envelope for any climate and any building type and a variety of decision-making aids, including combination and comparison options. To calculate the building's thermal performance, Solar5 requires the floor area, number of stories, location, and building type. SOLAR5 calculates the yearly needs using TMY data and assumes any other needed data to create an initial design with high thermal efficiency that the designer can later modify. SOLAR5

also produces a three-dimensional graphic output that relates time of day, time of year to heat gain or loss through windows, among other features.

SOLAR5 is very helpful during the earliest stages of the design and is extremely user friendly. The results of this software have been validated against DOE-2 and Blast, but its primary drawback is that it cannot be used for complex mechanical system design or equipment sizing (Mha 2001).

HOT2000 is a user-friendly energy analysis and design software useful in low-rise residential buildings. By using current heat loss/gain and system performance models, it aids in the simulation and design of buildings for thermal effectiveness, passive solar heating, and the operation and performance of heating and cooling systems. The input values needed include building geometry, construction characteristics (above and below grade), HVAC and domestic hot water specifications, geographical location of the house, fuel costs, and economic data (optional). Reports on the house analysis, weather file, economic and financial conditions, and fuel costs are available. The house analysis includes detailed monthly tables, as well as annual heat loss and HVAC load results (Building group 2001).

The main advantage of this program is its ability to perform whole-house energy analysis quickly. This analysis can then be used to determine annual energy use and the cost effectiveness of energy efficiency upgrades. The program takes into account thermal bridging through studs in assemblies, and it models both detailed air infiltration and foundation heat loss. Heat balance studies are performed on the basement, main floor, and attic levels. This system also can model five fuel types and many different HVAC systems, including heat recovery ventilators and heat pumps. it has been validated extensively against hourly simulation programs and monitoring of real houses. Its main shortcoming is that it cannot size HVAC equipment room-by-room (Building Group 2001).

2.5 THERMAL COMFORT

The ultimate objective of any building's heating, cooling, or ventilation system is to provide a comfortable environment for occupants. This comfortable environment is created by simultaneously controlling air temperature, mean radiant temperature,

humidity, air cleanliness, and air distribution. Therefore, as shown in Figure 2-6, thermal comfort in buildings depends on four design factors: air temperature, air movement, relative humidity, and the radiant temperature of surfaces. as shown in Figure 2-6. These design factors are weighed against other factors that consider the health, activity, and clothing of the occupants. Also, in order to ensure proper implementation of physiological, psychological and economic (energy conservation) comfort limits, the occupants' need to control their thermal environment must also be addressed (Rush 1986).

When two or more of these factors are combined into a single variable, the result is called an *environmental index,* which can be classified as either *rational* or *empirical*, depending upon how it was developed. Environmental indices include effective temperature (ET), the combining of temperature and relative humidity into a single variable; humid operative temperature (t_{oh}), defined as the temperature of a uniform environment at 100% relative humidity; heat stress index, a rational index defined as the ratio of the total evaporative heat loss E_{sk} required for thermal equilibrium to the maximum evaporative heat loss E_{max} possible for that environment under steady state conditions; and the skin wettness index, a ratio of the observed skin sweating E_{sk} to the E_{max} of the environment (ASHRAE 2001).

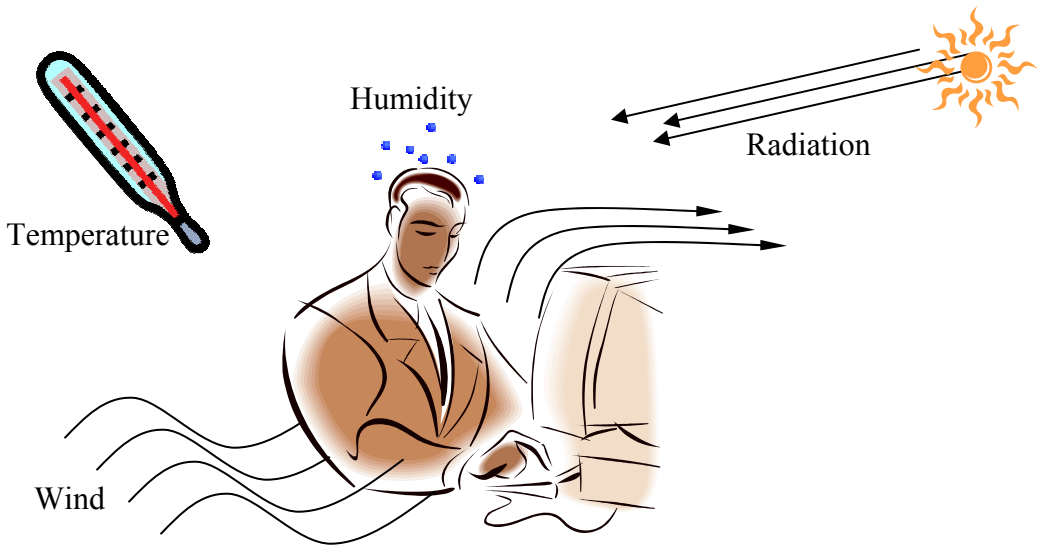

Figure 2-6. Factors Influencing Human Comfort

Evaluation of thermal comfort started in the 1970's when Fanger inferred a thermal index to articulate a client's feeling of thermal comfort "thermal sensation" whenever the surrounding environment deviated from the comfort zone. Based on this formulation, it was assumed that the subject's feelings of thermal comfort were a function of the body's thermal loads. To determine thermal loads, Fanger quantified results of experiments wherein subjects cast votes under different controlled conditions, including clothing, activity, air temperature, mean radiant temperature, relative air velocity, and humidity (Fanger 1972).

Other studies by Rohles ans Nevins (1971) and Rohels (1973) revealed correlations between other factors, including comfort level, temperature, humidity, gender, and length of exposure. Based upon these correlations, the ASHRAE thermal sensation scale was then developed:

+3	Hot
+2	Warm
+1	Slightly warm
0	Neutral
-1	Slightly cool
-2	Cool
-3	Cold

The ASHRAE thermal sensation scale (Y) can be calculated using the equations listed in Table 2-2, which indicates that women are more sensitive to temperature and less sensitive to humidity than are men. In general, a 5.4^{o}F change in temperature or a 3.0kPa (0.44psi) change in water vapor pressure is necessary to change a thermal sensation vote by 1.0 unit (Howell et. al. 1988). In addition, Fanger reduced the equations developed by Rohles and Nevins (1971) and Rohels (1973) to a single equation that assumes all sweat generated by an individual is evaporated:

$$\begin{aligned}(M-W) = {} & 1.196X10^{-9} f_{cl}\left[\left(t_{cl}+460\right)^4-\left(t_r+460\right)^4\right]+f_{cl}h_c\left(t_{cl}+t_a\right) \\ & +0.97\left[5.73-0.022(M-W)-6.9p_a\right]+0.42\left[(M-W)-18.43\right] \\ & +0.0173\,M\left(5.87-6.9p_a\right)+0.00077\,M\left(93.2-t_a\right)\end{aligned} \qquad (2\text{-}28)$$

where

M = level of metabolic activity (Btu/h.ft^2);

W = rate of mechanical work accomplished ((Btu/h.ft^2);

f_{cl}= clothing area factor = A_{cl}/A_D;

A_D = DuBois surface area (ft^2) = $0.108m^{0.425}l^{0.725}$, m = body mass and l = body height;

h_c = convective heat transfer coefficient (Btu/h.ft^2.^{o}F);

t_a = ambient temperature (^{o}F);

p_a = ambient partial vapor pressure(psi);

t_r = mean radiant temperature (^{o}F), and;

t_{cl} = temperature of the outer surface of the clothed body (^{o}F):

$$t_{cl} = 96.3 - 0.156(M - W) - R_{cl}\begin{bmatrix}(M - W)\\ -0.97[5.73 - 0.022(M - W) - 6.9p_a]\\ -0.42[(M - W) - 18.43]\\ -0.0173M(5.87 - 6.9p_a)\\ -0.00077M(93.2 - t_a)\end{bmatrix} \quad (2\text{-}29)$$

Table 2-2. Equations for Predicting Thermal Sensation (Howell et. al. 1998)

Exposure Period, h	Sex	Regression Equations
1.0	Male	Y = 0.122t + 1.61p – 9.584
	Female	Y = 0.151t +1.71p – 12.080
	Combined	Y = 0.136t + 1.71p -10.880
2.0	Male	Y = 0.123t + 1.86p – 9.953
	Female	Y = 0.157t +1.45p – 12.725
	Combined	Y = 0.140t + 1.65p -11.339
3.0	Male	Y = 0.118t + 2.02p – 9.718
	Female	Y = 0.153t +1.76p – 13.511
	Combined	Y = 0.135t + 1.92p -11.122

t (^{o}F) = dry bulb temperature and p (psi) = vapor pressure

The range of the measured thermal sensations can be expanded using a Predicted Mean Vote (PMV) Index, which predicts the mean response of a large group of people according to the ASHRAE thermal sensation scale. Using the following equation, Fanger related PMV to the imbalance between the actual heat flow from the body in a given environment and the heat flow required for optimum comfort during a specified activity:

$$PMV = \left[0.303\exp\left(-0.036M\right) + 0.028\right]L \quad (2\text{-}30)$$

where

L = thermal load on the body.

After calculating the PMV, the Predicted Percent Dissatisfaction (PPD) also can be calculated. The PMV-PPD model is a widely used method for design and field evaluation of comfort conditions; however, it can be used only to predict steady state comfort responses (ASHRAE 2001). In general, a PMV of ±1.0 is considered acceptable.

It should be noted that this model is based on a steady-state energy balance approach. To account for the transient nature of the process, where the subject interacts with its environment, a two-node model was developed that considers a human to possess two concentric thermal compartments, skin and core body. All heat is assumed to generate at the core compartment and is then passively conducted to the skin (Gagge 1986). The two-node model can be used to analyze responses in transient conditions, as well as predict physiological responses for low to moderate activity levels in cool to very hot environments.

As with the PMV-PPD model, the two-node model uses empirical expressions to predict thermal sensations and thermal discomfort, with the positive side representing heat and the negative side representing cold. However, the scale used in the two-node model is divided into 11 points instead of the 7 points previously used in the PMV-PPD model. The thermal sensation scale used in the two-node model is defined as follows:

+5	intolerably Hot
+4	Very hot
+3	Hot
+2	Warm
+1	Slightly warm
0	Neutral
-1	Slightly cool
-2	Cool
-3	Cold
-4	very cold
-5	intolerably cold

The thermal discomfort scale used in the two-node model is defined as follows:

+5	intolerable
+4	Limited Tolerance
+3	very comfortable
+2	uncomfortable and unpleaseant
+1	slightly uncomfortable but acceptable
0	comfortable

2.5.1 Recent Researches in Thermal Comfort

This section provides a brief overview of the research that has occurred on the topic under study during the last decade. To begin with, to help minimize their energy consumption, Braun developed a model for forecasting the cooling loads of large buildings that utilize thermal storage. Using a combined deterministic stochastic model, Braun estimated the load as a function of the ambient temperature, the solar radiation, occupancy, lightning, and electrical consumption (Braun 1987). These models were used in subsequent studies to identify practical optimal algorithms for thermal efficiency of plants with storage.

Braun also developed a methodology for dynamic optimization. Under this method, he could optimally control a building's thermal capacity to reach a more efficient level of energy consumption wherein the envelope, structure, interior, and mechanical were integrated to achieve a more efficient thermal performance. The harmony and architecture of the building, as well as its materials and systems, were used to maximize system effectiveness and to minimize the operating cost over a specific period while satisfying thermal comfort requirements. The operating cost of the system was given as the product of the power consumption and the cost of fuel at any specific point. Two constraints were used: the required thermal comfort (PMV = ±0.5) and the system's equipment operation limits. The control variables include set points derived from the PMV conditions, discharge air temperatures and plant control (Braun 1990).

The desire of a building's occupants to be in control of their environment led quite naturally to the development of personal environmental control (PEC) systems which allow individuals to control their own environment within an open-plan office through localized cooling or heating. These systems represent an integration between producing better air quality and increasing thermal performance. Through the use of computer simulations, the characteristics of energy systems incorporating personal

environmental control were compared with those of conventional designs. The TRANSYS simulation program was used to determine the building's heating and cooling loads. Results showed that, when compared with conventional systems, the effect of PEC systems ranges between 7% saving and a 15% penalty in building lighting and HVAC eclectrical, as well as an annual 0.08% increase in the worker's productivity. That increase in productivity offsets the worst case 15% penalty (Seem and Braun 1992).

Another early research project, involving a large office in Illinois, developed and tested a building control strategy that would utilize thermal mass to limit peak-cooling loads. This is accomplished through precooling of the building's thermal mass. The control strategy was first evaluated using simulation programs, then tested on two identical buildings-, one utilizing the newly developed control strategy; the other, acting as an experimental control, utilizing the existing control strategy. The simulation showed that, based upon cooling cost minimization, precooling control could result in a monthly savings of $25,000. The experimental setup validated the simulation outcome (Keeney and Braun 1997). The results of this work provide owners of large buildings with a strategy that can significantly reduce cooling costs.

In addition, through studying alternative ventilation control strategies for constant air volume (CAV) systems and evaluated their typical energy requirements, Brandemuehl and Braun (1999) examined the effects of integration for air quality and thermal performance. Their analysis was performed for four typical single-zone buildings using eight different ventilation systems placed under 20 different US climates. The building loads were calculated using the DOE2 simulation program. The results of the Brandemuehl and Braun study showed the possibility for significant energy savings with regard to both heating and cooling (Brandemuehl and Braun 1999).

Utilizing the concept of building's thermal inertia, Simmonds achieved an optimal design for its heating and ventilation systems. Using simple methods based on steady-state calculations, the system was evaluated by calculating the heat loss or gain through the envelope, as well as through basic ventilation and infiltration. Unfortunately, for the following reasons, these methods cause problems of insufficient capacity during installation (Simmonds 1993):

- The increasing energy costs require a higher degree of building insulation and air-tightness, resulting in a lower specific heat capacity within the insulation. This, in turn, lowers the accuracy of the calculations under any dynamic phenomena, such as heating or cooling the building.
- The client's consistent need to adhere to thermal comfort.

These concerns raised the need for utilizing hourly dynamic simulation programs that can estimate the annual thermal loads required to simultaneously satisfy the client's PMV requirements and minimize the building's overall energy demands (Simmonds 1993).

Simmonds also developed a procedure for predicting thermal comfort levels within a space while utilizing a predicted mean vote criterion for evaluation. Four factors were considered: dry-bulb air temperature, radiant temperature, air speed, and vapor pressure. Achieving these factors requires finding complete solutions to the complex air movement and thermal response equations under transient conditions, which calls for use of a dynamic simulation tool that would accurately model the dynamic effect of the building and HVAC system. To perform a comfort analysis, the model assumes the presence of a person standing at every point in the space and performs a heat balance at that person's surface, which considers the effect of long wave radiation. Since short wave radiation also can have a great effect on the median radiant temperature (MRT), its effects are considered using Fanger's *Form Factors* Theory. Under this theory, to include the effect of direct solar radiation if the point of analysis is not shaded, sunlight is tracked in the space and used to modify the MRT on an hourly basis. Weather test conditions were derived from a weather generator producing random ambient dry-bulb, wet bulb, and solar radiation based upon daily statistics (Simmonds 1993).

The dynamic optimization methodology developed by Braun (1990) for use in the aforementioned dynamic simulation tool involves discretizing the cost function in time and applying a non-smooth optimization algorithm to determine the set of controls for minimizing costs over time. The main difference between this work and Braun's is that in this study, the plant and building are not decoupled during analysis (Simmonds 1993). The optimization problem was stated as follows:

$$J = \sum_{k=1}^{K} \left(R(k) + P^* \left(PMV_z(k), f(k) \right) \right) \qquad (2\text{-}31)$$

The simulated system consisted of an office space with a low rate of air from primary ventilation means integrated with that from VHV units and a fresh air supply from slot diffusers mounted on the lower ceiling. The simulation model evaluated four different combinations of construction materials and systems to find the optimum operating conditions for each proposed integrated system. These systems represented examples of system integration between the mechanical, the envelope, the interior, and the structural systems. The system was simulated for two periods—summer and winter— and was based on a combination of simple equations that form a "quasi"-variable-volume strategy. For each thermal zone, the following equation was used to estimate the sensible cooling load needed to maintain comfort conditions at any stage (k) (Simmonds 1993):

$$Q_{z,k} = \sum_{K=1}^{N} \left[T_{a,k-1} + PMV_{z,k-1} + Q_{g,sk-1} + Q_{sol,k-1} \right] + \sum_{K=1}^{N} Q_{z,k-1} \qquad (2\text{-}32)$$

where

$Q_{z,k}$ = sensible cooling temperature for stage k;

$T_{a,k}$ = ambient temperature for stage k;

$Q_{g,s,k}$ = total sensible internal gains for stage k;

$Q_{sol,k}$ = total incident solar radiation on all exterior zone surfaces for stage k; and

N = number of stages in the day.

The simulation results showed that the PMV is within acceptable limits for the four combinations. They also indicated how, combined with low-ach primary ventilation, the VHV units could produce an alternative to conventional forms of air conditioning. A major advantage of this system is its ability to create separate zones, which gives the system more flexibility. Also, since it allows for systemic parametric studies of weather effects on dynamic control, the weather generator proves significantly more advantageous than the standard reference year. It has to be noted that Fanger's equation, used in the above procedure, is empirical and based on statistical data gathered in

working environments, so it should be applied with care to non-working spaces, such as commercial or residential spaces.

Research has also verified that pipes embedded in the flooring systems of buildings can be used for heating and cooling purposes. Such radiant floor systems employ envelope, mechanical, and interior integration as well as, to a lesser degree, structural integration. In these systems, heat is either radiated or conducted into the space or absorbed from it according to ambient conditions and internal loads. Using a simulation program, Simmonds developed for the Groninger Museum a strategy for controlling and evaluating such radiant floor systems. Simmonds's simulation calculates the aforementioned design factors for thermal comfort by solving energy and mass equations for the three modes of heat transfer: conduction, convection, and radiation. While different lighting levels and occupancies are simulated, the strategy controls within specified limits the temperatures and the PMV. The simulation results were used to size the hydronic system (Simmonds 1994).

To condition large spaces like airports, Simmonds developed a hybrid conditioning system that utilized a variable volume displacement radiant system and a radiant cooled floor. The control strategies used in this system within a required level optimize the energy consumption as well as contain the moisture level, which exemplifies integrating both thermal and air quality performance. After dividing the space into representative zones, computer simulations were used to calculate the building loads. Results showed that introducing radiant cooling floors into the system cover part of the cooling load and reduce the number of required air changes (Simmonds 2000).

In summary, it is worth noting that although significant advancements have been made toward integrating and evaluating separate components of a building in order to attain better thermal comfort levels, the work to date has always tackled a specific system, function, or objective. More research should be focused on combining the above efforts into one integrated technique that can simultaneously serve several objectives, systems, and functions.

3 FRAMEWORK AND DEMONSTRATION DESCRIPTION

3.1 INTRODUCTION

The main objective of this study is to develop a design-evaluation framework that can predict the overall energy savings in active solar systems and thus help create a new generation of cost-effective buildings with minimal need for non-renewable energy. This chapter describes the development of the proposed framework needed for evaluating any active thermal solar system. Implementation of the proposed framework in two case studies located in Blacksburg, Virginia and Minneapolis, Minnesota was used to verify and validate the design evaluation framework.

3.2 FRAMEWORK DESCRIPTION

As shown in Figure 3-1, the proposed evaluation framework consists of a decision module connecting six major stages:

I. Preliminary design stage,
II. Solar supply evaluation stage,
III. Building demand evaluation stage,
IV. Storage design and sizing stage,
V. Control system design stage, and
VI. Determination of overall system energy saving stage.

These six steps are connected through an iterative process that allows the designer to re-examine the design decisions in order to improve system performance. This iterative process is made possible through the decision-making module shown in Figure 3-1. In this module, the designer evaluates the design components against preset evaluation criteria. These criteria vary from project to project but in general will include: cost effectiveness, efficient thermal performance, aesthetics, and adequate service life with low maintenance needs. Based on the outcome of the evaluation, the designer reviews his design decisions or continues to the next step in the design evaluation framework.

This decision making evaluation process takes place after every step in the framework. Each of the six steps of the framework is fully described in the following sections.

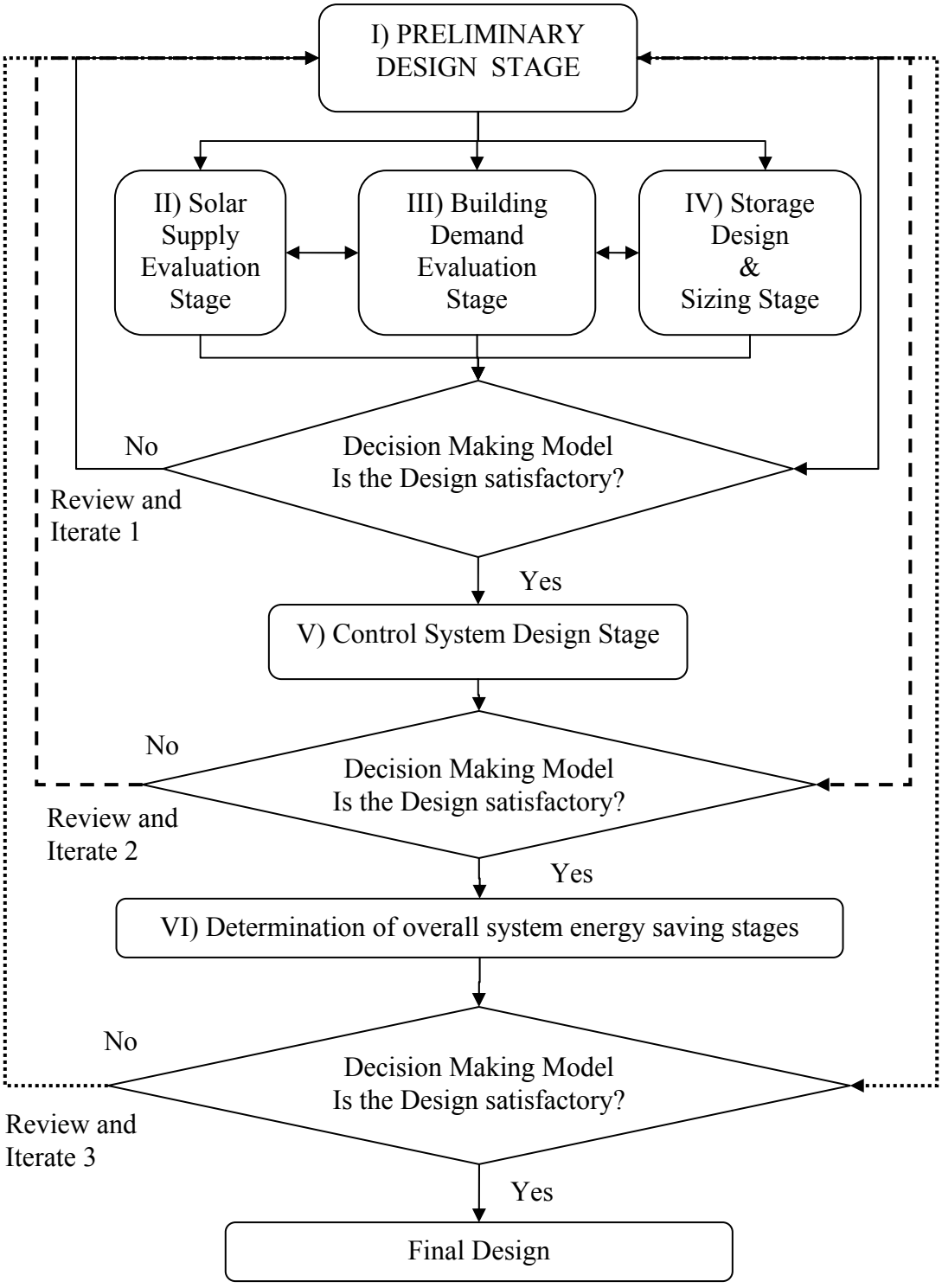

Figure 3-1. Framework Steps

3.2.1 Stage I: Preliminary Design Stage

The design evaluation process starts with the formulation of the preliminary building design. As evident in most building designs, traditional solar collection system designs possess several constraints. These constraints define the design process, which in turn is used to formulate the preliminary design. These constraints, which are shown in Figure 3-2, include the following criteria:

- Project budget,
- Building material and system selection,
- Building location,
- Building area,
- Collection system service life, and
- Occupancy schedule.

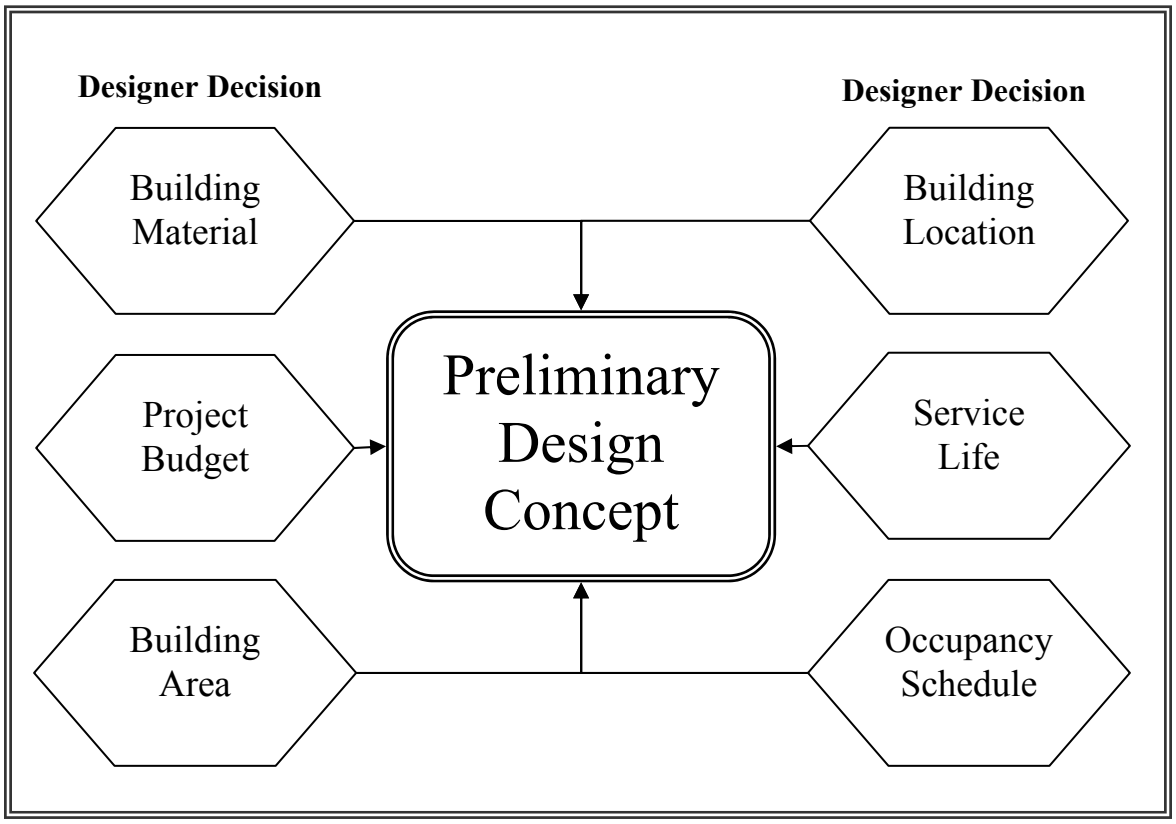

Figure 3-2. Factors Formulating the Preliminary Design Concept

The project budget determines the initial cost of the system; in turn, it eliminates some of the most expensive alternatives, even though they might improve overall performance. In addition, it sometimes dictates other constraints, i.e. building material, since using a specific type of material in a certain location may reduce system cost.

Since building material determines the amount of heat loss and/or gain that occurs, as well as how the building interacts with its environment from a thermal perspective, the building material greatly influences the system's thermal performance. Building location, on the other hand, determines the weather profile, which has the single most significant impact on the collection system. Building location also determines the ability of solar radiation to reach the collector—in some cases, for example, adjacent buildings could shade the collection area. When designing the building shape, these factors must be considered to ensure maximum exposure to solar radiation.

Area affects both the collection supply and the building demand. As the building area increases horizontally, both the solar energy supply and the building energy demand increase. However, as the building area increases vertically, energy demand increases, while the area of collection may remain constant—that is, if the designer decided to collect through the roof only. If the designer decides to collect through the building walls, more solar energy will be available to meet the demand.

Since the presence of people and their usage of equipment increases space gains, the building's occupancy schedule also will have a significant impact on determining thermal loads. In addition, the building's service life and the acceptable level of maintenance determine the acceptable initial cost of the collection system. Increasing the initial cost could be justified, as doing so could prolong the service life.

The combination of the aforementioned constraints shown in Figure 3-2 formulates the designer's decisions leading to a preliminary building concept. To transform this preliminary building concept into a preliminary design, the designer makes additional choices, as shown in Figure 3-3, with respect to the following variables:

- Method of solar collection,
- Type of collector,
- Collector-building assembly system,

- Supply system budget,
- Back-up supply system,
- Location of collector on building, and
- Inclination of collector.

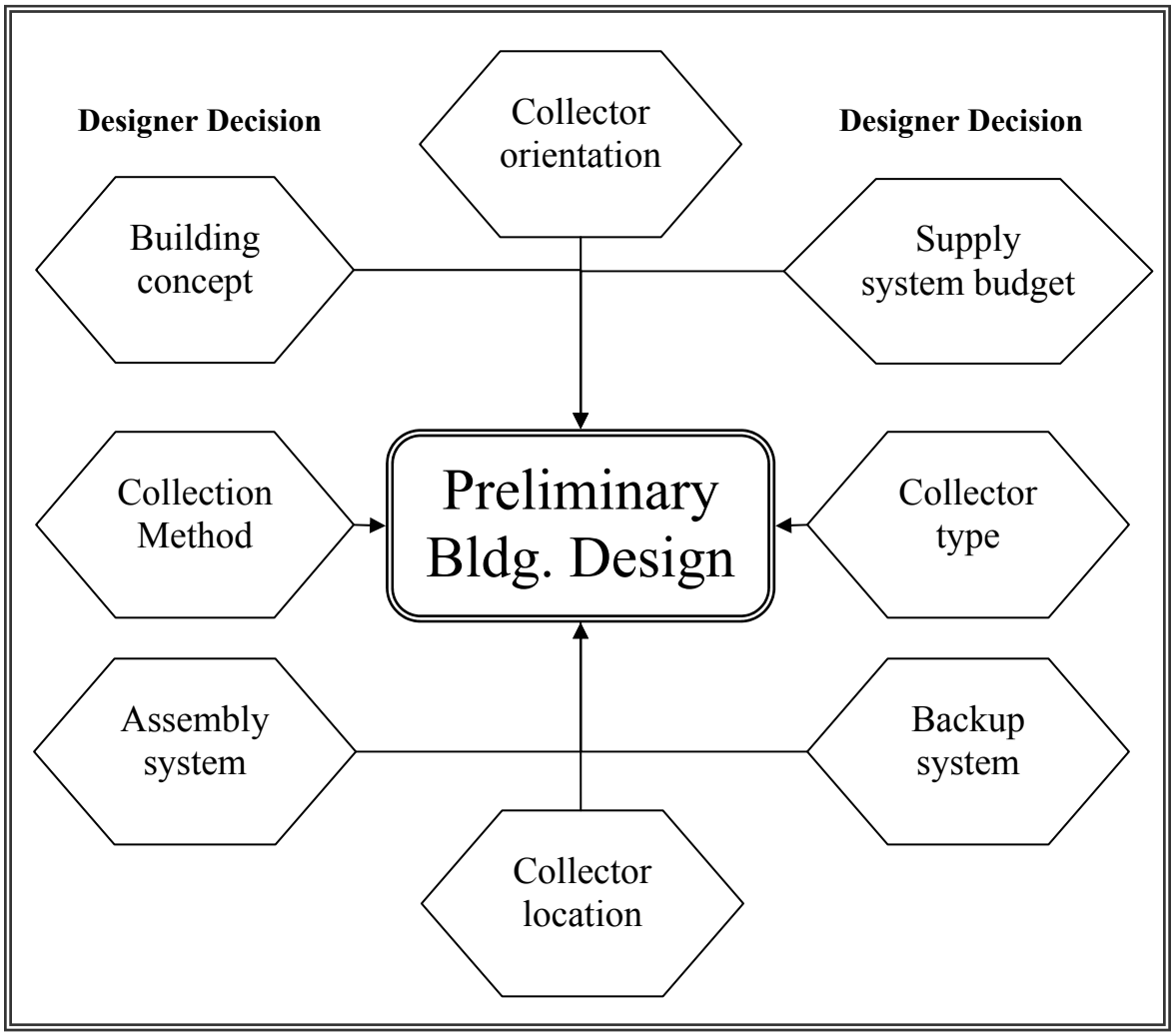

Figure 3-3. Preliminary Design Stage

During the first stage, the designer decides which collection method should be used in the energy supply system: active solar collection, passive solar collection, or a hybrid of active and passive. If active methods or a hybrid is chosen, the designer must then decide which type of solar collection system will be used: flat plate, concentrating, or photovoltaic (PV). As summarized in Chapter 2, each of these systems possesses distinct

advantages and disadvantages. While the photovoltaic system is typically the most expensive solar collector, the flat plate is the most cost-effective.

These decisions affect and are influenced by the decisions shown in Figure 3-2, as shown in Figure 3-3. For example, utilizing a passive system or a hybrid system indicates the need for an environmentally friendly building material and form. In such cases, the building interacts with its environment to absorb energy during cold weather and rejects it during hot weather.

A subsequent decision involves determining whether the collection system will be integrated within the building system. There are many advantages to integration, two of which are the system's ability to expand and cover a large area at a reasonable cost and its long service life, which results in decreased need for replacing materials and increased conservation. Should integration be chosen, the designer must define not only its process and shape, but also how that decision will affect both the building form and function. This process also becomes an iterative process between the initial building design concept (with respect to material choice and architectural design) and the process of integrating the solar collector within the building. If, on the other hand, the designer decides to avoid integration, the assembly process of the collector to the building shell would have to be defined. A balance must be reached between increases in system cost and savings in energy consumption costs during the lifetime of the structure.

It is worth noting that because of their direct impact on weather profile and solar collection variables, the location and budget of the building influences designer choices. For example, an increase in wind speed will increase the convection losses of the flat plate solar collector. Therefore, in a location with a high wind speed profile, the designer may consider using a different collector type, like a concentrating collector, to minimize convection losses. If the cost of concentrating collectors exceeds the project budget, another alternative must be chosen, such as using integrated collectors, so the collector can be shielded from wind by architectural features.

Another example in which cost and location highly affect the other four choices arises when the cost of energy in a particular location is cheaper than the initial cost of the storage system. In such a case, the designer might be inclined to eliminate or

downsize the storage system from the design and supply the rest of the needed energy using an online boiler or an electrical grid.

Since they affect how much solar radiation strikes the collection area, the collector's location and orientation must also be determined. For example, inclining the collector with the latitude of the building location will maximize annual heat gain. In addition, the designer must determine if a backup energy system is required. If it is, its type must be defined—e.g., online boiler, electric grid. The designer must also ensure that the addition of the backup system does not exceed the project's budget.

To summarize, in Stage I, the designer is required to make decisions that ensure better system integration and optimum design results. The outcome of this stage is the formulation of a building and collection preliminary design, which will be improved as the evaluation process continues. The resulting preliminary design will be used in Stages II, III, and IV of the design-evaluation framework. Since each of the decisions formulating the preliminary design will affect the selection process and performance of the solar collection system, this framework proposes an iterative process (presented by the decision making module). In this iterative process, the designer chooses a preliminary combination of these factors based on a preset design criterion. These criteria help the designer in making the best choice according to the project needs. The designer then goes through the proposed evaluation steps that follow to determine the system performance, and then reiterates to determine if any one or more aspect of these constraints may be modified depending upon the project priority.

3.2.2 Stage II: Solar Supply Evaluation Stage

This stage evaluates the ability of the proposed design to collect solar energy and determines the quantity of solar heat energy the proposed design can generate. This can be achieved by determining the amount of solar energy that can be collected under different environmental and operational conditions. A review of current literature indicates that the most important factors affecting solar collection (see Figure 3-4) are the following (De Wit and Augenbroe 2001):

- Wind speed / external convection coefficient,

- Dry bulb and wet bulb temperature,
- Solar radiation and incident angle,
- Initial and boundary conditions of collector,
- Collection media mass flow rate, if applicable,
- Collection area,
- Pipe diameter and spacing,
- Material properties, and
- Geometry (length, breadth, and height).

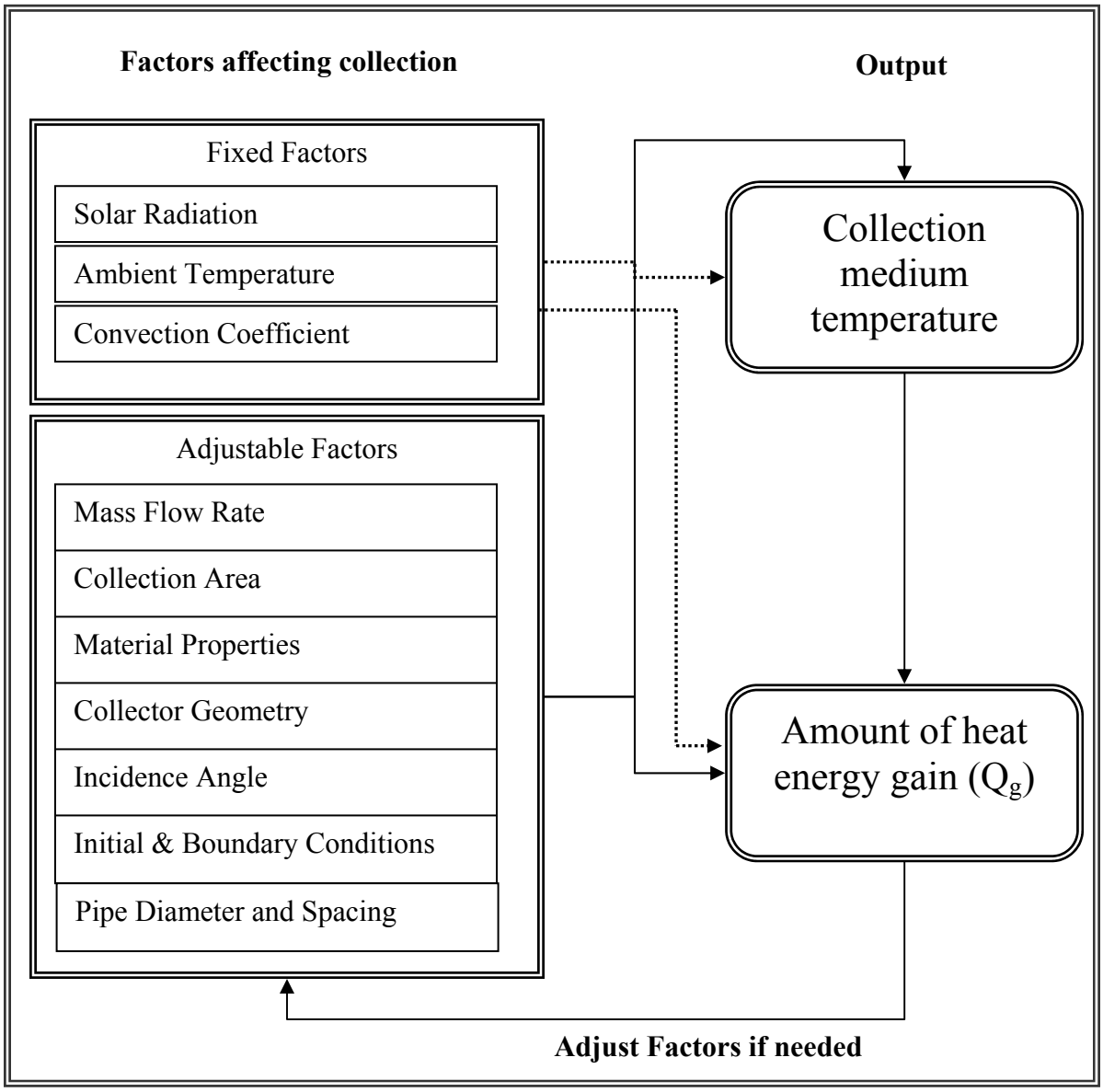

Figure 3-4. Factors Influencing Solar Energy Collection

To accurately determine the amount of solar gain collected by the system, the combined effects of the aforementioned factors must be considered. The output of the evaluation is defined in terms of (Figure 3-4):

- The collection medium increase in temperature, and
- The amount of energy collected (Q_g).

These two output parameters can be determined using any analytical or numerical methods, as mentioned in Chapter 2. Due to the accuracy they allow in the modeling process, however, the finite element method and the finite difference method are recommended in this evaluation framework. In addition, once the model is created, varying the different factors affecting the solar energy collection in order to perform a parametric study can be accomplished quite simply and will help the designer find solutions to different if-then scenarios. The proposed evaluation process thus consists of three steps (see Figure 3-5):

1. Creating a detailed model of the designed solar collector to predict the increase in the collection medium temperature.
2. Using the model iteratively, under different combinations of the factors affecting collection, to determine the collecting media's output temperature and the total amount of heat gain (Q_g) (see Figure 3-4). In each model iteration, the amount of increase in fluid temperature is obtained and the hourly heat gain (Q_g per hour) is divided by the modeled collection area to determine the amount of heat gain per meter square of collection area (q_g). This process helps the designer determine the required collection area according to the project budget and the building thermal loads.
3. Using statistical analysis tools to create a design equation for predicting the collecting media's output temperature and the total amount of energy collected (Q_g) under different conditions. This step may help the designer vary any of these parameters for the modeled collector design and improve the design without the need for repeated model execution.

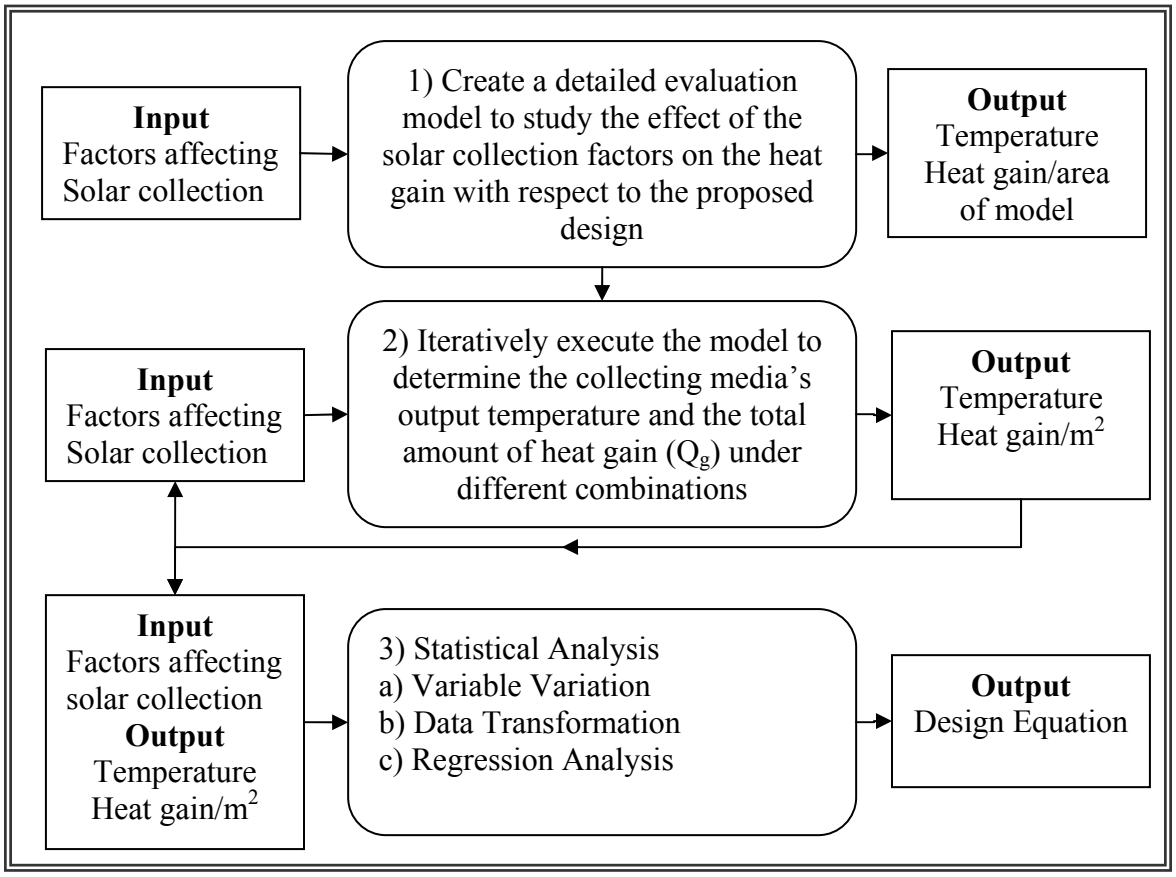

Figure 3-5. Summary of the Solar Collection Evaluation Process

Solar supply evaluation stage can be accomplished through conducting a parametric study that investigates the effects of the different controlling variables on the energy collected and predicting the most significant factor or set of factors. To ensure that weather data variability is accounted for, conditions such as solar radiation, solar incident angle, outdoor temperature, and wind speed, can vary according to the hourly TMY data files specified for the proposed location, as well statistical modifications of the TMY2 data, representing the best case scenario (95%) and the worst case scenario (5%). The rest of the parameters vary in two steps:

1. To find the range that maximizes energy gain for each, the parameters are varied one at a time while all the other parameters remain constant.

2. The range determined in Step 1 can vary in a matrix form with the rest of the parameters to evaluate the combined effect and develop a regression model for creating the design equation.

3.2.3 Stage III: Building Demand Evaluation Stage

Stage III involves determining the amount of energy required to maintain comfort-level heating conditions within the building. Building demand evaluation stage involves designing the mechanical system that will achieve this goal. Then, the amount of energy required can be estimated using simple or detailed methods. Simple methods include the heating degree day (HDD) and the heating degree hour, while detailed ones include detailed modeling of the system using programs like Blast, DOE2 and Energy Plus (see Chapter 2). Although simplified methods are easy to use, they cannot accurately predict energy impacts of features that have large hourly fluctuations (e.g., the amount of solar heat gain through windows with unique shading characteristics). Simplified methods also are unable to accurately predict the energy impacts of variations in a building's operation schedule. Therefore, detailed simulation methods are recommended. The main factors affecting the building's energy consumption, as shown in Figure 3-6, include:

- Weather conditions (all TMY2 indices),
- Building area,
- Mechanical system,
- Building construction and assembly (UA),
- Building occupancy schedule,
- Space gains (including people equipment lights, etc.), and
- Airflow (ventilation and infiltration).

The output of the building consumption evaluation is defined in terms of the building thermal zone temperature and humidity profile throughout the simulation period, as well as the amount of energy consumption (Q_c). As shown in Figure 3-7, the proposed consumption evaluation process consists of three steps:

1. Formulate a detailed energy consumption model using energy simulation software, i.e., DOE2 or Energy Plus, given the proposed preliminary design resulting from the first stage of Stage I, and the TMY2 weather conditions.
2. Use the model to determine the hourly energy consumption (Q_c) needed to ensure thermal comfort at all times.
3. Vary the adjustable factors to minimize the energy consumption while satisfying comfort level criteria.

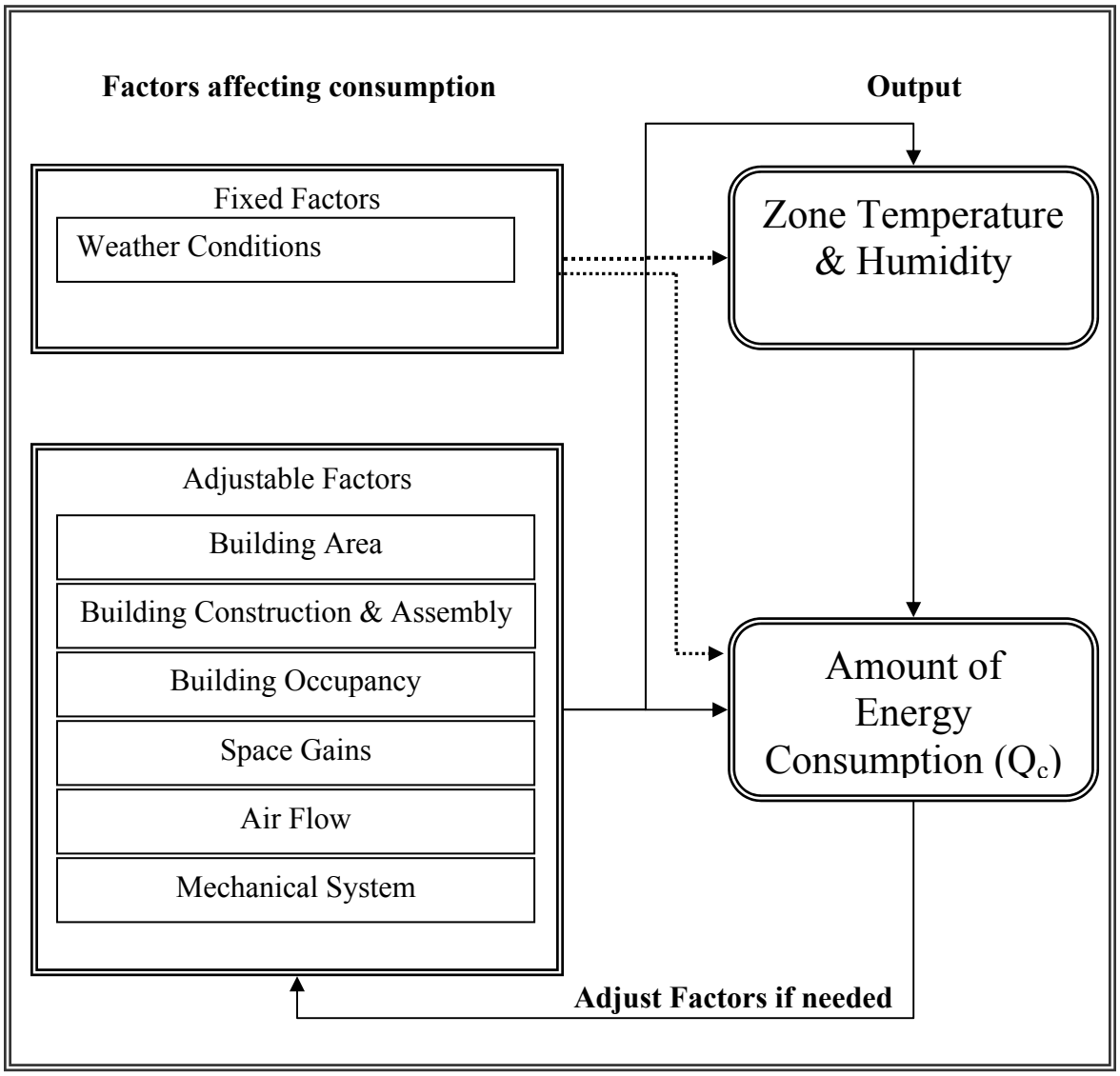

Figure 3-6. Factors Affecting Building Energy Consumption

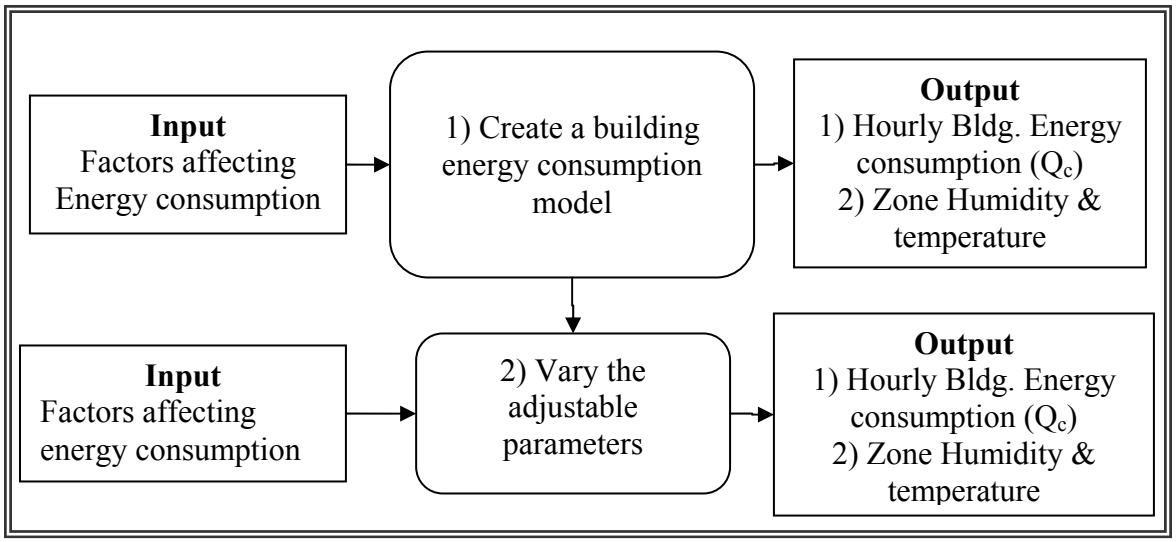

Figure 3-7. Summary of the Building Energy Consumption Evaluation Process

3.2.4 Stage IV: Storage Design and Sizing Stage

Stage IV involves designing and sizing of the solar collection system storage media. To achieve this design, the designer makes additional choices, as shown in Figure 3-8, with respect to the following criteria:

- Type of storage,
- Storage budget,
- Availability of secondary supply system, and,
- Cost of non-renewable energy.

The first decision the designer makes with respect to storage involves type. Three types of storage systems are available: sensible, latent, and thermochemical, each of which was described in Chapter 2. The choice of the storage type depends upon different locations and climatic conditions, (i.e. buildings located in cloudy cold weather will require larger storage capacity) as well as the dependence of the active solar system on storage, (i.e., whether storage supplies 100% of the remaining loads or not). After deciding on the type of storage system, the designer must balance the storage system's initial cost with its benefits in terms of energy savings and long-term costs. This analysis will help the designer size the storage system. System size can vary between a small tank that supplies

the needs of the night hours for one day in the winter to a large tank that can supply the whole building's energy needs. As the size of the tank increases, the cost effectiveness of the system decreases, and it becomes impractical, especially with regard to the residential construction industry.

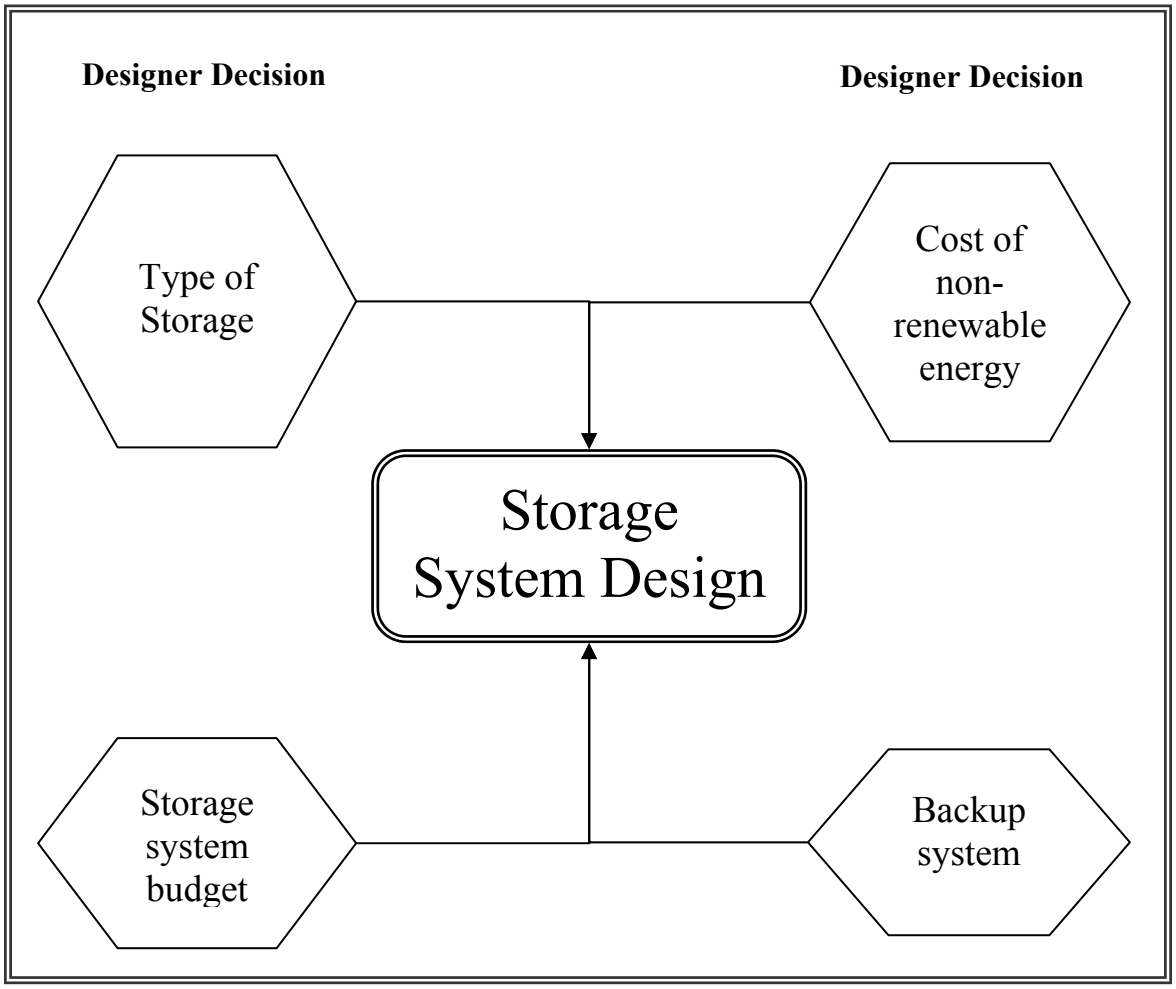

Figure 3-8. Storage System Design Stage

Therefore, the designer should increase tank size to support enough energy so that within three to five years potential savings can cover initial costs. For example, if the energy savings are $50 per month and the pay back period is 3 years, the maximum initial cost of the tank will be 3x50x12 = $US1800 (neglecting inflation rate). The following steps can be used to size the storage tank (see Figure 3-9):

1. Determine the type of storage tank to be used.
2. Determine the hourly, daily, monthly, and yearly solar energy (Q_g) collected from Stage II of the framework.
3. Determine the hourly, daily, monthly, and yearly building energy consumption (Q_c) from Stage III of the framework.
4. Determine alternative sizes for the storage tank based on the following guidelines:

   - Minimum size = Highest Daily (Q_c) – Lowest Daily (Q_g)
   - Maximum size = Yearly (Q_c) – Yearly (Q_g)
   - One Month under worst condition = Highest Monthly(Q_c)–Lowest Monthly(Q_g)
   - One day under worst condition = Highest Daily (Q_c) – Lowest Daily (Q_c)

5. Determine the mass and volume of the tank for each case, depending upon the type of storage system, using the approach presented in Chapter 2.
6. Determine the initial cost of the tank for each case.
7. Using the pay back period, compare the initial cost of the tank against savings in the cost of renewable energy to decide on the final size of the storage tank.
8. Design and size the backup energy supply system if needed.

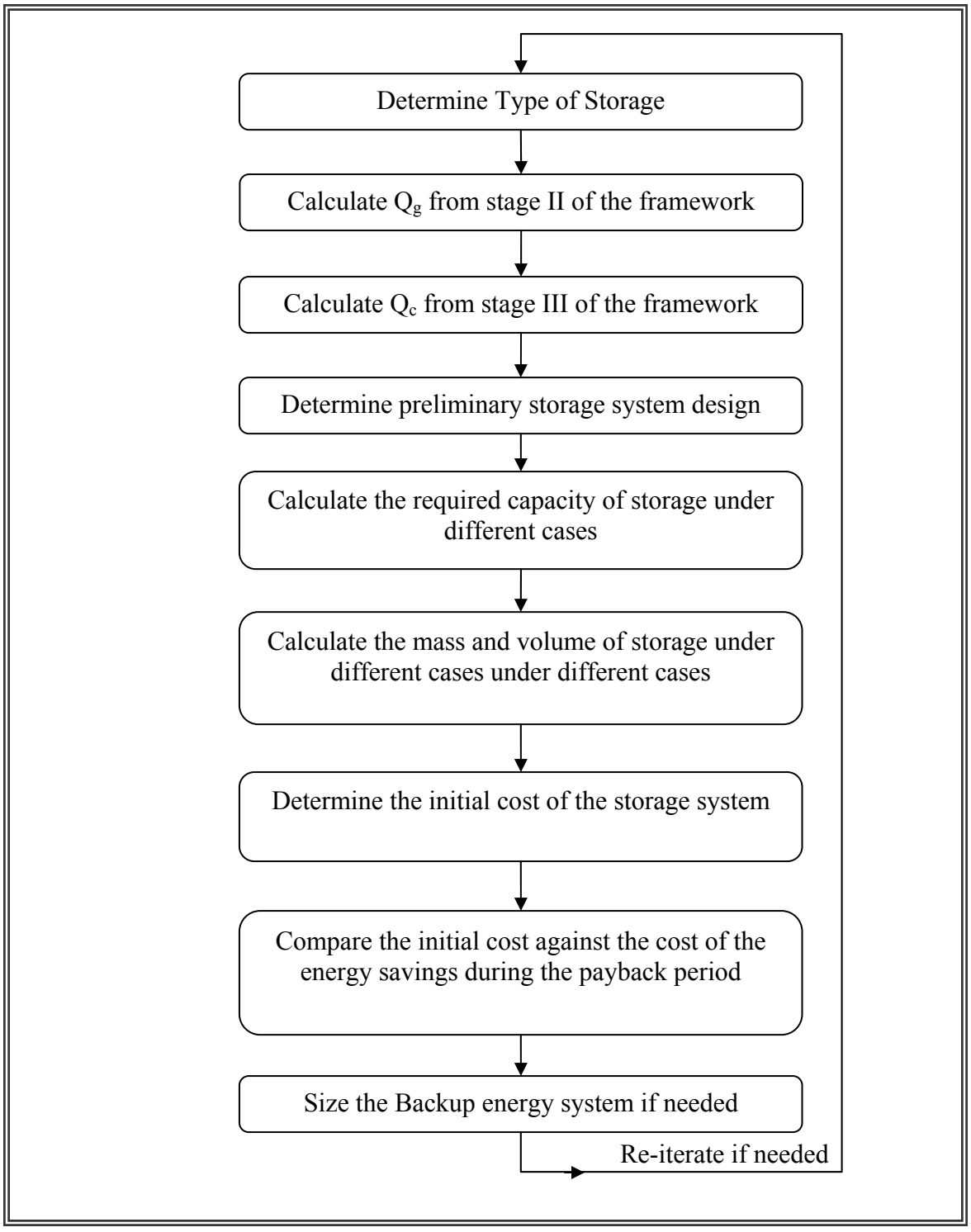

Figure 3-9. Summary of the Storage Design and Sizing Stage

The first decision making module of the framework is located after Stages II, III and IV. In this decision making module, the designer reviews the output of the three stages with

respect to each other and decides whether the design process can proceed or be iterated using review and iterate 1 as shown in Figure 3-1.

3.2.5 Stage V: Control System Design Stage

This stage helps the designer optimize system operation in the most energy efficient and cost-effective way. In this stage, the designer decides how the system components should be linked and what type of control system should be used. The main function of the system's control strategy is to regulate—by activating pumps, blowers, and valves—the automatic collection and distribution of solar energy either to the storage or to the load and to operate the auxiliary heating system in conjunction with the solar thermal system. The control system used for active solar collector is quite simple and in many ways is the same as that used for HVAC applications. The only difference is that in controlling the active solar system, the sensors sense a temperature differential instead of a single temperature and accordingly choose the fluid path, regulate the flow rates, and so on.

The second decision making module of the framework is located after stages V to ensure that the developed system operation is efficient. As in the first decision making module, the designer determines whether the evaluation criteria are satisfied. If they are, the design process continues otherwise, the design is iterated using review and iterate 2 shown in Figure 3-1. The design criteria that might be used will vary according to project priorities. Examples of the design criteria that might be used in the evaluation are cost effectiveness, efficient thermal performance, aesthetics, and adequate service life with low maintenance needs.

3.2.6 Stage VI: Overall System Energy Savings

Stage VI is the most important stage of the design evaluation process since it quantifies the usefulness of the system and examines alternatives for improving it. This quantification can be done as follows:

1. Compare the daily, monthly and yearly building energy consumption (Q_c) from Stage II to the building energy generation (Q_g) from Stage III and calculate the daily, monthly, and yearly percentage energy supplied (%SQ1) by the solar collector system according to Equation 3-1:

$$\%SQ1 = \left(\frac{Qc - Qg}{Qc} \right) * 100 \qquad (3\text{-}1)$$

2. Calculate the daily, monthly, and yearly percentage of energy supplied (%SQ2) by the storage system from Stage IV of the framework, and add it to (%SQ1) from Equation 3-1 to get the total percentage energy supplied by the collection system (SQ).
3. Utilize the design equation derived from Stage II to determine the percentage of system improvement that can be achieved if different parameters are altered.
4. Use the results from Step 3 to improve system design and performance.

After determination of the overall system energy savings, the designer uses the decision making module to determine if the system performance is satisfactory or needs further improvement. Criteria for determination of whether the design is satisfactory or not will vary from project to another and from design to another based on project priority as was mentioned earlier. If the design is satisfactory, the preliminary design becomes a final design. Otherwise, the process is iterated in review and Iterate 3 as shown in Figure 3-1.

3.3 STAGE I - DESCRIPTION OF CASE STUDIES USED FOR CONCEPT DEMONSTRATION

For verification and demonstration purposes, the proposed framework described above was used to evaluate the effectiveness of an active solar collection system proposed to be installed in a residential building. Two case studies were considered by studying the same design at two different locations: Blacksburg (VA) and Minneapolis (MN). This section briefly describes the proposed preliminary design that was used to validate the design-evaluation framework. This description presents the results of Stage I, which is

the preliminary design stage highlighted in Figure 3-10 and previously described in the framework.

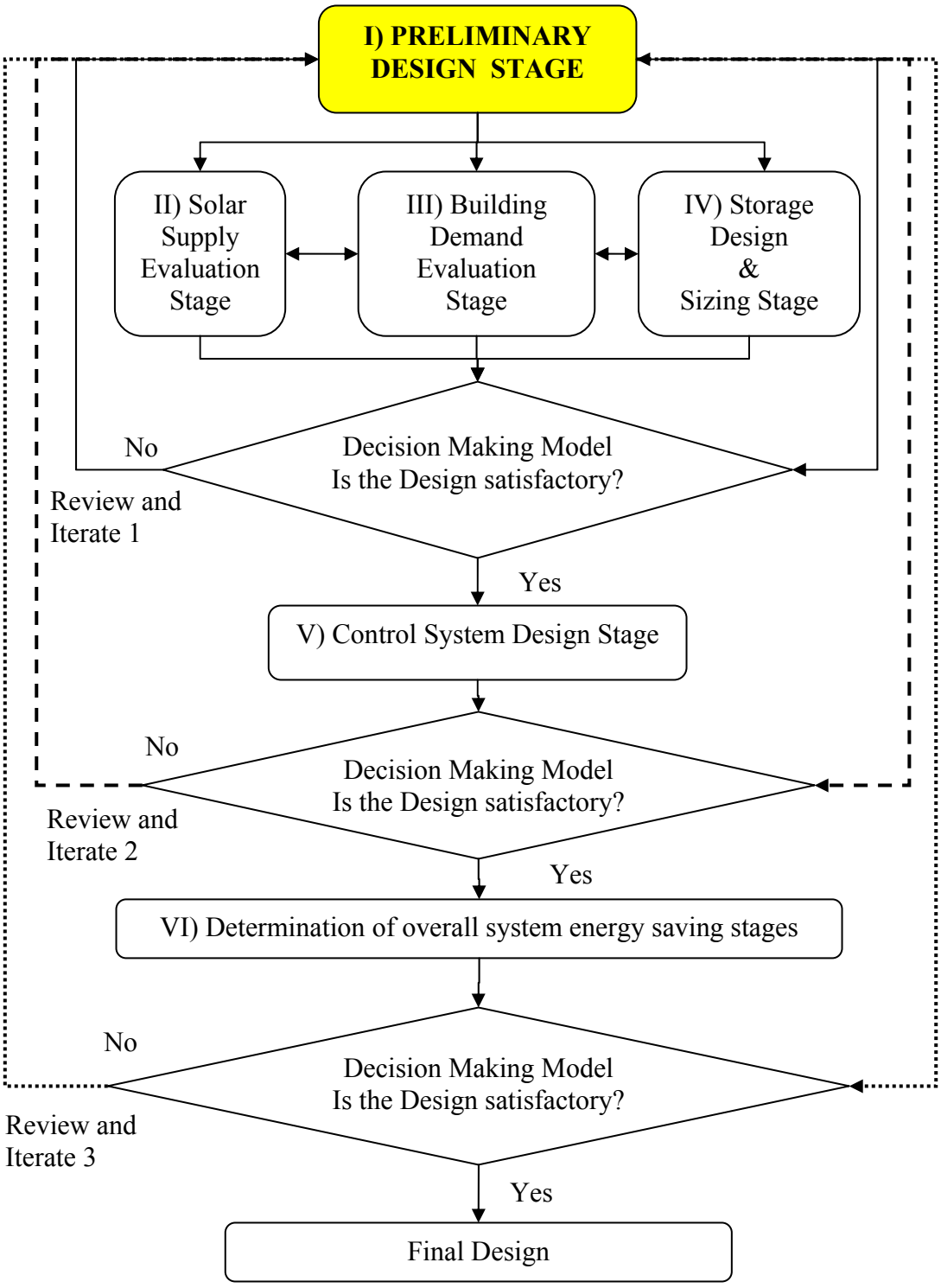

Figure 3-10. Stage I of the design evaluation framework

3.3.1 Building description

The proposed building is shown in Figure 3-11. A panelized system is proposed. As shown in Figure 3-12, the building shell utilizes insulated precast concrete sandwich panels in all exterior panels except the south roof. The panel is insulated using 75mm (3in) of polyurethane and is connected by fiber-reinforced plastic stirrups to provide tensile and shear strength. This feature allows the panel to act as a composite system, instead of a multi-layer system, so that it resists temperature and loading changes with minimal thermal bridging effect (Sauter 1991).

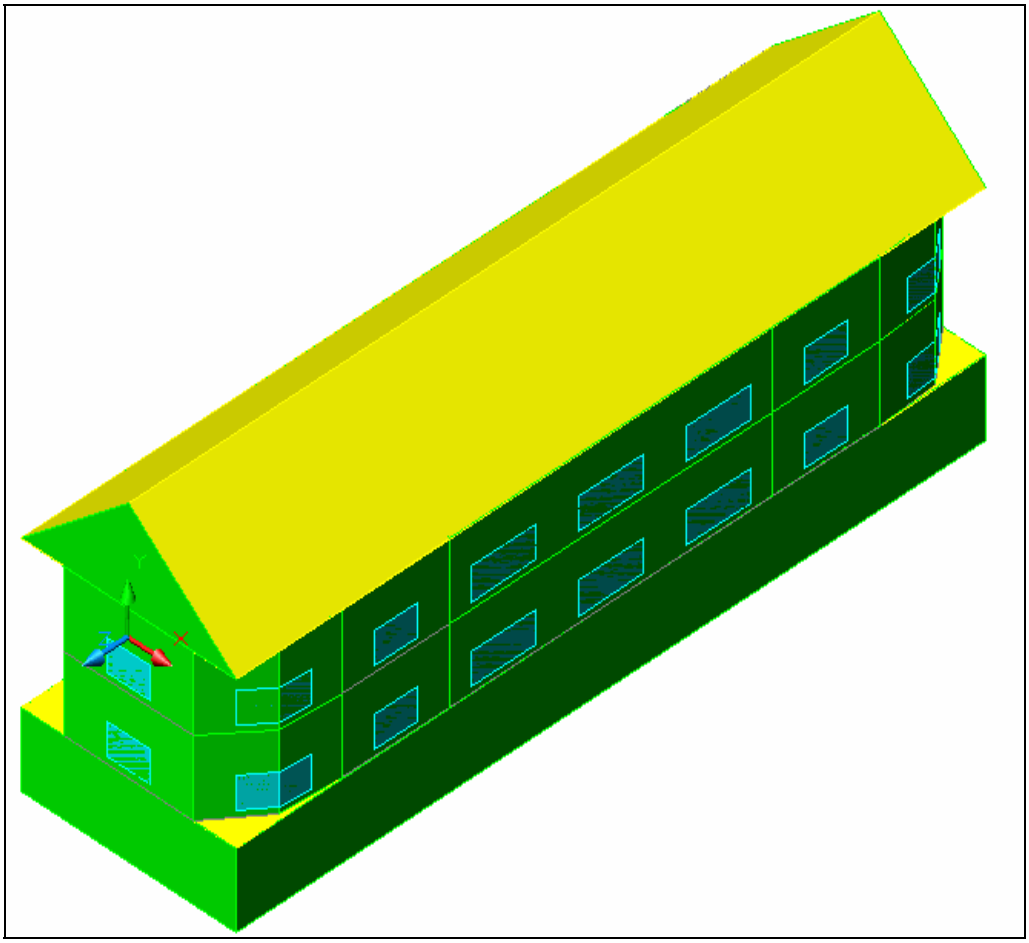

Figure 3-11. Proposed Building Preliminary Design

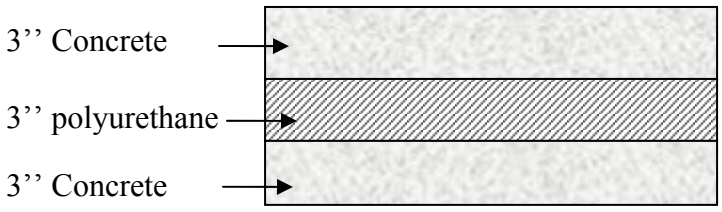

Figure 3-12. Cross section of the Building Shell Panels except for the South Roof

The south roof panels integrate the solar collector within the precast concrete building exterior panels, as shown in Figure 3-13. The design of the integrated roof solar collector went through an iterative process of design, performance evaluation, and redesign. Two alternatives made it to the final design stages. A cross- section of the first design is shown in Figure 3-13(a). It consists of a 6.35 mm (0.25 inch) single glass panel with an e-coating on the inner surface, followed by an air-gap. The thermal collecting medium consists of a fluid (water with antifreeze) enclosed in 12.7 mm (0.5 inch) diameter copper pipes painted black to ensure maximum solar absorption.

The pipes are laid within concrete cavities to minimize construction cost and time as well as to reduce convection losses. To ensure any radiation hitting the inner surfaces of the concrete cavity is reflected back to hit the copper pipes, they are surrounded with aluminum foil. The fluid absorbs the solar energy and transports it to its storage locations. The copper pipes are connected together by the aluminum foil layer surrounding them. The parts of the aluminum foil not surrounding the pipes are also painted black to ensure maximization of absorbed radiation. The foil absorbs the solar radiation and transmits it to the pipes by conduction (Duffie and Beckman 1980). The copper pipes are placed in groups of three every 800 mm (31.5 inch). This distance was selected to maximize the temperature gain while reducing the panel cost.

A 50.0-mm (2.0 inch) layer of insulation is attached to the back of the aluminum foil to reduce heat transfer to the adjacent 75.0 mm (3.0 inch) concrete. A 75-mm (3.0 inch) concrete layer is used as a building envelope. A 75.0-mm (3.0 inch) thick polyurethane foam is placed under the concrete to act as an insulation layer. The last layer consists of 75.0 mm (3.0 inch) concrete, to ensure structural stability as well as to

contribute to the thermal inertia on the inside of the facility. As in all the building shell panels, the south roof panels are connected by the aforementioned fiber reinforced plastic stirrups, used commonly in slab construction to provide tensile and shear strength.

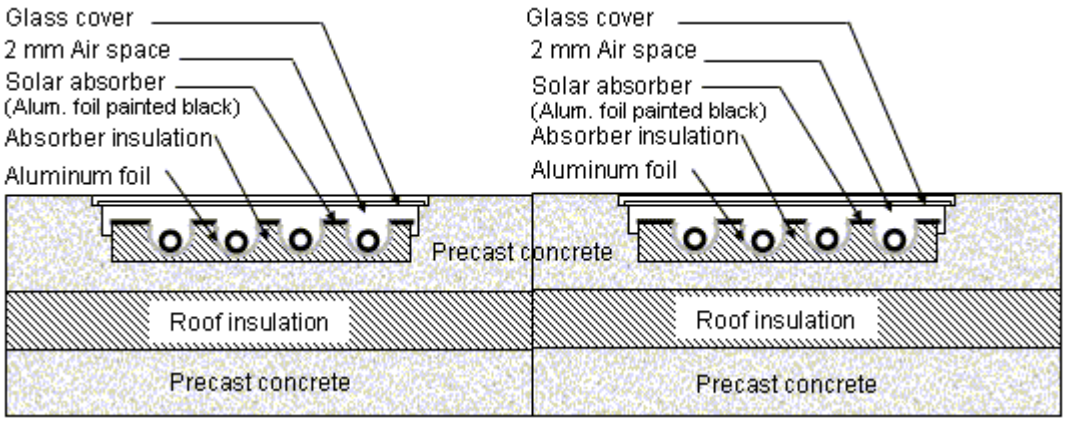

(a)

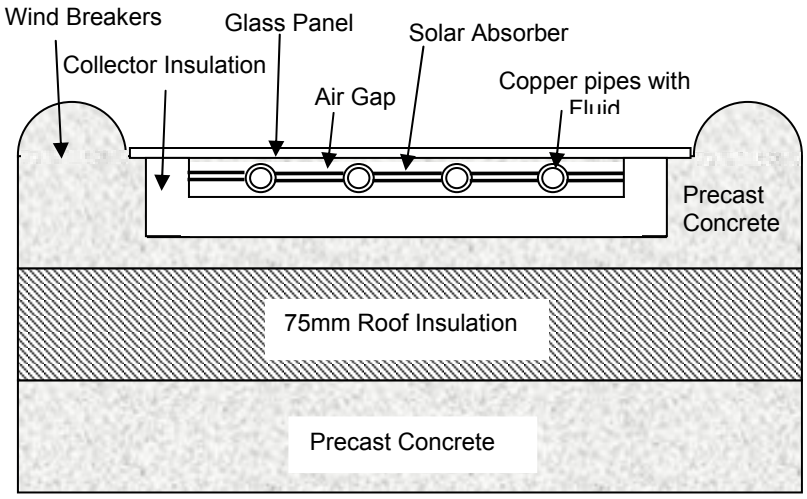

(b)

Figure 3-13. Cross Section of South Roof Panels: (a) First Design and (b) Final Design[5]

[5] This is the structure used in the finite element analysis model to evaluate the solar energy collection system described in stage II of the framework.

Unfortunately, early evaluations of the aforementioned design shown in Figure 3-13(a) indicated that it is difficult to construct and requires skilled labor. Therefore, it was simplified further to the final design (alternative B) shown in Figure 3-13(b). As shown in Figure 3-13(b), the upper layer of concrete is covered with a layer of insulation and the circular concrete cavities are replaced with a 610 mm (2 ft) square cavity containing four 12.7 mm (0.5 inch) connected pipes. These alterations further simplify construction. To ensure reduction of convection losses, the concrete has 75.0mm (3 inch) semi cylindrical wind breakers every 610 mm (2 ft) that reduce the wind speed. The sections shown in Figure 3-13 are repeated along the roof as needed to satisfy the building's heating and hot water requirements. The rest of the features remain the same as in the first design. Early cost evaluation showed that the proposed design may reduce the current market price of flat plate solar collection systems by two thirds.

3.3.2 Mechanical system

The proposed system consists of a collection system, a low-radiant heating, auxiliary heating systems, thermostats, humidistat, valves, and controllers. The proposed mechanical system allows the building to have the potential to heat itself throughout the year with a reduced dependency on non-renewable energy.

Low radiant heating and cooling systems (also known as hydronic) circulate hot or cold fluid through tubes embedded in the slab. Hence, energy is either added or removed from the space. The zone's occupants are conditioned by both radiation exchanges with the system, which increases their level of comfort, as well as convection from the surrounding air heated/cooled by the system. This system does not require fans, ductwork, or dampers.

For the purpose of minimizing the building's heating and hot water requirements, a combination of both active and passive solar collection techniques will be utilized. As previously described, the building has a low cost flat plate collector integrated within the roof structure. The flat plate collector supplies hot fluid to a moderate temperature phase change material (PCM) storage tank used for heat storage, as well as to the low radiant heating system that supplies heat to the zones, as shown in Figure 3-14.

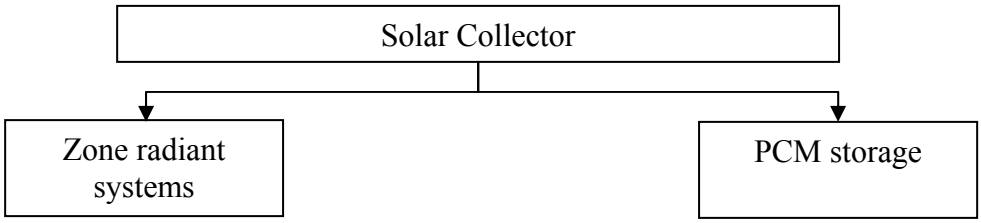

Figure 3-14. Heat Distribution

As shown in Figure 3-15, the hot fluid from the solar collector is circulated in the low radiant heating system embedded within the building's floor and is used to increase the temperature of the building zones.

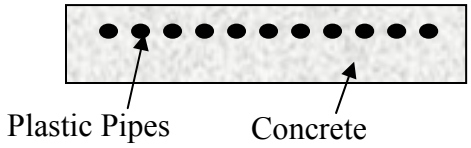

Figure 3-15. Building Floor Slab

The phase change material (PCM) chosen for heating storage, RUBITHERN RT 54, is based on a high crystalline, high n-paraffin content material. RUBITHERN RT 54 was chosen since it displays an absence of supercooling and is non-toxic and environmentally friendly. The main properties of this material are shown in Table 3-1. The main properties relevant for using water as a sensible thermal storage are also presented in Table 3-1 for comparison. The volume of the phase change material heating storage tank will be determined from the modeling analysis.

Table 3-1. Properties of heating phase change material (Material Data Sheet and Bejan 1995)

Property	Value (PCM)	Value (Water)
n-paraffin content (%)	85.1	N/A
Molar mass (Kg./Kmol)	377	N/A
Melting point (^{o}C)	55	0
Latent Heat Storage capacity (KJ/Kg) (from 46-61)	179	N/A
Density (solid (at 15^{o}C) Kg/l)	0.90	1.0
Specific Capacity (solid/Liquid) (KJ/Kg.K)	1.8 / 2.4	4.19
Density (liquid (at 70^{o}C) Kg/l)	0.76	1.0
Volume Expansion (%)	18	4.0
Heat conductivity (W/m.K)	0.2	0.58
Kinematic viscosity (70^{o}C) (mm^{2}/s)	5.80	1.30
Flash point (^{o}C)	220	N/A
Corrosion	Inert	Inert
Toxic	Non-toxic	Non-toxic

After presenting the output of Stage I of the design evaluation framework (the preliminary design), the following chapters will describe how the framework utilized detailed modeling techniques to evaluate the preliminary design for the case of Blacksburg, Virginia. Then a demonstration of the framework utilizing simplified modeling techniques under different thermal loading will be presented in Chapter 10 for evaluation of the Minneapolis, Minnesota case study.

4 FRAMEWORK WEATHER DATA PREPARATION

4.1 INTRODUCTION

After the preliminary design stage (Stage I of the framework), Stages II and III require evaluation of the building's energy consumption and collection. To demonstrate these two stages in the case of the Blacksburg, Virginia building, two detailed models were developed. The first model was used to simulate energy collection, (Stage II of the design evaluation framework), while the second was used to simulate energy consumption (Stage III of the design evaluation framework). The developed models were used to determine:

- The energy needed to keep the modeled building system within thermal comfort zone, as established by ASHRAE.
- The energy needed to supply the building's hot water requirements.
- The amount of energy that can be collected by the proposed active solar system under different weather conditions.

To ensure accurate simulation of the integrated components of the system, and to control potential errors, in the three models the same weather data were used as input. Moreover, since accurate interpretation of performance is possible only in relation to the test conditions applied to it, testing conditions should contain no uncertainties (DeWit 1997). However, it is often difficult to eliminate from simulation testing all sources of uncertainty. A good example is the variability of climatic conditions. Although significant work has been done to produce a typical reference year (TRY) of data in Europe or a typical meteorological year (TMY) in the USA (Argiriou et. al. 1999), the reliability of this data is still not well documented. This problem creates a situation wherein design evaluations of current building design practices— whether resulting from advanced building simulation, simple design guidelines, or even expert advice—rarely convey accurately the behavior of a simulated building.

Climatic conditions, especially wind speed and solar radiation, greatly impact the performance of active solar collection systems (De Wit & Augenbroe 2001). Therefore,

when designing such a system, it is vital to use the most accurate weather data available. Moreover, it is important that statistical analysis be used to minimize variability within the climatic data.

Initially, to represent climatic data, this simulation was to use the Typical Meteorological Years (TMY2) weather method, which provides hourly data standards for meteorological parameters over a period of one year. The represented climatic data is considered typical throughout a 30-year period. These files were specifically designed for long-term prediction of the annual performance of solar energy systems. Several methodologies have been reported in the literature for the generation of these files. Most of these methodologies promote using sequences of real, measured data, as in Klein et. al (1976), Schweitzer (1978), Hall et. al. (1978), Lund (1995), and Festa and Ratto (1993).

Unfortunately, the research's design location in Blacksburg, Virginia, does not have a TMY2 file. Therefore, in order to arrive at a more accurate simulation, the first two steps in the research design were to create a TMY2 file for Blacksburg and to eliminate variability within the climatic data. Attempting to eliminate the variability of the weather data took place through determination of the reliability of the weather data as well as manipulating the data to reflect high reliability. This section describes the process by which a TMY2 file was created for Blacksburg and how that file was manipulated to simulate average and extreme conditions.

4.2 SANDIA METHOD DESCRIPTION AND MODIFICATIONS

The TMY2 files were created based on the Sandia Method developed by the National Laboratories, which is an empirical approach that selects individual months from different years of the period of record (Hall et. al 1978). The Sandia Method selects a typical month based on nine daily indices: maximum, minimum, and mean dry bulb and dew point temperatures; maximum and mean wind velocity; and the total global horizontal solar radiation. For preparing the TMY2 files, this method was modified to include an index for direct normal radiation. Final selection of a month includes consideration of the monthly mean and median and the persistence of weather patterns. The process involves a series of steps as described below (Marion and Wilcox 1994):

For each month of the calendar year, five candidate months are selected with cumulative distribution functions (CDFs) for the daily indices closest to the long-term (30 years for the NSRDB). The CDF gives the proportion of the values that are less than or equal to a specified value of an index. Candidate monthly CDFs are compared to the long-term CDFs by using the Finkelstein-Schafer (FS) statistics (Finkelstein and Schafer 1971) for each index:

$$FS = \left(\frac{1}{n}\right)\sum_{i=1}^{n}\delta_i \qquad (4\text{-}1)$$

where

δ_i = absolute difference between the long-term CDF and the candidate month CDF, and;
n = the number of daily readings in a month.

Because some of the indices are judged more important than others, a weighted sum (WS) of the FS statistics is used to select the five candidate months that have the lowest weighted sums:

$$WS = \sum_{i=1}^{n} W_i S_i \qquad (4\text{-}2)$$

where

W_i= weighting of index, and

FS_i = FS statistic for index.

The five candidate months are ranked with respect to closeness of the month to the long-term mean and median. The persistence of mean dry bulb temperature and daily global horizontal radiation are evaluated by determining the frequency and run length above and below fixed long-term percentiles. The persistence data are used to select from the five candidate months to be used in the TMY. From the second step, the highest ranked candidate month that meets the persistence criteria is used in the TMY. The 12 selected months are then accumulated to form a complete year.

Since the months might be typical with respect to some indices, but not others, the following step involves weighting each of the 10 indexes. In this case, a month that has a better FS statistics for each index cannot be selected. By weighting the FS statistics, the

relative importance and sensitivity of the indices may be taken into account. The weights given to each of the TMY2 indices are shown in Table 4-1.

Table 4-1. TMY Weighting Values

Index	NSRDB TMY2 (Weightings)
Max Dry Bulb Temp	1/20
Min Dry Bulb Temp	1/20
Mean Dry Bulb Temp	2/20
Max Dew Point Temp	1/20
Min Dew Point Temp	1/20
Mean Dew Point Temp	2/20
Max Wind Velocity	1/20
Mean Wind Velocity	1/20
Mean Wind Velocity	1/20
Global Radiation	5/20
Direct Radiation	5/20

4.3 BLACKSBURG TMY2

The location of the first simulation case study, Blacksburg, VA, has no TMY2 file. Therefore, using weather files for adjacent cities, an interpolation approach was used to create TMY2 weather files for this location. Three cities forming a triangle around the location of Blacksburg (Latitude 37.20N, Longitude 80.24W) were selected:

- Charleston, (WVA) (n) (38.22N, 81.36W)
- Bristol, (VA) (t) (36.48N, 82.24 W)
- Roanoke, (VA) (k) (37.19N, 79.58W)

Assume that the latitude of any city be X and the Longitude be Z and that Blacksburg be represented by b, Bristol by t, Roanoke by k, and Charleston by n. Assume that by using

the following relation each weather index (W) radiation for a city can be related linearly to its longitude and latitude:

$$W = AX + BZ + C \tag{4-3}$$

where

A, B, and C = constants.

To obtain the three constants A, B, and C, three equations were formulated—one for each city—and simultaneously solved based on the available value for the solar radiation in Roanoke, Charleston, and Bristol. Solving the simultaneous equations yields the following:

$$A = R - BS \tag{4-4}$$

and

$$B = \frac{1}{V}[(W_t - W_k) - R(X_t\ X_k)] \tag{4-5}$$

and

$$C = W_n - AX_n - BZ_n \tag{4-6}$$

where

$$R = \frac{(W_k - W_n)}{(X_k - X_n)} \tag{4-7}$$

$$S = \frac{(Z_k - Z_n)}{(X_k - X_n)} \tag{4-8}$$

and

$$V = (Z_t - Z_k) - (S * (X_t - X_k) \tag{4-9}$$

Based on the available measurements for the three cities mentioned above, this approach was used to calculate the measured weather data for the location of Blacksburg. This procedure was repeated on an hourly basis for a period of 30 years (1961-1991). Samples

of the solar radiation data results are shown in Table 4-2. This sample shows part of the created Blacksburg data in January, 1964, Day 1.

Table 4-2. Samples of the Blacksburg Data for 1964

			Roanoke	**Bristol**	**Charleston**					**Blacksburg**
Month	day	hour	Global horizontal radiation	Global horizontal radiation	Global horizontal radiation					Global horizontal radiation
			W079	W082	W081	R	b	a	c	Sb
1	1	8	8	5	3	5.81	-1.61	-1.76	202.17	6.85
1	1	9	43	43	24	0.00	-2.38	-11.20	651.00	41.15
1	1	10	118	157	96	-75.48	10.00	-28.39	377.81	124.54
1	1	11	151	229	172	-150.97	28.14	-18.48	-1409.39	170.39
1	1	12	298	271	218	52.26	-18.84	-36.47	3165.53	284.22
1	1	13	336	286	210	96.77	-32.12	-54.48	4937.50	312.63
1	1	14	293	277	222	30.97	-14.12	-35.51	2747.24	282.54
1	1	15	227	263	156	-69.68	2.89	-56.08	2088.99	228.10
1	1	16	151	160	107	-17.42	-2.56	-29.49	1456.50	148.72
1	1	17	61	74	42	-25.16	1.87	-16.34	520.94	62.04
1	1	18	5	12	3	-13.55	2.04	-3.95	-10.73	6.36
1	1	19	0	0	0	0.00	0.00	0.00	0.00	0.00

The same procedure was repeated to create a TMY2 Blacksburg file, where the above equations were formulated into a spreadsheet and the weather data per hour for Blacksburg was calculated. A sample of the results is shown in Table 4-3. The analysis was performed for solar radiation data and then repeated for all other data within the TMY2 files. A copy of the resulting Blacksburg TMY2 file is shown in Appendix A.

After creating the TMY2 file for Blacksburg, we can estimate the reliability of this file by comparing it to actual measured weather data. To facilitate this task, a distribution function will be assumed and checked using the "Goodness of Fit" test, as shown in the next section.

4.4 GOODNESS OF FIT TEST

A Chi-Square "Goodness of Fitness" test was used to measure the equivalence of the sample data's probability density function to a normal distribution density function. This procedure tests a hypothesis of equivalence: it studies the sampling distribution using a statistic with an approximate chi-square distribution to measure the discrepancy between an observed probability density function and the theoretical probability density function (Bendat and Piersol, 2000).

Table 4-3. Samples of the Blacksburg TMY2 Created File – radiation data in W/m^2

			Roanoke	**Bristol**	**Charleston**					**Blacksburg**
Month	day	hour	Global horizontal radiation	Global horizontal radiation	Global horizontal radiation					Global horizontal radiation
			TMY2	TMY2	TMY2	R	b	a	c	TMY2
1	1	7	0.00	0.00	0.00	0.00	0.00	0.00	0.00	0.00
1	1	8	12.00	8.00	4.00	7.74	-0.50	5.38	-148.90	11.74
1	1	9	95.00	90.00	43.00	9.68	-5.88	-18.02	1237.88	90.59
1	1	10	168.00	254.00	119.00	-166.45	-16.90	-246.01	10699.44	152.16
1	1	11	330.00	383.00	165.00	-102.58	-27.28	-231.06	11134.00	307.13
1	1	12	483.00	496.00	233.00	-25.16	-32.91	-180.16	9837.98	457.02
1	1	13	526.00	527.00	148.00	-1.94	-47.43	-225.30	12726.28	489.12
1	1	14	439.00	500.00	210.00	-118.06	-36.29	-288.97	14124.82	408.87
1	1	15	367.00	409.00	184.00	-81.29	-28.16	-213.89	10600.52	343.80
1	1	16	242.00	267.00	113.00	-48.39	-19.27	-139.15	6975.67	226.24
1	1	17	81.00	102.00	46.00	-40.65	-7.01	-73.65	3389.75	74.89
1	1	18	9.00	13.00	4.00	-7.74	-1.13	-13.05	585.90	8.00
1	1	19	0.00	0.00	0.00	0.00	0.00	0.00	0.00	0.00

To perform such a test, it was assumed that the random weather data (x) has 30 (N) numbers of independent observations (one for each year of the 30 years) and a probability density function P(x). Let the N observations be grouped into K intervals, called *class intervals*, which together form a frequency histogram. Let the number of observations falling within the i^{th} class interval (the observed frequency in the i^{th} class), be denoted f_i. Let the number of observations that would be expected to fall within the i^{th} class interval (expected frequency), if the true probability density function of x was $p_o(x)$, (in our case a normal distribution function), (F_i), the discrepancy between the observed frequency and the expected frequency within each class interval be given by f_i-F_i. The observed

frequency for an hour in January is plotted against the expected frequency for the weather data in Figure 4-1.

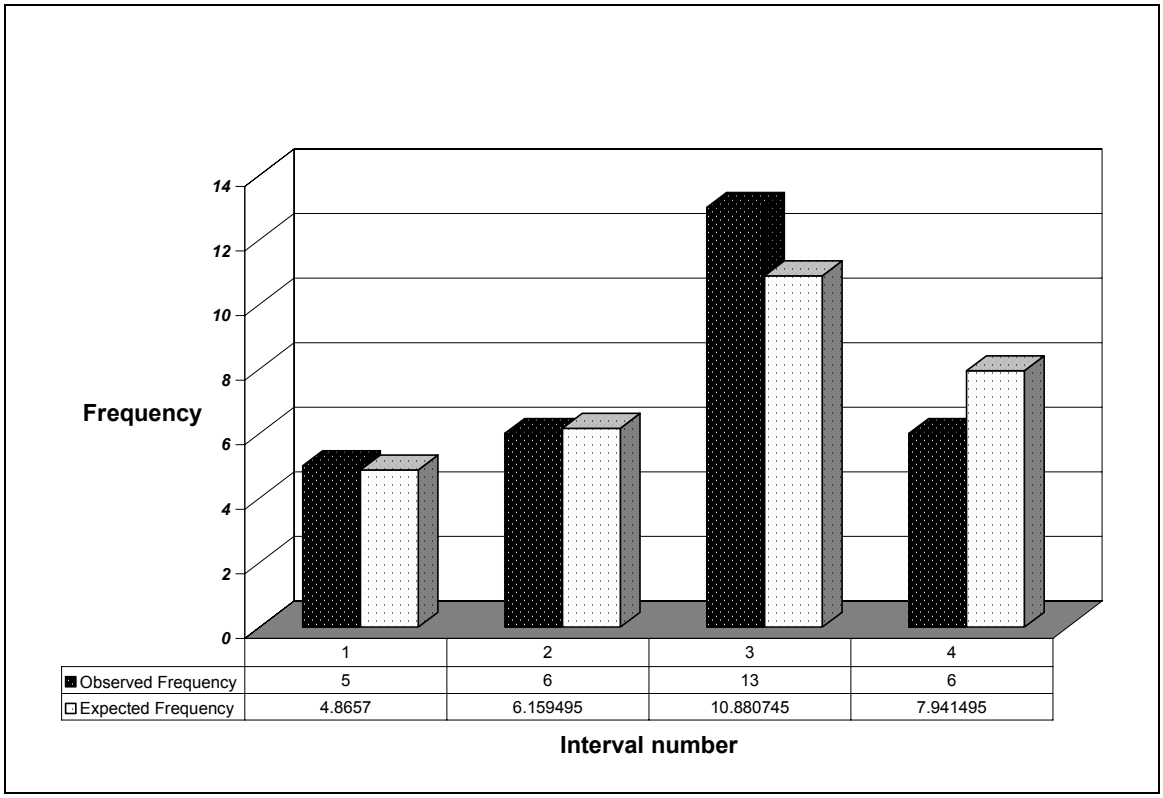

Figure 4-1. Observed versus Expected Frequency for an Hour in January

The total discrepancy for all class intervals (χ^2) is then measured by normalizing, then summing, the squares of the discrepancy in each interval by the associated expected frequency (Walpole and Myers 1985):

$$\chi^2 = \sum_{i=1}^{K} \frac{(f_i - F_i)^2}{F_i} \qquad (4\text{-}10)$$

If the observed frequency is close to the corresponding expected frequency, the χ^2 value will be small, indicating a good fit. The χ^2 is then compared against a critical value χ^2_α calculated based on statistical tables at a specific level of confidence α. For the purpose of this test, the level of confidence was chosen to be 95%. The number of degrees of

freedom in the case of a normal distribution is K-3 where K is the number of intervals (Bendat and Piersol 2000). The critical value χ_{α}^2 was found to be 7.16. The calculated χ^2 was found to be 0.895. Since $\chi^2 < \chi_{\alpha}^2$, then the weather data follows a normal distribution.

4.5 RELIABILITY OF TMY2 FILES

In general, *reliability* can be defined as the probability of an item or system to perform its required function adequately for a specified period of time under stated conditions. In that sense it can be expressed as the probability of that system's success (Harr 1987). The reliability of the specific weather input used in this study is defined as the probability that a value in the safe side of operation will occur for a specific period of time under defined operating conditions.

Since the data was proven to follow a normal distribution, the hourly average and standard deviation of the 30 years of data provided for Blacksburg were calculated. Then, the standardized z value of the data was calculated by:

$$z = (x - \mu_x)/\sigma_x \tag{4-11}$$

where

x = the value;

μ = the average; and

σ = the standard deviation.

To achieve the probability based on statistical tables, the z-value was used as an input. Then the reliability R(x) of the data was calculated as:

$$R(x) = 1 - P(x) \tag{4-12}$$

where

P(x) = the probability of failure.

4.6 RESULTS AND DISCUSSION

Results of the analysis showed that the TMY2 files have an inconsistent and low level of reliability. For example, the calculated reliability of the 12.00th hour of each day in the month of January is plotted in Figures 4-2 (a and b). These figures show that the reliability of January data fluctuates from 7% to 91%, while June's reliability fluctuates between 5% and 99%.

This analysis indicates that TMY2 files can be used only to describe the average performance of the system—not to size the system or indicate how it will perform under extreme weather conditions. To accomplish the latter tasks, three solutions were considered:

- Solution A - Modify the TMY2 file to provide high reliability (10th percentile).
- Solution B - Study the system's behavior based on random event occurrence.
- Solution C - Study the system's behavior under average conditions, high reliability conditions (5th percentile) and low reliability conditions (95th percentile).

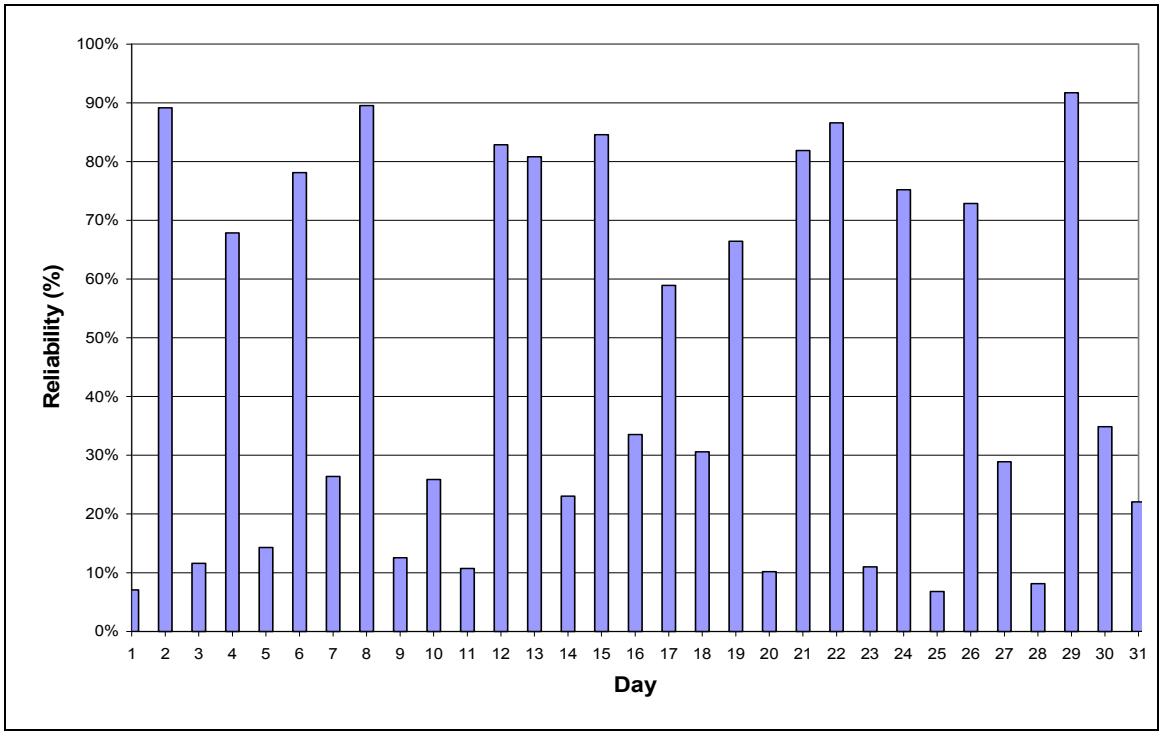

(a)

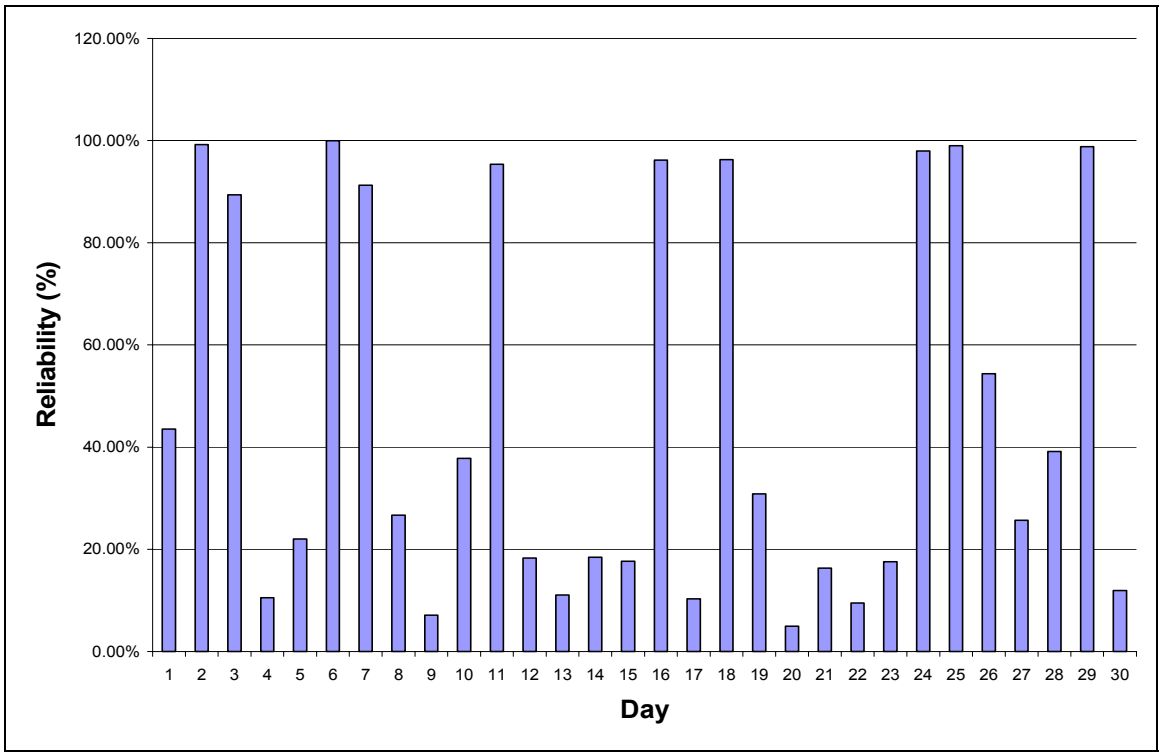

(b)

Figure 4-2. Reliability of the 12.00th Hour in (a) January and (b) June

4.6.1 Solution A

Solution A suggests that the TMY2 file can be modified to provide high reliability (10th percentile) by calculating the values of the solar radiation that corresponds to the desired reliability (90%). For example, to achieve a reliability of 90%, new solar radiation values were calculated for every hour. The solar radiation was calculated by satisfying the probability of failure as defined in Equation (4-12). The process then involved obtaining the corresponding Z-value (1.285) from statistical tables and calculating the new value (x) according to Equation (4-11). The new solar radiation data represent the minimum value that can occur 90% of the time every hour for 30 years. If that solution was considered, all indices included in the TMY2 file will be modified in the same manner to reflect a reliability of 90%. A major problem with this solution is that 90% of the time, the used value will be lower than the average solar radiation of the 30 years. Though this

ensures minimum system failures, the overall system will be over-designed 90% of the time.

4.6.2 Solution B

An alternative solution to this problem involves using the Monte Carlo Simulation method to generate random weather data and manage any uncertainties contained therein. This method represents a direct technique for propagating the uncertainties. In this case, the 30 years of hourly measured solar radiation data is represented by a probability density function (i.e., a normal distribution). The Monte Carlo process evaluates for a large number of trials (e.g., 1000) the occurrence probability of different solar radiation values. Each trial is obtained by a random sampling from the distribution. The procedure is repeated in each trial and the various solar radiation outcomes are sorted to obtain empirical estimates of desired top event attributes, such as mean median and the 95^{th} and 5^{th} percentiles. As the number of the trials increases, the precision of the estimate improves. This method possesses three main advantages:

- It is good for first order approximations.
- It is easy to implement.
- Its results are more realistic than those derived using analytical models.

On the other hand, this method presents two distinct disadvantages:

- It usually ignores time dependencies.
- It requires using a computer.

To create weather data for this research, Monte Carlo Simulation was implemented in a regular spreadsheet using an Excel add-in known as SIM.XLA, which was developed by Stanford University (Insight 1998). To apply Monte Carlo Simulation to the problem, three steps were followed:

- Calculation of the hourly median, maximum, and minimum solar radiation based on the available 30 years of hourly measured data. These values are referred to as low, most-likely, and high values.
- Using a random number generator (triangle distribution) and the low, most likely, and high values, the solar radiation was calculated for a given number of trials (e.g., 1000). After completion of the model, the simulation was conducted for the prescribed number of trials.

Results of this simulation for a given hour (8.00 am, 1st January) are shown in Figures 4-3 and 4-4, which use a histogram to depict the likelihood each solar interval (the number of intervals used is user-specified), as well as a cumulative distribution curve. As shown in this figure, it is more likely that a solar radiation of 10.06W/m^2 will occur. Its corresponding probability of occurrence is approximately 26%.

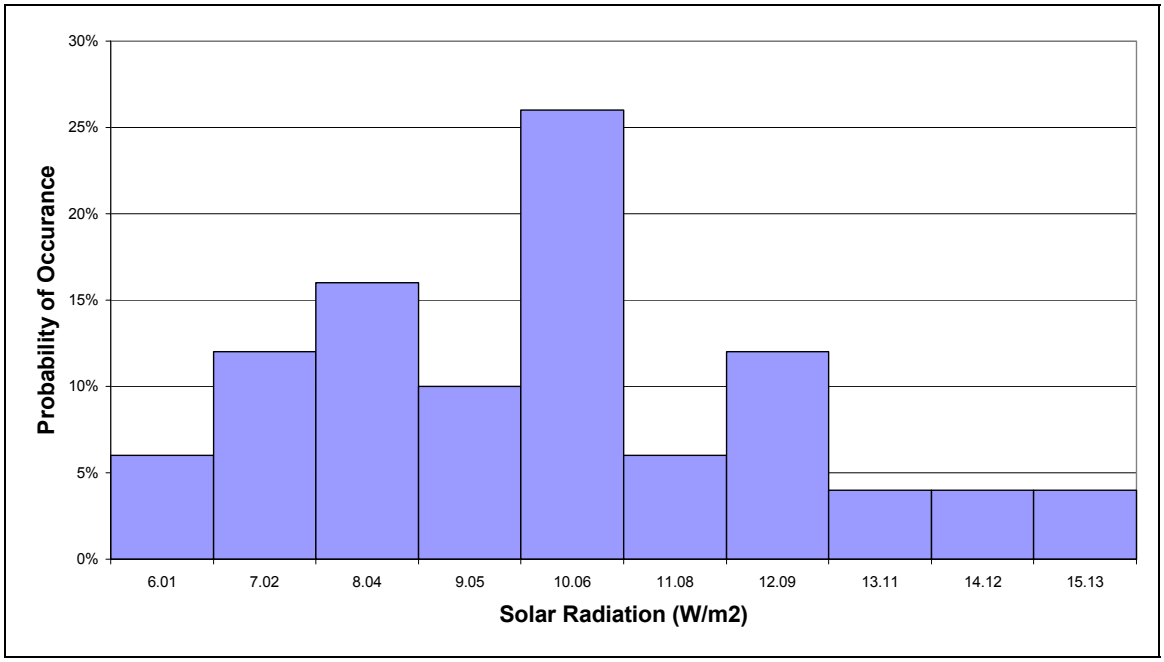

Figure 4-3. Likelihood of Occurrence of Each Solar Radiation Interval

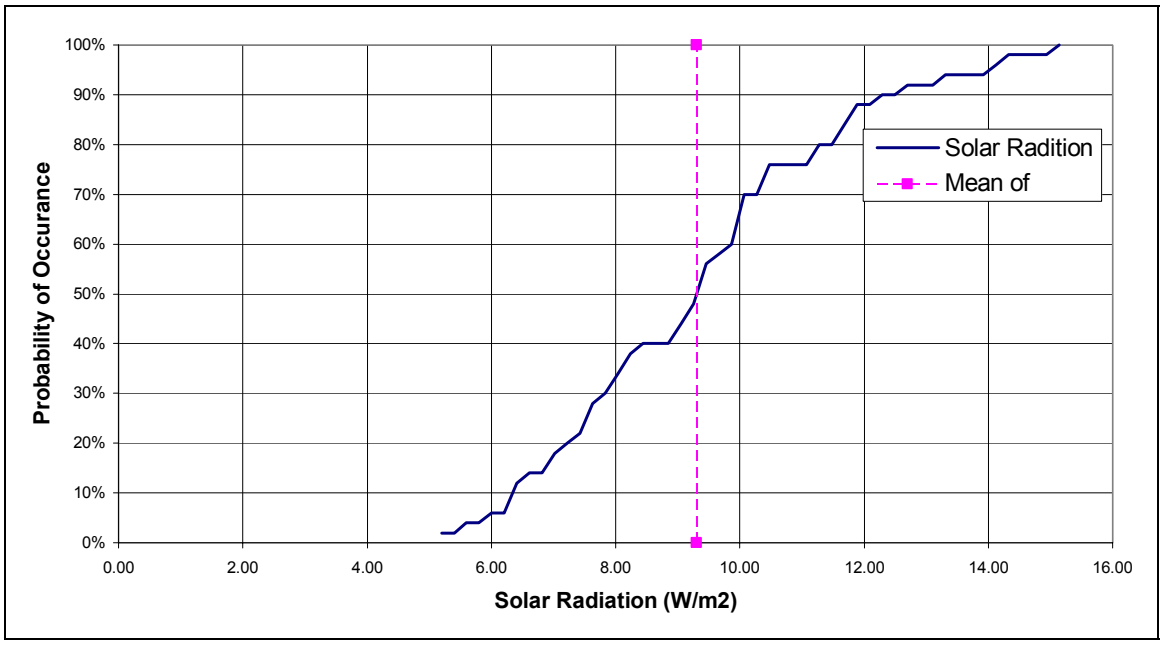

Figure 4-4. Cumulative Solar Radiation

It should be emphasized that selecting a low solar radiation value (for example 7 W/m^2) would result in estimating a low amount of generated energy. Hence, the solar panel generates a low amount of energy and therefore would be on the conservative side with respect to the benefit it provides. However, if a higher value of solar radiation occurs, more energy would have been available, therefore reducing the need for other non-renewable energy sources. On the other hand, if a high solar radiation was selected from the simulation (for example 13 W/m^2), the predicted energy saving would be considerably higher than what may actually occur. It is therefore reasonable to select a value that reflects a high percentage of occurrences. This value, which mainly depends on the amount of risk the decision maker is willing to take, should reflect an acceptable level of reliability.

Although Monte Carlo Simulation reflects an acceptable level of reliability, for the purpose of this research, it still does not evaluate the system's behavior under extreme climatic conditions. Therefore, using the cumulative solar radiation curve shown in Figure 4-4, it was suggested that one more trial based on random number generation should be conducted and the outcome of that trial should be used as input in the simulation. In that way, the system's behavior under any condition could be evaluated.

Unfortunately in order to fully utilize the method described above, we must control the bias between consecutive hourly values; otherwise the daily outcome will be similar to that shown in Figure 4-5 (Monte Carlo outcome 1000 trials or 1 trial). In case of the 1000 trials, a curve very close to that represented by the mean is obtained. This does not describe the system's response to extreme weather conditions. On the other hand, in the case of one trial, with no restriction on the bias, the simulation is allowed to take any values between the minimum and maximum, which results in a curve that does not resemble the daily variation curve, as shown in Figure 4-5.

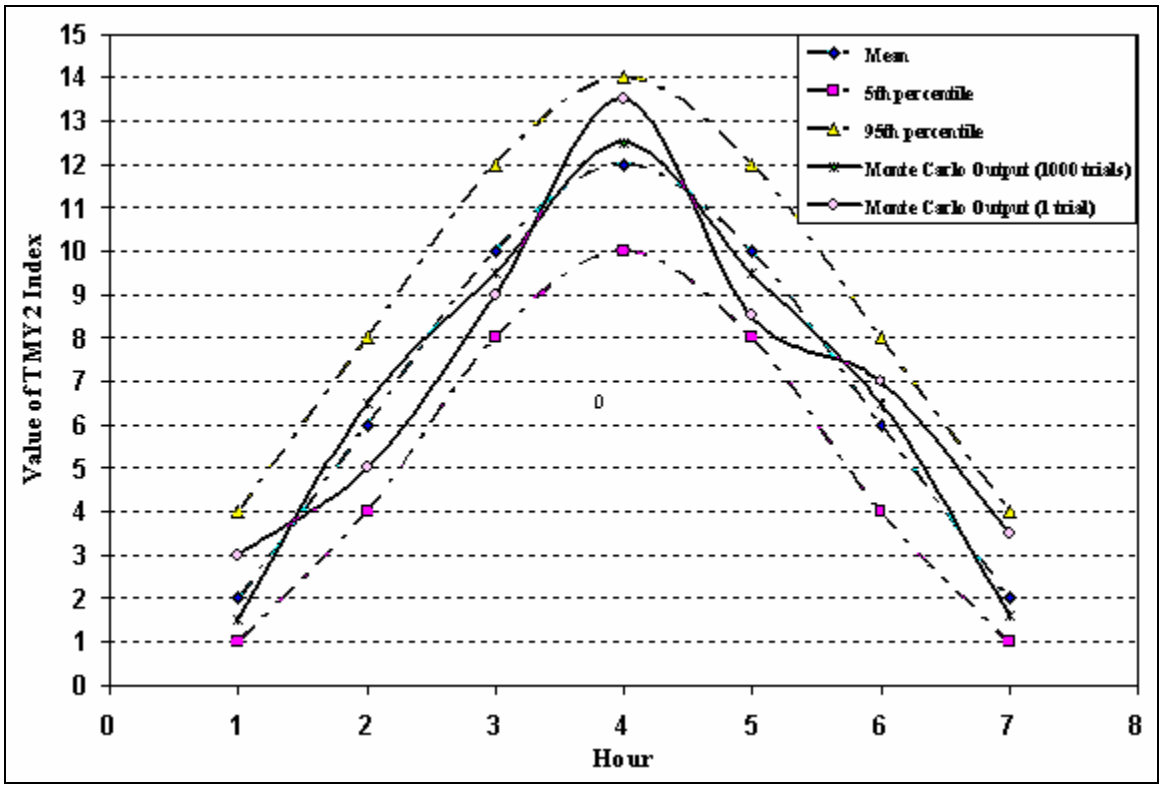

Figure 4-5. Problem with Monte Carlo Analysis

As a result, this research focused on finding a method for controlling the bias within consecutive runs. Members from Virginia Tech's Statistical Analysis Department were consulted for advice on the best method for controlling bias. Unfortunately, it was concluded that there is no proven reliable statistical method to control bias and relate the current outcome (the solar radiation of the second hour in the day) to its previous outcome (the solar radiation of the first hour in the day) with respect to weather data.

The team worked on a solution that would allow for (1) sizing of the system and (2) studying the system's behavior under average, as well as extreme weather conditions. The statistical team suggested Solution C, which is described in the next section and was eventually adopted for use in this research.

4.6.3 Solution C

This solution is divided into two segments. The first segment involves system sizing, while the second involves studying the system's behavior under normal conditions. For the purpose of system sizing, it was decided not to rely on the TMY2 files but to use two design days, a summer design day and a winter design day, that have weather data corresponding to a system reliability of 95%. These design days are used as input in Energy Plus, which calculates the required equipment and design parameter size required to maintain comfort level conditions in the space (see Chapter 5).

In order to study the system's behavior under different weather conditions, three steps were undertaken. First, to study the average performance of the system, the simulation was conducted using TMY2 data. Then the simulation was conducted using 95^{th} percentile values of the TMY2 files. Finally, in order to study the system's behavior under extreme weather conditions, it was conducted using the 5^{th} percentile values of the TMY2 files. The 5%, 95%, and TMY2 values for dry bulb temperature in January are plotted in Figure 4-6 as an example of the weather data that will be used during the analysis.

Due to time constraints, to study the average performance of the system using TMY2 weather data, it was decided to analyze two consecutive days in three of the winter months (December, January, and February), and two consecutive days in three summer months (June, July, August). Afterwards, to study the system under extreme conditions, two consecutive days will be considered in the month of January and the month of July using 5^{th} percentile weather data and 95^{th} percentile weather data. A schedule of the proposed runs is shown in Table 4-4.

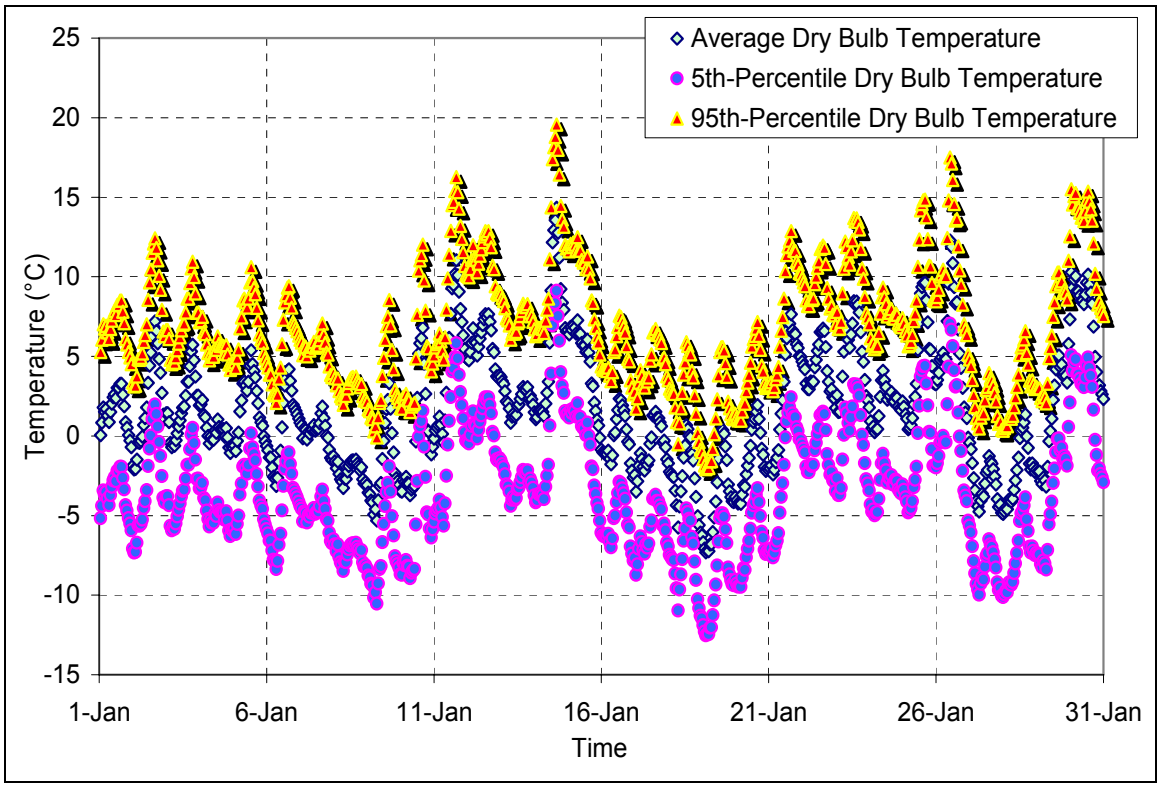

Figure 4-6. Dry Bulb Hourly Temperature Variation during January

Table 4-4. Proposed Run Schedule

Month	No. of Days	Cases for every hour	Equivalent run time (minutes)
December	2 days (48 hours)	TMY2	960
January	2 days (48 hours)	5%, TMY2, 95%	960
February	2 days (48 hours)	TMY2	960
March	0	-	0
April	0	-	0
May	0	-	0
June	2 days (48 hours)	TMY2	960
July	2 days (48 hours)	5%, TMY2, 95%	960
August	2 days (48 hours)	TMY2	960
September	0	-	0
October	0	-	0
November	0	-	0
Sum of run time			6.7 days

5 STAGE II - ENERGY COLLECTION MODEL – FINITE ELEMENT AND STATISTICAL ANALYSIS

5.1 INTRODUCTION

This chapter describes the developed model utilized to evaluate the energy collection in the Blacksburg, Virginia case study. This model demonstrates the solar supply evaluation stage (Stage II) of the design evaluation framework as shown in the highlighted area in Figure 5-1. Three-dimensional (3D) models were developed using the Finite Element Method (FEM) to simulate the proposed solar collector presented in the preliminary design (Stage I of the framework). The weather data presented in Chapter 4 were used as input parameters in the developed model. Moreover, this chapter also describes the design equations that were developed using statistical analysis based on the finite element model input and output.

5.2 BACKGROUND - PERFORMANCE EVALUATION

There are two main methods for evaluating the performance of low-cost solar collection systems: *analytical* and *numerical*, both of which are described in detail in the literature review. The second method holds distinct advantages over the first. For example, the formulations derived from the analytical method are accurate only under steady-state and one-cover transient conditions. In the case of two or more covers, the accuracy of the analytical method is reduced to around 15% (Duffie & Beckman 1980). Since numerical methods are much more stable and accurate under any transient condition, they were selected for evaluating the performance of the solar collector designed for this project.

There are two numerical methods that can be used to evaluate the solar collector's efficiency, the Finite Difference Method (FDM) and the Finite Element Method (FEM). Both methods are used whenever there are geometrical complexities or when multidimensional analysis is required. Also, they can be used for both transient and steady-state conditions, and they simplify the complexity of the analysis by coupling together the three modes of heat transfer. In general, however, FE methods are

considered more accurate than FD methods (Arpaci 1966). Therefore, Finite element analysis was used to quantify the benefits of the solar collector.

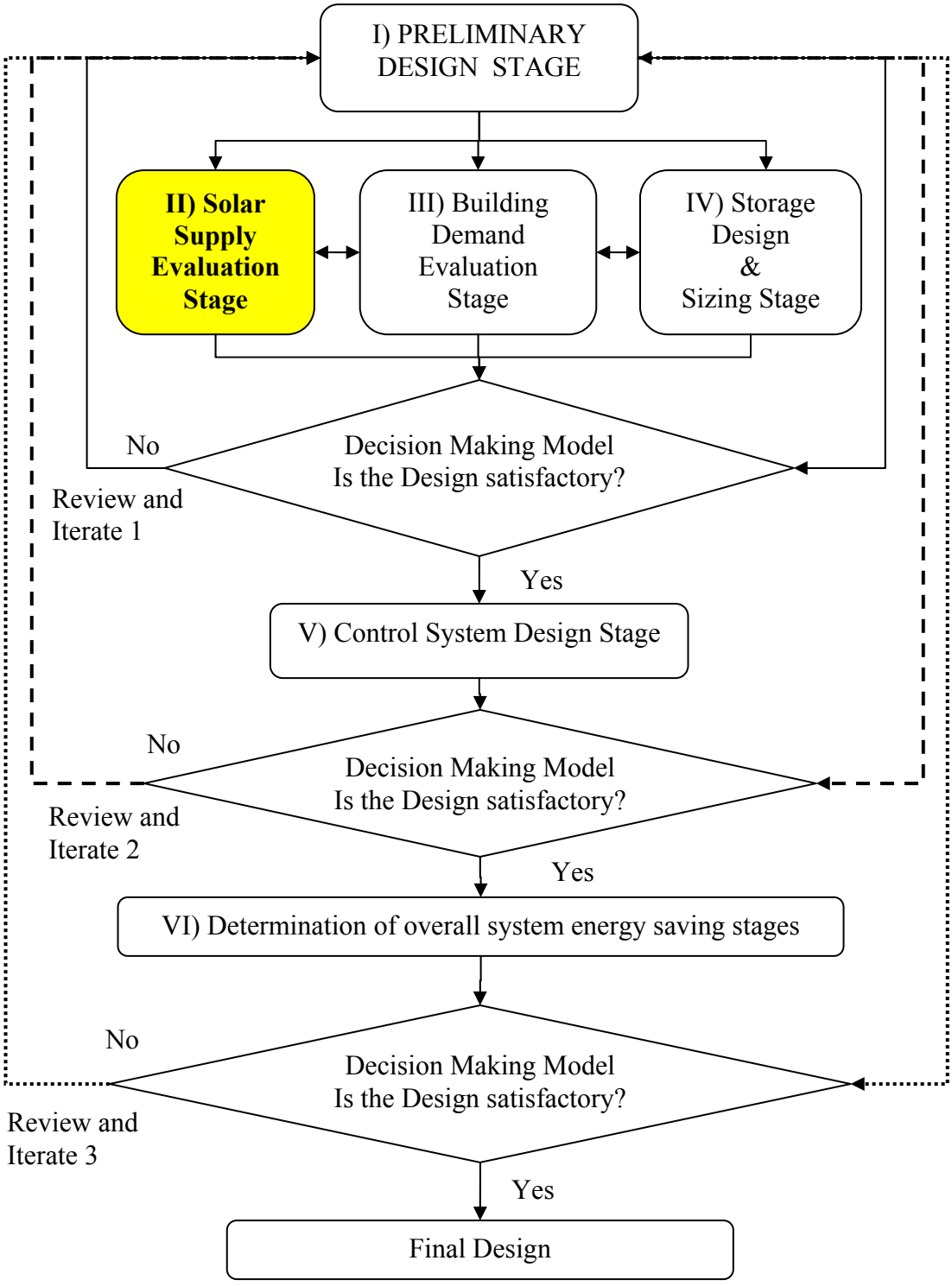

Figure 5-1. Stage II of the design evaluation framework

5.3 ENERGY COLLECTION MODEL

This section presents specifics of the energy collection model, including finite element formulations and model dimension and geometry, among other topics.

5.3.1 Finite Element Formulation

To predict the integrated solar collector's thermal performance, ABAQUS software Version 6.3 was used to develop finite element models of the solar roof panels (ABAQUS 2001). The developed FE code simulates the solar panels, as shown in Figure 5-2, with a typical length and width for an inclined two or three-story building roof. The roof's inclination is an input parameter, which in this case is modeled at 37^{o} to maximize solar gain for the considered location of Blacksburg, Virginia.

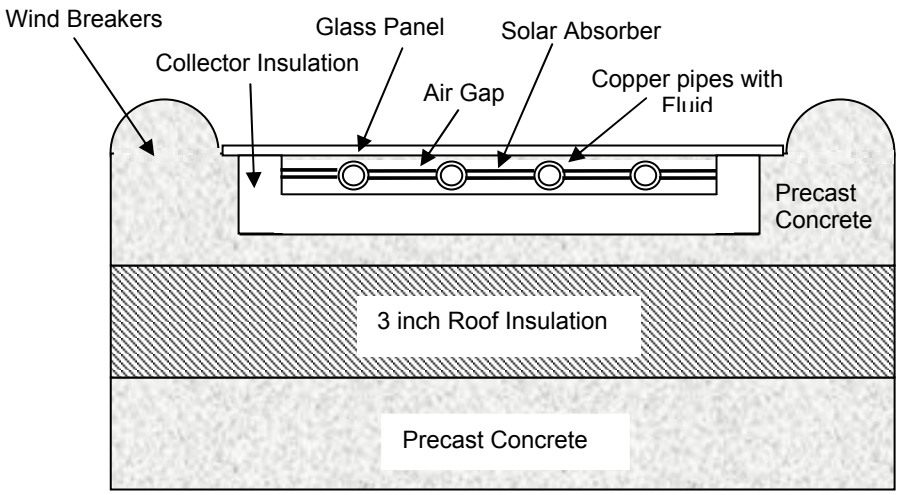

Figure 5-2. Solar Panel Cross Section for Integrated Solar Collector

To investigate the solar panel's effectiveness, for the design shown in Figure 5-2, 3D models were formulated. All material properties are listed in Table 5-1. In the developed models, coupled conduction, forced convection, and long wave thermal radiation modes of heat transfer were considered. The models were designed to fit any set of weather and

operational conditions, as well as differing times and locations. To simulate real field conditions, the models possess multidimensional and time dependent properties.

5.3.1.1 Model Dimension and Geometry

The dimensions of the modeled portion are 3500mm x 1500mm (138.0 inch x 59.0 inch). These dimensions were selected to keep the element size within acceptable limits (modeling constraints) but reduce potential edge effect errors. It is assumed that—in order to increase the amount of energy collected until the building's energy requirements are satisfied—the modeled parts will be repeated along the width [35m (115ft)] of the roof.

Table 5-1. Material Properties Used in the Models

(Adopted from Bejan 1995; Kakac and Yener 1993)

Material Name	Thermal Conductivity (W/m.K)	Density (Kg/m^3)	Specific Heat (J/Kg.K)	Emissivity
Glass	0.81	2800	800	0.94
Air	0.025	1.247	1006	N/A
Insulation	0.035	240	1.50	N/A
Copper	398	8954	383	1.0 (black coat)
Concrete	0.81	2200	880	N/A
Polyurethane	0.32	1200	2090	N/A
Rubber	0.2	1100	1670	N/A
Water	0.58	999.7	4192	N/A

Figure 5-3 shows the general layout of the developed model for the proposed integrated design. The generated mesh distribution was designed to give optimal accuracy; small elements (2.4mm) were used in the glass, pipe, air, and fluid, while larger elements (5mm) were used for the backing layers. The roof panel geometry dictated the element types and dimensions. Cubical 8-node brick continuum elements (DC3D8) were selected

for all layers, except for the fluid layer, where forced-convection diffusive elements (DCC3D8D-brick) were used to simulate the forced convection with dispersion control that would there take place. To preserve the continuity of nodes between consecutive layers, all layers were simulated with the same shape. In total, 38318 elements were needed to simulate this problem.

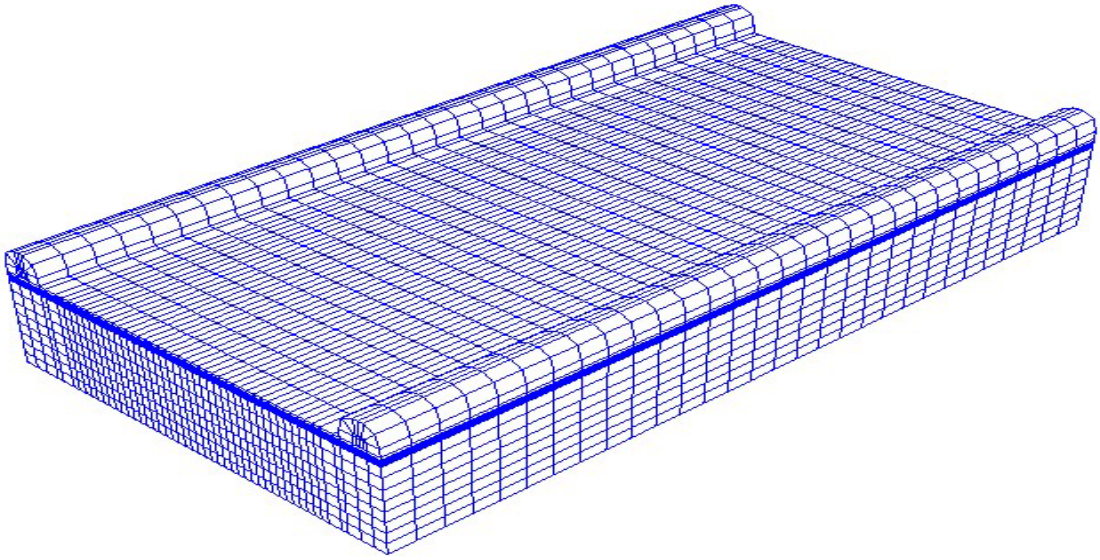

(a)

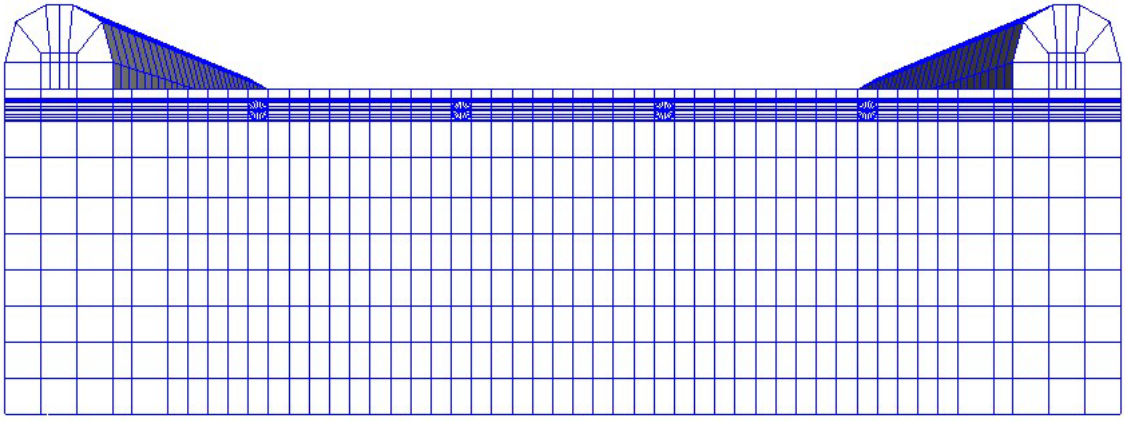

(b)

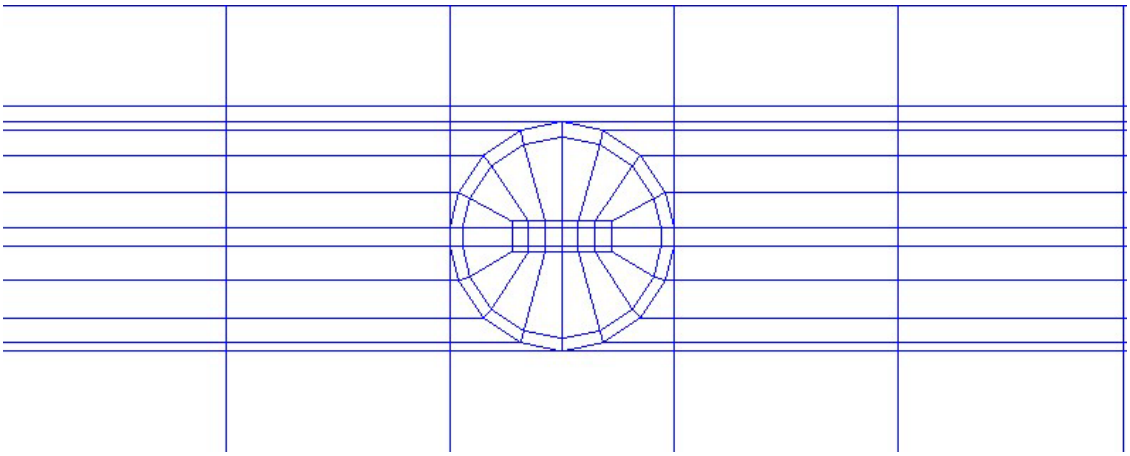

(c)

Figure 5-3. Shape of the Mesh used for Finite element analysis of the design shown in Figure 5-1. a) 3D view; b) Complete Model Meshing; c) Cross section through the Fluid and Pipe

5.3.1.2 Model Constraints

The heat transfer mechanisms taking place within the system include:

- Conductive, convective, and radiative heat exchange between the environment and the glass panels.
- Conductive and radiative heat transfer within the glass panel.
- Radiative heat transfer between the glass panel, the air gap, and the copper pipe walls.
- Convective heat transfer between the air gap and the adjacent walls.
- Absorption of solar radiation by the pipe walls.
- Forced convective heat transfer within the fluid.
- Conduction heat transfer through the opaque layers of the panel.
- Conductive and convective heat transfer between the 75 mm (3.0 inch) concrete layer and the inside space.

The main thermal models governing these mechanisms are shown in Figure 5-4. From weather data in TMY2 files (see Chapter 4), the user defines solar intensity, as well as inside and outside temperatures. A convection boundary condition and a solar radiant flux govern the heat exchange taking place between the environment and the glass surface. The convection coefficient (h_c) is defined as (Duffie and Beckman 1980):

$$h_c = \max\left[5, \frac{8.6\,V^{0.6}}{L^{0.4}}\right] \qquad (5\text{-}1)$$

where

v = the wind speed in m/s, and

L = the cube root of the house's volume.

According to its angle of incidence, the radiative flux is reduced as it passes through the glass. The level of reduction is estimated using a FORTRAN subroutine that calculates the absorption, reflection, and transmittance according to the properties of the glass. This subroutine is presented in Appendix C.

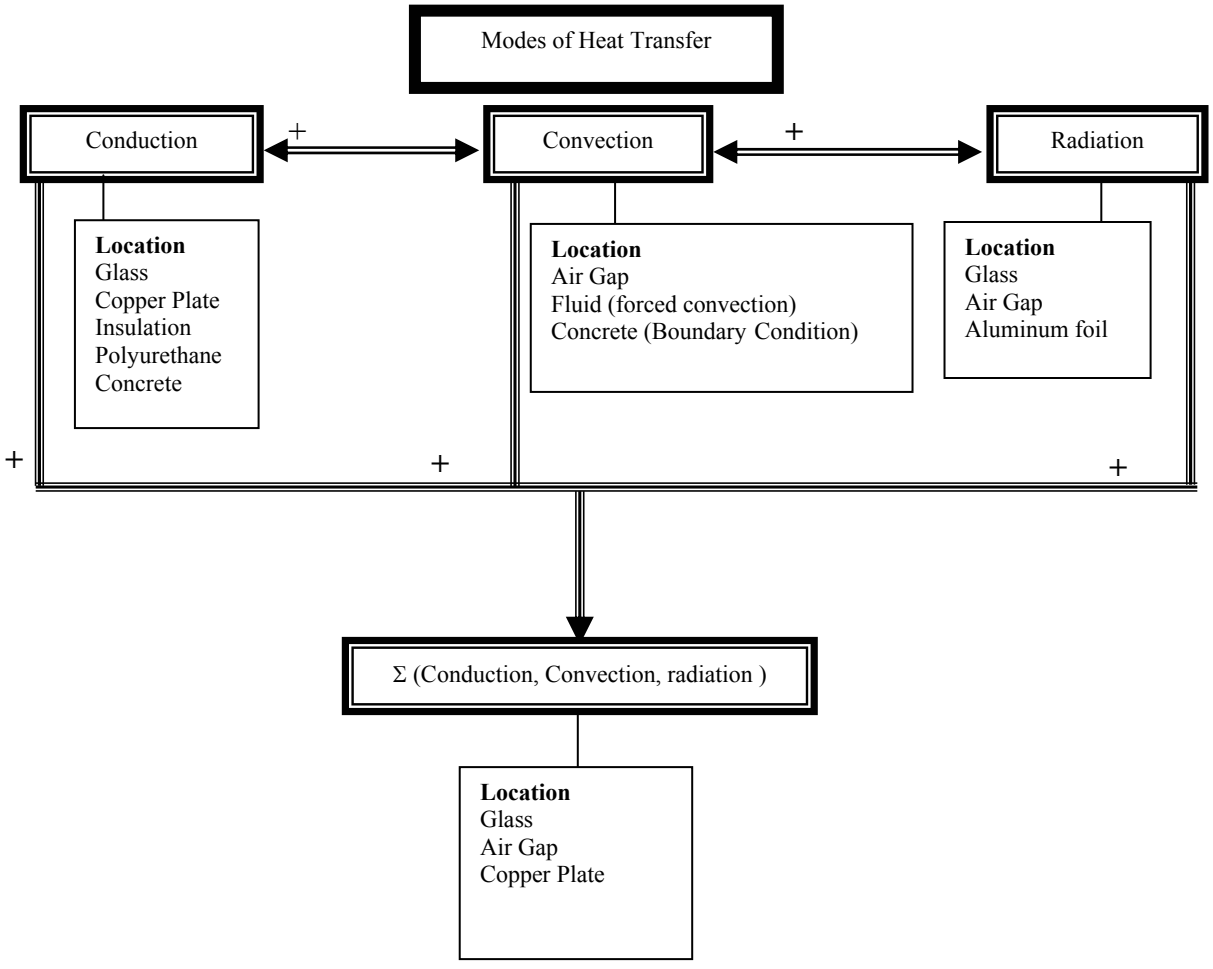

Figure 5-4. Modes of Heat Transfer Present in the Panel

5.3.2 Heat Gain Calculations

The resulting outlet fluid temperature ($T_{f,o}$) is converted to heat gain using:

$$Q = \dot{m} C_p \Delta\theta \tag{5-2}$$

where

$\dot{m}$ = fluid mass flow rate (Kg/hr);

C_p = fluid specific heat (KJ/Kg.K), and

$\Delta\theta$ = change in fluid temperature between the inlet and the outlet (K).

The resulting hourly heat gain (Q) is compared with the heat energy needed to satisfy the building's heating and hot water requirements. Q is also converted to heat gain per unit of collector area (q) by dividing it by the modeled collection area. The resulting figure determines the collection area needed to fully satisfy the building's needs, given adequate available roof area.

5.3.3 Model Verification

The solar collector model was verified by simulating a steady-state case and comparing its results to the analytical solution developed by Duffie and Beckman, which was summarized in Chapter 2. Based on this analytical solution, an Excel spreadsheet was developed to calculate the fluid exit temperature. The first step formulated in the spreadsheet involved calculating the loss coefficients—top, bottom, and edge—for the considered collector, according to the following equations (Duffie and Beckman 1980):

$$U_t = \left(\frac{N}{\frac{C}{T_{p.m}} \left[\frac{T_{p,m} - T_a}{N + f} \right]^e} + \frac{1}{h_w} \right) + \frac{\sigma \left(T_{p,m} + T_a \right) \left(T_{p,m}^2 + T_a^2 \right)}{\left(\varepsilon_p + 0.00591 N h_w \right)^{-1} + \frac{2N + f - 1 + 0.133\varepsilon_p}{\varepsilon_g} - N} \tag{5-3}$$

where

N = number of glass covers;

$f = (1+0.089h_w - 0.1166h_w \varepsilon_p)(1+0.07866N)$;

$C = 520(1-0.000051\beta^2)$ $\beta$is the collector tilt $=37^o$ in this simulation;

$T_{p,m}$ = mean plate temperature (K);

T_a = ambient temperature (K);

$e = 0.43(1-100/T_{p,m})$;

ε_g = emittance of glass;

ε_p = emittance of plate, and

$h_w = h_c$ = wind heat transfer coefficient (W/m^2C).

$$U_b = \frac{1}{R_4} = \frac{k}{L} \tag{5-4}$$

where

k = backing material's thermal conductivity (W/m^2C), and;

L = backing material layer thickness (m).

$$U_e = \frac{(UA)_{edge}}{A_c} \tag{5-5}$$

where

Ac = backing collector area (m^2);

U = K/L, L is the edge insulation thickness (m), and;

A = insulation perimeter (m) x collector thickness (m).

The collector overall loss coefficient U_L equals the sum of these three loss coefficients and is equal to 4.86 W/m^2C for T_{pm} of 28^oC and a T_a of 7^oC. The second step is to calculate the Fin efficiency (F) of the collector (Duffie and Beckman 1980):

$$F = \frac{\tanh\left[m(W-D)/2\right]}{m(W-D)/2} \tag{5-6}$$

where

W = pipe spacing (m);

D = pipe Diameter (m), and

$$m = \frac{U_L}{T_p * K_p} \tag{5-7}$$

where

T_p = Plate thickness (m);

K_p = Plate conductivity (W/m C), and

U_L = Collector overall loss coefficient.

The Fin efficiency (F) of the considered collector—0.982—was in turn used to calculate the collector efficiency factor (F′) which represents the ratio of actual useful energy gain to the useful energy gain that would result if the collector's absorbing surface had been at the local fluid temperature (Duffie and Beckman 1980).

$$F' = \frac{\frac{1}{U_L}}{W\left[\frac{1}{U_L\left[D+(W-D)F\right]} + \frac{1}{C_B} + \frac{1}{\pi D_i h_{f,i}}\right]} \tag{5-8}$$

where

W = Pipe spacing (m);

D = Pipe Diameter (m);

D_i = Inside Pipe Diameter (m);

F = Fin efficiency;

$h_{f,i}$ = Fluid heat transfer coefficient inside the pipe ($W/m^{2o}C$) and is calculated from the Reynolds number, the Prandtl number, the Nusselt number, the mass flow rate, the thermal conductivity, and the diameter and length of the pipe; and

C_B = bond conductance.

In this simulation, the bond conductance CB was assumed to be in "full bonding" condition. Thus, the collector efficiency factor (F′) was found to be 0.924. The third step involved calculating the absorbed solar energy (S) from the incident radiation in both cases: where the radiation incidence angle was perpendicular to the collector surface, as

well as where it was inclined. The results of this step were used to verify the FORTRAN subroutine used to calculate the amount of radiation passing through the glass. The fourth step involved calculating the fluid outlet temperature ($T_{f,o}$) according to Equation 5-9 (Duffie and Beckman 1980):

$$T_{f,o} = \left\{ \left[e^{-\left(\frac{A_c U_L F'}{\dot{m} C_p} \right)} \right] \bullet \left[T_{f,i} - T_a - \frac{S}{U_L} \right] \right\} + \frac{S}{U_L} + T_a \qquad (5\text{-}9)$$

where

$\dot{m}$ = fluid mass flow rate (Kg/s);

F' = collector efficiency factor;

S = absorbed solar energy (W/m^2);

$T_{f,i}$ = inlet Fluid Temperature (C);

T_a = ambient Temperature(C), and

C_p = specific Heat (J/KgK).

The fifth step consisted of calculating the resulting amount of useful energy and mean plate temperature:

$$Q_u = A_c \left[S - U_L \left(T_{p,m} - T_a \right) \right] \qquad (5\text{-}10)$$

and

$$T_{p,m} = T_{f,i} + \frac{Q_u / A_c}{U_L F_R} (1 - F_R) \qquad (5\text{-}11)$$

where

$$F_R = \frac{\dot{m} C_p (T_{f,o} - T_{f,i})}{A_c \left[S - U_L \left(T_{f,i} - T_a \right) \right]} \qquad (5\text{-}12)$$

The procedure is iterated until the mean plate temperature ($T_{p,m}$) converges. Using the finite element model and the analytical solution, a number of trials were executed involving varied rates of solar radiation and mass flow. The results of both models are compared in Figures 5-5, 5-6, 5-7, and 5-8. The calculated error was found to be less than 5% in all cases.

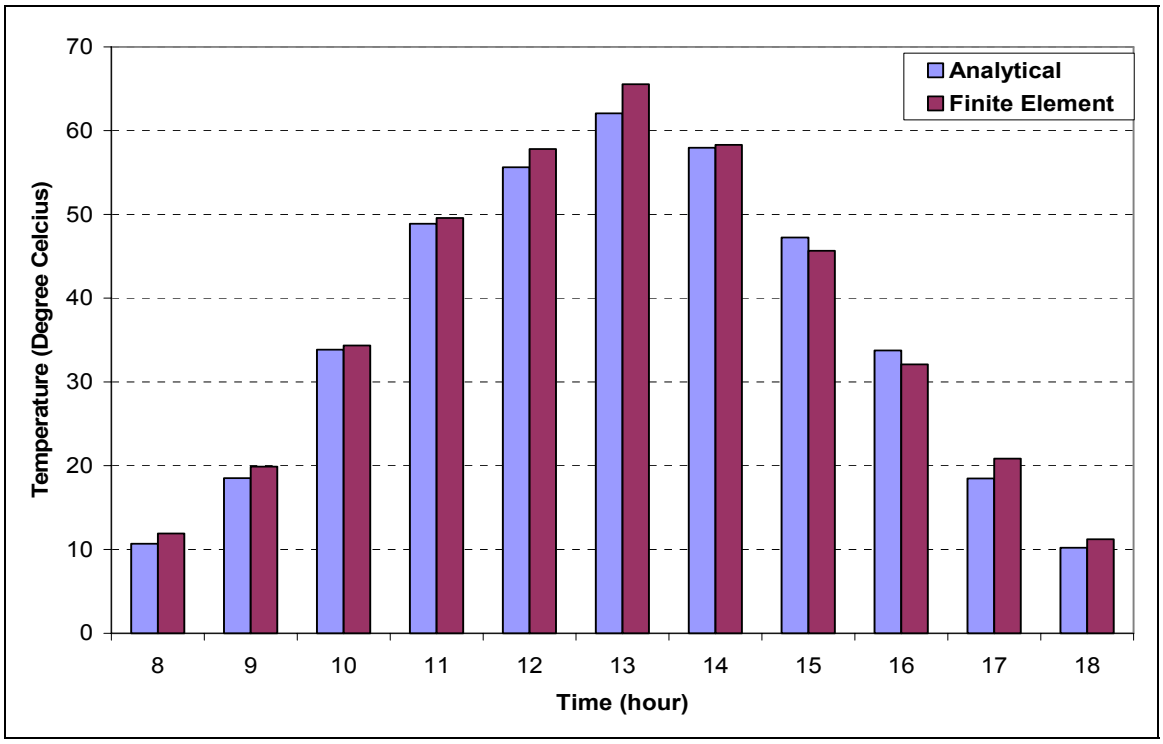

Figure 5-5. Analytical versus Finite element Solution for a Day in January at a Mass Flow Rate of 0.0005 m^3/hr

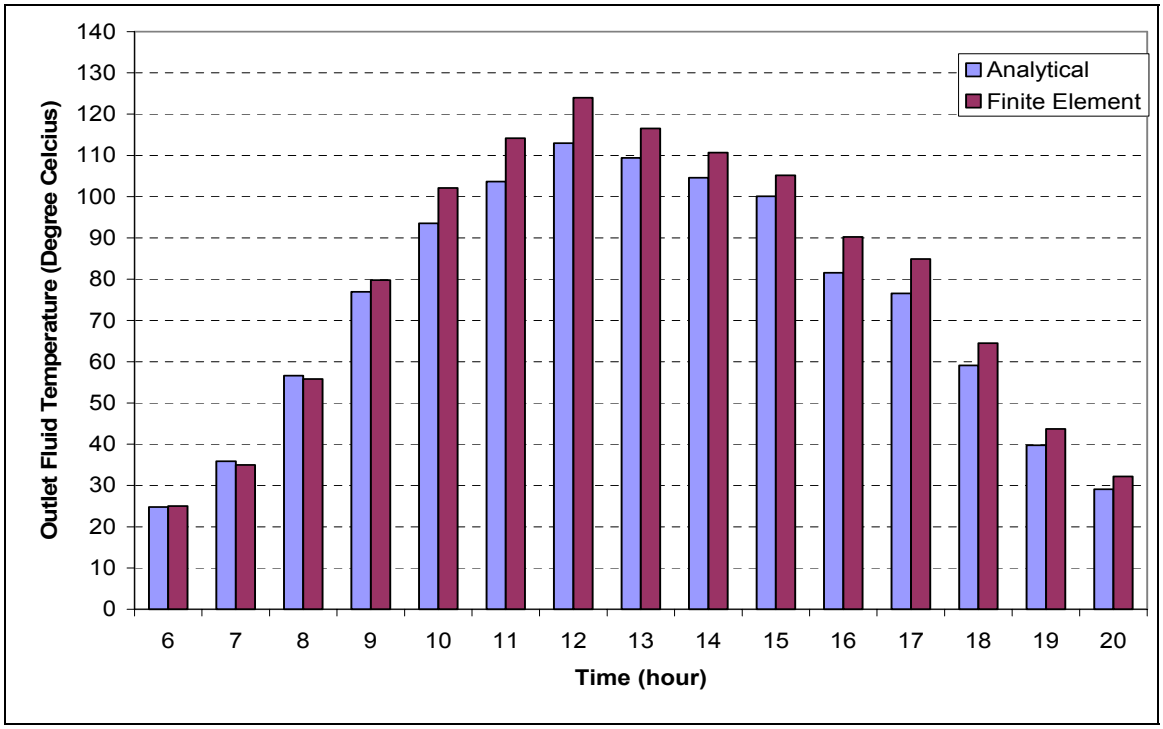

Figure 5-6. Analytical versus Finite element solution for a Day in July at a Mass Flow Rate of 0.0005 m^3/hr

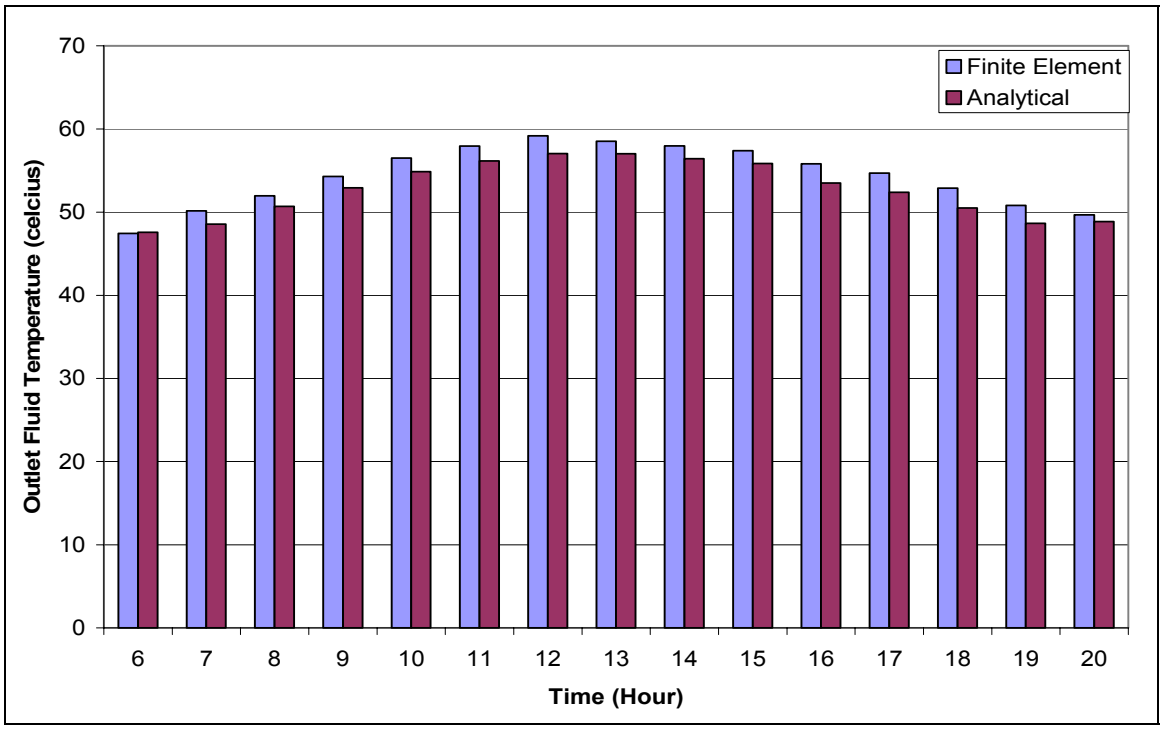

Figure 5-7. Analytical versus Finite Element Solution for a Day in July at a Mass Flow Rate of 0.01 m^3/hr

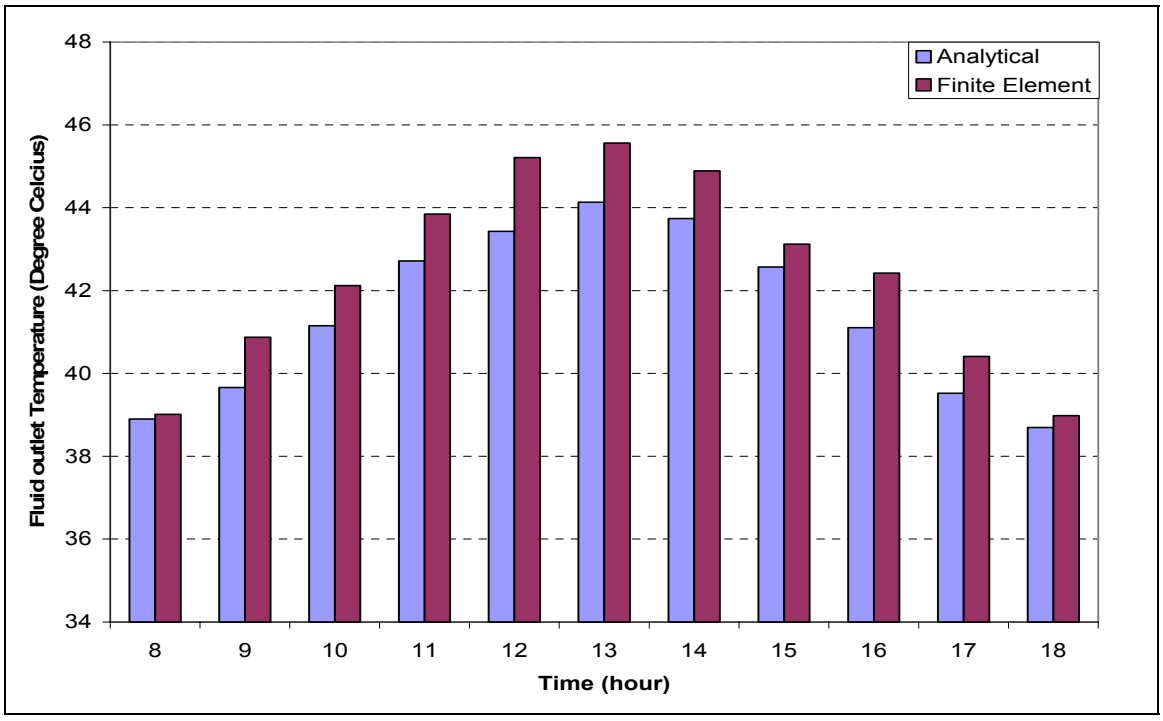

Figure 5-8. Analytical versus Finite Element Solution for a Day in January at a Mass Flow Rate of 0.01 m^3/hr

5.3.4 Variation of Design, Environmental, and Operational Variables

After the developed models were verified, the effects of the different collection controlling parameters on overall heat gain were investigated. These parameters can be classified according to three sets:

1) Environmental parameters:

- Solar radiation;
- Wind speed expressed in terms of convection coefficient (h_c), and
- Ambient temperature.

2) Operational parameters:

- The fluid mass flow rate, and
- Inlet fluid temperature.

3) Design parameters:

- Collection area;
- Pipe diameter; and
- Pipe spacing.

Within the environmental parameter set, the variables were varied simultaneously according to data available from the TMY2 files and the 95% and 5% developed weather files. As for the operational parameters, the inlet fluid temperature was varied based on the developed control strategy and according to the output of the Energy Plus simulator by varying each of these parameters one at a time, while keeping other variables constant, three critical levels of fluid mass flow were identified to maximize overall energy gain. The three levels of mass flow rate were 0.1, 0.25, and 0.0005m^3/hr. Although the third mass flow rate maximizes the outlet fluid temperature ($T_{f,o}$), it does not maximize the overall heat gain calculated by Equation (5-2), since the effect of the mass flow rate is more significant when compared to the increase in temperature.

The design parameters proved to be the most challenging because more models were needed to compare the changes in geometry. Therefore, three models were developed for each of the considered pipe diameters and pipe spacings. Three pipe diameters were simulated: 25.4mm, 12.7mm, and 6.35mm. Similarly, three pipe spacings

were considered: 138mm, 65mm, and 190mm. The first dimension is based on the available market size for flat plate solar collection fins, while the other two levels were calculated by increasing the original size 1.5 times and reducing it by half. The collection area was varied based on comparing the hourly amounts of energy collected versus those needed.

5.4 STATISTICAL ANALYSIS

As previously proposed in the design evaluation framework, the complexity and length of the analysis may hinder the designer's ability to iteratively evaluate the effectiveness of the preliminary solar active system. Therefore, the design evaluation framework recommended the incorporation of a simple regression model that could be used in a routine design to facilitate the iterative process. For demonstration purpose, a predictive model was developed for the flat plate collector design used in this study. This model may be used to predict the outlet fluid temperature under different environmental, operational, and design parameters. These parameters were the fluid mass flow rate, the inlet fluid temperature, the solar radiation, the convection coefficient, the ambient temperature, and the pipe diameter and spacing.

To develop this regression model, the relation between each controlling variable and the outlet fluid temperature was identified by varying each parameter at a time while keeping the rest of the parameters constant. For example, to identify the effect of solar radiation on the fluid temperature increase, solar radiation was varied while the rest of the parameters were kept constant, and the temperature was calculated and plotted as points. Afterwards, curve fitting was used to determine how the relation between the independent and dependent variables may be described (linearly, logarithmically, etc.). This relationship is used as an input in the regression analysis to identify the combined effect of all the controlling variables on the outlet fluid temperature.

5.4.1 Correlation and Trends

The objective of this section is to identify the relationship between each controlling variable and the outlet fluid temperature in order to use it in the regression analysis. This

was first accomplished through identifying the existing trend between each independent variable (i.e., mass flow rate, inlet fluid temperature, solar radiation, incident angle, convection coefficient, ambient temperature, and pipe diameter) and the dependent variable (outlet fluid temperature). This necessitated varying each factor while keeping all other variables constant. It is worth noting that the objectives of identifying the trend between independent and dependent variables consist of two parts:

- Define positive and negative correlations between the dependent and independent variables. This was accomplished to check the adequacy of the model in reacting to the change in each variable. For example, it is well known that the greater the solar radiation, the greater the expected increase in fluid temperature. Therefore, in this case, a positive correlation was expected.
- Identify possible trends between the dependent and independent variables. This was limited to trends found helpful in improving the developed model.

Figure 5-9 illustrates the relation between the solar radiation and the fluid outlet temperature. As shown in this figure, as the solar radiation increases, the fluid outlet temperature also increases. An exponentional relationship seems to exist among these variables.

Similarly, Figure 5-10 illustrates how the fluid outlet temperature varies with the ambient temperature. In this case, as the ambient temperature increases, the outlet fluid temperature also increases. An exponentional relationship may be used to describe the variation of the outlet fluid temperature with the ambient temperature.

As previously mentioned, this analysis indicates only the trend between the dependent and the independent variables. The specific use of the equations presented on the trendlines shown in Figures 5-9, 5-10, 5-11, 5-12, and 5-13 is not valid, since it is of no interest in predicting the dependent variable from a single independent variable. Instead, these trendlines were only used to identify the relationship that was used in the regression analysis, which describe the combined effects of all the design parameters.

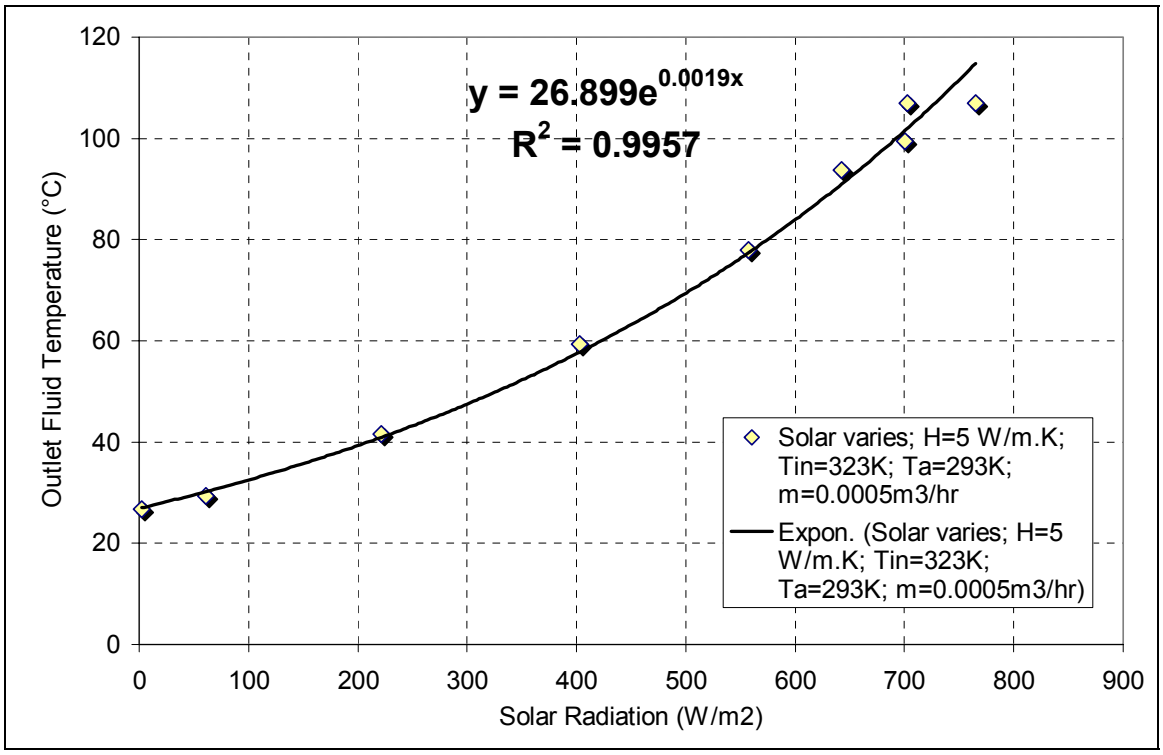

Figure 5-9. Variation of Fluid Outlet Temperature with Solar Radiation

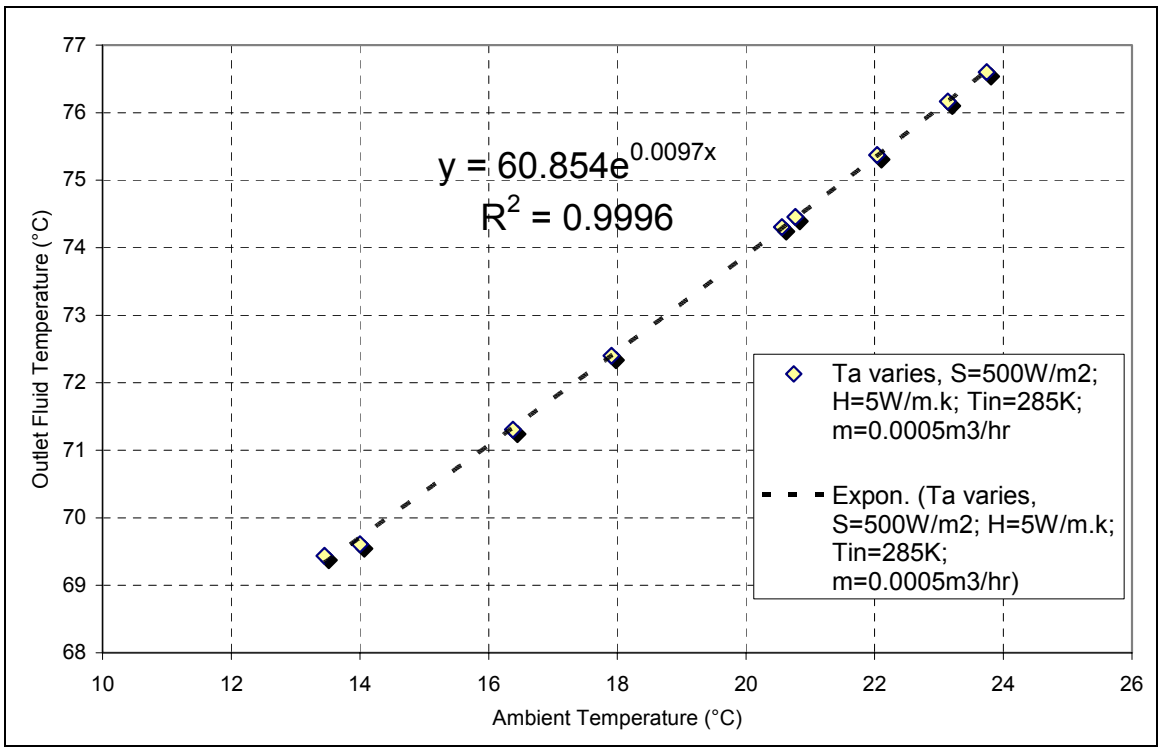

Figure 5-10. Variation of Fluid Outlet Temperature with Ambient Temperature

Figure 5-11 illustrates the variation of the outlet fluid temperature with the inlet fluid temperature. As shown, there is a positive correlation between the two variables, which can be described in terms of a linear relationship.

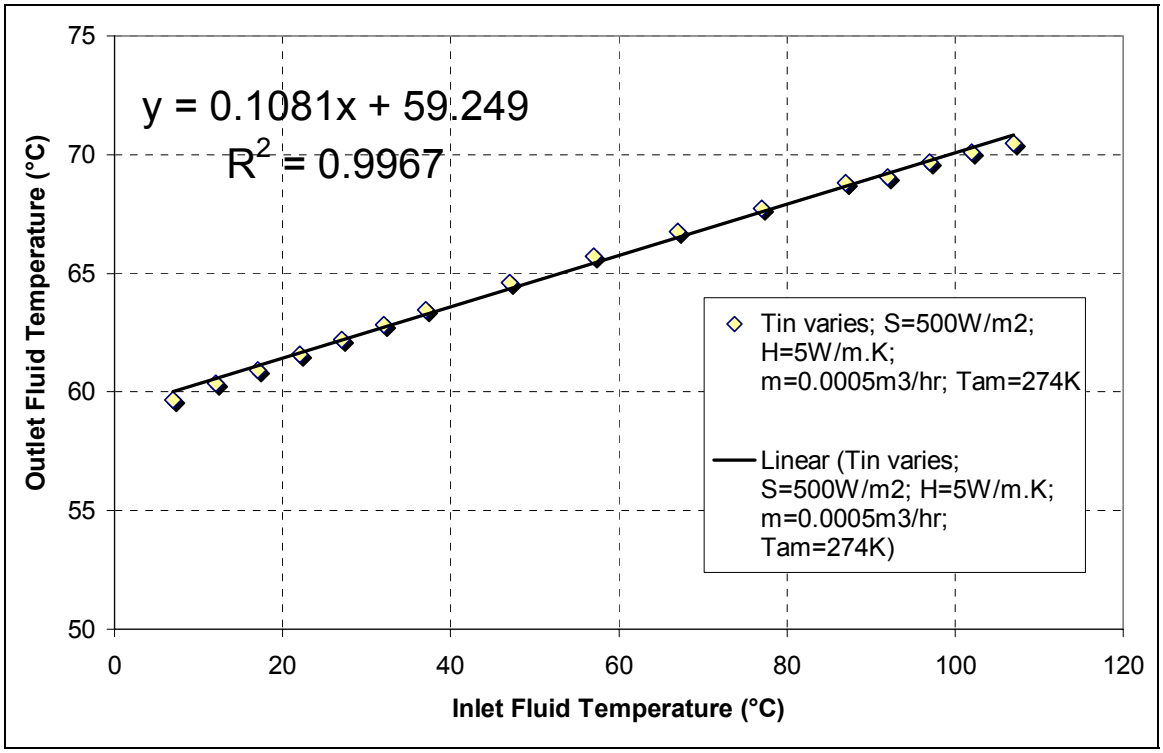

Figure 5-11. Variation of Fluid Outlet Temperature with Inlet Fluid Temperature

Similarly, Figure 5-12 illustrates the variation of the outlet fluid temperature with the ambient convection coefficient (h_w). A negative correlation can be identified between these two variables. In this case, a power law model is suitable to describe the variation of the outlet fluid temperature with the convection coefficient.

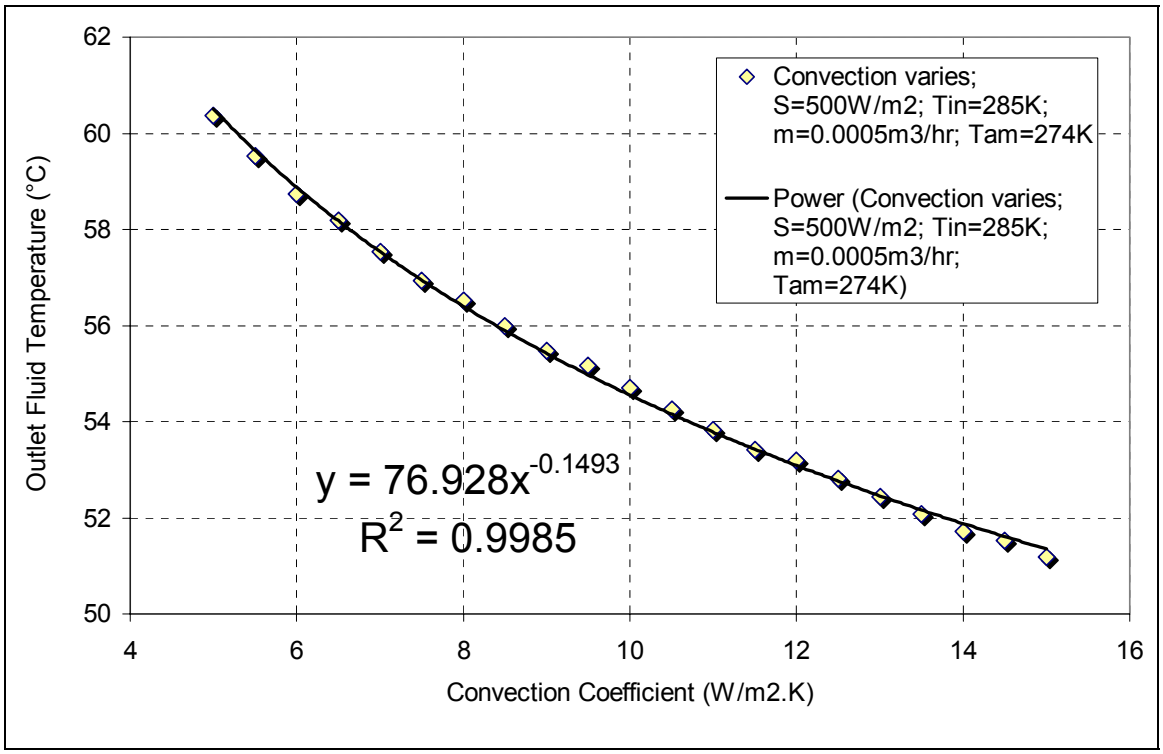

Figure 5-12. Variation of Fluid Outlet Temperature with Convection Coefficient

Figure 5-13 presents the variation of fluid outlet temperature with the mass flow rate. As shown, a negative correlation exists between these two variables. In general, as the fluid mass flow rate decreases, the fluid outlet temperature increases. In this case, a power law model was used to describe the relation between the mass flow rate and the outlet fluid temperature.

The use of a specific mass flow rate is critical since it determines the temperature difference between the outlet fluid temperature from the collector and the building supply temperature. In addition, it has to be noted that many piping materials have a recommended maximum velocity requirement. For example, copper pipe has maximum velocity criteria for both cold and hot water lines. In general, a maximum speed of 2.45m/sec (8ft/sec) is recommended for cold-water piping and 1.22m/sec (4ft/sec) for hot-water piping. This means that a 12.7-mm (0.5 inch) cold-water copper pipe should operate only at a maximum flow rate of 1.25m^3/hr (44.14 ft^3/hr).

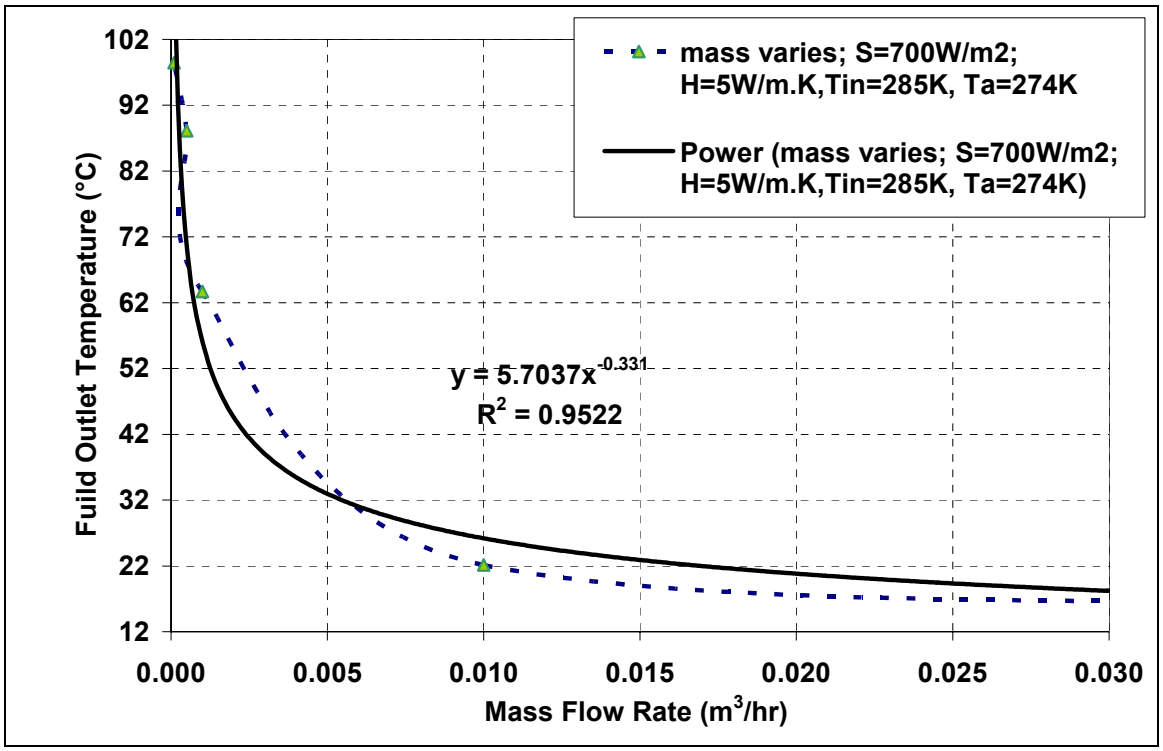

Figure 5-13. Variation of Fluid Outlet Temperature with Mass Flow Rate

The last independent variables are pipe diameter and spacing. Since only three values were considered for the pipe diameter (i.e. 6.35, 12.7, and 25.4mm) and the pipe spacing (i.e. 62.5, 128, and 188.5mm), it was not possible to draw a clear relationship between these variables and the outlet fluid temperature. Therefore, a linear trend was assumed.

5.4.2 Model Development

5.4.2.1 Model Selection Criteria

A multiple regression analysis was conducted to develop a simple model that may be used to predict the outlet fluid temperature. Model selection was based on several criteria defined as follows:

- Goodness of fit, based on the best combination of coefficient of determination (R^2), and root mean square error (RMSE). The use of the R^2 alone is usually not a good indicator of the goodness of fit since this coefficient can be improved by including additional independent variables (Jones 1996).

- The developed model, which utilizes the least square procedure, should satisfy the assumptions of this approach. These assumptions, which are dealt with in the following sections, are the following (Jones 1996):

    - **Linearity of the regression model**: the dependent variable can be expressed in terms of a linear combination of the independent variables.
    - **The variance of the error is zero**: This means that the average of the residual is zero.
    - **Constant variance and independence of the error**: The error has the same variance (S_e^2) across the different levels of X's, i.e. the variance of the error is homoskedastic (constant variance of the error) and not heteroskedastic (variance of the error changes for different levels of X's). In addition, the error is uncorrelated with the independent variables and independent of each other, i.e. not auto-correlated or serially correlated (correlation over time).
    - **Independent variables are not linearly correlated**: Any of the predictors should not be linearly related with any or all others. This assumption becomes serious if the correlation between any two independent variables increases above 0.9.
    - **Normality**: The error term is assumed to follow a normal distribution.
    - **X's are non-stochastic**: The selected set of independent variables does not change given the tested conditions.

5.4.2.2 Analysis of Variance

An analysis of variance (ANOVA) is the process of subdividing the total variability of the observations into portions attributable to recognized sources of variation. An analysis of variance (ANOVA) was conducted to study the statistical significance of the considered independent variables on the outlet fluid temperature. Table 5-2 illustrates the results of the analysis of variance for the modeled data. The probability (P value) shown in table 5-2 indicates how important an independent variable is in explaining the behavior of the dependent variable. The rest of the variation is then attributed to the error

(residual). In total, up to 260 different cases were used in this analysis. As shown by the P-Value[6] in this table, the most influential factors are fluid mass flow rate, solar radiation, convection coefficient, and ambient temperature. Although, the inlet fluid temperature was statistically insignificant, the use of this variable allows the designer to link the outlet fluid temperature on each run to the following hour, therefore, simulating transient conditions. On the other hand, the pipe diameter and spacing were also insignificant, but were thought useful in iterative evaluation of the panel geometry (design parameters). Therefore, all the considered variables were included in the developed model.

Table 5-2. Analysis of Variance for the Outlet Fluid Temperature

Variable	DF	Mean Square	F-Value	P-Value
Mass Flow Rate	1	2.599907	96.57	<0.0001
Pipe Diameter	1	0.092412	3.43	0.0651
Pipe Spacing	1	0.000207	0.01	0.9302
Solar Radiation	1	1.822091	67.68	<0.0001
Convection Coefficient	1	1.991649	73.98	<0.0001
Inlet Fluid Temperature	1	0.028001	1.04	0.3088
Ambient Temperature	1	0.430161	15.98	<0.0001
Residual	256	6.89		

5.4.2.3 Model Transformation

Based on the trend analysis and the relationship established between the dependent and independent variables, it appears that the relationship between the outlet fluid temperature and the independent variables is not a linear function. The model should take the following form:

$$T_{out} = c_1 \dot{m}^{c_2} + c_3 D_p + c_4 D_s + c_5 \exp(c_6 .\text{Solar}) + c_7 h_w^{c_8} + \\ + c_9 \exp(c_{10} . T_{am}) + c_{11} T_{in} + c_{12} \quad (5\text{-}13)$$

where

T_{out} = outlet fluid temperature (°C);

Solar = solar radiation (W/m^2);

[6] P-value is a measure of statistical significance, the lower the P-value the more significant the parameter.

T_{in} = inlet fluid temperature (°C);

T_{am} = ambient temperature (°C);

h_w = convection coefficient ($W/m^2.C$);

D_s = pipe spacing (m);

D_p = pipe diameter (m);

$\dot{m}$ = mass flow rate (lit/hr); and

c_1 to c_{12} = partial slope coefficients.

The use of this model in the regression analysis presented several difficulties:

- The regression process includes 12 different regression coefficients (c_1 to c_{12}) in a nonlinear form. If this model was used, the results of this analysis will not be robust enough. Moreover, to ensure validation of this model, convergence of the analysis should be met, which was not always the case.
- The goodness of fit of the model was not acceptable, since the root mean square error was 15°C in average.

To facilitate and to linearize the fitting process, transformations were used for the independent and dependent variables. Taking the natural logarithms of both sides of Equation (5.13), and applying the transformation process independently on each component of the equation results in the following model:

$$\begin{aligned} \ln T_{out} &= a_1 \ln \dot{m} + a_2 \ln D_p + a_3 \ln D_s + a_4 Solar + a_5 \ln h_w + \\ &+ a_6 \ln T_{in} + a_7 T_{am} + a_8 \end{aligned} \tag{5.14}$$

where

a_1 to a_8 = partial slope coefficients.

As shown in Equation (5.14), the number of regression coefficients decreased from 12 to eight coefficients, which will improve the robustness of the analysis.

5.4.2.4 Model Formulation

Based on the conducted regression analysis, the developed model for evaluation of the outlet fluid temperature is as follows:

$$\begin{aligned} \ln T_{out} &= 2.8862 - 0.0512 \ln \dot{m} - 0.0461 \ln D_p + 0.005081 \ln D_s \\ &+ 0.000475\,Solar - 0.3321 \ln h_w + 0.304 \ln T_{in} + 0.0132 T_{am} \\ R^2 &= 0.99 \qquad RMSE = 0.1637 \end{aligned} \tag{5-15}$$

The goodness of fit parameters of the model is shown in Table 5-3. Due to the used transformation, the shown mean square error (MSE) is not representative of the actual error, but rather to the error in the natural logarithmic domain. After transforming back the predicted outlet fluid temperature using an exponentional function, the actual RMSE was calculated manually, and was found to be 8.5°C.

Table 5-3 also presents the estimate of the coefficients, as well as the test for significance using a t-test. In general, a t-Value greater than ±2.0 indicates a significant variable. The sign of the t-Value also indicates whether a positive or negative correlation is present. Based on this fact, the solar radiation, the pipe spacing, the inlet fluid temperature, and the ambient temperature are all positively correlated to the outlet fluid temperature. This is in agreement with the theory which indicates that increasing the solar intensity increases the outlet fluid temperature due to the increase in radiation gains. In addition increasing the pipe spacing, (assuming the pipe spacing is covered by a collection fin connected to the pipes), increases the collection area therefore increases the radiation heat gain increasing the outlet fluid temperature and increasing the inlet fluid temperature increases the outlet fluid temperature. Similarly, increasing the ambient fluid temperature increases the outlet fluid temperature since it reduces the convection losses.

In contrast, the mass flow rate, the pipe diameter, and the convection coefficient are all negatively correlated to the outlet fluid temperature. This is also in agreement with the theory since increasing the mass flow rate reduces the fluid's exposure to the source of heat (the solar radiation) reducing the outlet fluid temperature. Moreover, increasing the pipe diameter decreases the outlet fluid temperature. Similarly, increasing the convection coefficient increases the convection losses to the environment resulting in a

decrease in the outlet fluid temperature. The results of the t-test indicate that the model fits the expected theory As previously mentioned, although the pipe diameter, the pipe spacing, and the inlet fluid temperature, were not strongly correlated to the dependent variables, they were included to facilitate the design iterative process proposed by the design evaluation framework.

Table 5-3. Multiple Regression Analysis Results

Source	DF	Sum of Squares	Mean Square	F Value	Approx Pr > F
Regression	7	4078.3	582.6	63.85	<.0001
Residual	257	6.8935	0.0268		
Uncorrected Total	264	4085.2			
Corrected Total	263	17.1695			

Variable	Estimate	Error	t-Value	P-Value
Intercept	2.8862	1.493	1.69	0.0924
Mass Flow Rate	-0.0512	0.0052	-9.83	<0.0001
Pipe Diameter	-0.0461	0.0253	-1.85	0.0651
Pipe Spacing	0.00508	0.0430	0.09	0.9302
Solar Radiation	0.000475	0.000058	8.23	<0.0001
Convection Coefficient	-0.3321	0.0389	-8.60	<0.0001
Inlet Fluid Temperature	0.304	0.3926	1.02	0.3088
Ambient Temperature	0.0132	0.00314	4.00	<0.0001

5.4.2.5 Sensitivity Analysis

This section analyzes the prediction of the model in terms of its coefficients. Each parameter is varied while keeping the rest of the parameters constant, and the response of the model is monitored with respect to partial slope coefficients. The parameters were kept as follows: mass flow rate=5liter/hr, inlet fluid temperature= 12^{o}C, ambient temperature=17^{o}C, solar radiation=500W/m^{2}, wind convection coefficient=5W/mK, pipe diameter=12.7mm, and pipe spacing=128mm. Afterwards each of the parameters was varied. First, consider the variation in the mass flow rate. The change in mass flow rate from 1 liter/hr to 2 liter/hr results in a decrease of the outlet fluid temperature of 1.656°C. This shows the high dependency of the outlet fluid temperature on the operational mass

flow rate. This is in agreement with the results of the t-test of significance (t-Value=-9.83). However, the change of a mass flow rate from 100 liter/hr to 101 liter/hr results in a decrease in the outlet fluid temperature of only 0.017°C. This indicates the capability of the model to behave nonlinearly with respect to the mass flow rate.

Similarly, the change in the pipe diameter from 0.012m to 0.013m results in a decrease of the outlet fluid temperature of -0.162°C. On the other hand, the change in the pipe spacing from 0.128m to 0.129m results in an increase of the outlet fluid temperature of 0.002°C. This is considered a small effect, as indicated by the t-test (t-Value=0.09).

The change in the solar radiation from 150W/m^2 to 151W/m^2 results in an increase of the outlet fluid temperature of 0.0179°C. This shows the high dependence of the outlet fluid temperature on the solar radiation. This is in agreement with the results of the t-test of significance (t-Value=8.23). Moreover, the change of the solar radiation from 300W/m^2 to 301W/m^2, 400W/m^2 to 401W/m^2 , 500W/m^2 to 501W/m^2 600W/m^2 to 601W/m^2 results in an increase in the outlet fluid temperature of 0.0193°C , 0.0202°C , 0.0212°C , 0.0222°C. This also indicates the capability of the model to behave nonlinearly with respect to the solar radiation.

The change in the convection coefficient from 5W/m.C to 6W/m.C results in a decrease of the outlet fluid temperature of 2.358°C. This also shows the high dependence of the outlet fluid temperature on the convection coefficient. This is in agreement with the results of the t-test of significance (t-Value=-8.60).

The change in the inlet fluid temperature from 15^{o}C to 16°C results in an increase of the outlet fluid temperature of 0.859°C if the ambient temperature is lower than the inlet fluid temperature (e.g. 10^{o}C). Nevertheless, if the ambient temperature is higher than the inlet fluid temperature (e.g. 25^{o}C), a change in the inlet fluid temperature results in an increase of the outlet fluid temperature of 1.047°C. This shows some dependence of the inlet fluid temperature on the ambient temperature. It also indicates the presence of some correlation between the two variables as shown in Table 5-4 (page 123) in the following section, (correlation factor = -0.78). However, since the correlation factor is below 0.9, this level of correlation is acceptable. On the other hand, the change in the ambient temperature from 17^{o}C to 18^{o}C results in an increase of the outlet fluid temperature of 0.632°C.

5.4.2.6 Appropriateness of the Model

It was previously indicated that in order for the proposed model to be valid, several assumptions need to be verified. First, consider the assumption of the average of the residual is zero and constant variance and independence of the error. In the case of multiple regression analysis, these two assumptions may be verified by plotting the residuals against the fitted values (Myers 1990). Figure 5-14 shows the plot of the residuals against the predicted outlet fluid temperature. Since this figure indicates a random pattern of residuals around zero, a homoskedastic behavior (constant variance of the error) may be assumed. Moreover, since the slope of the trendline shown in Figure 5-14 is very close to zero, the assumption that the average of the residual is zero is validated.

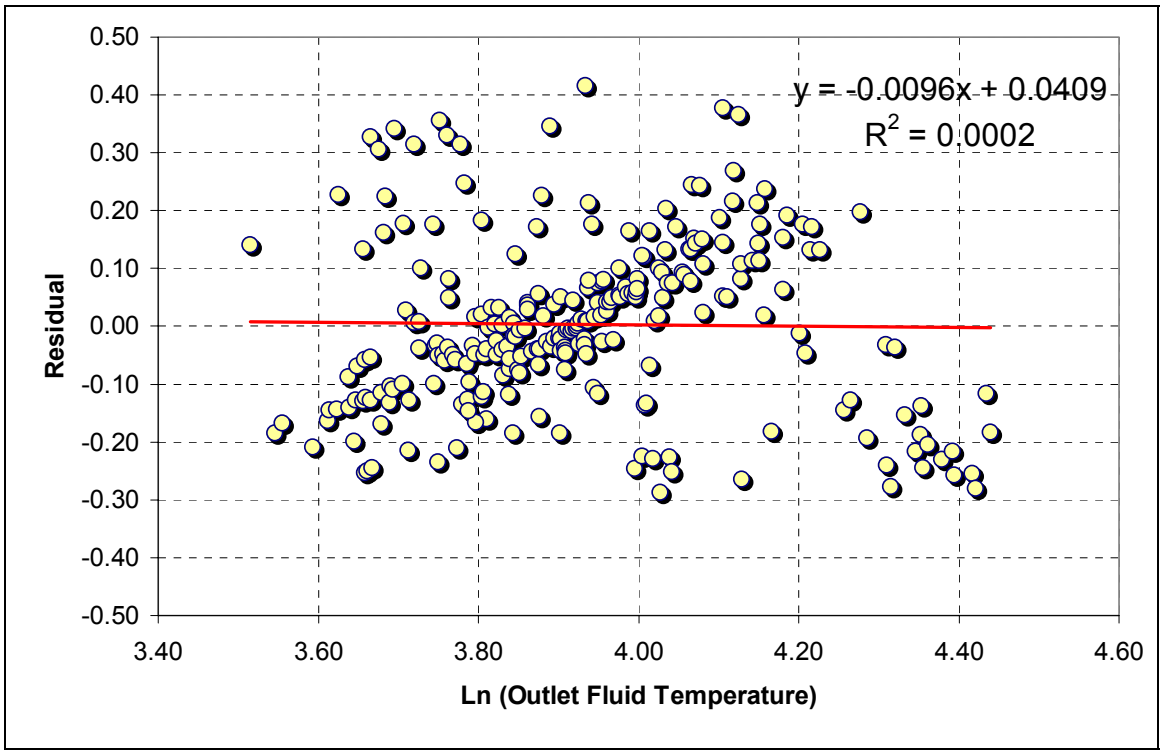

Figure 5-14. Plot of the Residual against the Predicted Values

Consider now the assumption of serial correlation. In this case, residuals are correlated with residuals lagged from previous time steps. This assumption can be tested using Durbin-Watson d-statistic (Younger 1979). The d parameter, which may be computed

using any computer packages, ranges from zero to four. A d-value around two indicates that no serial correlation is present. A d-value greater than two indicates a negative serial correlation. A d-value less than two shows a positive serial correlation. For the considered model, a d-value of 0.85 was calculated, indicating the presence of some positive serial correlation. Presence of serial correlation indicates that the model prediction in one time period is affected by the model prediction in the next period. Therefore, the residual in one time period is related to the residual in the next; i.e., the error is time dependent. This indicates that the error will follow a specific trend with respect to time; i.e., accuracy of the model will be higher in some instances and lower in others. However, since the RMSE of this model is acceptable and as shown in the next section, the prediction of the model is accurate, and for reasons of parsimony (simplicity), the serial correlation was not considered further in the analysis. Moreover, it was previously shown that fixation of this problem may cause the violation of the multicollinearity assumption (Jones 1996).

Consider the assumption of multicollinearity. Multicollinearity is manifested when the regressor variables are not independent, and describe redundant behavior. Table 5-4 presents the correlation matrix for the regressor variables used in the developed model. A correlation greater than 0.9 indicates violation of the multicollinearity assumption. As shown in Table 5-4, no variable violates this assumption.

Table 5-4. Correlation Matrix

		Coefficients						
		a1	a2	a3	a4	a5	a6	a7
Coefficients	a1	1.00	-0.11	-0.19	-0.27	-0.23	-0.05	-0.27
	a2	-0.11	1.00	-0.01	0.15	0.08	0.04	0.15
	a3	-0.19	-0.01	1.00	0.09	0.05	0.03	0.11
	a4	-0.27	0.15	0.09	1.00	-0.13	-0.24	-0.36
	a5	-0.23	0.08	0.05	-0.13	1.00	-0.28	0.26
	a6	-0.05	0.04	0.03	-0.24	-0.28	1.00	-0.78
	a7	-0.27	0.15	0.11	-0.36	0.26	-0.78	1.00

Consider the assumption of the regressor being a non-stochastic matrix. This assumption suggests that the selected variables would adequately describe the behavior for different sets of data under controlled conditions. In general, the selected set of regressor has been

previously used in analytical predictive models to describe the behavior of flat plate collectors (Duffie and Beckman 1980). Moreover, the influential factors affecting collections identified in Figure 3-4 of the design evaluation framework were all considered in the developed model.

Finally, consider the assumption of residuals having a normal distribution. To test this assumption, the standardized residuals were plotted against the abscissa of the normal distribution function (Z). Figure 5-15 illustrates the results of this analysis. As shown in this figure, an approximate straight line is obtained indicating the validity of the assumption.

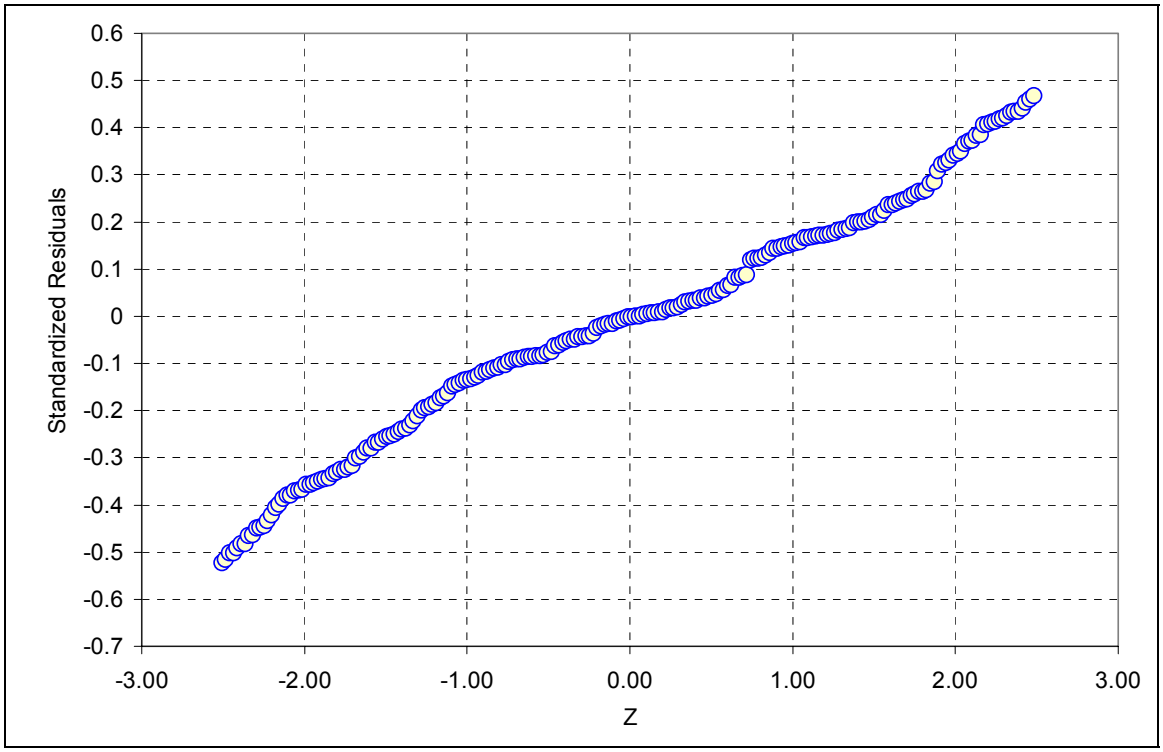

Figure 5-15. Normality Probability Plot

5.4.2.7 Model Validation

To validate the proposed model, a typical day in August (from 8:00AM to 17:00PM) was selected from the Blacksburg TMY2 file. For this specific day, predictions from the model were compared against results from the finite element simulation. Figure 5-16

illustrates the comparison between the two approaches. The RMSE for this day was 4.80°C.

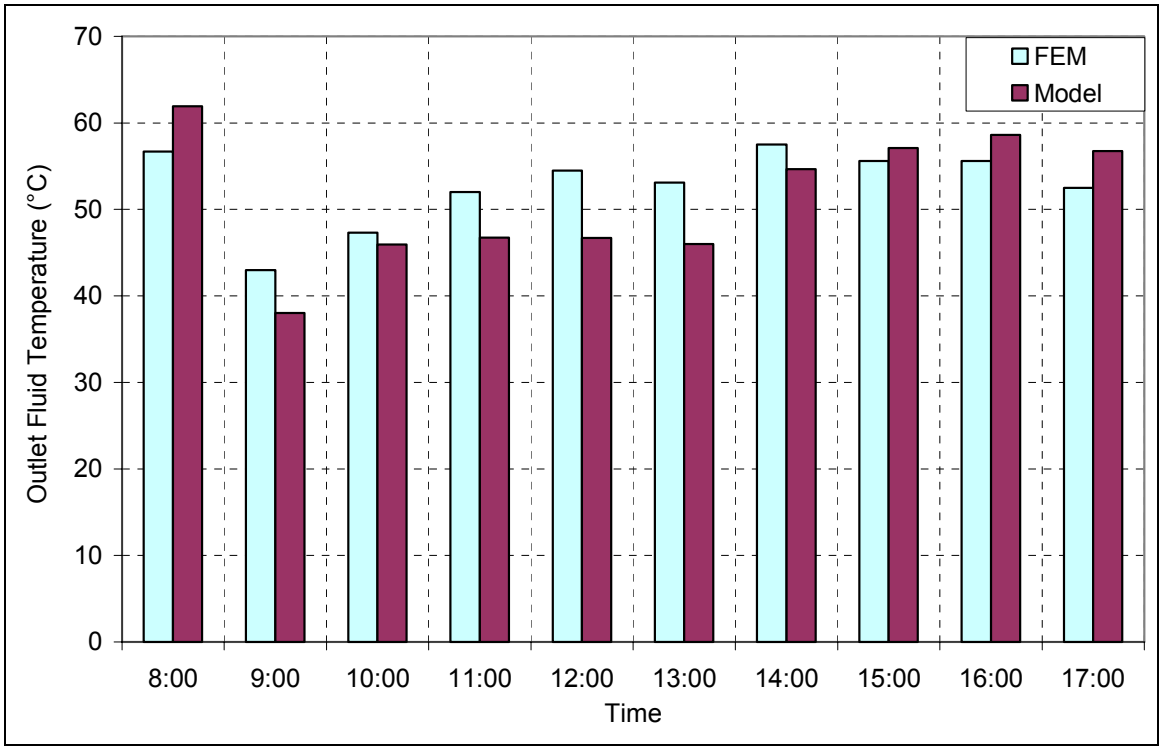

Figure 5-16. Comparison between Results from the Finite Element and the Predictive Model

5.4.2.8 Energy Estimation from the proposed model

Based on the estimated outlet fluid temperature, the amount of energy collected can be calculated as follows:

$$Q(MJ) = \frac{\dot{m}\, c_p}{1.5(D_s + D_p)}(T_{out} - T_{in})A_c \qquad (5\text{-}16)$$

where

Q = Energy collected per hour;

$\dot{m}$ = mass flow rate (kg/hr);

c_p = specific heat of the fluid (J/kg.°C);

A_c = area of collection (m^2); and

All other variables as previously defined.

5.4.3 Design Example

Assume that, based on the weather records for a given day; a designer determines the following expected conditions (see Table 5-5).

Table 5-5. Weather Data used in the Design Example

Time	Solar Radiation (W/m^2)	Convection Coefficient (W/m.°C)	Ambient Temperature (°C)
8.00	265.66	5	4
9.00	472.38	5.42	5.69
10.00	613.99	5	7.86
11.00	700.31	6.44	9.83
12.00	650.49	5	10.95
13.00	627.95	5.42	11.4
14.00	549.63	5.42	12.04
15.00	439.24	5.42	12.07
16.00	228.37	5.42	11.62
17.00	81.51	5.42	10.56

For this specific day, the designer is to determine the outlet fluid temperature and then the collected energy based on two alternative designs and choose the design that maximizes the heat gain for the given weather conditions. The two alternative designs consist of the following:

Design and operational Parameter	Alternative A	Alternative B
Mass Flow Rate	$0.0005m^3/hr$	$0.001m^3/hr$
Pipe Spacing	128mm	128mm
Pipe Diameter	12.7mm	12.7mm

The designer estimates that at the beginning of this analysis, the fluid inlet temperature is 20°C and varies according to the outlet fluid temperature in both alternatives as shown in Table 5-6. However, if the outlet fluid temperature exceeds 40^oC, the building supply

temperature, the inlet fluid temperature automatically becomes 40°C. Using Equation 5-15, the designer can predict the hourly outlet fluid temperature for the two alternatives A and B. The calculated outlet fluid temperatures are shown in Table 5-6.

It appears that for this specific day, collection of solar energy will occur between 8.00 am and 5.00 pm for both alternatives. Using Equation 5-16 and assuming that a $50m^2$ collection area will be used, the amount of energy collected this day can be estimated at 369.01MJ (349754Btu) for a mass flow rate of $0.0005m^3$/hr and 656.54 MJ (622279.9Btu) for a mass flow rate of $0.001m^3$/hr. Therefore, the designer is advised to use alternative B.

Table 5-6. Design Example Output

Time	Inlet Fluid Temperature Alternative A	Inlet Fluid Temperature Alternative B	Alternative A Outlet Fluid Temperature*	Alternative B Outlet Fluid Temperature**
8.00	20.0	20.0	39.2	37.8
9.00	39.2	37.8	52.8	50.4
10.00	40.0	40.0	60.0	57.9
11.00	40.0	40.0	59.0	56.9
12.00	40.0	40.0	63.6	61.4
13.00	40.0	40.0	61.6	59.5
14.00	40.0	40.0	59.8	57.8
15.00	40.0	40.0	56.8	54.9
16.00	40.0	40.0	51.1	49.4
17.00	40.0	40.0	47.0	45.4

* Mass flow rate = $0.0005m^3$/hr

** Mass flow rate = $0.001m^3$/hr

Furthermore, the designer decides to investigate the effect of changing the pipe diameter from 12.7mm to 6.35 on the outlet fluid temperature and the heat gain using Alternative B. The resulting outlet fluid temperature is shown in Table 5-7. As shown in Table 5-7, decreasing the pipe diameter increased the outlet fluid temperature. Similarly, using Equation 5-16 and assuming that a $50m^2$ collection area will be used, the amount of energy collected this day can be estimated at 656.54 MJ (622279.9Btu) for a pipe diameter of 12.7mm and 799.45MJ (757732.4Btu) for a pipe diameter of 6.35mm. Since using smaller diameter pipes resulted in an increase in the overall collected energy and at

the same time reduces the cost of the collector, the designer may decide to modify Alternative B to use 6.35mm diameter pipes instead of 12.7mm ones. As demonstrated in this example, the developed equation allows the designer to test the effect of different alternatives at minimal cost and time.

Table 5-7. Design Example Output – Effect of Changing the Pipe Diameter

Time	Inlet Fluid Temperature D=6.35	Inlet Fluid Temperature D=12.7	Outlet Fluid Temperature D=6.35	Outlet Fluid Temperature D=12.7
8.00	20.0	20.0	39.1	37.8
9.00	39.1	37.8	52.5	50.4
10.00	40.0	40.0	59.8	57.9
11.00	40.0	40.0	58.8	56.9
12.00	40.0	40.0	63.4	61.4
13.00	40.0	40.0	61.4	59.5
14.00	40.0	40.0	59.7	57.8
15.00	40.0	40.0	56.7	54.9
16.00	40.0	40.0	50.9	49.4
17.00	40.0	40.0	46.9	45.4

6 STAGE III - BUILDING AN ENERGY CONSUMPTION MODEL – ENERGY PLUS

6.1 INTRODUCTION

This chapter describes the energy consumption model developed for the Blacksburg, Virginia building case study. This model was used in the building demand stage (Stage III) of the design evaluation framework highlighted in Figure 6-1. There are two commonly used methods for energy modeling: simplified and detailed. Simplified methods use integrated weather representations, like degree-days or degree-hours, to predict building's response to the exterior environment. Such methods possess drawbacks. They are unable to predict accurately the impact on energy consumption of either features that have large hourly fluctuations (e.g., the amount of solar heat gain through windows with unique shading characteristics) or variations in a building's operation schedule. On the other hand, for every hour of every day of the year, detailed modeling performs a whole building heat loss/heat gain calculation. On an hourly basis, it accounts for exact sun angles, cloud cover, wind, temperature and humidity, thereby accounting for the effects of thermal time lag and thermal storage within the building.

A number of computer programs are available for building energy simulation and evaluation. They range from full-building energy analysis programs with passive solar capabilities to programs for active solar energy systems with some passive or hybrid capabilities. In general, building energy analysis programs are more appropriate for passive and/or hybrid solar applications, which require the details of energy transfer between walls and rooms, or for multi-zone applications in which HVAC system simulation is important.

In general, the main disadvantage of building analysis simulation programs is that although they provide a detailed picture of thermal energy flows and of the interaction between heating and cooling loads and equipment, they include simplifications that might not fully account for all significant energy terms. Another disadvantage is the large amount of input information required to simulate a simple passive structure. The level of

complexity encountered usually requires the advice of an analyst with training or experience in computer simulation.

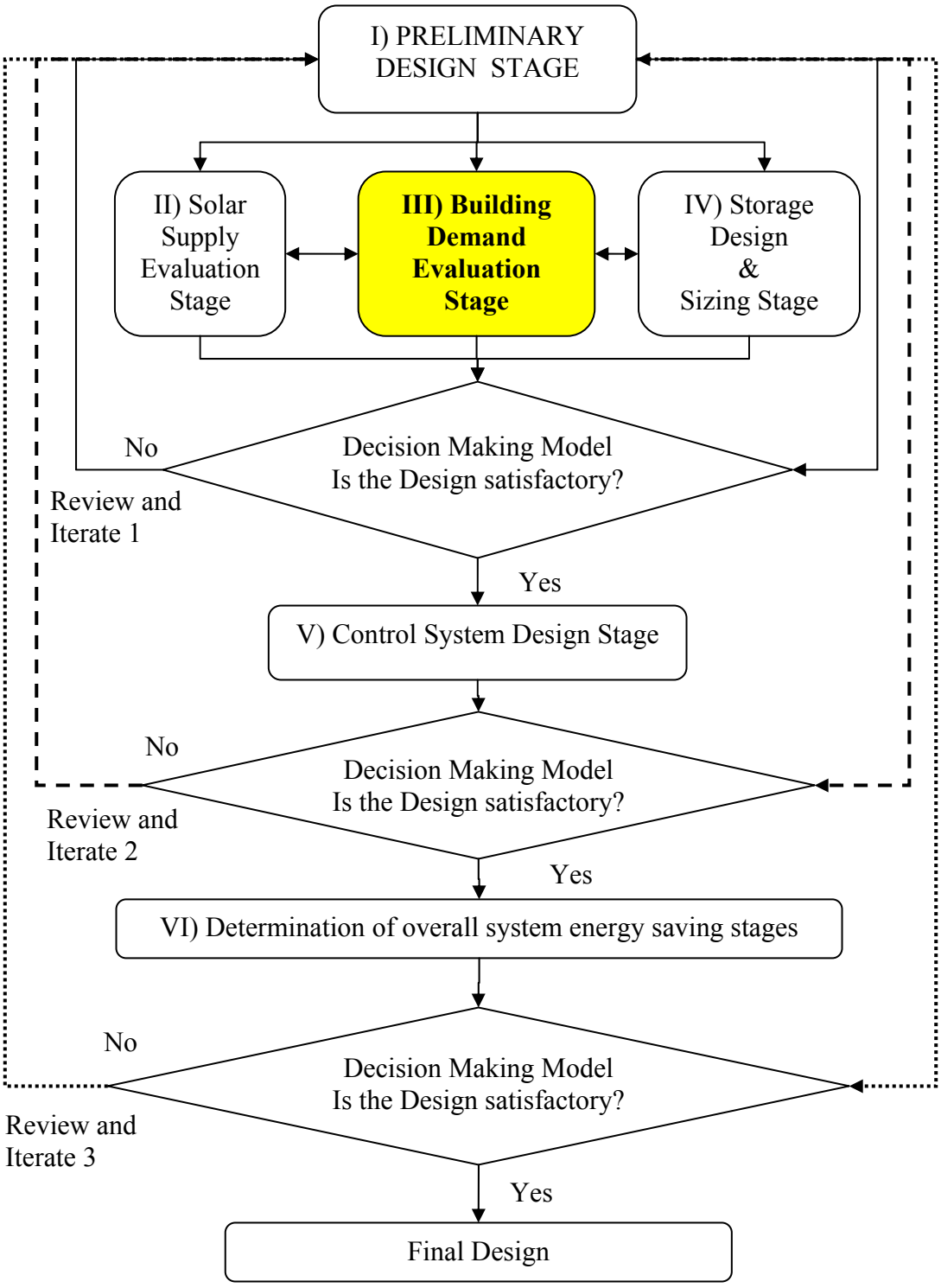

Figure 6-1. Stage III of the design evaluation framework

The most common energy simulation software are DOE2, BLAST, TRANSYS and Energy Plus (see Chapter 2). Since it represents state of the art technology in building performance simulation, Energy Plus was selected to simulate heating requirements in the first case study's building located in Blacksburg, Virginia. Energy Plus, which is based on both BLAST and DOE-2 energy simulation programs, is an energy analysis and thermal load simulation program. Using primary and secondary HVAC systems and coils, it calculates the heating and cooling loads necessary to maintain within the building user-specified thermal control set points. Energy Plus is divided into different modules named for their various roles or simulation purposes: sky model, shading, daylighting, window glass, heat transfer calculation, airflow, air loop, PV, plant loop, zone equipment, and condenser loop. A successful simulation requires that the user input different parameters in some or all of these modules. Then, to perform the required simulation in hourly or sub-hourly time intervals, Energy Plus integrates the building description, the text weather files, and the defined HVAC system. Figure 6-2 shows how the different modules within Energy Plus interact with each other.

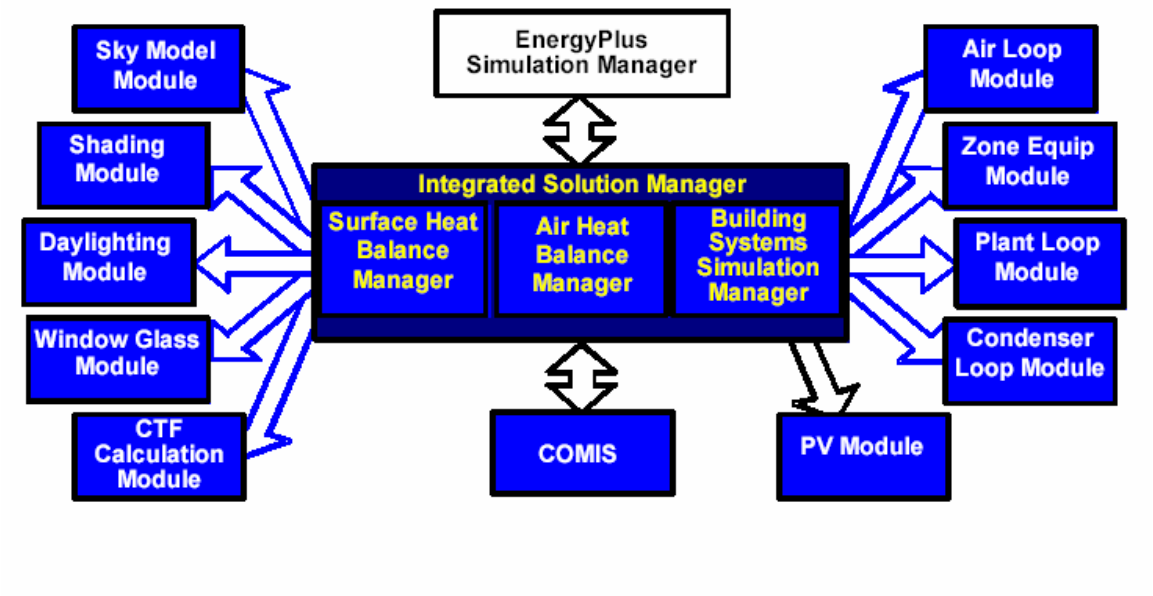

Figure 6-2. Energy Plus Modules Interaction (Energy Plus 2002)

This chapter demonstrates the framework's ability to utilize detailed modeling techniques (in the form of Energy Plus), to simulate the Blacksburg, Virginia building's energy consumption. The following sections will introduce the input parameters used in each module to simulate energy consumption in the Blacksburg, Virginia building, as well as highlight any assumptions used within it. The Energy Plus simulation input file is presented in Appendix B.

6.2 MODEL FORMULATION

This section discusses the steps required in formulating the heating energy consumption model, from simulation parameters to location and weather data to geometry and materials, among others considerations. It is important to emphasize that the cooling cycle was not considered in the model, as the major focus of this study is on the heating cycle. However, infiltration and ventilation in the building were considered in the developed model to accurately calculate heating thermal loads.

6.2.1 Simulation Parameters

The first step in formulating the energy consumption model is identifying the different simulation parameters, such as solution algorithm, loads, and temperature convergence tolerances. The time-step-per-hour is also here defined, as are the inside and outside convection algorithm, the required airflow model, and the different run control parameters.

This simulation used the conduction heat transfer functions (CTF) solution algorithm, which represents a sensible heat-only solution and does not take into account moisture storage or diffusion into the construction element. This method was chosen because the building design does not rely on the construction to store or diffuse moisture.

For higher accuracy without elongating the simulation run time, the time-step-used-per-hour was six. To achieve higher accuracy, the loads and temperature convergence limits were 0.04W and 0.4^{o}C. The convection algorithm used was ASHRAE detailed, while COSMIS was used for airflow simulation. Sizing calculations of the zones, the system, and the plant were requested.

6.2.2 Location and Weather Data

In this module, various building site data are identified, including longitude, latitude, time zone, monthly ground temperatures, and elevation. The location specified for this simulation is Blacksburg, Virginia, which possesses a latitude of 37.34, longitude of -80.67, and an elevation of 670m (2000ft). The module also specified two design days, one for winter and one for summer. The required design day data include maximum dry bulb, daily temperature range, wet bulb temperature at maximum temperature, barometric pressure, wind speed and direction, sky clearness, and rain and snow indicator (see Appendix B). The program uses the design day data for system and plant sizing and uses the daily temperature range given in this data to create the daily cycle distribution for the design day, as shown in Figure 6-3. Two design days were specified, as shown in Table 6-1.

Table 6-1. Summer and Winter Design Days

Design day Data	**Summer**	**Winter**
Maximum Dry-Bulb Temperature (°C);(^{o}F)	32 (90)	-12 (10)
Daily Temperature Range (°C);(^{o}F)	10 (50)	0 (32)
Wet-Bulb Temperature At Max. Temp (°C);(^{o}F)	23 (73)	-12 (10)
Barometric Pressure (Pa);(psi)	99433.54 (14.4)	99782.25 (14.5)
Wind Speed (m/s); (ft/sec)	3.81 (12.5)	11.6 (38.1)
Wind Direction (deg)	180	326
Sky Clearness	0.98	0
Rain Indicator	1	0
Snow Indicator	0	0
Day Of Month	21	21
Month	July	January

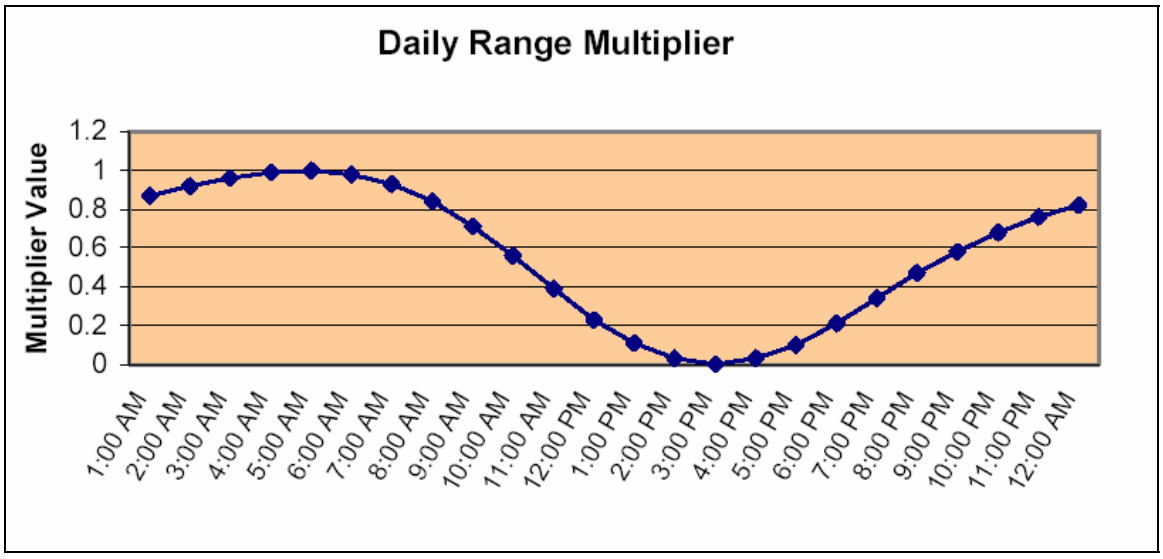

Figure 6-3. Energy Plus Design Day Daily Range Multiplier (Energy Plus 2002)

After system sizing, for energy consumption calculations, the model uses the weather data file described in Chapter 4 (TMY2, 5th percentile and 95th percentile). As shown in Appendix A, the TMY2 weather data file contains the following hourly indices: dry bulb temperature, dew point temperature, direct and diffuse radiation values, relative humidity, atmospheric pressure, wind speed, wind direction, total sky cover, visibility, precipitation, illuminance values, aerosol optical depth, broadband turbidity, snow depth, and days since last snow.

6.2.3 Geometry and Construction Material

The construction materials and their properties are specified in this section by types and names. In order to perform at CTF analysis, the designer must identify the following material properties: roughness, layer thickness, conductivity, density, specific heat, and thermal, solar, and visible absorbance. The definition of different material properties affects the analysis. For example, if moisture-related properties were not identified, the model could perform only CTF calculations.

There are three ways to define opaque material properties: material regular, material regular-r, and material air. If material regular is used, the simulation is capable of taking the thermal mass effect into account and thus allowing for the evaluation of

transient conduction effects. If material regular-r is used, steady state analysis is assumed. Material air should be used only if needed to define properties of air gap between construction layers. To allow for simulating transient effects, this simulation defined the material properties using the material regular option. Construction of the opaque layers was previously presented in Chapter 3.

Glass windows and doors are defined separately either as "Material: window glass" or "Material: window glass all input." The former allows the front and back optical properties of the glass to be different, while the latter does not. This model defined all windows as "Material: window glass." The glass properties defined include light transmittance and reflectance for the inward and outward surfaces, short wave reflectance of the inward and outward surfaces, emissivity, and thermal conductivity. All windows were modeled using double layers of glass, with an appropriate air pocket between the layers, as shown in Figure 6-4.

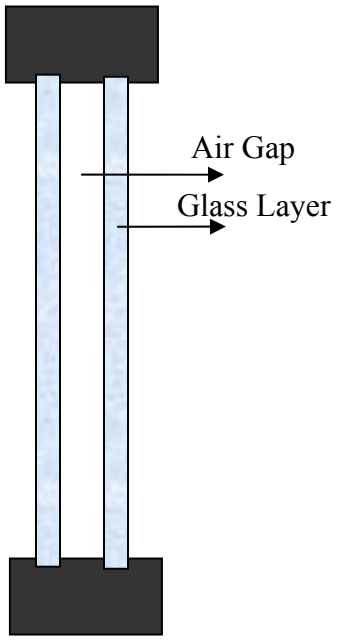

Figure 6-4. Window Construction

Afterwards, the defined materials are used to assemble the construction composition of different components, i.e. roof exterior walls, interior walls, and so on. Finally, surfaces are specified for the building with geometric coordinates as well as referenced

construction. Radiant systems are modeled by construction with internal sources. Since the modeled heating and cooling systems are based on low radiant heating/cooling technology, all floor slabs in the building were modeled as construction with internal sources.

The geometry of the model consists of a square basement floor, two circular floors, and a loft with an inclined roof. The area of the basement is 350m^2 (3767.37 ft^2), while the area of the first and second floors is 328.5m^2 (3535.94ft^2). Figure 6-5 shows an isometric of the building modeled in Energy Plus.

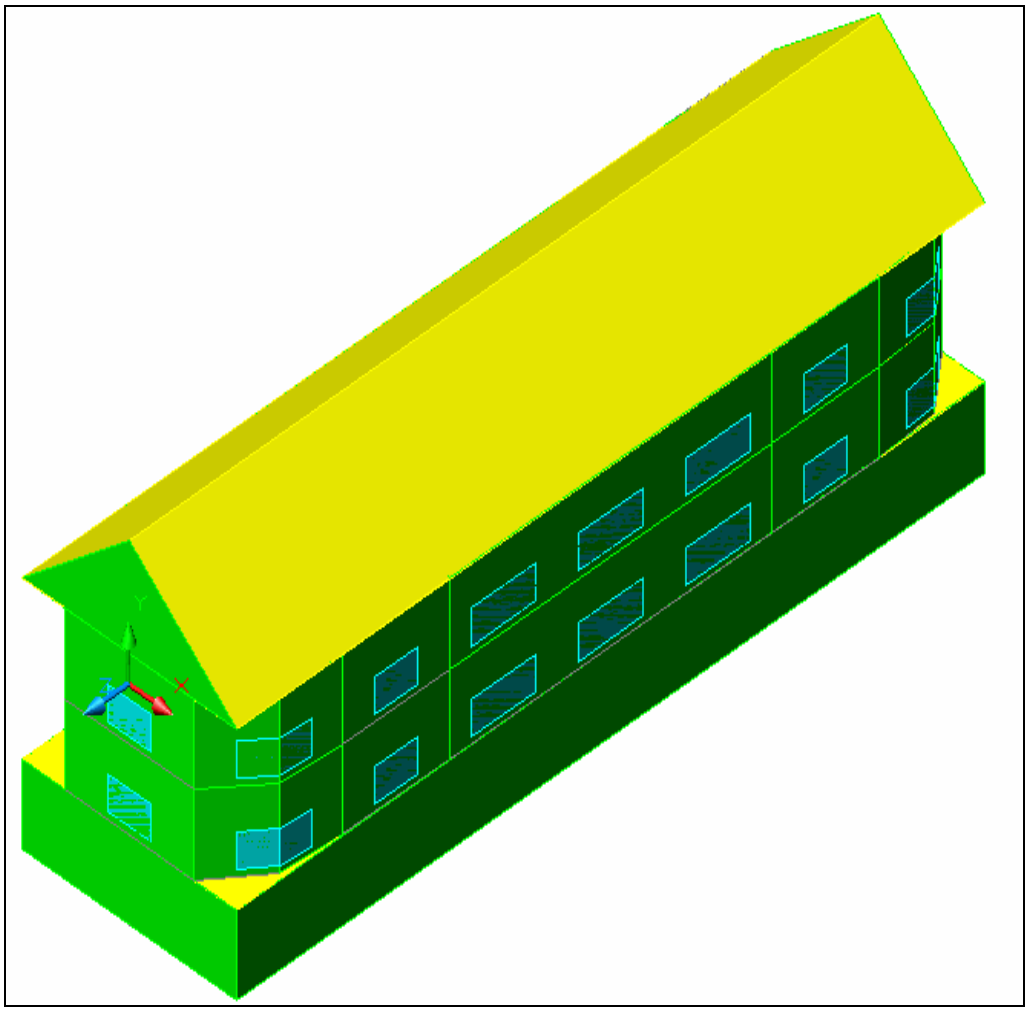

Figure 6-5. Isometric of the Energy Plus Model (Energy Plus 2002)

To study the effects of area changes on building energy consumption, two additional models were created by scaling the modeled area, as shown in Table 6-2. The three

models were formulated as thermal load cases and were used to predict the fraction of the load the solar collection system is able to supply.

Table 6-2. Proposed Area Variation

Description	Area CASE II (M^2)	Area CASE I (M^2)	Area CASE III (M^2)
Basement	3.5 (3.5*1)	350 (35x10)	35000 (350*100)
1st Floor	3.285 (3.285*1)	328.5 (32.85*10)	32850 (328.5*100)
2nd Floor	3.285 (3.285*1)	328.5 (32.85*10)	32850 (328.5*100)
Loft	3.5 (3.5*1)	350 (35*10)	35000 (350*100)
Height (m)	3	3	3

The first and second floors were divided into 15 thermal zones each, as shown in Figure 6-6, while the basement and loft were modeled as a single thermal zone, as shown in Figure 6-7. The thermal zones were divided according to orientation: north, south, east, west, northeast, northwest, southeast, and southwest.

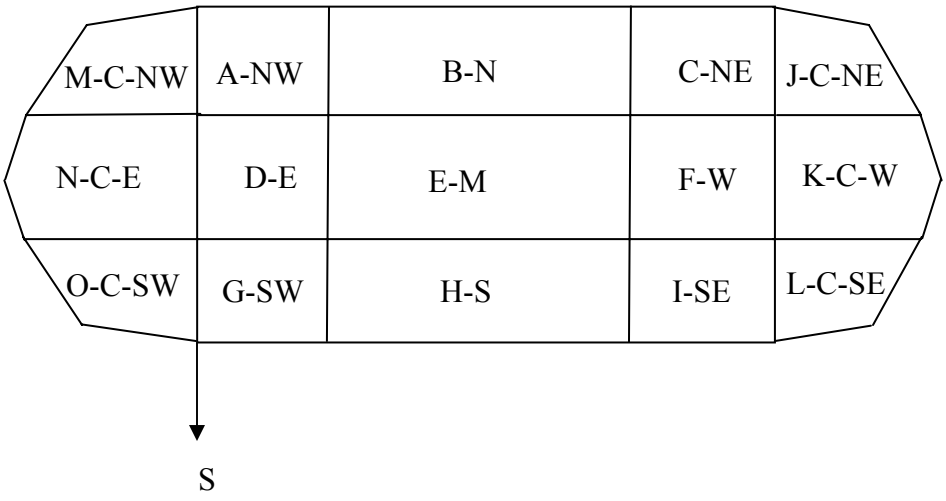

Figure 6-6. Thermal Zones – First and Second Floor

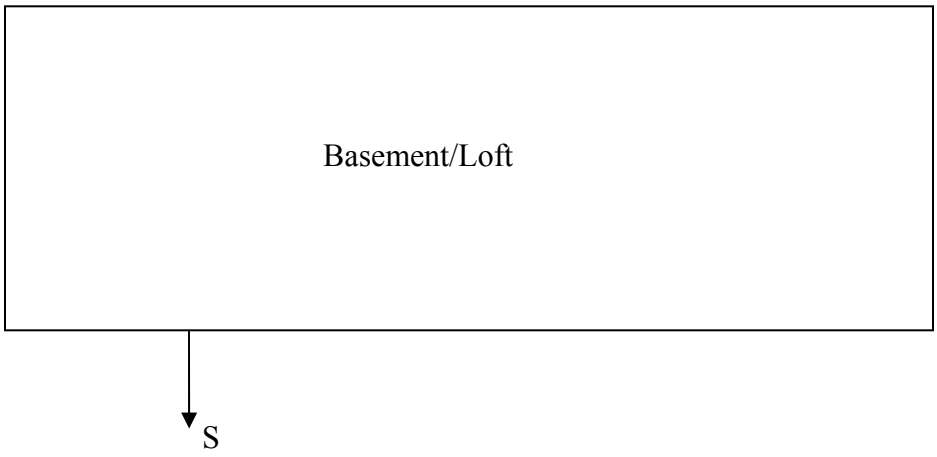

Figure 6-7. Thermal Zones – Basement and Loft

6.2.4 Thermal Comfort Calculations

Through the "people statement," Energy Plus simulates the effect of occupants on space conditions. Thermal comfort can be calculated based on Fanger's Thermal Model or on Pierce's Two-Node Thermal Model. To calculate the thermal comfort, one must identify the maximum number of people in each thermal zone, calculate the fraction of heat radiated by them, and determine their occupancy schedule, as well as a schedule of their activity level, clothing schedule, and work efficiency. Moreover, the air velocity within the space must be identified at all times.

The Mean Radiant Temperature (MRT)[7] in the zones can be calculated in Energy Plus using zone-averaged or surface-weighted calculations. Using the zone average method, the MRT is calculated for an average point in the zone. In that case, the calculation is based on an area emissivity weighted average of all zone surfaces (Energy Plus 2001). On the other hand, the surface weighted calculation estimates the thermal comfort of a person in the space close to a particular surface without having to define the exact view-factors for the rest of the surfaces or the location of that person in space. In that case the MRT used is the average temperature of the surface to which the person is closest (Energy Plus 2002).

[7] Mean radiant temperature (MRT) is a temperature measure that accounts for the temperature impact of surrounding surfaces according to the angle of influence. It is calculated by summing the multiplying of the object's angle of exposure to each surface in the room by the temperature of that surface. A combination of MRT and mean air temperature produce comfort conditions.

Zone average thermal comfort calculations were used in this simulation. The space thermostats were adjusted to provide a Fanger PMV Index ranging within ± 0.75 at all times.

6.2.5 Airflow

Two types of airflow statements need to be defined, infiltration and ventilation. Ventilation is the purposeful flow of air, using no mechanical means, from the outside to the thermal zones. For the purpose of this model, no ventilation was defined under this statement because the building ventilation (2/3 of the volume of the house air exchanges per hour) was achieved using forced air exchange (as shown in the air loop section). Infiltration is defined as the unintended flow of air from the outside environment to the zone. Usually, infiltration is caused by window cracks or the opening and closing of exterior doors. Infiltration in this model was simulated using the COSMIS software link in Energy Plus. COSMIS, a stand-alone airflow program developed in 1994, gets called on by Energy Plus during each time step to calculate the airflow between the outside and inside and from zone to zone.

6.2.6 Mechanical System Simulation

In Energy Plus, HVAC system simulation is more complex than that of either building geometry or thermal comfort because the interconnection between the various components must be defined. In reality, these components are connected together through ducts and pipes. In the simulation, each component is identified by a number of nodes, usually two (an inlet node and an outlet node). In some cases, more nodes must be identified, such as internal ones in which heat calculations need to be performed. Energy Plus evaluates the heat transfer fluid properties at these nodes then passes the output to the next piece of equipment in the simulation.

The aforementioned components are then linked together to form various loops in the simulation. Therefore, the outlet node from one component serves as an inlet node to the next component. Four main loop sections must be identified in Energy Plus: plant, condenser, air, and zone equipment (Energy Plus 2002).

Since Energy Plus cannot simulate active systems, the solar collector (Stage II model of the design evaluation framework) and PCM storage system (Stage IV model of the design evaluation framework) were simulated using Finite Element Analysis (FEA) (see Chapters 5 and 7) and input into Energy Plus as "purchased hot water" equipment.

6.2.6.1 Plant Loop

The first loop in the simulation, which involves the plant, describes the equipment used for heating the building. The plant loop is divided into two secondary loops: a supply side and a demand side. The plant loop supply side involves energy supplied by various components like pumps, boilers, and purchased heating, among others. The plant loop demand side describes those loop components that demand the energy supplied by the supply-side equipment. Examples of equipment appearing in this loop include coils and radiant heating system.

Figure 6-8 shows the heating plant loop modeled in this simulation. The heating plant supply side consists of a solar collector, modeled as purchased hot water, which served as a link to the solar collector described in Chapter 5. The supply temperature of the fluid in the simulation was fixed at 50^{o}C (122^{o}F) for three reasons. First, this is the supply temperature of most commercially available radiant systems. Second, it is a safe temperature to use; in other words, the concrete and plastic pipes embedded within can withstand it without any sign of deterioration. Finally, by using this supply temperature, the simulation was able to satisfy the preset comfort criterion (a PMV index of ±0.75) throughout the year period.

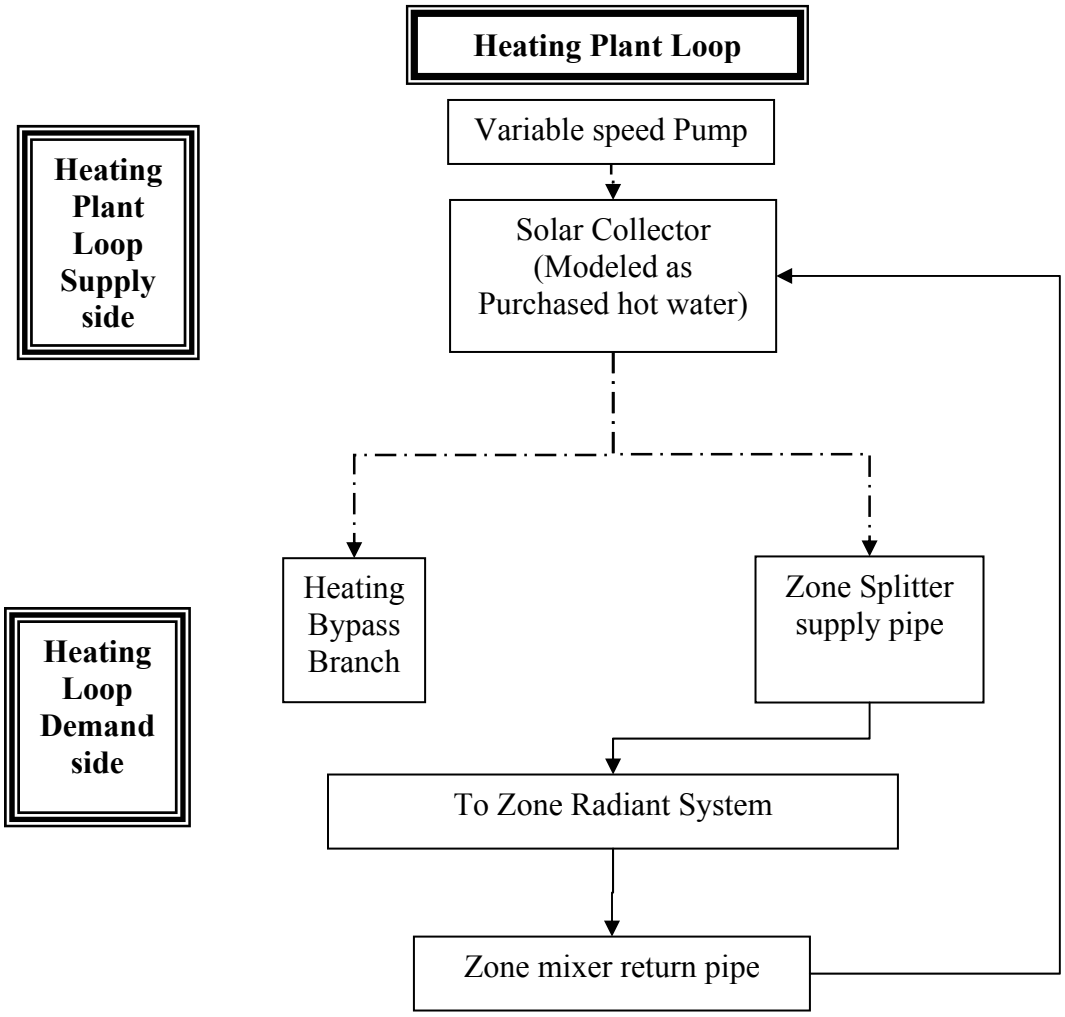

Figure 6-8. Heating Plant Loop

The heating supply side loop is connected to a zone splitter supply pipe that is itself controlled by a thermostat. If the zone requires heating, a valve opens the flow from the purchased heating, and vice versa. The zone splitter then distributes the fluid flow to the low radiant hydronic pipes embedded within the slabs of the different zones. The control temperature thermostat is programmed to heat the space when the temperature drops below 22^{o}C (72^{o}F). In practice, the control thermostat will be adjusted by the occupants to ensure their physiological satisfaction and comfort. The heating demand side loops has a bypass branch to prevent overflows. After the fluid exits the thermal zones it is collected into a zone mixer return pipe that re-circulates it for conditioning to the purchased heating supply side.

6.2.6.2 Condenser Loop

A condenser loop is similar to a plant loop except in one aspect. In a condenser loop, energy is demanded by a chiller condenser. Since the mechanical system being modeled in this simulation has no chiller condenser, this loop was not used.

6.2.6.3 Air Loop

Air loops in Energy Plus define the section of airflow within the system that begins after the zone air return stream and continues until the zone air supply stream. Since all the heating needs should be satisfied using the low radiant system (the plant loop), the air loop described in this model was used only for ventilation. Because ventilation is beyond the scope of this research, the air loop was only modeled to ensure that the simulation replicates real field conditions. The mass flow rate of the incoming air exchanged was fixed at 2/3 of the building volume air exchanges per hour. The building volume for Area Case I is 4071m^3 (143766ft^3). Therefore, the mass flow rate was fixed at 0.75m^3/s (1591cfm). The mass flow rates of the three area cases are shown in Table 6-3.

Table 6-3. Simulated Air Loop Mass Flow Rates for the Three Area Cases

Area (m^2)	**CASE I**	**CASE II**	**CASE III**
Volume (m^3)	4071	407.1	40710
Mass Flow rate (m^3/sec)	0.75	0.075	7.5

Figure 6-9 depicts the simulated air loop. Using a sensible heat recovery air-to-air heat exchanger, outside air is mixed with the zone exhaust air. The air is then passed from the heat recovery system to the zone distribution ducts through the zone supply fan.

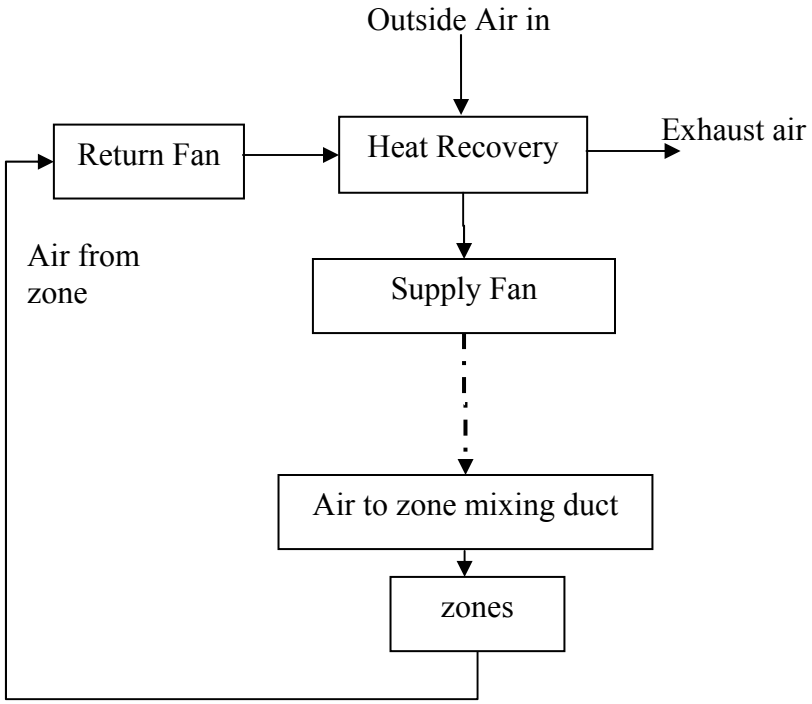

Figure 6-9. Simulated Air Loop

6.2.6.4 Zone Equipment

The zone equipment defines everything, from where the ducts and pipelines are split to serve various zones to where the ducts and pipelines are combined into a single duct. Therefore, any HVAC equipment present within the zone is included in the zone equipment loop. In addition, this loop connects both the air and plant loops to the zones.

In cases where a zone is heated by both an air loop and a plant loop, the zone equipment meets the zone thermal loads according to the equipment priority list. For example, if the designer gave a priority "1" to the air-handling unit and a priority "2" to a low radiant system unit, the program first tries to satisfy the load using the air-handling unit; if this proves insufficient, it will then attempt to use the low radiant system. Zone equipment can also include dampers and reheat coils

The zone equipment modeled in this simulation includes the heating low radiant system, as well as the pipes and ducts serving the zones with ventilated air. The low radiant heat/cool system models a hydronic system that transfers heat by radiation using

water as a heat transfer fluid to supply energy to a building surface. The hydronic system is controlled to meet the zone loads. The modeled hydronic system consists of plastic pipes embedded within the concrete floor slabs, as described in the preliminary design (Stage I of the design evaluation framework) described in Chapter 3. The system is connected to an availability schedule, which in this simulation indicates that the equipment operates 24 hours a day, 7 days a week. The equipment is controlled by throttling hot water flow to the unit. Thus, the mass flow rate of the water varies in order to satisfy zonal comfort conditions.

6.2.7 Design and Sizing Parameters

Energy Plus uses specified design days—at least two, one for winter and another for summer—to calculate each zone's heating and cooling loads and air flow rates. Energy Plus can use these calculated outputs to size the different HVAC components. In addition, in order to satisfy safety concerns, the designer can request the use of a global sizing factor. Only controlled zones can be included in the zone and system sizing simulation. The different component parameters automatically sized by Energy Plus for this simulation include hydronic tubing length, hot water mass flow rates, the volume of the plant loop, and the flow rates and power consumption of the variable speed pump.

6.2.8 Energy Plus Output

Many types of output can be requested from Energy Plus, including outdoor weather conditions; zone window heat gains and losses; internal and external building surface temperatures; convection coefficients; heat gain and losses; zone mean radiant temperature; zone mean air temperature; zone latent, radiant, and convective heat gains/losses; people radiant; and convective, sensible and latent heat gain. In addition, such output as the following can be requested: thermal comfort indices (Fanger and Pierce), sensible heating, and inlet and outlet nodal temperatures of any equipment in the mechanical system being simulated.

Reports of the different outputs can be requested. In this simulation, in order to ensure that thermal comfort needs are always satisfied, requested outputs included the zone mean radiant, mean air temperature, and the Fanger PMV index.

7 STAGE IV - ENERGY STORAGE MODELS – FINITE ELEMENT ANALYSIS

7.1 INTRODUCTION

This chapter presents the storage model that was used in Stage IV of the design evaluation framework for the Blacksburg, Virginia building case study as highlighted in Figure 7-1. A two-dimensional (2D) Finite Element model was developed to determine the temperature profiles in the fluid and phase change material used in this study for energy storage.

Whenever there is a mismatch between available energy and demand, the need for energy storage arises. Such storage also eliminates one of the major disadvantages of solar energy, which is inconsistent supply. Therefore, in this project, it was essential to integrate energy storage into the building's heating system. This section describes that storage system, as well as the finite element formulation used to simulate the heat energy storage and its results.

For this research, latent heat storage was selected. According to this method, heating energy is stored in a phase change material RUBITHERM RT 54, which is itself stored in a well-insulated cylindrical tank, as shown in Figure 7-1. The storage tank contains parallel 6.35mm (0.25in) diameter copper pipes connected to the solar collector. To allow for heat transfer through them, hot fluid is transferred from the solar collector to the phase change material.

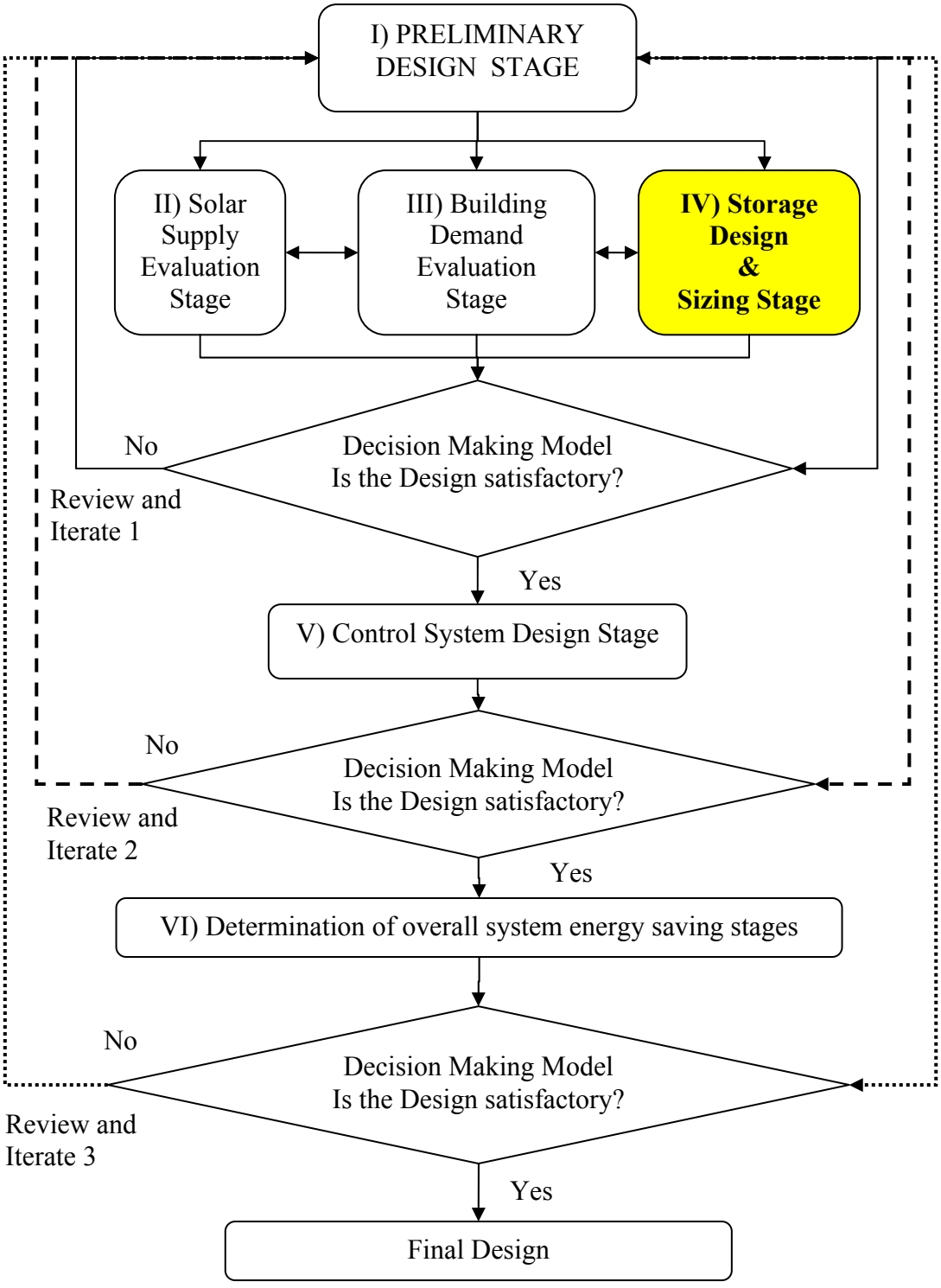

Figure 7-1. Stage IV of the design evaluation framework

7.2 FINITE ELEMENT FORMULATION

A 2D Finite Element model was developed to predict the phase change material temperature, as well as the temperature of the fluid exiting the storage tank. To develop the finite element model of the phase change material storage tank, ABAQUS software Version 6.2 was used (ABAQUS 1998). The developed finite element code represents Section A from the storage tank, as shown in Figure 7-2. Section A, shown enlarged in Figure 7-3, represents a copper pipe serving two phase-change material sections, each of which has a length of 187.5mm (7.4in) and a thickness of 6.35mm (0.25in).

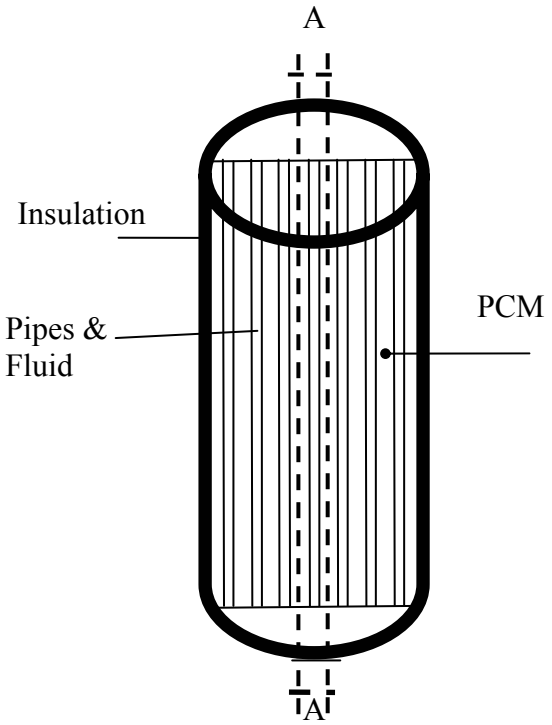

Figure 7-2. Storage Tank

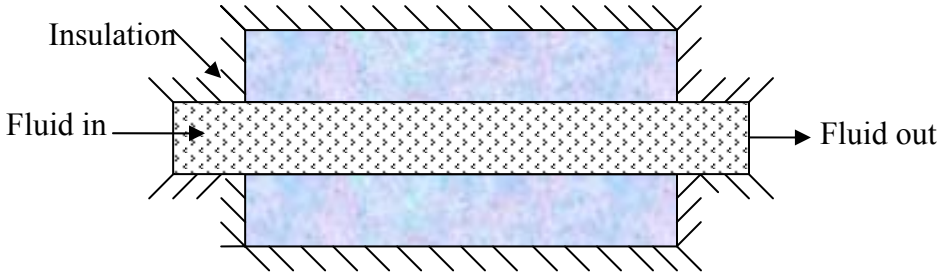

Figure 7-3. Section A Enlarged

The properties of the phase change material chosen for use are listed in Table 7-1, while the properties of the other materials were previously shown in Table 5-1. Thermal properties of water are also shown in Table 7-1 for comparison. Water is usually used for sensible storage (between 1°C and 99°C). In the developed model, conduction and forced convection modes of heat transfer were considered. Additionally, to simulate field conditions, the model is time dependent.

Table 7-1. Phase Change Material Properties

Property	Value (PCM)	Value (Water)
n-paraffin content (%)	85.1	N/A
Molar mass (Kg./Kmol)	377	N/A
Melting point (°C)	55	0
Latent Heat Storage capacity (KJ/Kg) (from 46-61)	179	N/A
Density (solid (at 15°C) Kg/l)	0.90	1.0
Specific Capacity (solid/Liquid) (KJ/Kg.K)	1.8 / 2.4	4.19
Density (liquid (at 70°C) Kg/l)	0.76	1.0
Volume Expansion (%)	18	4.0
Heat conductivity (W/m.K)	0.2	0.58
Kinematic viscosity (70°C) (mm^2/s)	5.80	1.30
Flash point (°C)	220	N/A
Corrosion	Inert	Inert
Toxic	Non-toxic	Non-toxic

7.2.1 Model Dimension and Geometry

The dimensions of the modeled portion (Section A) were 197.5mm x 19.05mm (7.78 inch x 0.75 inch). These dimensions were selected to reduced the potential for edge effect errors while keeping the element size within acceptable limits (modeling constraints). Figure 7-4 shows the general layout of the developed model.

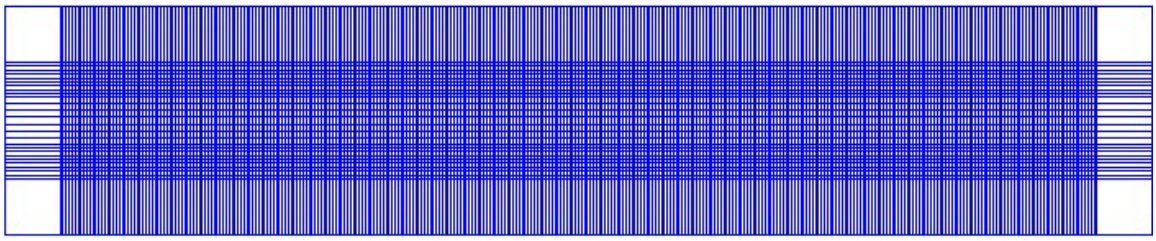

Figure 7-4. General Layout of the Finite Element Used in the Heat Storage Model

The generated mesh distribution was designed to give an optimal accuracy, as can be seen in Figure 7-4. Small elements of 0.8mm were used in the phase change material; elements of 1.27mm, in the fluid; and larger elements of 10mm for the insulation layers. Model geometry dictated the element types and dimensions. Rectangular (DC2D4) elements (4 noded elements) were selected for all materials in the three models, except for the fluids where rectangular (DCC2D4) continuum elements were used to simulate the forced convection with dispersion control that would here take place. All layers were simulated with the same shape to preserve the continuity of nodes between consecutive layers. In total, 9504 elements were needed to simulate the model.

7.2.2 Model Constraints

The heat transfer mechanisms taking place within the system include:

- Convective heat exchange between the environment and the PCM tank insulation.
- Conductive heat transfer within the PCM.
- Conductive heat transfer between the copper pipe's outside wall, and the PCM.
- Convective heat transfer between the fluid and the copper pipe's inside wall.
- Forced convective heat transfer within the fluid.

The main thermal modes governing these mechanisms are shown in Figure 7-5. The control strategy indicates that inlet fluid temperature is a user-defined parameter, which varies according to the fluid outlet temperature calculated by the solar collection model and the fluid path taken.

7.2.3 Sizing of the Storage Tank

The size of the storage tank is determined based on the difference between energy collected and consumed, according to Equation 2-24:

$$Q = mc_{ps}\,\Delta\theta_s + m\lambda + mc_{pl}\,\Delta\theta_l \qquad (7\text{-}1)$$

where

$\Delta\theta_s$ = the change in PCM temperature from its initial solid temperature to the temperature where it starts to change phase;

$\Delta\theta_l$ = the change in PCM temperature from the temperature where phase change ends, to its final liquid temperature;

m = the mass;

c_{ps} = the specific heat of the solid PCM;

c_{pl} = the specific heat of the liquid PCM; and

λ = the heat of phase transformation.

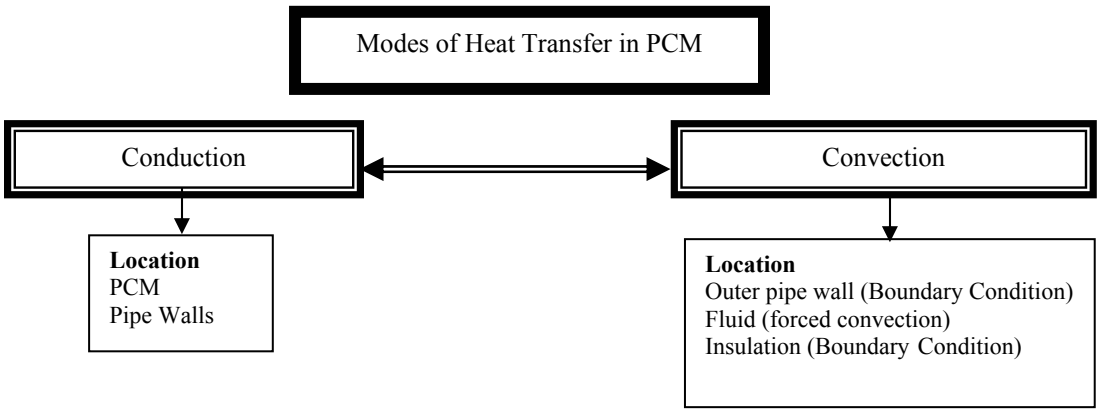

Figure 7-5. Modes of Heat Transfer in the Heat Storage Model

Ideally, the storage tank should satisfy 100% of the building's energy needs left unsatisfied by collection alone. However, the size of a tank that would achieve this goal is quite large, and thus quite impractical and probably cost-prohibitive. Therefore, this research will measure against the potential savings in renewable energy the alternative storage sizes that can satisfy a) the night cycle under worst conditions, b) one-day energy consumption in January, c) three-day energy consumption in January, and d) the consumption of an average winter month (i.e. February). The outcome of this analysis represents a trade off between the size of the storage tank and the potential energy savings.

8 STAGE V - CONTROL STRATEGY

8.1 INTRODUCTION

It is generally recognized that how a building is operated significantly impacts its energy use and that a poorly operated building can overwhelm even the best energy-conserving design. It is also accepted that the use of control will lead to improved system efficiencies (Farris et. al. 1980). Therefore, in this research, it was essential to integrate within the proposed active solar system a simple yet efficient method of control.

This chapter describes the development of the control system design for the Blacksburg, Virginia building - (Stage V of the proposed design-evaluation framework highlighted in Figure 8-1). The output of the three developed models for Stages II, III and IV of the design evaluation framework, described earlier, were used to determine the best control strategy for minimizing energy consumption while keeping the thermal zones within the comfort level and satisfying the building's hot water requirements. This control strategy regulates and ensures efficient operation of the active solar collection system.

The control system of any building can be compared to a central computer the branches of which extend to all components, ending in sensors and activators. In that respect, it also acts very much like the human brain, which controls all parts of the body's central nervous system. The main function of the control system is to integrate and control the transfer of energy from one component of the network to another, whether that component is a zone, a storage tank, the grid, or the collector. Therefore, it can be concluded that the controls in an active solar system have to:

1. Regulate the automatic collection and distribution of solar energy either to the storage or to the load by activating pumps, blowers and valves.
2. Operate the auxiliary heating system in conjunction with the solar thermal system.

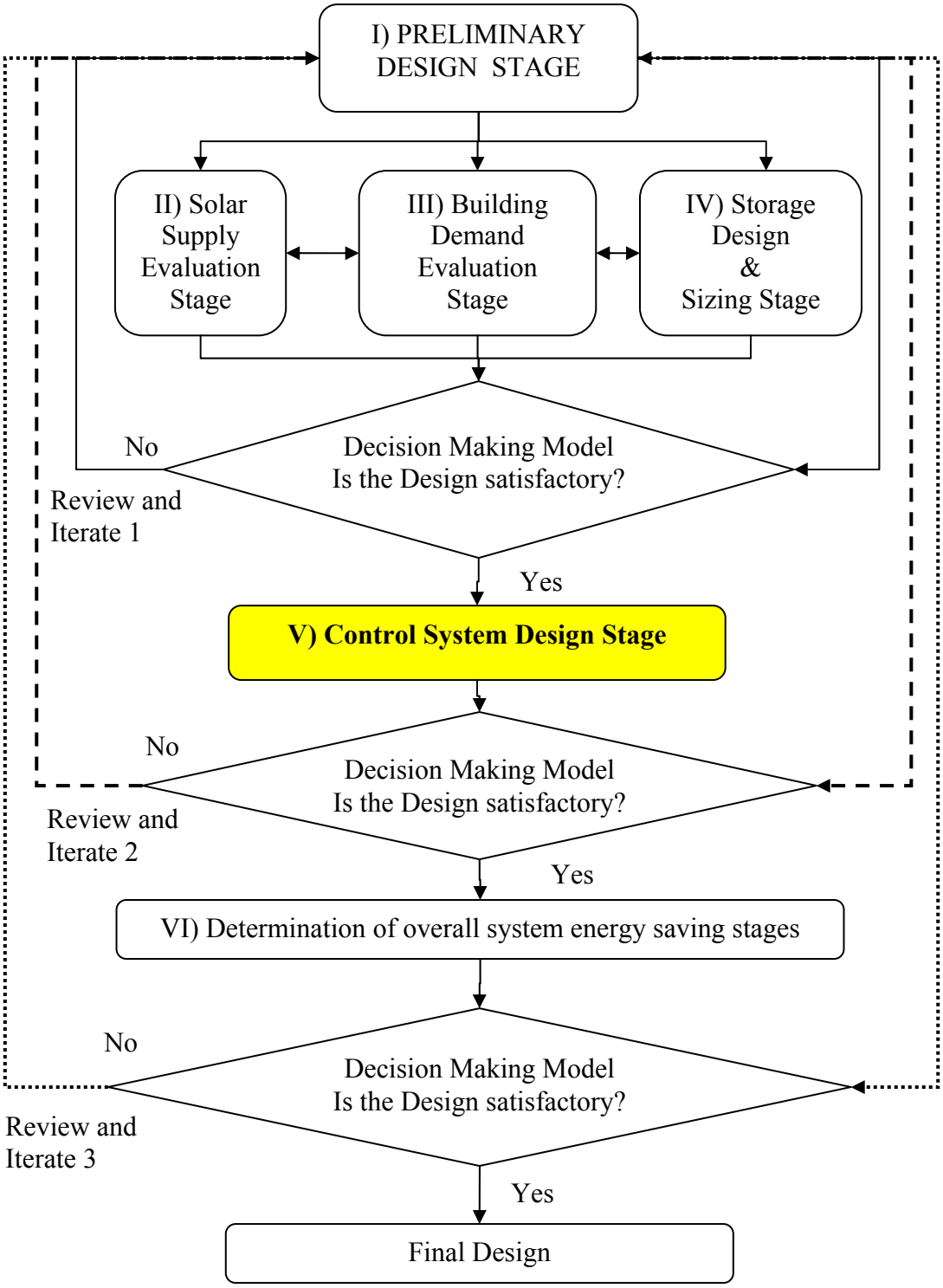

Figure 8-1. Stage V of the design evaluation framework

The control strategies and equipment that can be used to serve solar collection systems are quite simple; in several aspects, they are similar to those of conventional systems. The main difference between the controls used for solar collection systems and those used for conventional ones is the need for differential temperature (e.g. a collector storage differential or storage building differential) measurement rather than simple temperature sensing. The temperature differential can be measured using a temperature measuring instrument e.g. thermocouples or thermistors, while the room temperature is measured using conventional thermostats. The next section will describe the proposed control strategy, then suggest different hardware components that can be used to build the control system.

8.2 CONTROL SYSTEM DESCRIPTION

Automatic control of the solar thermal system can be accomplished by controlling the fluid circulation pump as well as the fluid path. The latter can be altered based on changes either in system and service temperatures or in the level of solar irradiance and ambient temperatures. The control system sends electrical signals to the fluid pump to adjust the flow rate and to the pipe valves to alter the fluid path. The mechanical configuration of the space heating and hot water system is shown in Figure 8-2.

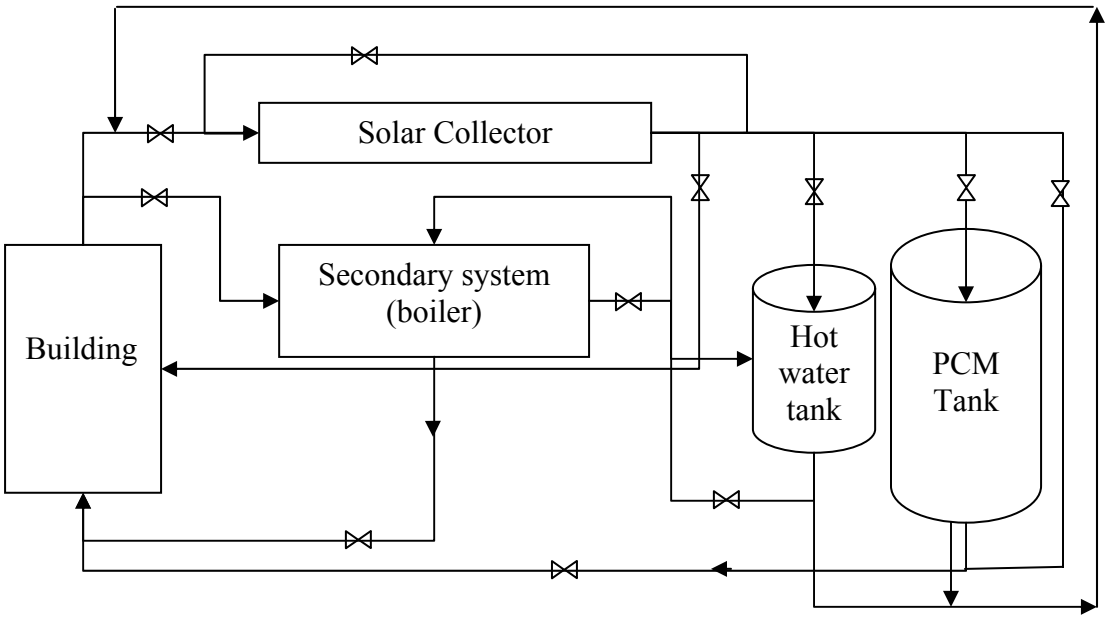

Figure 8-2. Combined Space Heating and Hot Water Configuration

The control strategy utilized for this research was divided into four levels. The first level defines the fluid flow path and mass flow rates of nearly all components shown in Figure 8-2; the other three levels are used to control the simulation within the building thermal load block. The first control level contains five fluid paths, as shown in Figure 8-3:

- If the fluid outlet temperature (T_o) from the solar collector (output of Stage II of the design evaluation framework) lies between 40°C and 60°C, Path A becomes operational. In Path A, to satisfy the building's thermal loads and hot water requirements (input to stage III of the design evaluation framework), the hot fluid is circulated between the solar collector and the building thermal zones and hot water tank.

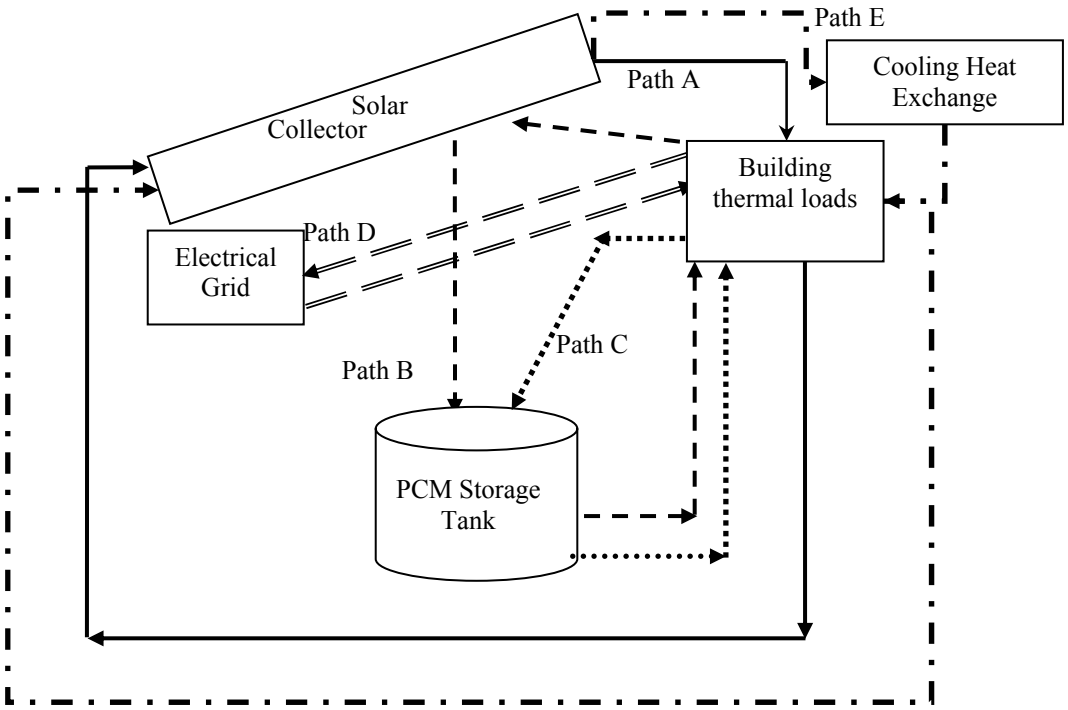

Figure 8-3. Alternative Energy Supply Passages

- If the fluid exiting the solar collector's temperature (T_o) (output of Stage II of the design evaluation framework) increases above 60°C but is less than 100°C, and the temperature of the storage tank (Stage IV of the design evaluation framework) is 5°C or more below the fluid temperature, the fluid path is switched to Path B. Path B transports the hot fluid from the solar collector, (output of Stage II of the design evaluation framework), to the storage tank (input to Stage IV of the design evaluation framework), where the excess energy is stored until the fluid's temperature is around 50°C, at which it can be released from the tank. The fluid is then transferred to the thermal zones and the hot water tank (input to stage III of the design evaluation framework), where it supplies the building's thermal loads before being returned to the solar collector (input to stage II of the design evaluation framework), This path is followed until the temperature of the fluid exiting the tank falls below 60°C.

- If the fluid temperature (output of stage II of the design evaluation framework) increases above 100^{o}C, two actions take place:

1) The fluid path is switched to Path E. Path E transports the hot fluid from the solar collector (output of stage II of the design evaluation framework) on the south roof to the cooling heat exchanger embedded in the north roof. This process ensures that the structural integrity of the building remains unaffected by the temperature of the fluid as it passes through. Fluid exiting the heat exchanger can join either Path A (input to stage III of the design evaluation framework) or Path B (input to stage IV of the design evaluation framework) depending upon its temperature and the need for storage (for example, if there is a temperature differential between the fluid and the storage tank).
2) The mass flow rate of the fluid increases until the fluid outlet temperature drops below 100^{o}C, then it remains constant.

- In cases where the change in the fluid temperature (output of stage II of the design evaluation framework) as it passes through the solar collector equals zero or less (e.g., night hour and low solar radiation hours), the flow within the solar collector will shut itself off. During that time, the needed energy is drawn either from the PCM storage tank (Path C) (output of stage IV of the design evaluation framework) or, if the stored energy is insufficient, from the grid (Path D).

As described in Chapter 6 and as shown in Figure 8-2, the building's thermal load blocks consist of a hot water tank that supplies the building with its needed hot water and 32 different thermal zones. The fluid path within the building starts at the hot water tank, (T_w^{o}C), then, beginning at the top floor to minimize loss during transportation, travels through each zone in turn. The control within the building blocks is achieved on three levels: a macro-level, the zone control; a micro-level, the equipment on/off and heat/cool control; and a level that links the micro and the macro levels. The macro-level control determines the thermal load required to maintain the zone's thermal comfort conditions, as defined by the designer, while the micro-level control allows the equipment to supply the zones' heating/cooling demands.

The zones are controlled using thermostatic control. The thermostat sets the temperature within the zone to a specific set point specified by the designer. If the temperature within the zone falls below the set point, the control will use the heating equipment to heat the zone.

On the other hand, the micro-level control regulates the operation of heating equipment, which is controlled by both on/off switch and space condition schedules. The on/off switch control allows the tenants to specify when the equipment will be shut down, regardless of space conditions. This feature is very useful in cases where the occupants are away from the residence for long periods, such as during vacation. The space condition control evaluates the conditions within the space and alters the fluid mass flow rate to maintain comfortable conditions. This process is achieved as a result of heating and cooling set point schedules being defined for every zone. These schedules can differ from those specified for the zone control (the macro-level).

The third or linking level control reads the system's demand, which is determined by the macro-level or zone control, and determines, based upon the designer's maximum capacity specifications, which component of the equipment should meet the load. After the linking control assigns the task to a specific piece of equipment, in order to meet the demand, the micro-level control takes over.

8.3 CONTROL SYSTEM ALGORITHM

In the simulation, the control system described in the previous section was used. The level one control algorithm is as follows:

- Input start and finish dates and hours of the simulation.
- Read the ambient temperature, the solar radiation, and the wind speed from the weather files.
- Calculate the convection coefficient and the incidence angle of the solar radiation.
- Update the collector model file and execute for an hour period.
- Read the output temperature of all model layers (copper pipe, concrete layers, insulation, glass and air) and write them in a text file.
- Update the initial temperature of the aforementioned layers for the second iteration.

- Read the output fluid temperature from the collector model result.
    - If the output fluid temperature (T_{out}) is below fluid inlet (T_{in})temperature:
        - Shut collector model off.
        - Check the temperature differential between the storage tank and the zone temperatures. If $T_{storage} > 5^{o}C$, supply the radiant system from storage tank; otherwise, heat the fluid using an electric heater, then supply from the radiant system
    - If the output fluid temperature is $T_{in} < T_{out} < 60^{o}C$:
        - Supply fluid to the radiant system (update energy plus plant loop schedule using T_{out}) to heat the building and execute the Energy Plus model.
        - Read the output fluid temperature of the radiant system from the energy plus model and input that temperature as Tin in the solar collector model to prepare for the simulation of hour 2.
    - If the output fluid temperature is $T_{in} < 60^{o}C < T_{out} < 100^{o}C$:
        - Supply fluid to the storage tank model.
        - Execute storage model.
- Read the output temperature of all storage model layers (PCM and copper pipe) and write them in a text file.
- Update the initial temperature of the layers for the second iteration.
- Read the output fluid temperature ($T_{storage\ out}$) from the storage model result.
    - If the $T_{storage\ out} < 60\ ^{o}C$:
        - Input that temperature as T_{in} in the solar collector model to prepare for the simulation of hour 2.
        - Increase mass flow rate of fluid in tank until temperature = $60\ ^{o}C$.
    - If the $T_{storage\ out} \geq 60\ ^{O}C$:
        - Supply fluid to the radiant system (update energy plus plant loop schedule using T_{out}) to heat the building.
        - Execute the Energy Plus model.

        - Read the output fluid temperature of the radiant system from the energy plus model and input that temperature as Tin in the solar collector model to prepare for the simulation of hour 2.
        - If the output fluid temperature is $T_{in} < 100^{o}C < T_{out}$
        - The mass flow rate of the fluid is increased by 0.25% until the temperature drops below $100^{o}C$.
- Read next date and repeat.

The process is repeated until the specified simulation dates are accomplished. The other three control levels within the building thermal load block were simulated using Energy Plus software, (the model used in stage III of the design evaluation framework), using the zone control (macro control), the low radiant system control (the micro control), and the plant condenser control (the linking control). The macro-level control (the zone control) consists of a thermostatic controller for each zone. Within Energy Plus, the thermostatic control set point is defined according one of five control choices:

- Uncontrolled.
- Single Heating/Cooling Set Point: specifies that at a specific single set point, the zone needs to be heated, while above that set point, the zone needs to be cooled. Only heating or cooling can be specified at any given period under this control type.
- Single Heating Set Point: specifies a heating-only thermostat with a set point. Below that specific set point, the space must be heated.
- Single Cooling Set Point: specifies a cooling-only thermostat with a set point. Below that specific set point, the space will need to be cooled.
- Dual Set Point with Dead Band (heating and cooling): used for a heating and cooling thermostat, where set points for both can be scheduled for any given period.

The macro-level control (the zone control) used in this simulation involves a single heating set point. The heating schedule specifies that the building should be heated whenever the zone temperature is below $22^{o}C$ ($71.6^{o}F$) in the winter and $15^{o}C$ ($59^{o}F$) in the summer.

The micro-level controls the low radiant system by both on/off switch and space condition schedules. In this simulation, the on/off schedule is always *on*. For every zone, the space condition schedule specifies a heating set point schedule, which can be different from the schedules specified for the zone control (the macro-level). The low-radiant system heating and cooling temperature schedule specifies a set point temperature wherein the flow rate to the system is at half the maximum flow rate. In addition to a user-specified (or system-sized; see Chapter 6) maximum mass flow rate, Energy Plus uses the set point schedules to control the fluid mass flow rate to each zone: the flow rate is varied between zero and the maximum value until comfort conditions are met. The low radiant heating and cooling set points can vary with the mean air temperature, the mean radiant temperature, or the operative temperature, according to designer preference. In this simulation, whenever the zone temperature is below heating set point 26^{o}C (78.8^{o}F), hot fluid is allowed inside the space.

As determined by the macro-level or zone control, the plant condenser control reads the system's demand and then uses the designer's maximum capacity specifications to choose which equipment should meet the load. After the plant condenser control assigns the task to specific equipment, the micro-level control takes over to meet the demand. In this simulation, the plant condenser control assigns the system to *purchased heating* (Chapter 5) simulating the solar collector (heating supply).

8.4 DEVIATIONS FROM THE ALGORITHM

The Level 1 control strategy described above was programmed using Java to serve as a link for automatically executing the three simulation models used for evaluation of Stages II, III, and IV of the design evaluation framework (Suman 2003). A copy of the Java program is presented in Appendix C. Unfortunately, the Energy Plus program works only in a Windows or a Linux environment, and the FE models are executed in an SGI-IRIX environment, a situation making it difficult to link them in a single environment. To solve this problem, a simplification was introduced into the control algorithm.

Whereas the initial algorithm proposed changing the plant loop supply temperature, the simplification involved executing the Energy Plus program under Windows using a constant heat loop supply temperature of 50^{o}C for a year period. That

temperature was chosen because it is the supply temperature of most commercially available radiant systems, it is a safe temperature to use, and with it, the simulation was able to satisfy the preset comfort PMV criteria (+/-0.5) throughout the year period. The resulting Energy Plus output nodal temperature of the fluid exiting the radiant system was written in a text file (EP.txt) that was placed in the SGI-IRIX where finite element analysis was executed. In the revised algorithm, whenever the control strategy requested that Energy Plus be executed, the execution step was replaced by reading the output temperature of Energy Plus from the Energy Plus solution text file.

To ensure that this simplification does not affect the accuracy of the simulation, it was assumed that whenever the collector heats the fluid to a temperature below 50^{o}C (Energy Plus supply temperature), the electrical grid boosts the fluid temperature back to the needed supply temperature. The need for conventional energy supply throughout the year is discussed in the Results section of this study. Using the Energy Plus model, the collected hourly heat energy was compared against the building's required hourly heat energy. The amount of energy supplied by the collector is determined by this comparison, the results of which are presented in Chapter 9.

8.5 CONTROL SYSTEM COMPONENTS

A primary component of the control system is the closed or feedback loop, which is utilized when the actual changes in the controlled variables—the fluid mass flow rate, the fluid temperature, the zone temperature, and the humidity—are measured, and the controller changes the controlled device based upon these measurements. The corrective action continues until the variable is brought to a desired value within the design limitations of the controller. This loop can be used in the solar collector to adjust the fluid mass flow rate when the fluid temperature increases over 100^{o}C in the summer and in the storage tank to ensure the exit fluid temperature is more than or equal to 50^{o}C (the low radiant system supply temperature). A typical feedback control loop is shown in Figure 8-4.

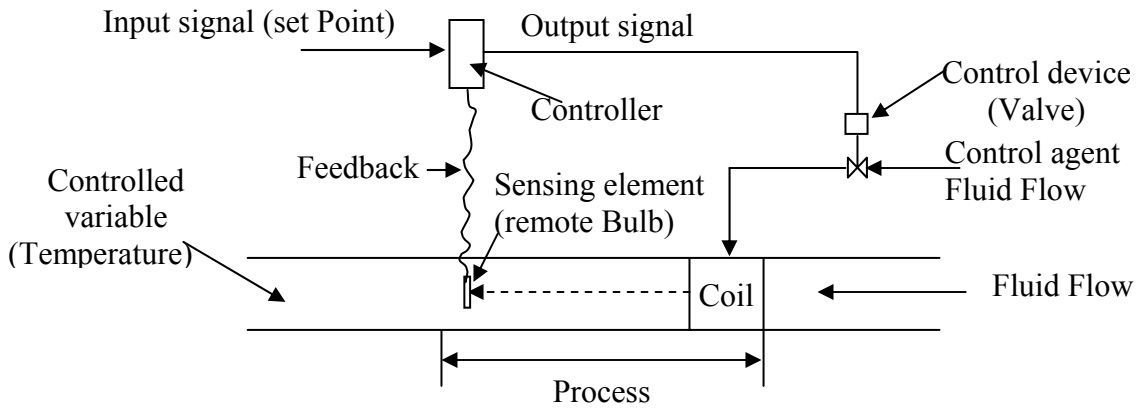

Figure 8-4. A Typical Feedback Control Loop

The feedback loop consists of a sensor (e.g. a thermocouple), that measures the controlled variable (e.g. fluid temperature) and transmits to the controller (e.g. data acquisition system) a signal having a pressure, voltage, or current value proportional to the value of the variable being measured. The controller compares this value with the set point and signals the controlled device to undertake corrective action

The controller generally includes hardware, as in thermostats and humidistats, or software, as in any digital device that receives and acts on data on a sample rate basis, e.g. digital algorithms (ASHRAE 2001). A digital controller automatically uses a series of if-then rules that emulates the way a human operator might control the processes. The controlled devices used to regulate the fluid flow are known as *valves*, of which there are many automatic types:

- A Single-Seated Valve: designed for tight shut off.
- A Double-Seated Valve: designed so that the media pressure acting against the valve disk is balanced. This type usually is used if the fluid pressure is too high to be shut off using a single seated valve; however, it cannot be used for a tight shut off.
- A Three-Way Mixing Valve: contains two inlet connections and one outlet. It is used to mix two fluids entering the inlet connection.
- A Three-Way Diverting Valve: contains one inlet and two outlet connections and has two separate disks and seats. It is used to divert flow to either of the outlets or to proportion the flow to both outlets.

The three way diverting valve and the single seated valves will be used to distribute the flow within the predetermined fluid passages (see Figure 8-2 and 8-3) or to shut down the flow. A pneumatic valve actuator, consisting of a spring-opposed flexible diaphragm attached to the stem valve, can be adjusted to regulate the fluid mass flow rate (ASHRAE 2001).

The device that responds to the change in the controlled variable is called a *sensor*. Its response is usually a change in some physical or electrical property available for translation or amplification by the controller. The following should be considered when selecting a sensor for a special application:

- Operating range of the controlled variable,
- Compatibility of the controller's input,
- Accuracy and repeatability,
- System response time,
- Control agent properties, and
- Durability of the sensor.

In the proposed control system, three main types of sensors are used: temperature, humidity, and flow rate. Temperature sensing elements fall into one of three general categories: a) those that use a change in relative dimension due to differences in thermal expansion; b) those that use a change of a state in a vapor or a liquid; and c) those that use a change in some electrical property. Many different types of sensors exist in each category. Those most commonly used in heating, ventilation and air conditioning include (ASHRAE 1999):

- A *bimetal element*, which consists of two thin strips of dissimilar metals fused together. Since the two metals have different coefficients of thermal expansion, the element bends and changes position as the temperature varies. This type is commonly used in room and immersion thermostats.
- A *rod and tube element*, which consists of a high expansion metal tube containing a low temperature rod. One end of the rod is attached to the rear of the tube. The tube

changes length with changes in temperature, causing the free end of the rod to move. This element is commonly used in certain insertion and immersion thermostats.

- A *remote bulb element*, which consists of a bulb or capsule connected to a sealed diaphragm by a capillary tube; the entire system is filled with vapor, gas or liquid. Temperature changes at the bulb cause volume or pressure changes that are transferred to the diaphragm through the capillary tube. The remote bulb element is useful where the temperature measuring point is remote from the desired thermostat location.
- A *thermistor*, which is a semiconductor that changes electrical resistance with temperature. Its resistance decreases as the temperature increases. Thermistors are relatively low cost and have a large charge in resistance for small changes in temperature.

All of the above temperature sensors can be used in our control system. They will be installed in the building thermal zones, as well as in the hot water storage tank, solar collector, and PCM tank. They will also be installed in the fluid flow to measure its inlet and outlet temperatures.

Humidity sensors, also called *hygrometers*, are used to measure relative humidity, dew point, or absolute humidity of ambient or moving air. The most important of these measurements for our control system is relative humidity, since if the psychometric chart was programmed and measured it as well as the temperature; human comfort conditions can be verified. Relative humidity can be detected using either mechanical or electronic hygrometers. Mechanical hygrometers operate on the principle that a hygroscopic material, like nylon, retains moisture and expands when exposed to water vapor. The change in size or form is detected by a mechanical linkage and converted to an electronic signal. Electronic hygrometers use either resistance or capacitance sensing elements. The resistance element is a conductive grid coated with a hygroscopic or water absorbent substance. The conductivity of the grid varies with the amount of retained water; thus the resistance varies with relative humidity. The capacitance element involves a stretched membrane of nonconductive film. It is coated on both sides with metal electrodes and mounted in a perforated plastic capsule. Although it responds non-linearly to relative

humidity, the signal can be linearized (ASHRAE 2001). The relative humidity will be measured in all of the building thermal zones.

There are many devices that can be used to measure fluid mass flow rate, some of which are less expensive and simple to use, like the orifice plate, pitot tube, and venturi. However, these devices possess a limited range, so accuracy depends on their location. Other devices—like turbine, magnetic, and vortex-shedding meters—usually have better range and are more accurate over a wide range (ASHRAE 2001). In our system, to avoid high costs, we recommend using the less expensive devices and locating them close to the regulating device.

9 BLACKSBURG CASE STUDY RESULTS AND ANALYSIS

This chapter presents the results of the three developed models, presented in chapters 4, 5, 6 and 7, for the Blacksburg, Virginia building case study representing Stages II, III, and IV of the design evaluation framework, as well as provides a comparative analysis of the building energy consumption versus the collection system energy supply. This analysis was used in determining the overall energy savings of the system (Stage IV of the design evaluation framework). The results of each model are presented first, and then the overall saving analysis is described.

9.1 STAGE II - ENERGY SUPPLY

To evaluate the solar supply evaluation stage (Stage II of the framework, the solar collection system was evaluated using the model described in Chapter 5 on an hourly basis for a year period. The major output of the finite element analysis was the fluid outlet temperature exiting the collector. For a typical day in May, January, and July, the fluid temperature in the solar collector and the collector temperature distribution are shown in Figures 9-1 (a and b), 9-2 (a and b) and 9-3 (a and b) at an operational mass flow rate of $0.0005 m^3/hr$. These figures show that the fluid temperature increases as it enters the collector and that it reaches its maximum as it exits. The temperature profile of the solar collector indicates that since it minimizes collector backing and edge losses the insulation thickness is quite adequate.

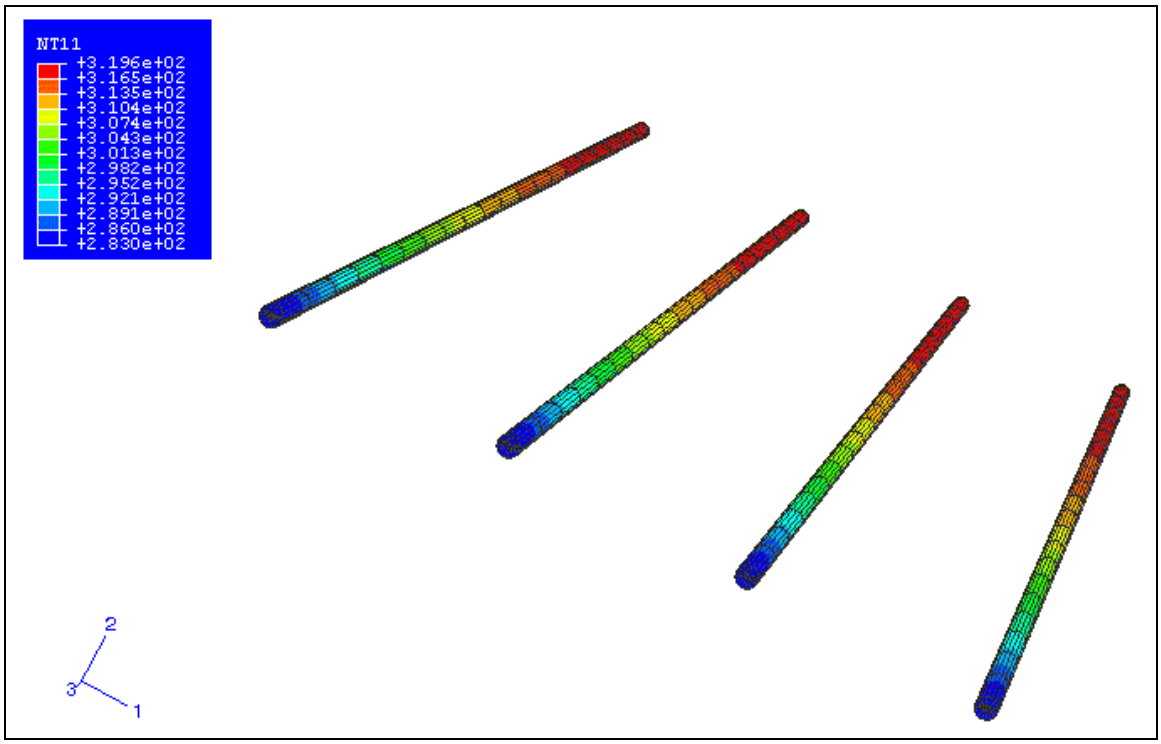

(a)

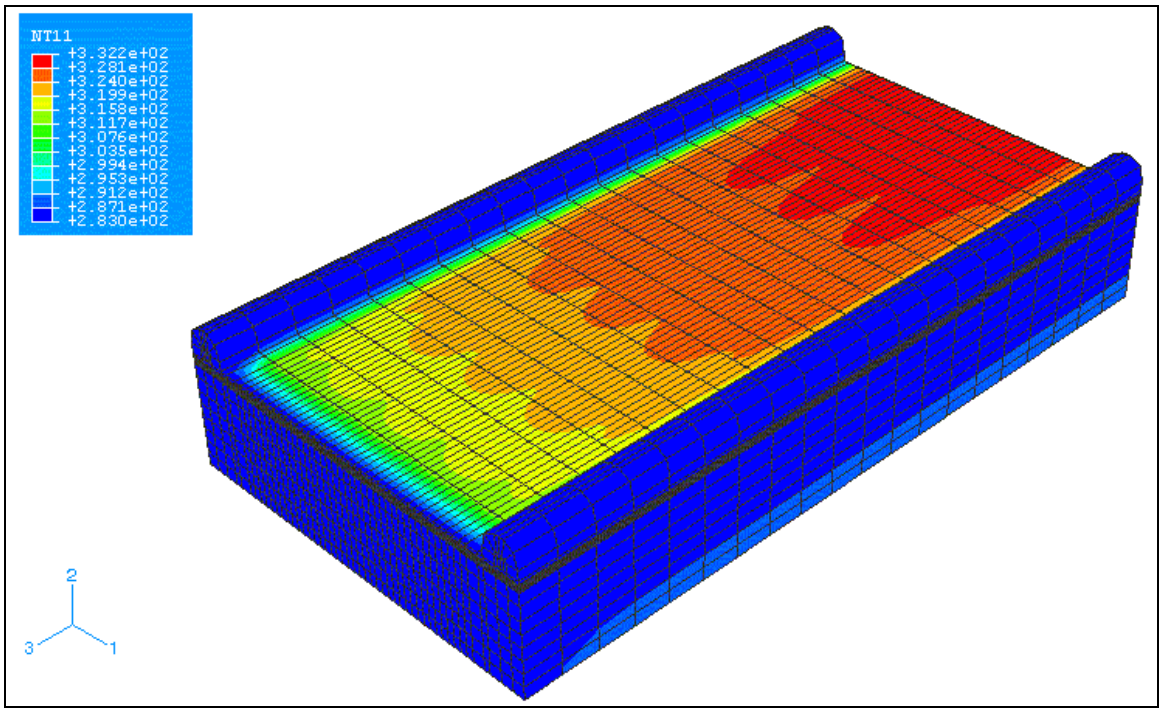

(b)

Figure 9-1. Temperature Distribution in the (a) Fluid and (b) Solar Collector during noon in May (600W/m^2)

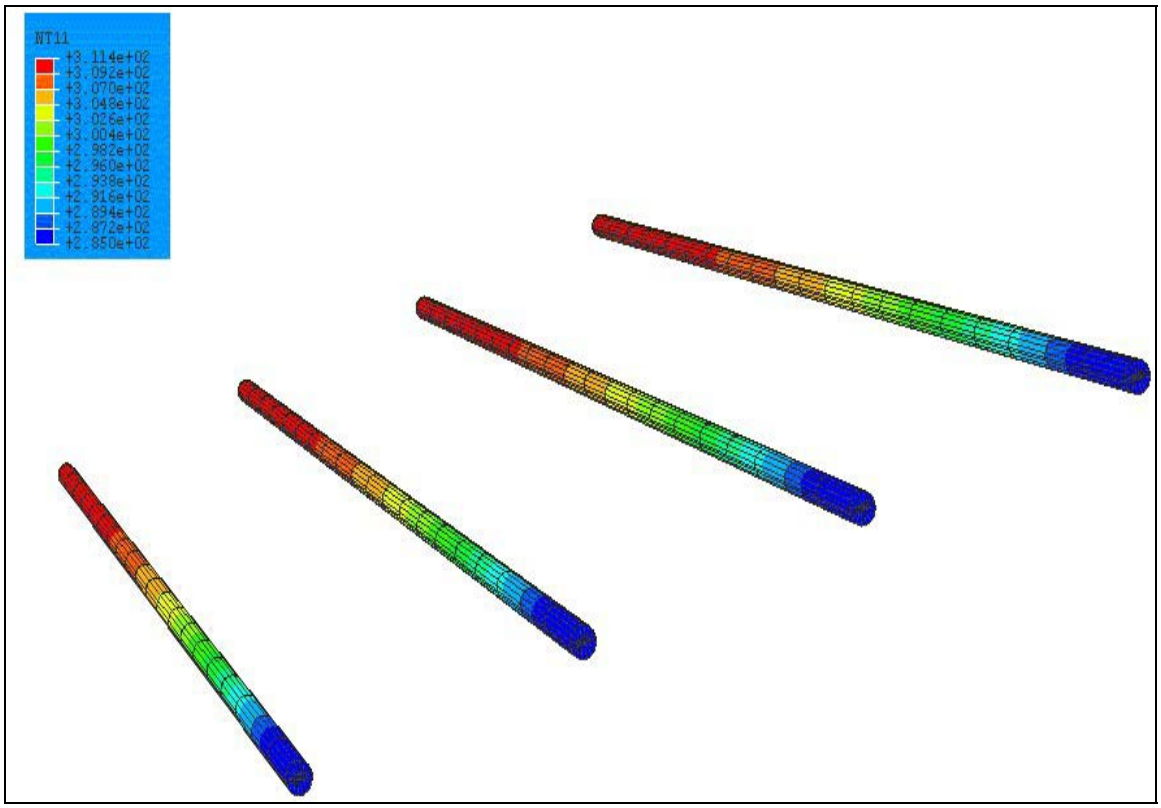

(a)

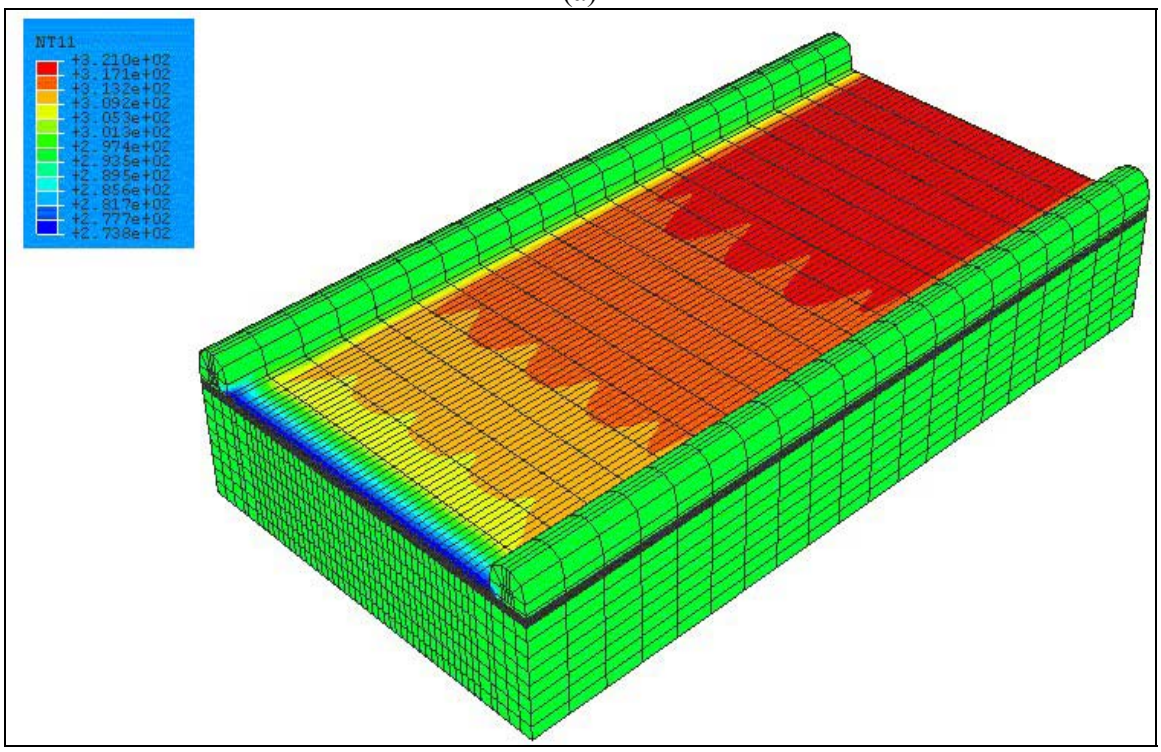

(b)

Figure 9-2. Temperature Distribution in the (a) Fluid and (b) Solar Collector during noon in January (540W/m^2)

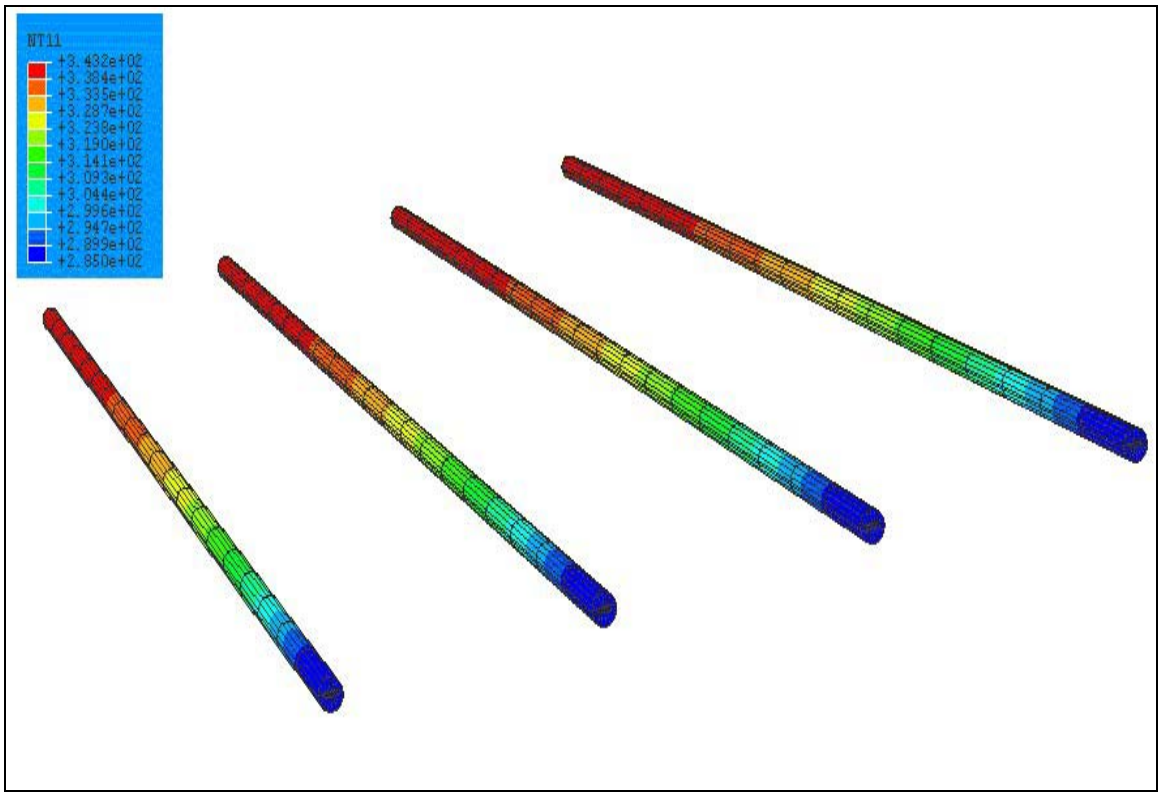

(a)

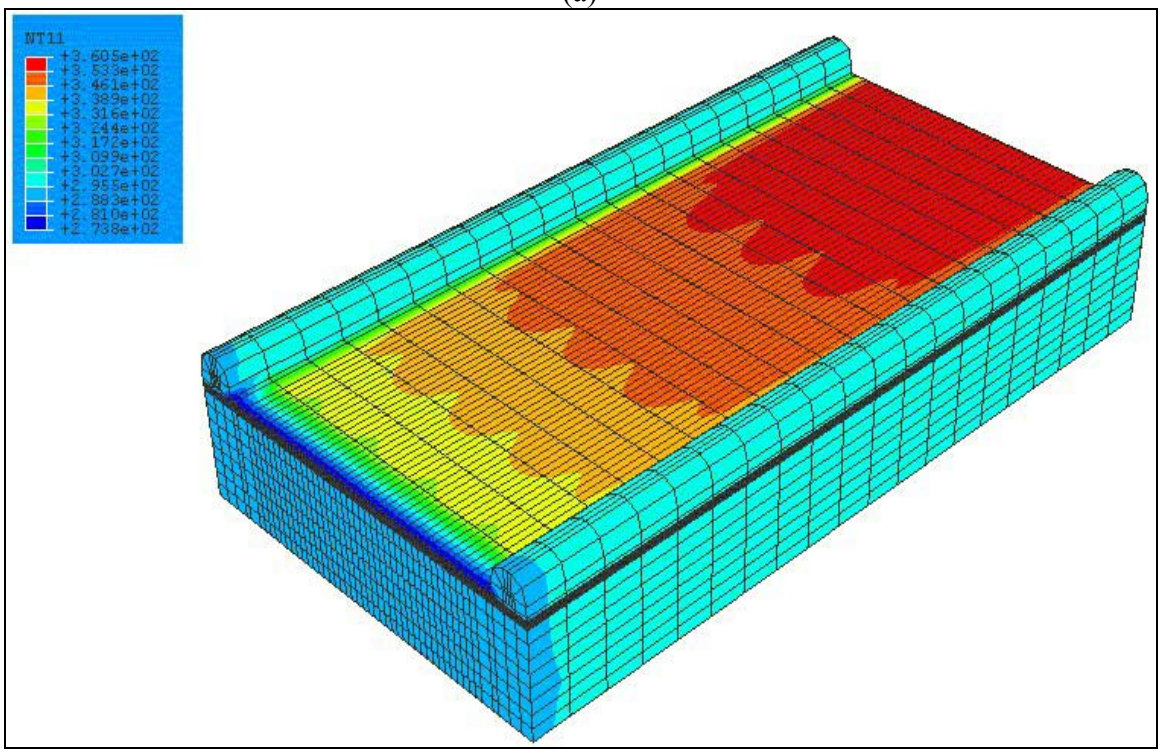

(b)

Figure 9-3. Temperature Distribution in the (a) Fluid and (b) Solar Collector during noon in July (850W/m^2)

Figure 9-4 presents the fluid temperature exiting from the solar collector under winter and summer conditions. For a mass flow rate of 0.0005m^3/hr, the maximum temperature achieved in the summer is 111°C, corresponding to an 86°C increase above the ambient temperature. During January, the maximum fluid temperature exiting the collector is 59°C. The temperature increases to a maximum of 74°C in February, and it continues to increase gradually until it reaches its peak in July.

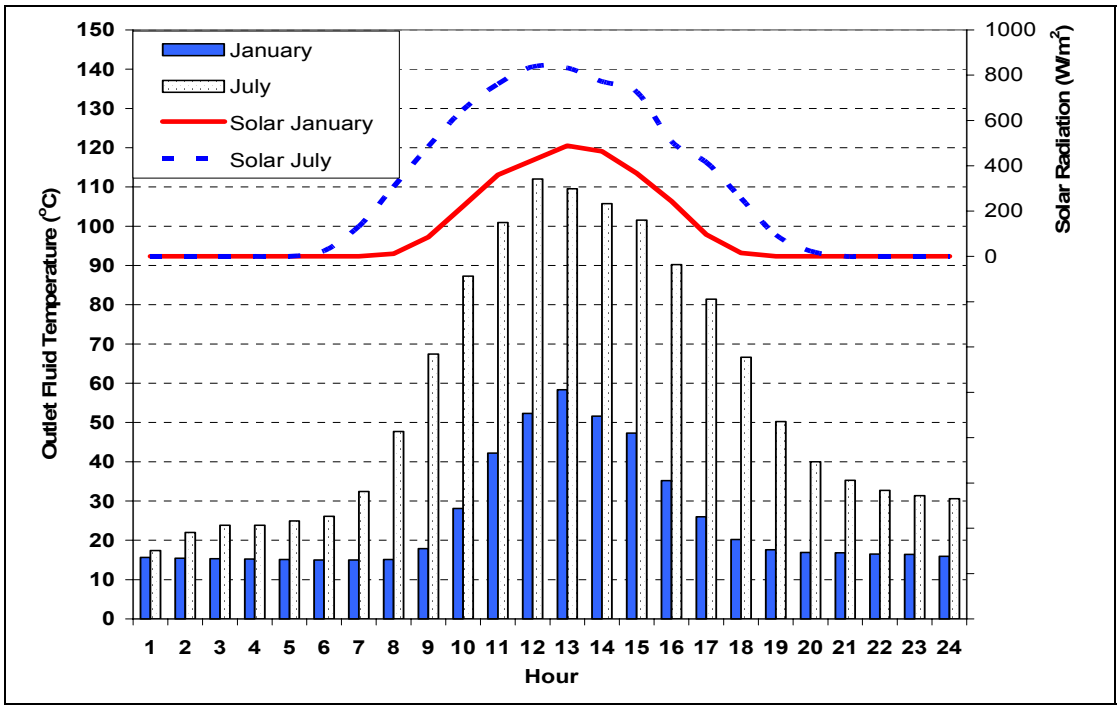

Figure 9-4. Performance of the Solar Collector under Winter and Summer Conditions

Whenever a solar heat flux of 150W/m^2 or lower is encountered under all weather conditions, the collector experiences losses. Therefore, it is recommended that the solar panel be switched off not only during night hours but also below a solar flux of 150W/m^2 so that it can act as a normal insulated roof. As the solar intensity increases to between a solar heat flux of 150 and 300W/m^2, the heat gain increases slightly. There are no losses experienced in this range, but the temperature increase is not enough to be used as a heat source for the building. When the solar flux is greater than 300 W/m^2, the panel can generate enough energy to heat the structure and to act as a supplementary energy source, if needed.

The solar evaluation design stage recommends varying the different operation and design parameters to maximize the outlet fluid temperature and the heat gain. Therefore, each of the design and operation parameters was varied. The outcome of this variation is summarized in the following paragraphs.

Different pipe diameters—25.0 mm (1.0 inch), 12.7 mm (0.5 inch), and 6.35 mm (0.25 inch)—were simulated to maximize thermal efficiency. The most efficient diameter was found to be 6.35mm (0.25 inch), since it both allows for a more consistent temperature distribution within the cross section of the fluid and is more cost effective. When larger diameters were used, the temperature distribution was less uniform within the fluid's cross section. Figure 9-5 shows how the fluid nodal temperature varied for different cross sections.

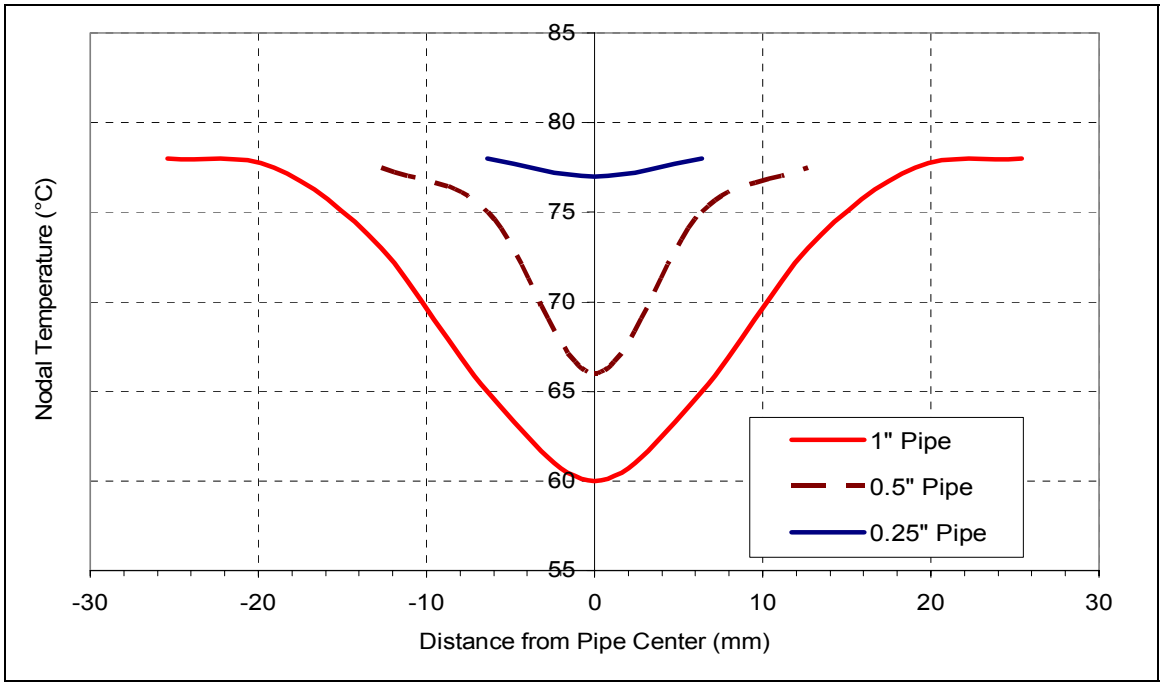

Figure 9-5. Variation of Fluid Nodal Temperature across the Pipe Diameter at a Solar Intensity of 800W/m^2

Varying the operational parameters—the mass flow rate and inlet fluid temperature—greatly impacts the amount of heat gain (Q). In general, since it is exposed for a longer period to the solar radiation, as the fluid mass flow rate decreases, the fluid temperature increases. Figure 9-6 shows how the maximum water temperature varies with the mass flow rate.

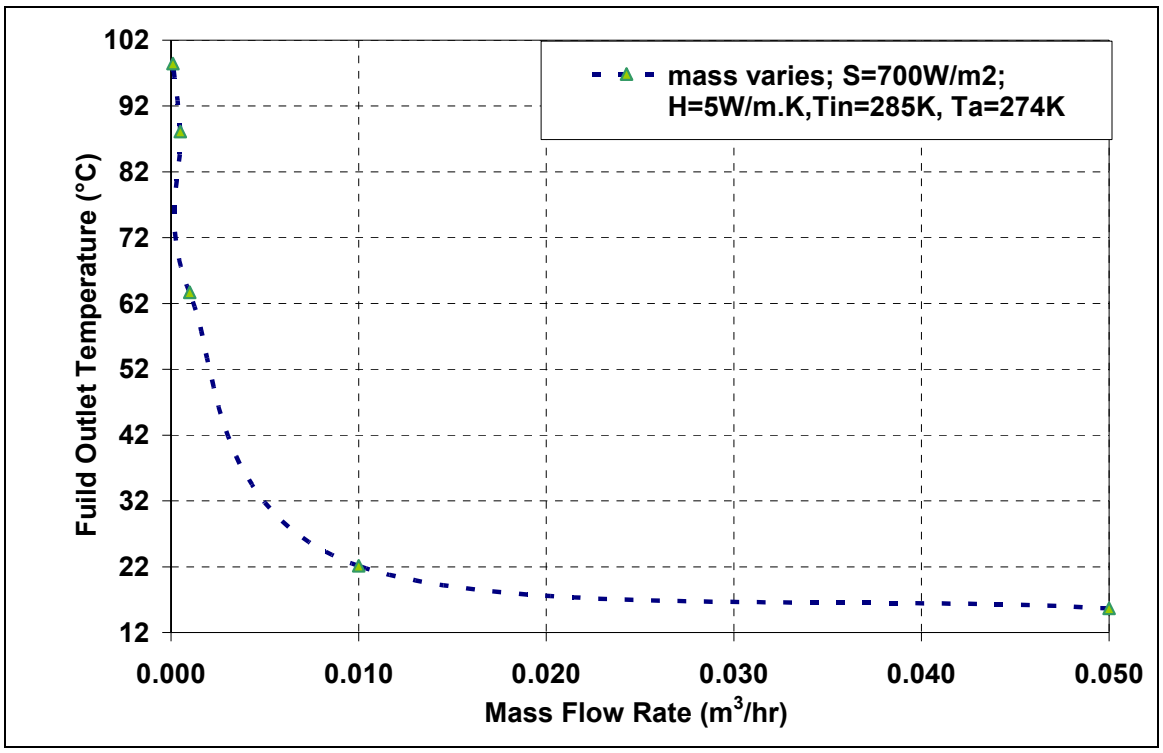

Figure 9-6. Variation of Maximum Fluid Temperature with respect to Mass Flow Rate at a Solar Intensity of 700W/m^2

Since the mass flow rate has a greater impact on overall heat gain (Q) than the increase in the fluid temperature (Duffie and Beckman 1980), it is essential to select the mass flow rate that allows for a reasonable temperature gradient between the fluid and the building operation temperatures. The model results showed that a mass flow rate of 0.0005m^3/hr to 0.005m^3/hr can be used during the winter season corresponding to an average supply temperature of 50°C. During the summer season, a mass flow rate of 0.1m^3/hr or more can be used to minimize the temperature increase in the fluid and dissipate the excess heat energy. It was also found that the closer the inlet fluid temperature was to the temperature of the absorber and collector, the larger the increase in the outlet fluid temperature.

For the different building area cases, the monthly amount of energy collected (Q_c) is plotted in Figures 9-7, 9-8, and 9-9. The daily amount of energy that can be collected per square meter for each month is shown in Figure 9-10.

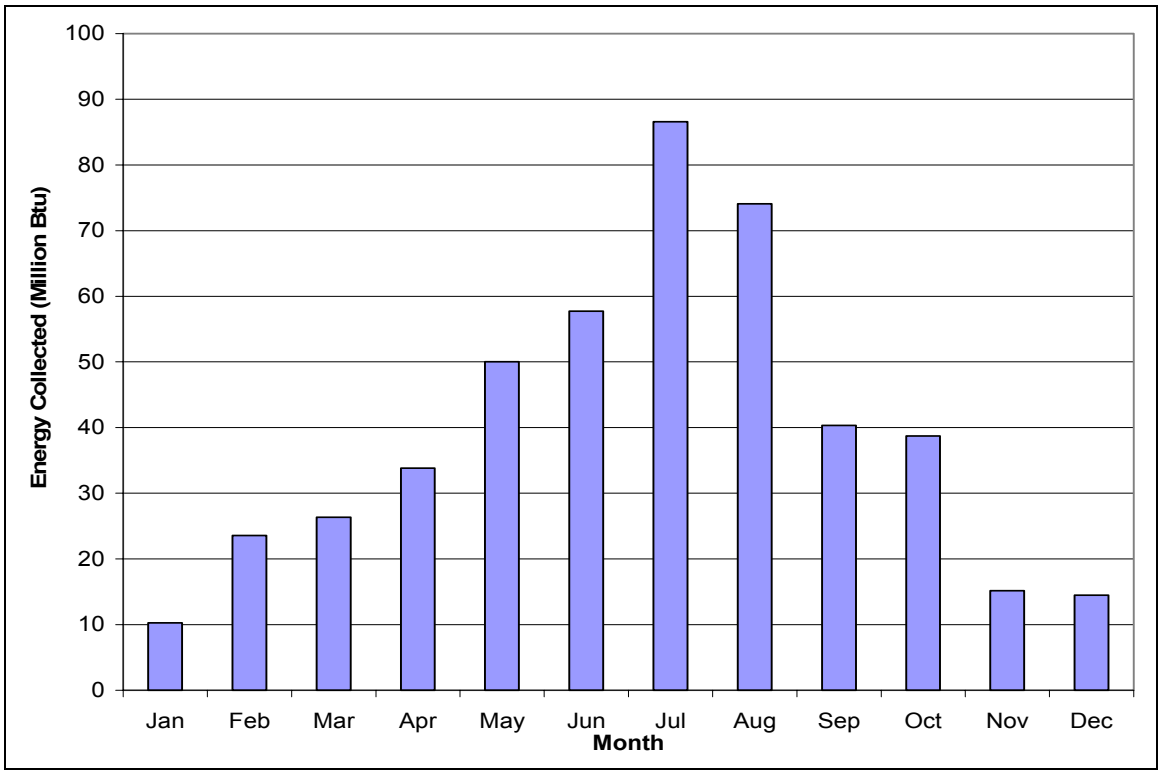

Figure 9-7. Monthly Building Energy Collection using a collection area of 150m^2

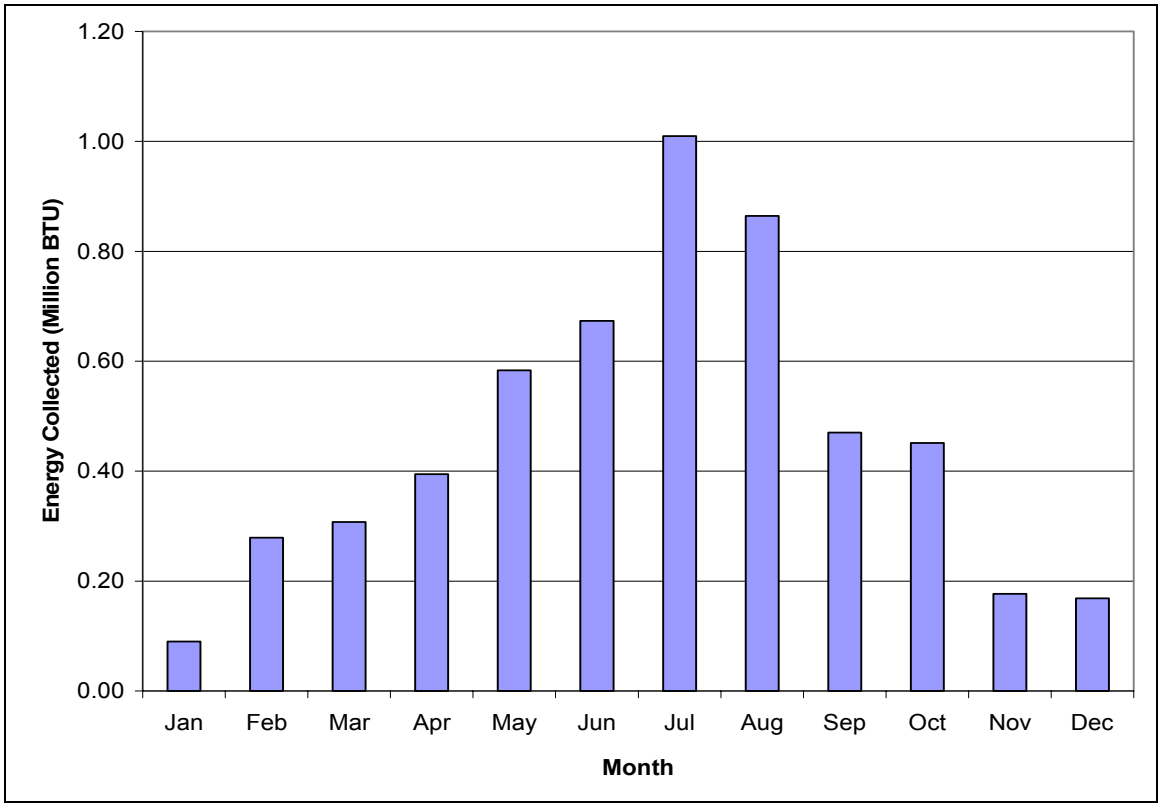

Figure 9-8. Monthly Building Energy Collection using a collection area of 1.75m^2

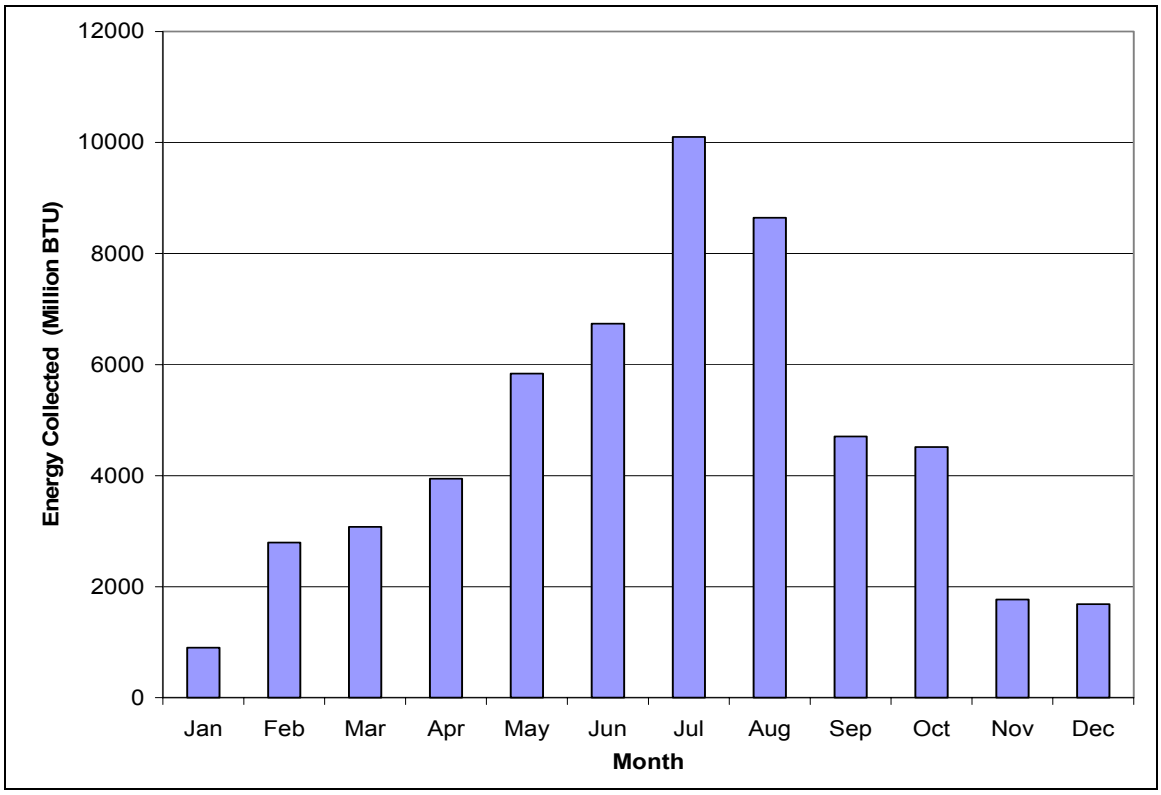

Figure 9-9. Monthly Building Energy Collection using a collection area of 17500m^2

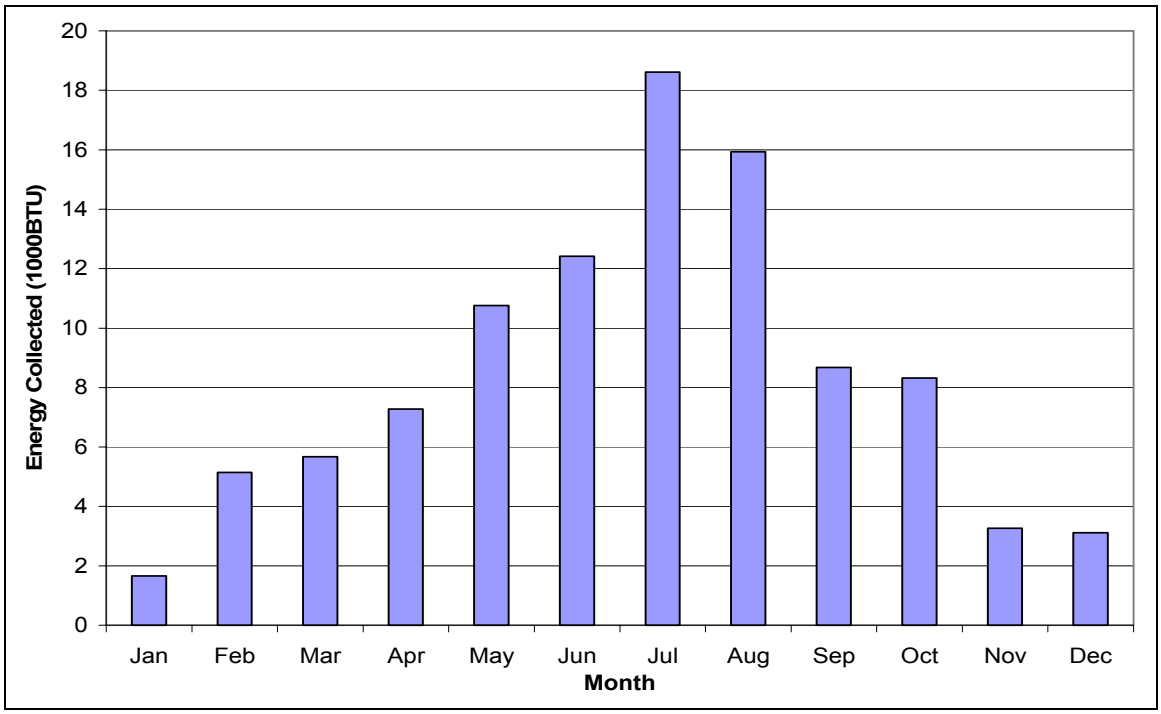

Figure 9-10. Monthly Building Energy Collection per Square Meter

Figure 9-7 assumes that the section of the collector modeled using the finite element is repeated along the width of the roof to cover a collection area of 150m^2. Similarly, Figure 9-8 assumes an area of 1.75m^2; Figure 9-9, 17500m^2.

9.2 STAGE III - ENERGY CONSUMPTION

This section quantifies the building's monthly heating energy consumption (the output from Stage III if the design evaluation framework) for the building located in Blacksburg. Virginia. As discussed previously, the Energy Plus program was used to determine the thermal loads, given the selected mechanical equipment, to achieve a consistent, acceptable comfort level for the building's occupants. For the three area cases or buildings presented in Chapter 6—which possessed areas of 13.57m^2, 1357m^2, and 135700m^2—Energy Plus calculated energy consumption. Figures 9-11, 9-12, and 9-13 show the monthly building energy consumption for the three cases.

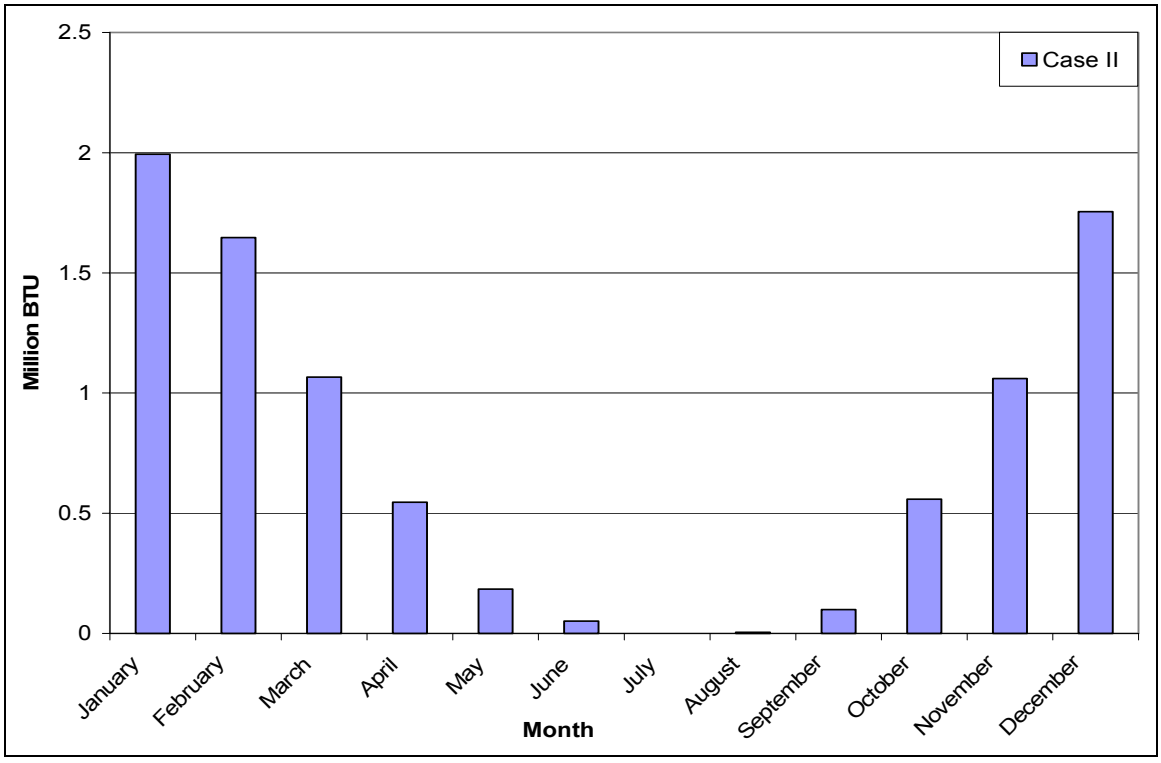

Figure 9-11. Monthly Building Energy Consumption for an Area of 13.57m^2

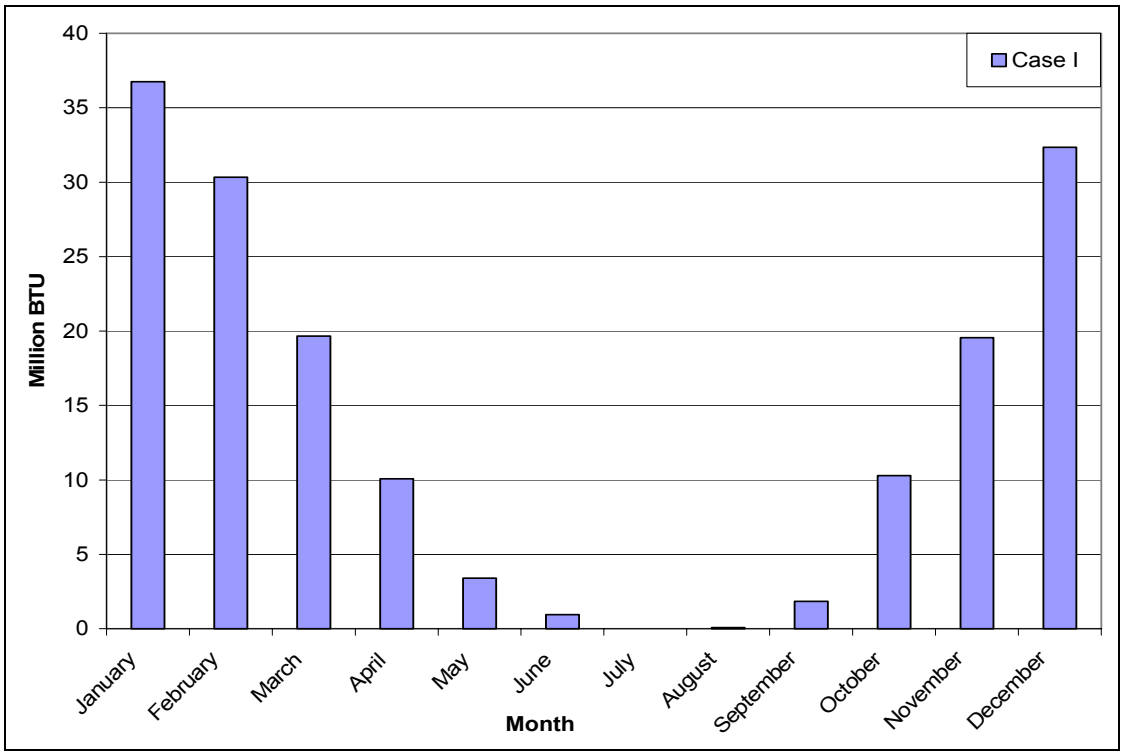

Figure 9-12. Monthly Building Energy Consumption for an Area of 1357m^2

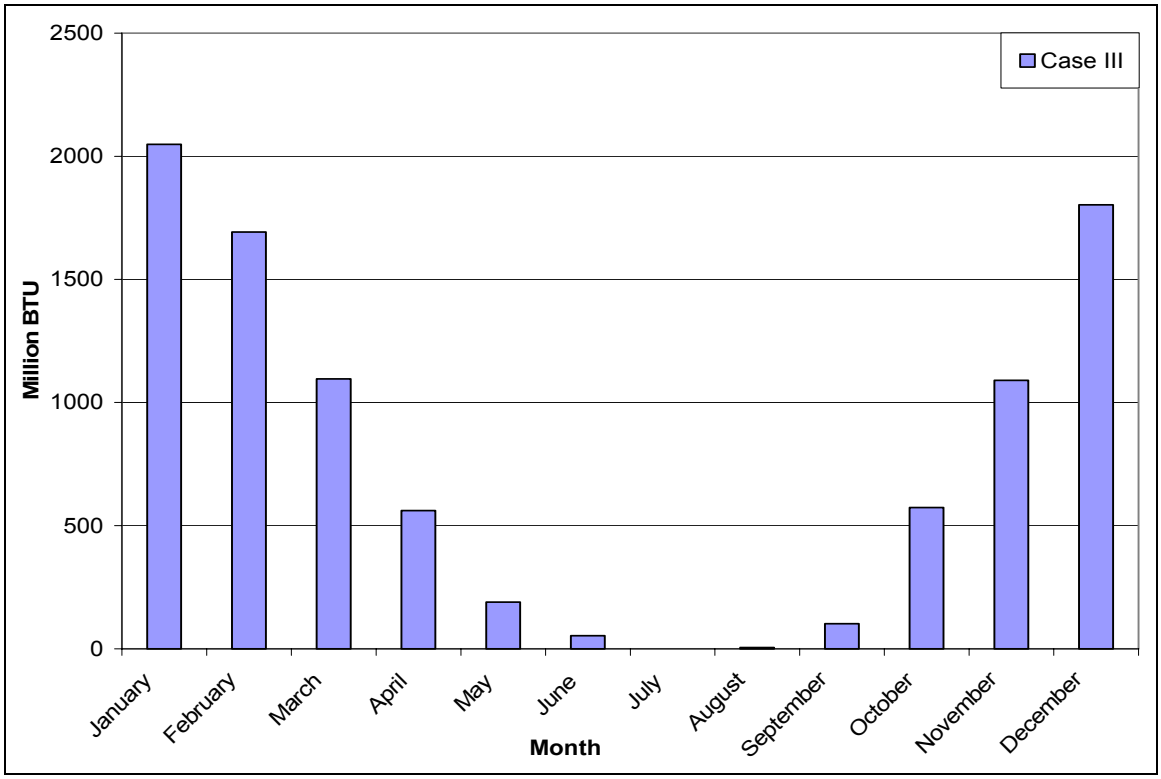

Figure 9-13. Monthly Building Energy Consumption for an Area of 135700m^2

As shown in these figures, as building area increases, so does energy consumption. For Case III, the total energy consumption in January was estimated at 2048.7 Million BTU. As the area decreased to 1357m^2 (Case I), January's building consumption decreased to 36.8 Million, while a minimum of 2 million BTU were needed for the smallest area (13.57m^2), Case II. For all three cases, the highest energy consumption took place during January; the second highest, December; the third, February; and tied for fourth, March and November. For the remaining months of the year, heating energy consumption decreased, becoming nearly negligible in July. Total energy consumption for the three cases is shown to be nearly linear when plotted on a semi-logarithmic scale (see Figure 9-14).

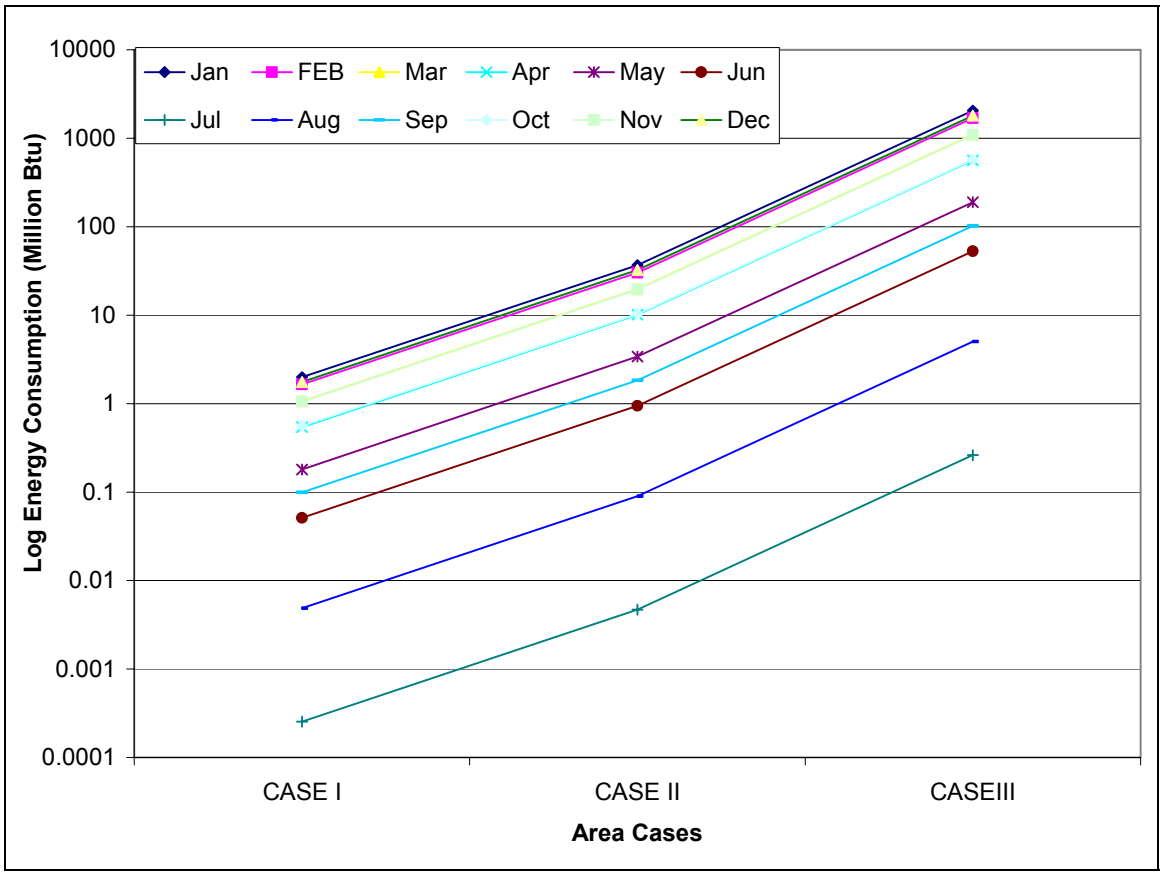

Figure 9-14. Monthly Building Energy Consumption for the Three Cases

Since the design evaluation framework recommends maintaining comfort level conditions within the space at all time, the comfort level within the space was measured for the three area cases using Fanger's PMV previously discussed in Chapter 2. For all cases, the selected mechanical equipment was sufficient to maintain a preset comfort

criterion of ±0.75 at all times throughout the year, as measured by the Fanger PMV Index. Figure 9-15 shows the Fanger PMV Index of the building's 32 thermal zones during winter months (i.e., January, February, September, October, November and December), while Figure 9-16 focuses on thermal comfort conditions during the spring and summer (i.e., March, April, May, June, July and August).

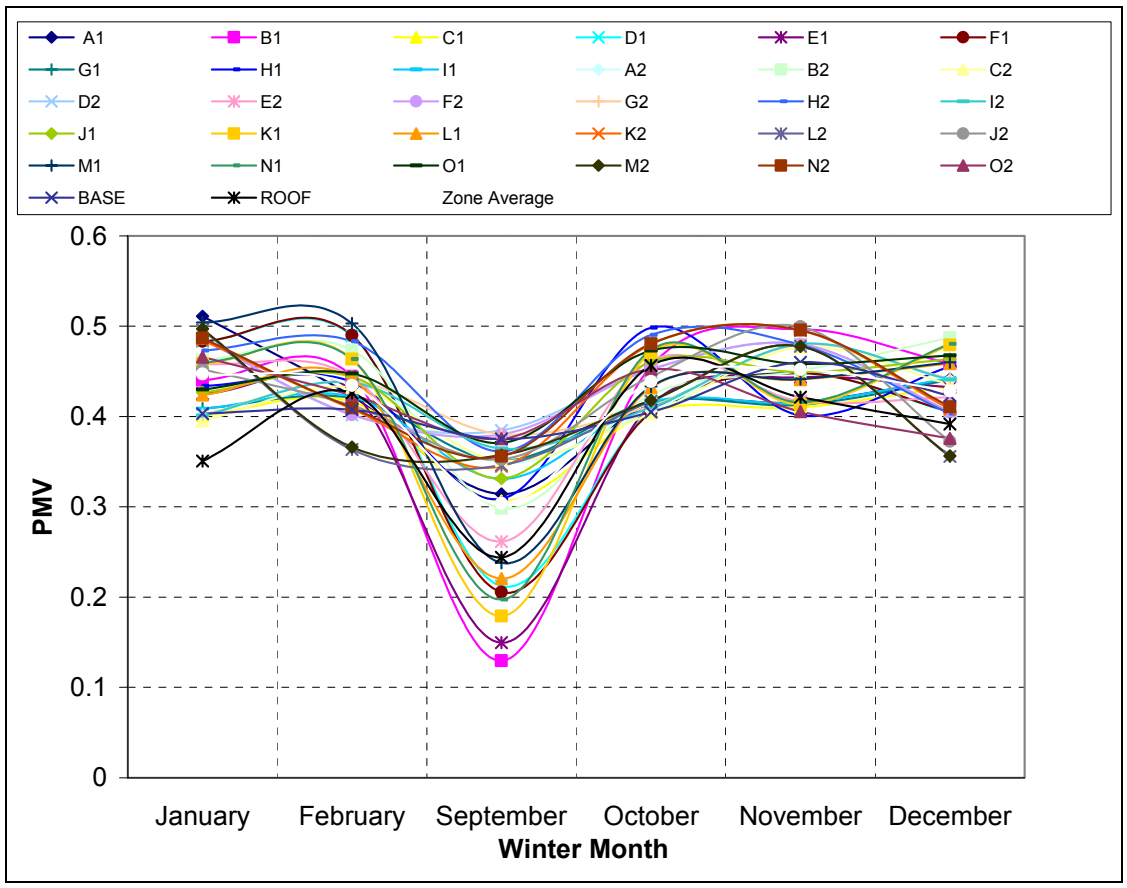

Figure 9-15. Fanger PMV Index Variation in the Zones during the Winter (Area Case I)

Figures 9-17 and 9-18 depict the results of the zone mean radiant and mean air temperatures. As the former indicates, the mean radiant temperature within the space varied between 20.5°C and 25.5°C (68.9°F and 77.5°F) at all times. Similarly, the mean air temperature varies between 20°C and 25.5°C (68°F and 77.5°F). These figures also depict the fact that the winter month temperature is higher than the summer month temperature, which indicates that, in order to reduce energy consumption and remain

within the comfort level, the heating set point temperatures may be reduced in the zone thermostatic control. The same phenomenon appears in the PMV graphs: the PMV index is above zero in winter and below in summer, which indicates that the control set points may be reduced to save more energy and still maintain the space within comfort conditions.

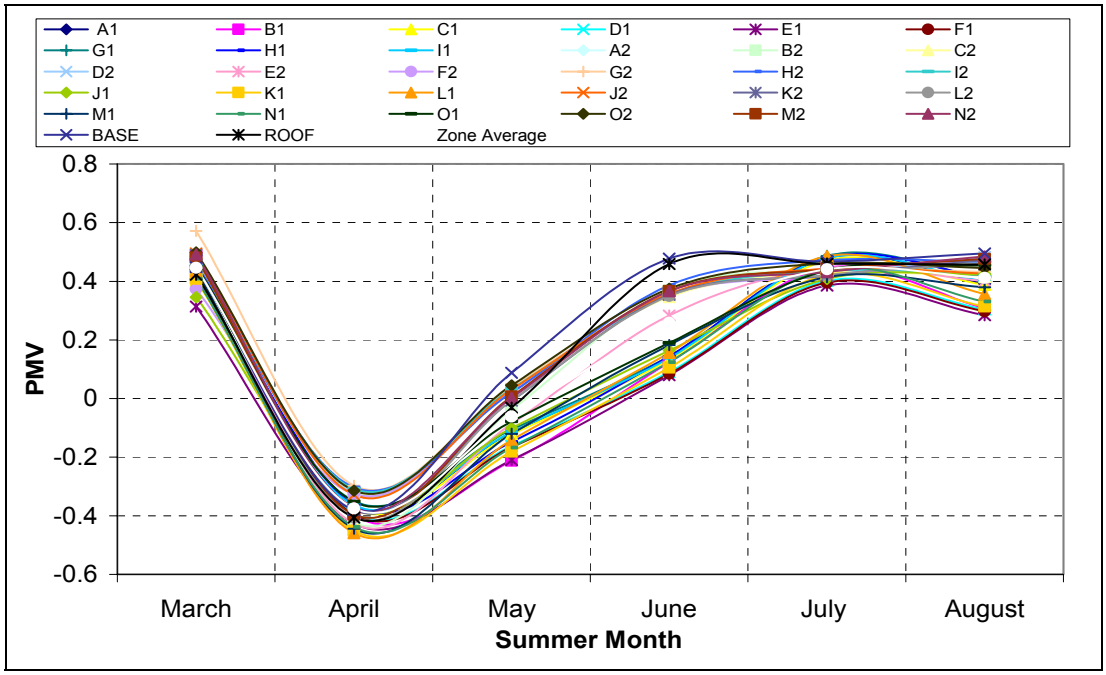

Figure 9-16. Fanger PMV Variation in the Zones during the Summer (Area case I)

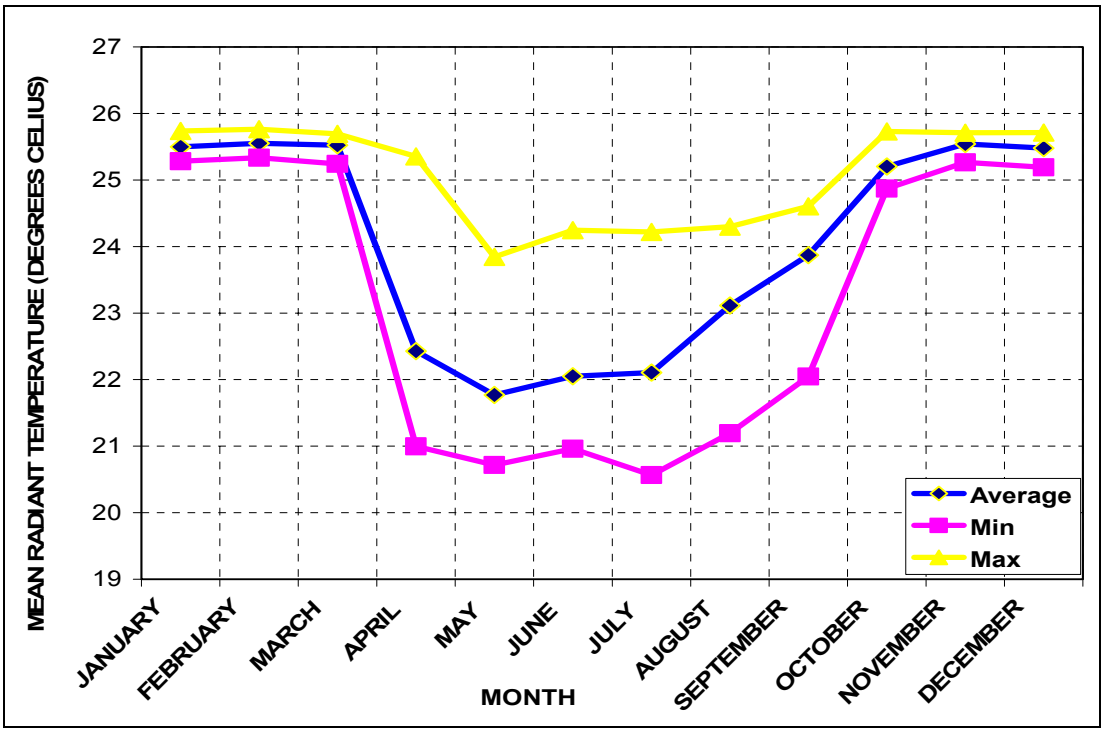

Figure 9-17. Minimum, Maximum, and Average Mean Radiant Temperature inside the Thermal Zones during the Year

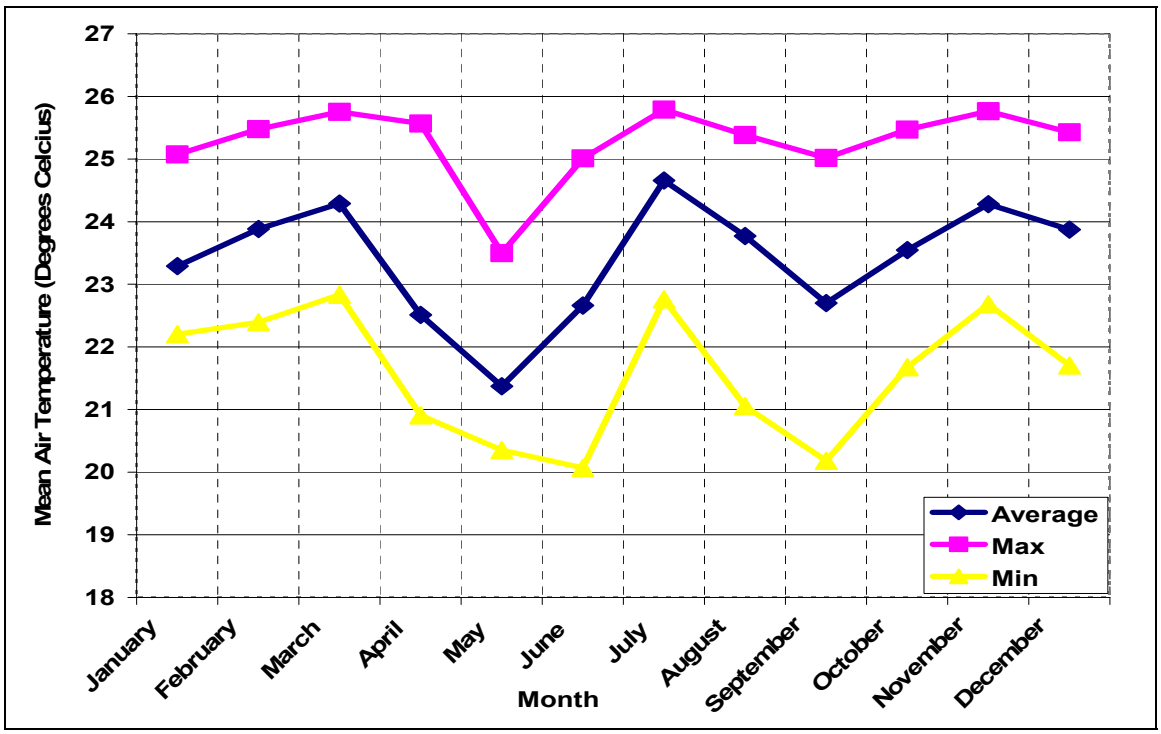

Figure 9-18. Minimum, Maximum, and Average Mean Air Temperature inside the Thermal Zones during the Year

9.3 STAGE IV - ENERGY STORAGE

The energy storage model (developed for Stage IV of the design evaluation framework) was evaluated on an hourly basis for a year period. The major output of this model was the fluid outlet temperature exiting the storage tank. According to its temperature and the control algorithm, this temperature was used as an inlet fluid temperature in one of two paths: the solar collector or the building low radiant system (see Chapter 8). Figure 9-19 shows the temperature distribution within the storage tank. Figure 9-20 depicts the first part of the tank enlarged. The fluid entered the storage tank at a temperature of 70.6°C and exited at an average temperature of 52°C. As a result, the PCM temperature increased from 12°C to an average of 50.8°C. The temperature of the insulated layer remained constant at 23°C. These results indicate that the selected PCM material was effective in storing heat energy throughout the year.

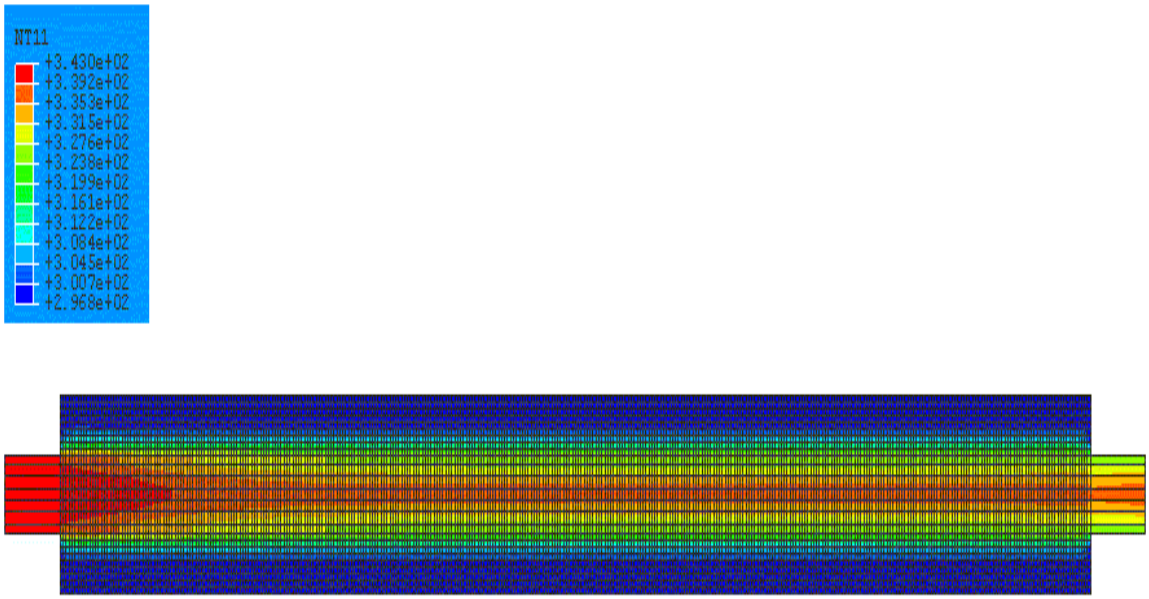

Figure 9-19. Temperature Distribution in the PCM Storage Model with an Inlet Fluid Temperature of 70°C

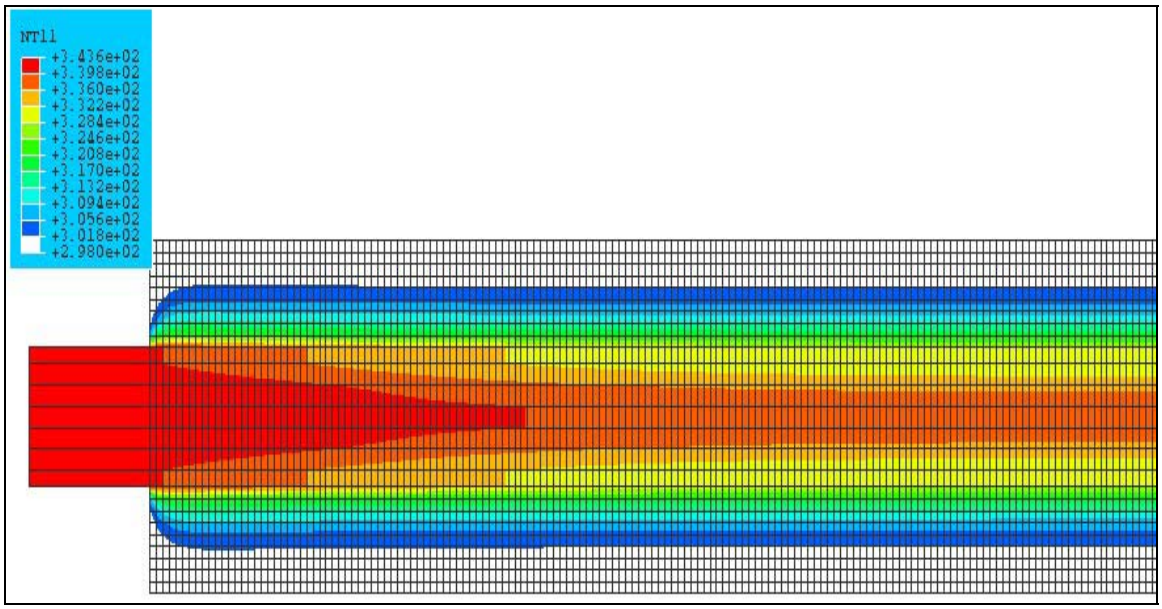

Figure 9-20. Temperature Distribution in the PCM Storage Model with an Inlet Fluid Temperature of 70°C – Beginning Enlarged

The size of the storage tank for area case I was selected based on a cost comparison of the potential sizes as recommended in the design evaluation framework. Area case I was the only case considered in terms of storage sizing because it is the only case that represents a practical residential area. The following alternative storage sizes were proposed:

- Alternative 1: 70% of the energy needed for January (Q = 21.8 Million BTU)
- Alternative 2: 47% of the energy needed for December (Q = 13 Million BTU)
- Alternative 3: 12% of the energy needed for February (Q = 2.95 Million BTU)
- Alternative 4: 16% of the energy needed for November (Q = 2.64 Million BTU)
- Alternative 5: Three consecutive bad weather days in January (Q = 2.08 Million BTU)
- Alternative 6: Two consecutive bad weather days in January (Q = 1.32 Million BTU)
- Alternative 7: One bad weather day in January (Q = 0.71 Million BTU)
- Alternative 8: Largest night cycle from January (Q = 0.26 Million BTU)
- Alternative 9: Two night cycle from January (Q = 0.522 Million BTU)

The size of the PCM storage tank was calculated based on an operating temperature range of 32^{o}C (90^{o}F) to 71^{o}C (160^{o}F) using equation (7-1). The price of the chosen phase change material is $3.3 per pound (manufacturer's quote). Listed in Table 9-1 can be

found the corresponding mass, in Kg, and tank volume, in m^3, for each of the aforementioned seven alternatives.

Table 9-1. Storage Tank Sizes

Alternative	Storage Capacity (MBtu)	Mass (Kg)	Volume PCM (m^3)	Volume water (m^3)	Price PCM (US$)
1	21.8	88872	98.75	120.06	646563.6
2	13.0	53166	59.07	71.83	386799.4
3	2.95	12026	13.36	16.24	87494.5
4	2.64	10767	11.96	14.55	78333.1
5	2.08	8500	9.45	11.48	61845.2
6	1.32	5409	6.01	7.31	39356.0
7	0.71	2859	3.18	3.86	20802.5
8	0.26	1066	1.18	1.44	7753.3
9	0.522	2131	2.37	2.88	15506.6

As shown in Table 9-1, PCM storage was found to be quite expensive. Therefore, it was decided in this study that if PCM storage is used, to utilize the smallest possible storage tank —i.e. one that would accommodate only the night cycle—and assume that the remaining needed heating energy would be supplied by the secondary supply system. Therefore, the selected storage solution was Alternative 8, with a storage capacity of 0.26 Million BTU, a mass of 1066Kg, and a volume of $1.18m^3$. The initial cost of that alternative solution is US$7753.3, as shown in Table 9-1.

As was shown in the design evaluation framework and highlighted in Figure 9-21, the results of the different stages are compared against the design criteria using the decision making module. When the results of stage IV were compared against the design criteria, cost and thermal efficiency, it was revealed that although the phase change material storage tank can be quite effective from a thermal perspective, Table 9-1 also indicates that it can be costly. Therefore, the design process was iterated to examine alternative storage capabilities. Hence, sensible storage in the form of a water tank was presented as an alternative to the PCM tank. Moreover, the building slab thermal mass

was presented as a potential storage to supply the building needs during the night cycle. Both alternatives were studied in the iterated design evaluation process.

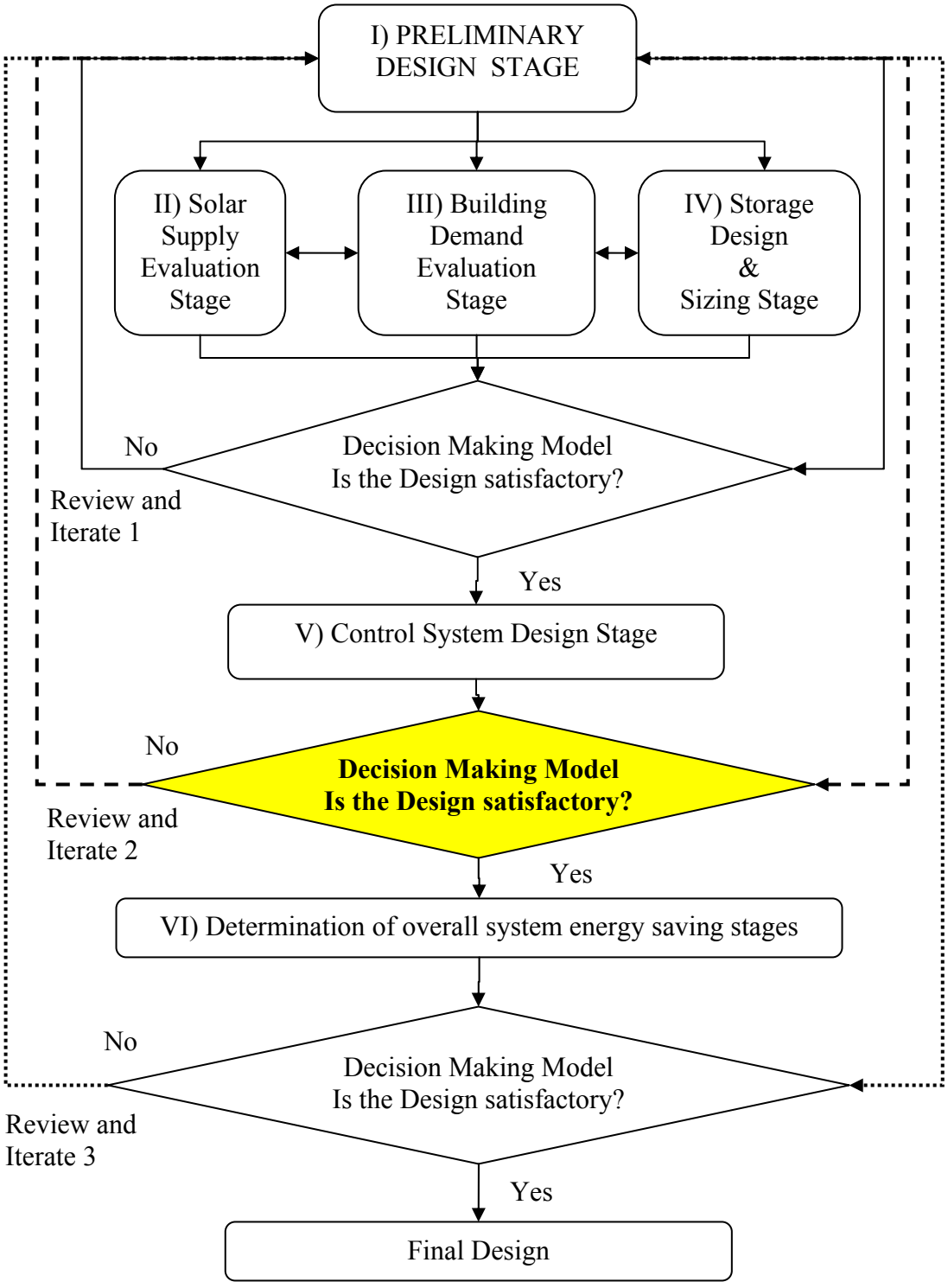

Figure 9-21. Decision Making Module of the design evaluation framework

Accommodating the aforementioned nine storage alternative storage sizes using sensible storage in the form of a large water tank was calculated using Equation 9-1 and is also shown in Table 9-1:

$$Q = mc_p\Delta\theta \qquad (9\text{-}1)$$

where

$\Delta\theta$ = the change in water temperature (^oC);

m = the mass (Kg); and

c_p = the specific heat of the water.

The calculation assumes an operating range of 32°C (90°F) to 71°C (160°F). Therefore, the corresponding change in water temperature ($\Delta\theta$) is 39°C. As shown in Table 9-1, the size of the water tank needed is close to the size of the PCM tank but utilizing water is more cost effective since water is much cheaper than PCM. Therefore, it can be concluded that utilizing water as a sensible storage medium is recommended rather than using the selected PCM due to its cost efficiency. If a water tank was used for thermal storage, two consecutive bad weather days in January (Alternative 6) can be accommodated at a reasonable cost. Since this alternative provides a larger storage capacity, this case study will utilize a 7.31 m^3 hot water tank instead of the PCM tank for thermal storage.

Results also showed that accommodating the night cycle needs using the building slabs' thermal mass is possible. Heat will be supplied to and withdrawn from the slabs using the radiant heating system. The quantity of heat energy that can be stored in the building's concrete floor slabs, a volume of 68.5m^3 (52.4 $yard^3$) was calculated. The building slabs was found capable of storing 132.6 MJ (0.13 Million Btu) for every 1°C increase in temperature. Therefore, it can be concluded that if the building slab's thermal mass was used for sensible storage, increasing its temperature by 2°C can supply one night cycle in January, while an increase of 4°C can supply two consecutive night cycles in January. Further work is required to develop control strategy to efficiently utilize the building slab's thermal mass for storage.

9.4 OVERALL ENERGY SAVING ANALYSIS

As recommended in stage VI of the design evaluation framework highlighted in Figure 9-22, the amount of energy required by the building was compared against that collected by the solar collection system consisting of a flat plat solar collector and a hot water tank for a year period for the three area cases considered. The results of the comparison are shown in Figures 9-23, 9-24, and 9-25.

With respect to Case I, (Building area = 1357m^2, collection area = 150m^2), the energy collected sufficiently provided 100% of the hot water requirements. In addition, it was able to provide 31% of the heating space needs in January, 51% during December, 88% during November and February, and more than 100% for the rest of the year. On average, throughout the calendar year, the system can supply 85% of the building's heating and hot water requirements.

In Case II, (Building area = 13.57m^2, collection area = 1.75m^2), as the building area and its corresponding collection area decreased, the ability of the building to supply energy likewise decreased. The energy collected was not sufficient to provide hot water requirements during the month of January and December, but it provided 100% of the hot water requirements throughout the rest of the year. The collection system was able to provide 4.5% of the heating space needs in January, 9.6% during December, 16.7% during November and February, 28.8% during March, 72% during April, 80% during October and more than 100% for the rest of the year. On average, the system can supply 56.8% of the building's heating and hot water requirements throughout the year.

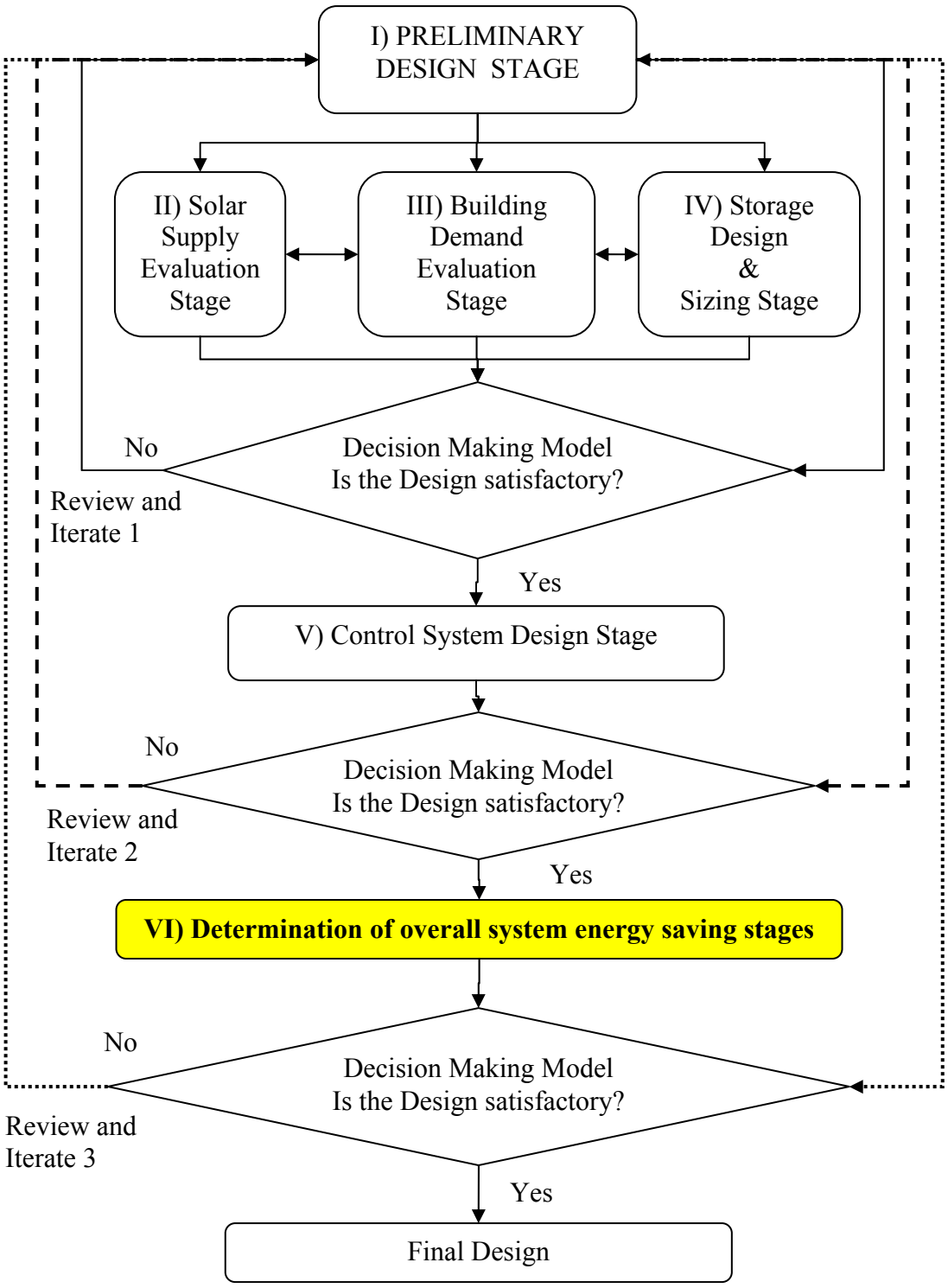

Figure 9-22. Stage VI of the design evaluation framework

In Case III, (Building area = 135700m^2, collection area = 17500m^2) as the building area and its corresponding collection area increased, so did the ability of the building to supply energy. In fact, the energy collected provided 100% of hot water requirements. Moreover, the collection system was able to provide 44% of the heating space needs in January, 93.5% of the heating space needs in December and more than 100% for the rest of the year. On average, the system can supply 94.5% of the building's heating and hot water requirements regardless of season. Table 9-2 shows the percentage of the amount of energy that can be supplied by the collection system in the three cases throughout the year. As can be seen from Table 9-2, increasing the area of the building in the east-west direction enables the collection system to supply more of the building needs.

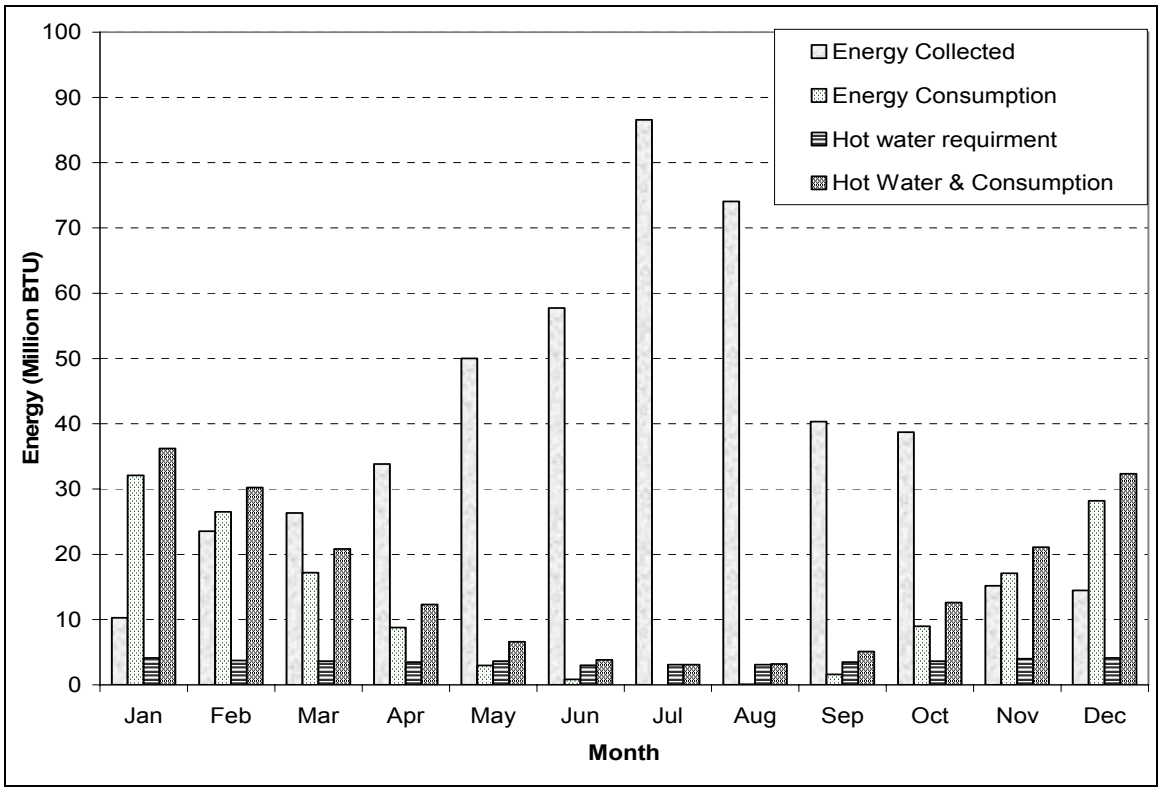

Figure 9-23. Monthly Building Energy Collection versus Consumption for Area Case I

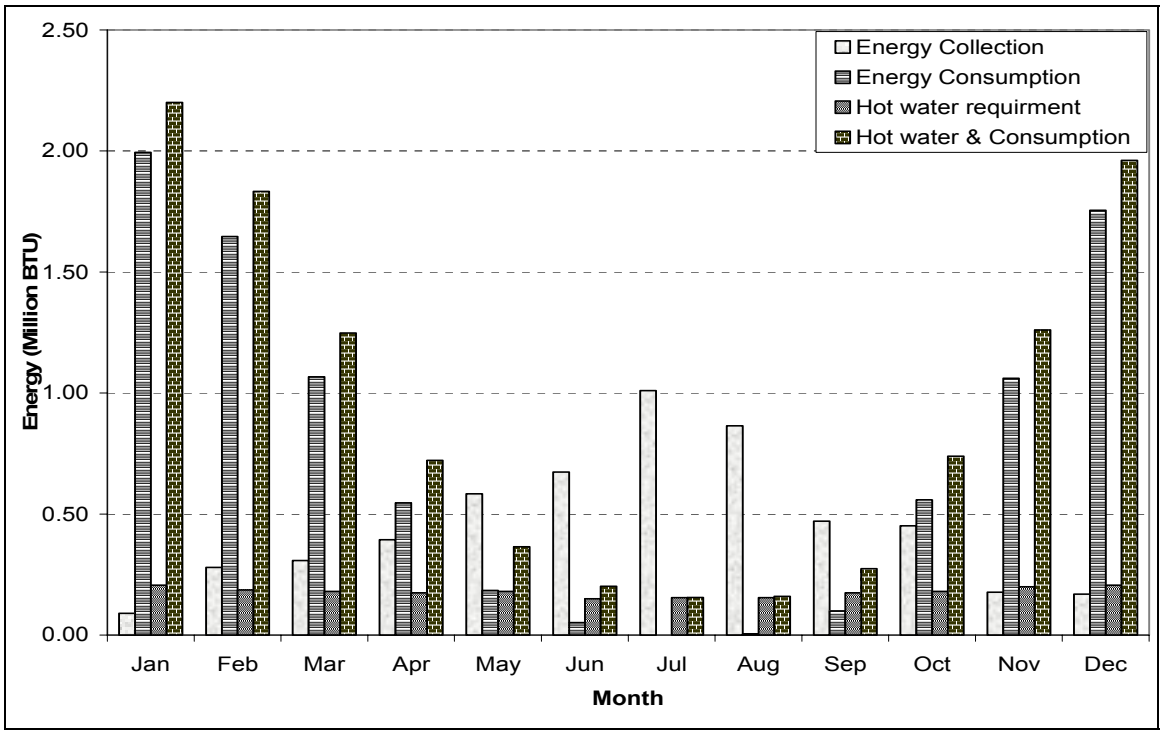

Figure 9-24. Monthly Building Energy Collection versus Consumption for Area Case II

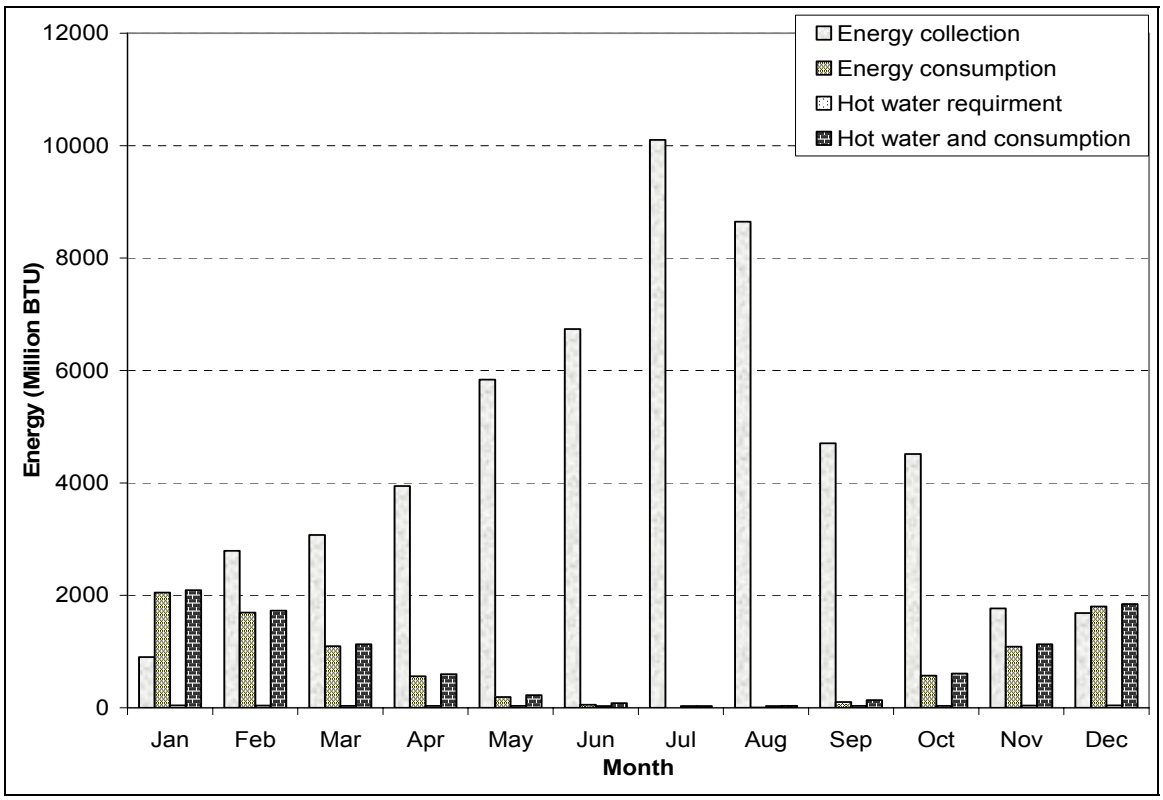

Figure 9-25. Monthly Building Energy Collection versus Consumption for Area Case III

Table 9-2. Percentage of Building Energy Supplied by the Solar Collection System

Percentage of Energy consumed supplied by collection	Case II 13.75m^2	Case I 1375m^2	Case III 135700m^2
January	4.08	31.96	43.05
February	15.23	88.88	>100
March	24.6	>100	>100
April	54.6	>100	>100
May	>100	>100	>100
June	>100	>100	>100
July	>100	>100	>100
August	>100	>100	>100
September	>100	>100	>100
October	61.08	>100	>100
November	14.03	88.65	>100
December	8.59	51.27	91.46

9.4.1 Effect of Weather Data Variation on Energy Gain

To estimate the effect of weather variability on the overall performance of the system, the 5% and 95% January and July weather data were used in the simulation, then the results were compared against the system performance under Blacksburg TMY2 weather conditions. Figure 9-26 shows the amount of energy collected in January and July under 5%, 95%, and TMY2 climatic conditions.

As this figure indicates, the weather data variability significantly impacts system performance. In January, the 5% weather data reduces the amount of energy collected by 41%. Under 5% weather conditions in January, the building is only able to satisfy 22% of the needed energy consumption, as opposed to the 31% mentioned previously. Similarly, under 95% weather conditions, the performance improved significantly. The energy collected under 95% weather conditions in January is 125% of the energy collected under the TMY2 data; additionally, it was sufficient to satisfy 81% of the heating and hot water requirements during January. In July, the collected energy shows a

similar variability trend. However, the July case was not as critical as that of January because under 5% weather conditions, TMY2 weather conditions, the collection system was able to satisfy 100% of the heating and hot water requirements. Table 9-3 shows the percentage of the building energy needs that can be supplied using the collection under 5%, TMY2, and 95% in January and July. Assuming that the percentage of increase and decrease in the collected energy remain constant for the rest of the year, the remaining 10 month collection was estimated under 5% and 95% conditions and are also shown in Table 9-3.

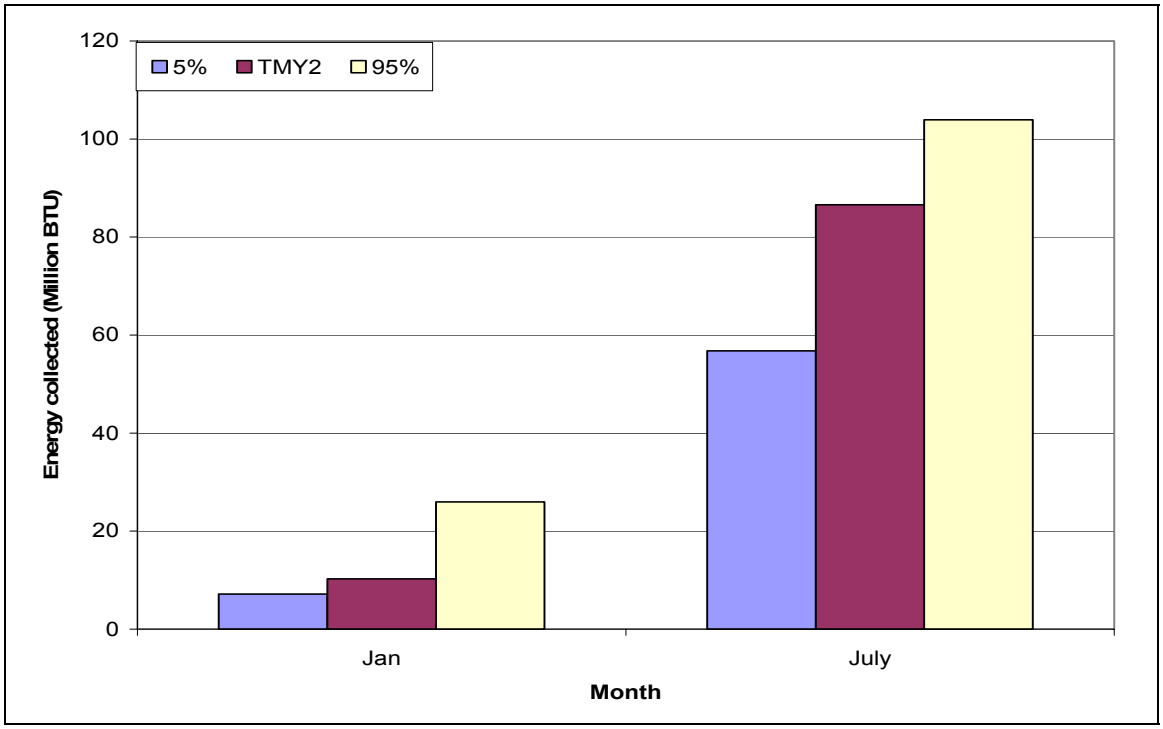

Figure 9-26. Energy Collection under 5%, TMY2, and 95% for a Collection Area of 150m^2

Table 9-3. Percentage of Building energy supplied by the solar collection system for case I under TMY2, 5%, and 95% weather conditions

Percentage of Energy consumed supplied by collection	5%	TMY2	95%
January (Actual)	22	31.96	>100
July (Actual)	>100	>100	>100
February (Estimated)	61.11	88.88	>100
March (Estimated)	>100	>100	>100
April (Estimated)	>100	>100	>100
May (Estimated)	>100	>100	>100
June (Estimated)	>100	>100	>100
August (Estimated)	>100	>100	>100
September (Estimated)	>100	>100	>100
October (Estimated)	>100	>100	>100
November (Estimated)	61.11	88.65	>100
December (Estimated)	35.23	51.27	>100

10 FURTHER DESIGN EVALUATION FRAMEWORK VALIDATION: MINNAPOLIS, MINNESOTA

10.1 INTRODUCTION

For further demonstration of the decision making process presented by the design evaluation framework, a second case study located in Minneapolis, Minnesota (latitude 44.9 and elevation 837) was evaluated using simplified modeling techniques. The heating Degree day (HDD) method was used to calculate the energy consumption and the predictive statistical design equation presented in Chapter 5 was used to calculate the energy collection. The same preliminary building design (Stage I) that was presented in Chapter 3 was used in this case study as was previously mentioned. A TMY2 file is available for Minneapolis, Minnesota and was used as input for the climatic parameters.

10.2 STAGE II - SOLAR SUPPLY EVALUATION STAGE

The design equation developed using the statistical analysis presented in Chapter 5 was used in Stage II of the design evaluation framework. This design equation was used to estimate the quantity of energy collected by the flat plate collector of the building located in Minneapolis, Minnesota. The design equation was also used to iteratively alter the operational parameters (e.g. mass flow rate) to maximize the heat gain (Q). The design parameters that were used to calculate the amount of heat gain are: solar radiation, wind speed (convection coefficient), ambient temperature, inlet fluid temperature, mass flow rate, pipe diameter = 0.5 inches, and pipe spacing = 128mm. The used environmental parameters are based on Minneapolis Minnesota's TMY2 file. The monthly energy collected is shown in Figure 10-1. As can be seen from Figure 10-1, the maximum amount of heat gain takes place during July with 44.1 million BTU. The heat gain decreases gradually to reach its minimum in December and January with a total heat gain of 0.8 million BTU in December and 1.37 million BTU in January. Comparing the collection ability of the building in Blacksburg (VA), with the building in Minneapolis (MN) shows that the ability to collect energy in Minneapolis Minnesota is decreased by more than 50% due to the severe weather conditions. To improve the efficiency of the

collector, several modifications may be utilized such as increasing the collection area, changing the type of fluid used to obtain better energy absorption, and using a different energy collection method (e.g., concentrating collectors). In addition, passive collection techniques with night shading can also be utilized.

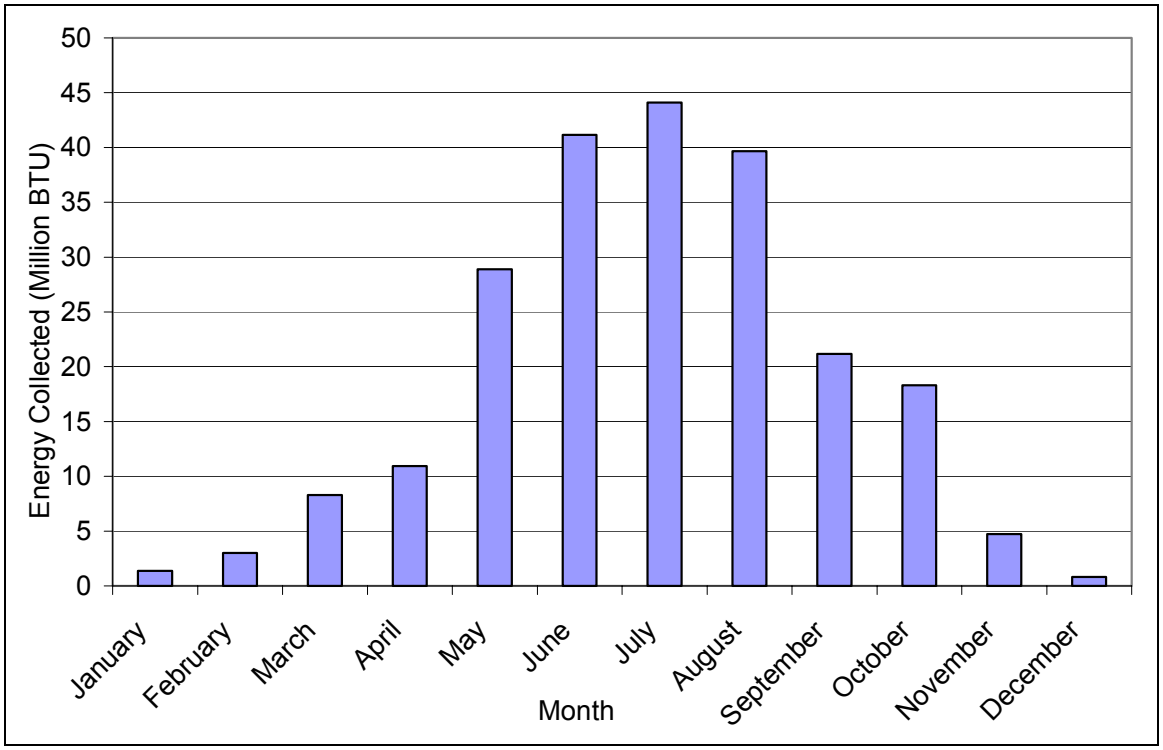

Figure 10-1. Monthly Building Energy Collection for a Building Located in Minneapolis (MN) with a Collection Area of 150m^2

10.3 STAGE III – BUILDING DEMAND EVALUATION STAGE

The monthly energy consumption of the second case study was evaluated using the heating degree-day method previously described in Chapter 2. It has to be noted that simplified methods does not allow the monitoring of the hourly temperature and humidity of the zones. Therefore, the design evaluation framework recommends utilization of detailed simulation techniques for energy evaluation. The heating degree days (HDD) was estimated based on a heating balance point of 60^{o}F. The monthly energy consumption for the preliminary design is plotted in Figure 10-2. As shown in Figure 10-2, the total energy consumption was estimated at 318 Million BTU per year compared to

165 Million BTU in case of the building located in Blacksburg, Virginia. As was the case in building located in Blacksburg, Virginia, the highest energy consumption took place during January with a value of 72.24 Million Btu; the second highest, December; the third, February; followed by March and November. Comparing the energy needed for the winter month in the case of Minneapolis, Minnesota and Blacksburg, Virginia reveals that the demand was nearly doubled in case of the Minneapolis building. For the remaining months of the year, heating energy consumption decreased, becoming nearly negligible in July.

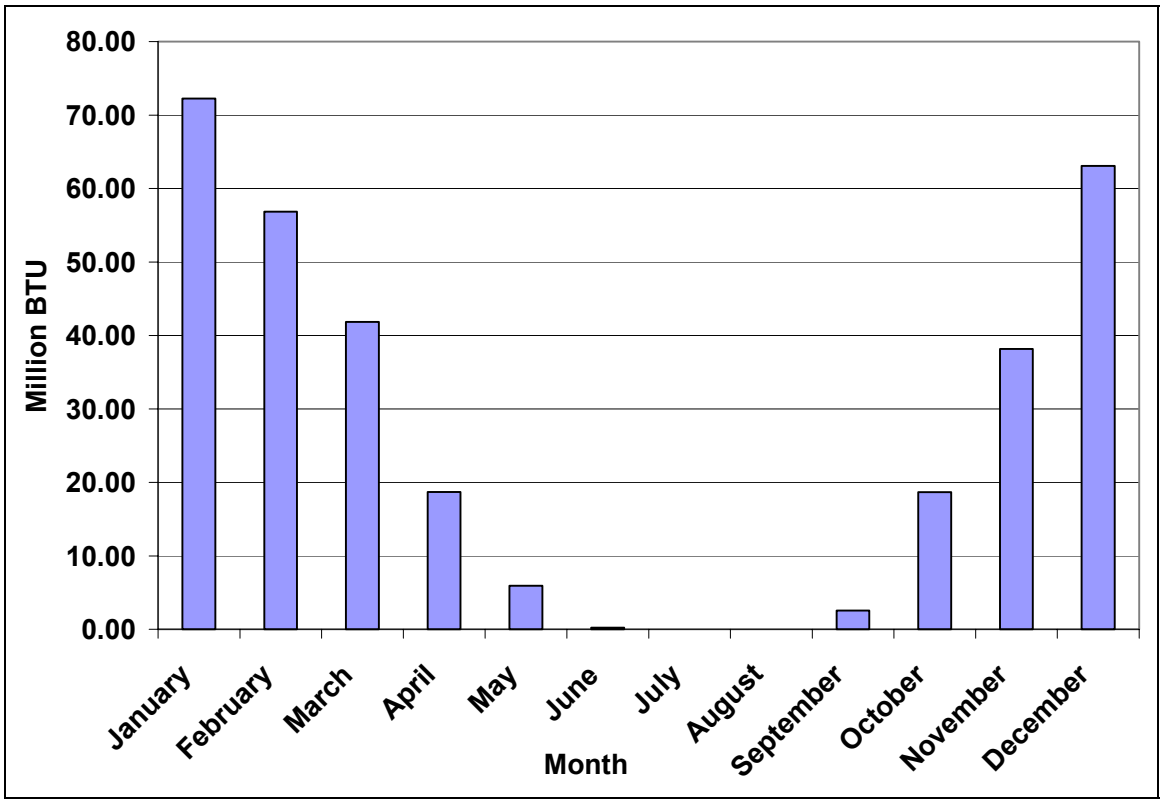

Figure 10-2. Monthly Building Energy Consumption for a Building Located in Minneapolis (MN) with an Area of 1357m^2

10.4 STAGE IV – STORAGE DESIGN AND SIZING STAGE

The first step in the storage design proposed by the design evaluation framework is determination of the type and cost of the storage system. Since the phase change material storage system proposed by the preliminary design (Stage I of the framework) was

rejected in case of the building located in Blacksburg, Virginia because of its cost inefficiency, it will not be utilized in this case study. Instead, the proposed storage system type will be a hot water tank and utilization of the building thermal mass slabs.

Sizing the storage tank was based on a cost comparison of the potential sizes as recommended in the design evaluation framework. The following alternative storage sizes were considered:

- Alternative 1: 98% of the energy needed for January (Q = 70.86 Million BTU)
- Alternative 2: 98% of the energy needed for December (Q = 62.25 Million BTU)
- Alternative 3: 94% of the energy needed for February (Q = 53.84 Million BTU)
- Alternative 4: 80% of the energy needed for March (Q = 33.54 Million BTU)
- Alternative 5: 41% of the energy needed for April (Q = 7.76 Million BTU)
- Alternative 6: Three consecutive bad weather days in January (Q = 6.9 Million BTU)
- Alternative 7: Two consecutive bad weather days in January (Q = 4.57Million BTU)
- Alternative 8: One bad weather day in January (Q = 2.28 Million BTU)
- Alternative 9: Largest night cycle in January (Q = 0.66 Million BTU)
- Alternative 10: Two night cycle in January (Q = 1.33 Million BTU)

The result of accommodating the ten storage alternative sizes using sensible storage in the form of a large water tank was calculated using Equation 9-1 and is shown in Table 10-1. The calculation assumes an operating range of 32^{o}C (90^{o}F) to 71^{o}C (160^{o}F). Therefore, the corresponding change in water temperature ($\Delta\theta$) is 39^{o}C. As shown in Table 10-1, the size of the water tank needed is quite high. Therefore, the selected water tank that is to be used for thermal storage can accommodate two night cycles from January (Alternative 10) at a reasonable cost with a storage capacity of 1.33 Million BTU, a mass of 7324Kg, and a volume of 7m^3. The rest of the needed energy will be supplied using the secondary supply system.

On the other hand, utilization of sensible storage in the form of a water tank may be eliminated if the building thermal mass can supply the night cycle needs, especially if the capacity of the sensible storage system can only supply the building night cycle needs. Therefore, the amount of energy that can be stored in the building slab thermal

mass was determined. Results showed that the building slabs are capable of storing 132.6 MJ (0.13 Million Btu) for every 1°C increase in temperature. Since we need to store 0.66 million BTU for every night cycle, an increase of at least 5°C is needed. Since such an increase can disrupt the thermal comfort level within the space, this option can be disregarded or used in conjunction with the sensible storage water tank to supply part of the needed energy, thus reducing the size of the storage tank. It has to be noted though that to properly utilize the building thermal mass to supply part of the load without disrupting thermal comfort conditions, integrating optimization techniques in the control strategy is needed. Therefore it is recommended to investigate utilization of optimization techniques for thermal storage in future research work. In such a study, the thermal comfort requirements will be regarded as the optimization boundary and the objective will be minimizing the building's energy consumption.

Table 10-1. Storage Tank Sizes

Alternative	Storage Capacity (MBtu)	Mass (Kg)	Volume water (m^3)
1	70.86	390259	390
2	62.25	342840	343
3	53.84	296522	297
4	33.54	184720	185
5	7.76	42738	43
6	6.90	38001	38
7	4.57	25169	25
8	2.28	12557	13
9	0.66	3634	4
10	1.33	7324	7

10.5 STAGE V – CONTROL SYSTEM DESIGN

The framework requires the development of a control strategy to optimize the system operation in the most energy efficient and cost-effective way. The control strategy proposed in Chapter 8 for the Blacksburg, Virginia case study can be utilized in the Minneapolis, Minnesota case study with some modifications. However, to maximize the efficiency of the solar collection system, given the high demand and the low supply, integrating optimization techniques in the control strategy to regulate the flow of heat to

the building may help reduce the consumption. Therefore, it is recommended to further investigate the effect of integrating optimization techniques in the control strategy in future work.

10.6 STAGE VI – OVERALL SYSTEM ENERGY SAVING STAGE

In this stage the benefits of the active solar system can be quantified. As recommended in the design evaluation framework, the amount of energy required by the building was compared against that collected by the solar collection system for a year period for the three area cases considered. The results of the comparison are shown in Figures 10-3.

As can be seen in Figure 10-3, the energy collected provided 33% of the hot water requirements in January, 80.6% in February, 19% in November, and 100% for the rest of the year. In addition, it was able to provide 18.3% of the space heating needs in March, 49% during April, 11% during November, and more than 100% for the rest of the year. On average, throughout the calendar year, the system can supply 55.75% of the building's heating and hot water requirements. Table 10-2 summarizes the percentage of energy needed that can be supplied by the solar collection system.

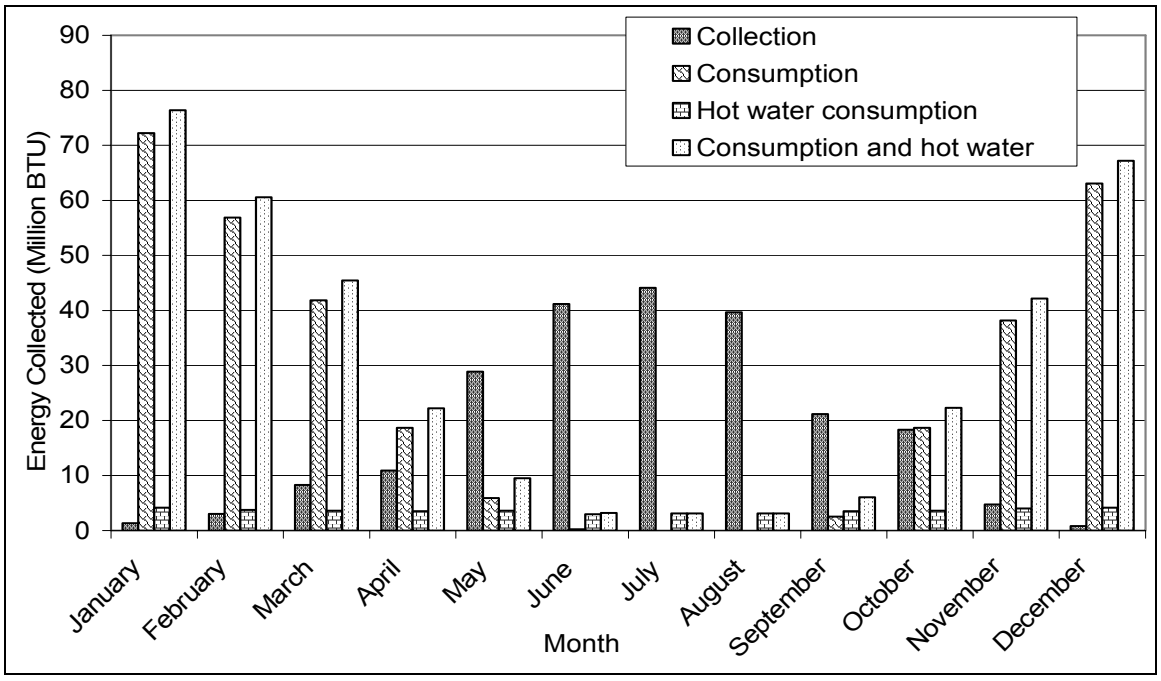

Figure 10-3. Collection versus Consumption for a year period

Table 10-2. Percentage of Building Energy Supplied by the Solar Collection System

Month	% of Energy Supplied
January	1.80
February	4.97
March	18.27
April	49.27
May	>100
June	>100
July	>100
August	>100
September	>100
October	82.16
November	11.26
December	1.22

10.7 DECISION MAKING MODULE

The framework recommends evaluating the results of the preliminary design with respect to the design criteria three times within the evaluation process, after stages II, III, & IV, after stage V, and after stage VI. In this case study, the design criteria is thermal efficiency and cost effectiveness. Therefore, examining the results of the six stages of the design evaluation framework against the thermal efficiency and cost effectiveness design criteria reveals that the building has a very high energy demand compared to its ability to collect. That raises the need for the designer to review and iterate to improve the preliminary design. Alternative improvement techniques include, changing the building material and construction to improve its thermal efficiency, for example increase the insulation from 3 in to 6 in will reduce the building consumption by more than 21%. This decrease in energy consumption can be evaluated against the increase in cost using life cycle costs, and if it proves effective, the preliminary design can be adjusted accordingly. The energy consumption resulting from increasing the thickness of the insulation is shown in Figure 10-4. Other alternatives include utilize passive collection techniques through the building's glass while improving the R-factor of windows and using night

shading to reduce losses. Figures 10-5 and 10-6 show the reduction in the energy consumption in case of using a window R-factor of 5 and a window R-factor of 11. As can be seen in figures 10-5 and 10-6, the energy consumption of the building was reduced on average by 20% in each case.

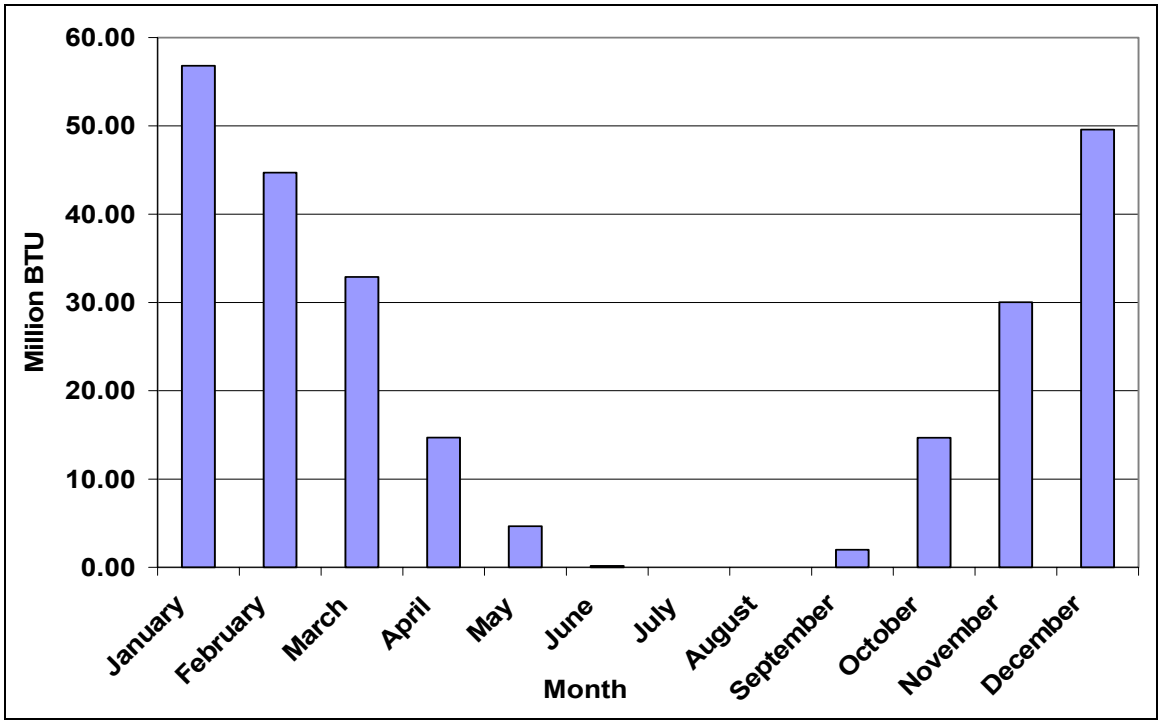

Figure 10-4. Monthly Building Energy Consumption – (after increasing insulation from 3 to 6 inches)

On the other hand, it is recommended to investigate different solar collection methods (e.g. concentrating techniques and photovoltaic) to maximize the amount of heat gain. These investigations are beyond the scope of this research but are recommended for future work. Also, the increase in the active solar system cost needs to be compared against the life cycle cost of the energy to determine the effectiveness of the system. A third alternative is to investigate the benefits of utilizing passive techniques alone. That alternative will reduce the building's energy consumption and reduce the cost of the building by eliminating the initial cost of the overall solar collection system. Depending upon the selected alternative, the new design should be evaluated using the design evaluation framework until the design criteria becomes satisfied, where the preliminary design becomes a final design.

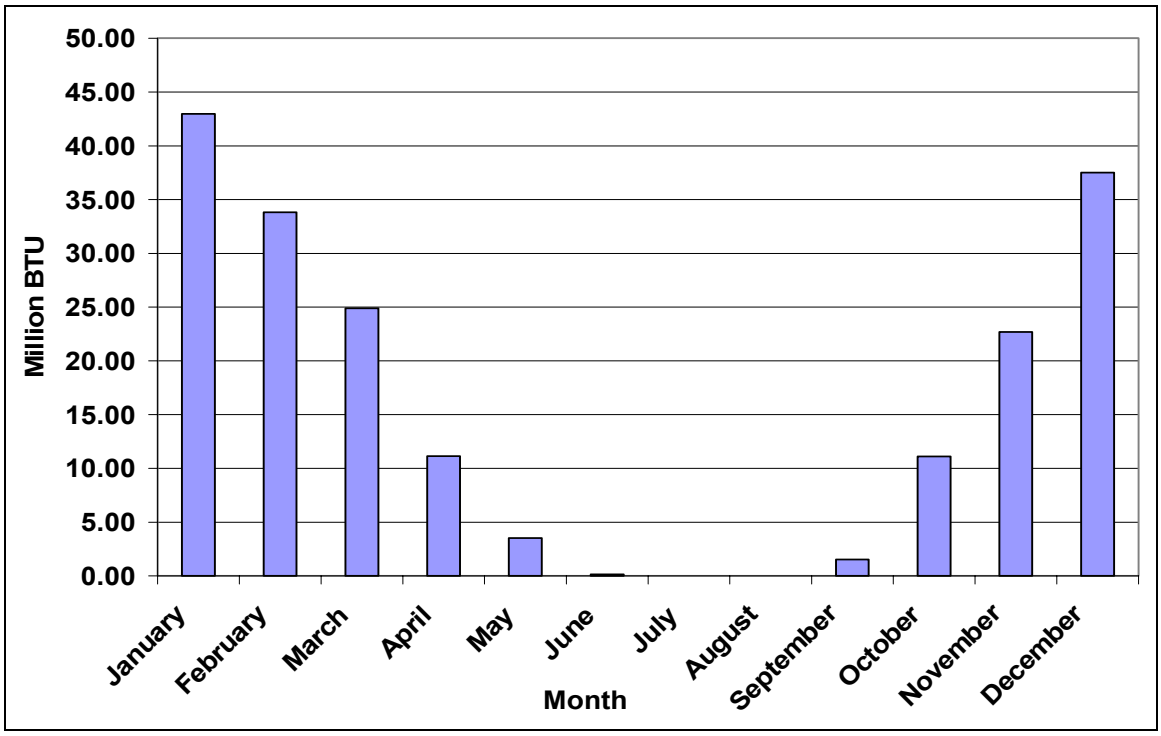

Figure 10-5. Monthly Building Energy Consumption – (after increasing window R-factor from 2 ^{o}F ft^{2} h to 5 ^{o}F ft^{2} h)

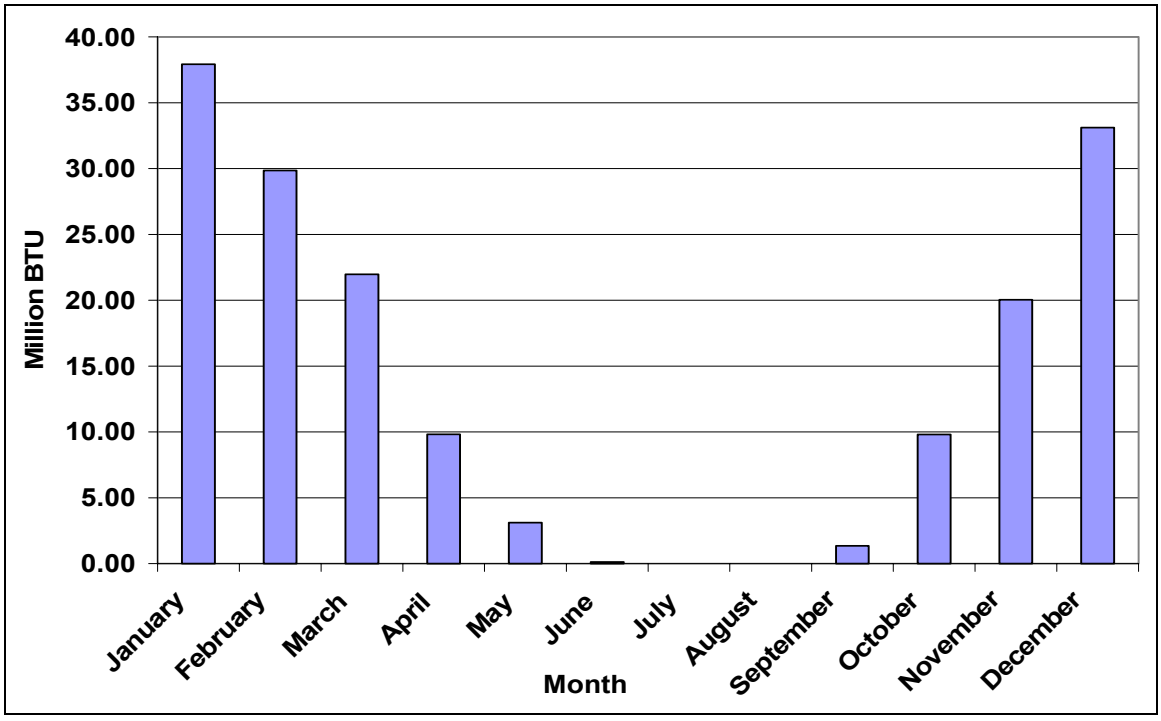

Figure 10-6. Monthly Building Energy Consumption – (after increasing window R-factor from 2 ^{o}F ft^{2} h to 11 ^{o}F ft^{2} h)

11 FINDINGS, CONCLUSIONS, AND RECOMMENDATIONS

This study presents a framework that can be used by both researchers and designers for design-evaluation of active solar collection systems. Although this design evaluation framework emphasizes the importance of using detailed modeling to simulate building performance, it also presents a process through which the detailed results of modeling can be reused in a simplified, flexible, iterative procedure that allows revision and improvement of preliminary designs. The framework utilizes an integrative approach that allows for overall system performance evaluation, as well as for subsystem component performance.

To demonstrate the proposed methodology, a preliminary design was developed for a roof solar collection system that would consist of an integrated flat plate solar collector and a storage tank. The developed preliminary design was evaluated, revised, and improved using the design evaluation framework. The considered locations to virtually demonstrate the framework are Blacksburg, VA, and Minneapolis, MN. cThe proposed solar collection system's ability to supply heating energy and hot water requirements to the building was simulated for one year.

To theoretically quantify the benefits of the new integrated design located in Blacksburg (VA), finite element (FE) models were developed to predict the integrated solar system's thermal performance and compare it against the building's energy requirements. The latter requirements were simulated using Energy Plus software, which represents state-of-the-art technology in terms of passive building energy simulation. Analytical results showed the ability of the new design to supply the building with energy. The FE modeling results were used to develop a statistical design equation that allows the designer to vary the different operational and design parameters and predict the amount of energy collected. The developed equation was used to estimate the amount of energy collected for the building located in Minneapolis (MN). The energy consumption of the building located in Minneapolis (MN) was estimated using the heating degree day method. Results of both case studies were compared. The comparison showed that the proposed preliminary design was energy efficient if located in Blacksburg, Virginia but needed modifications and improvements to be thermally

efficient in case of Minneapolis Minnesota. The design evaluation framework recommends using the decision making modules to iteratively improve and reevaluate the preliminary design to reach an energy efficient final design in case of Minneapolis Minnesota. Suggested improvements include using passive collection techniques and a different active collection method as well as increasing the thickness of the insulation layer and the windows to reduce the building's thermal consumption. For the building in Blacksburg, the framework presented in this dissertation predicted that the solar collector was able to supply 85% of the building's heating and hot water requirements, while for the building located in Minneapolis, the solar collector was only able to supply 56% of the building's heating and hot water requirements.

11.1 FINDINGS

The findings of this study are the following:

11.1.1 Case Study Findings

- For the first case study located in Blacksburg (VA), detailed modeling of the building energy consumption using Energy Plus software revealed the following:
    - The mechanical equipment that was selected ensured an acceptable level of comfort for all occupants at all times. The level of comfort condition acceptance was measured using the Fanger PMV index. For 95% of the year, the PMV ranges measured between ± 0.5.
    - Building energy consumption was calculated by Energy Plus for the three area cases of 13.57m^2, 1357m^2, and 135700m^2. As expected, energy consumption increased as the building area increased. On a semi-logarithmic scale, the increase in energy consumption was found to be approximately linear.

- For the second case study located in Minneapolis (MN), simplified modeling (Heating Degree Day) method was used to calculate the energy consumption. Results showed that the building has a very high energy consumption rate. This can be

attributed primarily to the severe climatic conditions, and secondly to inaccuracies in the simplified modeling techniques.

- To simplify design iterations, a regression model was developed to predict the outlet fluid temperature depending upon the different design environmental and operational factors:

$$\ln T_{out} = 2.8862 - 0.0512 \ln \dot{m} - 0.0461 \ln D_p + 0.005081 \ln D_s + 0.000475 Solar - 0.3321 \ln h_w + 0.304 \ln T_{in} + 0.032 T_{am} \quad (11\text{-}1)$$

$$R^2 = 0.99 \qquad RMSE = 0.1637$$

where

T_{out} = outlet fluid temperature (°C);

Solar = solar radiation (W/m^2);

T_{in} = inlet fluid temperature (°C);

T_{am} = ambient temperature (°C);

h_w = convection coefficient ($W/m^2.C$);

D_s = pipe spacing (m);

D_p = pipe diameter (m); and

$\dot{m}$ = mass flow rate (lit/hr).

- The regression model was used to predict the amount of energy collection for the second case study.
- In the preliminary design of this case study, phase change material was chosen to serve as a storage medium. Results showed that although the selected Phase Change Material (PCM) material was effective throughout the year in storing heat energy, it is not cost effective.
- Phase change material storage was compared to sensible storage using a water tank and. Results showed that the needed size of the water tank is close to the size of the needed phase change material tank at a fraction of the cost. Therefore, this research recommends the use of water as sensible storage for energy collection systems.
- Increasing the temperature of the floor slabs by 2^oC can accommodate the energy needed for a night cycle in January in case of the building located in Blacksburg, VA.

On the other hand, to accommodate the night cycle needs in Minneapolis, MN, the temperature of the building floor slabs need to be increased by as much as 5^{o}C.

- The building can store up to 1.58 Million Btu using sensible storage (in the form of water and building mass). This energy can accommodate two consecutive bad weather days in January as well as the largest January night cycle in case of the building located in Blacksburg. In case of the building located in Minneapolis, this energy can only accommodate one night cycle in January. To reduce the energy consumption in case of Minneapolis, MN, passive techniques including night time insulation for windows and a better R- factor for the exterior shell skeleton can be utilized.

11.1.2 General Findings

- Seasonal variations exposed the solar collector to excessive gains during summer days and losses during winter times.
- Losses took place below a solar intensity of 150W/m^2 in most cases. Therefore, operation of the solar collector should be stopped whenever the solar intensity is below 150W/m^2.
- The temperature profile through the thickness of the solar collector indicated that, since it minimizes collector backing and edge losses, the insulation thickness is effective.
- The maximum temperature attained in summer was 111^{o}C, corresponding to an 86^{o}C increase above the ambient temperature, while the maximum fluid temperature attained during January was 59^{o}C.
- Decreasing the fluid mass flow rate increased the fluid temperature but reduced the overall heat gain. The fluid temperature does not increase when the mass flow rate increases above 0.06 m^3/hr. In general, a reasonable temperature difference should be preserved between the fluid and the building operation temperatures. Therefore, it is essential to identify the optimum mass flow rate. The model results showed that the optimum mass flow rate was 0.0005m^3/hr to 0.005m^3/hr during the winter season and 0.1m^3/hr during the summer season.

- The most efficient and cost effective pipe diameter was 6.35 mm (0.25 in), since it allows for a more consistent temperature distribution within the fluid cross-section and is more cost efficient.
- Although phase change material storage is thermally efficient, it is not cost effective.

11.2 CONCLUSIONS

Based on this study, the following conclusions can be drawn:

- A framework has been developed to serve as an accurate design-evaluation tool for active solar systems. That framework consists of six major steps: preliminary design, solar supply evaluation, building demand evaluation, storage design and sizing, control system design, and determining of overall system energy savings. It also includes a decision-making module. These six steps are connected through an iterative process that allows the designer to re-examine design decisions in order to improve efficiency, and thermal performance. The developed design evaluation framework regards and evaluates active solar buildings as a unified system.
- The developed framework was demonstrated through design and evaluation of two cases studies located in Blacksburg (VA), and Minneapolis (MN). The evaluation process made use of detailed simulation techniques in case of Blacksburg, Virginia and simplified modeling techniques in case of Minneapolis, Minnesota.
- Virtual demonstration of the framework showed its capability to predict the energy supply and demand for heating and hot water consumption for different building sizes, types, solar collection system, and climatic conditions. Moreover, the design evaluation framework can be utilized to iteratively evaluate any active solar preliminary design to reach an energy efficient final design and quantify the overall energy savings of the system.
- The developed design evaluation framework provides a method for design evaluation and maximization of energy benefits through usage of parameter variation.

11.3 RECOMMENDATIONS AND FUTURE WORK

This study presents only the first step to quantify the effects of detailed modeling and simulation on designing and evaluating the benefits of active solar energy collection systems. Based on the above findings and conclusions of this study, the following future research is recommended:

- Additional studies are needed that utilize the developed framework to design and evaluate different active solar designs (different solar collector types and different storage systems). These studies should be conducted to simulate, in the least, the four climatic environments in the US using different solar collection methods. These studies should recommend using different types of collection and storage systems to improve the environmental design with respect to different climates.
- Studies should be conducted to test the effect of using different building materials, assembly systems, construction methodologies, and architectural designs and present combinations of schemes that make buildings more energy efficient under different climatic conditions.
- Studies should be conducted to quantify the benefits of integrating the solar collection system within the building envelope and collaborate with the industry to enhance the manufacture of systems that can further reduce the cost of the integration because integration in building performance design can reduce the project cost, improve its quality, and reduce the need for maintenance and repair. Furthermore, life cycle cost analysis studies should quantify the benefits of the integration.
- Research is needed to quantify the benefits of using hybrid active and passive solar system in residential and commercial construction. These benefits should be compared against the increase in the upfront cost of the system under different US climatic conditions.
- Studies should be conducted to compare the results of using simplified design methods versus using detailed simulation methods as evaluation tools in the framework. These studies should quantify the error resulting from using the simplified design methods and determine their significance under different design and environmental conditions.

- Further research is needed to develop a design-evaluation framework to minimize the need of non-renewable energy for cooling and dehumidification. These studies should recommend making use of the design and environmental conditions for passive cooling as well as integration of active renewable cooling systems and dehumidification to reduce the building energy consumption while satisfying the space comfort requirements. This design evaluation methodology should evaluate the building as a unified system and develop the needed steps for linking the different system components. The aforementioned research recommendations should be conducted to further develop the design-evaluation framework that minimizes the need of non-renewable energy for cooling.
- There is great potential in storing energy within the thermal mass of the building but increasing the temperature of the building slab thermal mass by more than 2 to 3^{o}C will negatively impact the thermal comfort conditions within the space. Therefore, it is recommended to investigate the effects of integrating optimization techniques in the control strategy for heating and cooling of buildings to effectively utilize the building thermal mass for storage and minimize the residential and commercial building's energy consumption while keeping the building thermal zones within comfort level.
- Studies that can integrate the aforementioned optimization studies into the control strategies of the building should be conducted. These studies can optimize the utilization of the structure's thermal mass for energy supply and storage. The research should provide methodologies as to how the energy needed will be supplied to heat/cool the space while maintaining thermal comfort conditions. For example, for the case studies of the buildings presented in this research, the building thermal mass in the floor slabs can be used to supply and store the energy needed for night cycles. In addition, energy can be supplied and absorbed from the floor slabs using the embedded radiant system.
- Future statistical work should concentrate on producing more accurate climatic data to better serve the building construction industry. Studies should be conducted to study the feasibility of using Monte Carlo simulation techniques to predict climatic conditions while bounding the consecutive inputs to simulate real field conditions.

- Future research should concentrate on quantifying and eliminating errors present within the detailed modeling and simulation. Quantification and elimination of the errors can be conducted through identification of the potential sources of errors in both process and modeling.
- The results of this study should be verified using a full-scale experimental setup. Experimental validation will help in identifying and elimination of the modeling errors. That will lead to a "calibrated" model that accurately predicts the system behavior. In addition, it will increase the level of confidence in future simulation studies that can be validated using the results of this studies' experimental validation.

REFERENCES

Agnoletti, L., Cortella, G., and Manzan, M. (1995) "Finite element thermal analysis of special building components." *Energy and Buildings*, Vol. 22, 115-123.

Ahuja A. (1997). *Integrated M/E Design – Building Systems Engineering*, Chapman & Hall, NY.

Allen, E. (1999). *Fundamentals of Building Construction – Materials and Methods*, John Wiley & Sons, NY.

Ametek. (1985). *Solar Energy Handbook*, Chilton Book Company, Pennsylvania.

Andersen, B., Eidorff, S., Lund, H., Pedersen E., Rosenorn S., and Valbjorn O. (1977) "Meteorological data for design of buildings and installation: a reference year." Report no. 66, 2nd ed., Thermal Insulation Laboratory, Denmark.

Arpaci, S., (1966). *Conduction Heat Transfer*, Wesley Pub.

ASHRAE Handbook Heating, Ventilation and Air Conditioning Applications, ASHRAE Inc., Atlanta, (1993), 32.6-32.21.

ASHRAE Handbook Heating, Ventilation and Air Conditioning Applications, ASHRAE Inc., Atlanta, (1999), 32.6-32.21.

ASHRAE Handbook Heating, Ventilation and Air Conditioning Applications, ASHRAE Inc., Atlanta, (2001), 15.1-15.17.

Augenbroe, G. (1994). "Integrated building design systems in context of product data technology." *Journal of Computing in Civil Engineering*, Vol. 8 (4): 420-435.

Augenbroe, G. (1992). "Integrated building performance evaluation in the early design stages." *Building and Environment*, Vol. 24 (2): 149-161.

Beckman, W. A. (1993). "Detailed simulation methods and validation." *Active Solar Systems*. MIT Press, 19-38.

Beckman W., Klein S., and Duffie J. A. (1977). *Solar Heating Design by the f-chart Method,* Wiley Interscience, New York.

Bendat J. S., and Piersol A. G. (2000). *Random Data: Analysis and Measurement Procedures,* John Wiley & Sons, NY.

Brandemuehl, Michael J. and James E. Braun, (1999). "Impact of demand-controlled and economizer ventilation strategies on energy use in buildings." *ASHRAE Transactions*, Vol. 105(2), 39-50.

Braun, J., (1987). "Performance and control characteristics of a large cooling system." *ASHRAE Transactions,* Vol. 93(1), 1830-1852.

Braun, J., (1990). "Reducing energy costs and peak electrical demand through optimal control of building thermal storage." *ASHRAE Transactions,* Vol. 96(2), 876-885.

Buchberg, H., and Roulet J. R., (1968). "Simulation and optimization of solar collector and storage for house heating." *Solar Energy*, 12, 13-27.

Butz, L. W., Beckman, W.A., and Duffie, J.A., (1974). "Simulation of a solar heating and cooling system." *Solar Energy*, 16, 129-135.

Connolly, M., (1976). "Solar heating and cooling computer analysis-a simplified sizing design method for non-thermal specialists." *Proc., ASES/ISES Annual Meeting,* Winnipeg, Canada, 220-243.

Crawley D. B., Lawrie L. K., Pedersen C. O., and Winkelmann F. C. (2000). "Energy plus: energy simulation program." *ASHRAE Journal*, 42(4), 49-50.

CISH. (1999). *Center for Integrated Systems in Housing*, Proposal Submitted to National Science Foundation.

Department of Energy, (2001), http://www.eren.doe.gov/solarbuildings.

DOE-2 Engineers Manual. (1982). Los Alamos National Laboratory, Los Alamos, Version 2.1A.

De Wit, M. S. and Augenbroe. (2001). "Uncertainty analysis of building design evaluations." *Proc., Building Simulation '01*, Seventh International IBPSA Conference, August 13-15, Rio de Janeiro, Brazil.

Dorer, V., and Weber A. (1999). "Air contaminant and heat transport models: Integration and application." *Energy and Buildings*, 30, 97-104.

Duffie, J. A. (1993). "Overview of modeling and simulation." *Active Solar Systems*, MIT Press, 3-19.

Duffie, J., and Beckman W. (1980). *Solar engineering of thermal processes*, John Wiley & Sons, NY.

Fanger, P. O. (1972). *Thermal comfort analysis and applications in environmental engineering*, Mcgraw-hill, NY.

Farris D. R., and Mcdonald T. E. (1980). "adaptive optimal control – an algorithm for direct digital control." *ASHRAE Transactions*, Vol. 86 (1), 880-893.

Festa, R., and Ratto, C. F. (1993). "Proposal of a numerical procedure to select reference years." *Solar energy*, 40(4), 309-313.

FMI. (2003). *The 2003-2003 U.S. markets construction overview*, FMI corporation, NC.

Gagge, A. P., Fobelets, A. P., and Berglund, L.G. (1986). "A standard predictive index of human response to the thermal environment." *ASHRAE Transactions*, Vol. 92 (2B), 709-731.

Gan, G. (1998). "A Parametric Study of Trombe Wall for Passive Cooling of Building." *Energy & Building*, Vol 27, 37-43.

Garg, H.P., Mullick, S.C., and Bhargava, A. K., (1985). Solar Thermal Energy Storage, D. Reidel Publishing Company, Boston.

Gerics, L. J., and Nichlas, M.H. (1996). "A building integrated high temperature solar thermal system for industrial applications." *Proc., 1996 Annual Conference*, ASES: 88-93.

Goswami, D. Y., Kreith, F., and Kreider, J. F., (1999). *Principals of Solar Engineering*, G.H. Buchanan Company, Philadelphia.

Green, G., W., and Jerrold, E., W., and, Kretschmann, E. E. (1999). "Mechanical properties of wood." Wood Handbook-Wood as an Engineering Material, Madison, 4.1-4.45.

Guyer, G., C., (1989). "Handbook of applied thermal design." McGraw Hill, Newyork.

Hall, I., Prairie, R., Anderson, H., and Boes, E. (1978). "Generation of typical meteorological years for 26 SOLMET stations." SAND78-1601, Sandia National Laboratories, Albuquerque, NM.

Harr, M. E., (1987). *Reliability Based Design in Civil Engineering*, Mcgraw Hill, NY.

Hartkopf, V., Loftness V., Mahdavi A., Lee S., and Shankavaram J. (1997). "An integrated approach to design and engineering of intelligent buildings – the intelligent workplace at carneigie mellon university." *Automation in Construction*, Elsevier, Vol. 6:401-415.

Hartkopf, V., and Loftness V. (1999). "Global relevance of total building performance." *Automation in Construction*, Elsevier, Vol. 8, 377-393.

Hartkopf, V., Loftness V., and Duckworth, S. (1994). "The intelligent workplace retrofit initiative." *DOE Building Studies*.

Hottel, H., and Woertz B. (1942) "Performance of flat plate solar heat collectors." *Transaction of the American Society of Mechanical Engineers*, Vol. 64, 91.

Howell, R. H., Harry, S., and Coad, W. (1998). "Principiles of heating, ventilating and air conditioning." American Society of Heating, Refrigerating and Air-Conditioning Engineers, Inc. 4.2-4.10

Incropera, F. P., and De Witt, D. P. (1996). *Fundamentals of Heat and Mass Transfer*, John Wiley & sons, NY.

Jones, J. (1996). *Predictive Equations for Nighttime Ventilation Control Based on Building Mass Temperature*, University of Michigan.

Jurinak, J. J., and Abdel-khalik S. I. (1979). "Sizing phase change energy storage units for air-based solar heating systems." *Solar Energy*, 22, 355-367.

Kakac S., and Yener Y. (1993). *Heat conduction*, Taylor and Francis, DC.

Kanazu, T. (1996). "An experimental study on physical properties of concrete exposed to high temperature for eight years." CRIEPI Report no. U95037.

Keeney K. R., and Braun, J. E. (1997). "Application of building precooling to reduce peak cooling requirements." *ASHRAE Transactions*, Vol. 103(1), 463-469.

Khedari, J., Hirunlbh, J., and Bunnag T. (1997). "Experimental study of a roof solar collector towards the natural ventilation of new houses." *Energy and Buildings*, Vol. 26, 159-164.

Klein S. A. (1993). "Design methods for active solar systems." *Active Solar Systems*, MIT Press, 39-81.

Klein. S. A., Beckman W. A., and Duffie J. (1979). "A design procedure for solar heating systems." *Solar Energy,* 18, 113-124.

Klein S. A. (1993). "Design methods for active solar systems." *Active Solar Systems*, MIT Press, 39-81.

Klein. S. A., Beckman W. A., and Duffie J. (1979). "A design procedure for solar heating systems." *Solar Energy,* 18, 113-124.

Klein. S. A., Beckman W. A., and Duffie J. (1976). "TRNSYS-A transient simulation program." *ASHRAE Transactions*, 82(1), 623-635.

Lane, G. A. (1983). "Solar heat storage: Latent heat materials." Vol. I Background & Scientific Principals, CRC Press, BOCA Raton, Fla.

Lane, G. A. (1983). "Solar heat storage: Latent heat materials" Vol. II Background & Scientific Principals, CRC Press, BOCA Raton, Fla.

Lewis R. W., (1996). *The Finite Element Method in Heat transfer analysis*, John Wiley & Sons, NY.

Lof, G. O., and Tybout, R. A. (1973). "Cost of house heating with solar energy." *Solar Energy*, 14:253-264.

Lund, H. (1995). "The design reference year user's manual." Report No. 274, Thermal Insulation Lab., Technical University of Denmark.

Lundsager, P. (1996). "Integration of renewable energy into local and regional power supply." *The World Renewable Energy Congress*, Denver, 117-122.

Mamlouk, M. S., and Zaniewski, J. P. (1999). *Materials for Civil and Construction Engineers*, Addison-Wesley, California.

Marion, W.; Wilcox, S. (1994). "Solar radiation data manual for flat-plate and concentrating collectors." NREL/TP-463-5607. Golden, CO: National Renewable Energy Laboratory.

Mohsini, R. A. (1989). "Performance and building: problems of evaluation." *Journal of Performance of Constructed Facilities*, Vol. 3 (4): 235-243.

Mutch, J. J. (1974). *Residential Water Heating, Fuel Consumption, Economics, and Public Policy*, RAND Corp., NSF.

Myers, R. H. (1990). *Classical and Modern Regression with Applications*, Library of Congress, California.

NSRDB - Vol. 1 (1992). "User's Manual - National Solar Radiation Data Base (1961-1990)." Version 1.0. Golden, CO: National Renewable Energy Laboratory and Asheville, NC: National Climatic Data Center.

Pasqualetto, L., Zmeureanu, R., and Fazio, P. "A case study of validation of an energy analysis program: micro-DOE2.1E." *Building and Environment*, 33(1), 21-41

Pepper D. W., and Baker, A. J. (1988). "Finite differences versus finite elements." *Handbook of Numerical Heat Transfer*, John Wiley & Sons.

Reddy, T. (1987). *The Design and Sizing of Active Solar Thermal systems*, Oxford Science Publications, Oxford.

Rincon, J., Almao, N., and Gonzalez, E. (2000). "Experimental and numerical evaluation of a solar passive cooling system under hot And humid climatic conditions." *Solar Energy*, 71(1), 71-80.

RSMeans, (2001). Residential Cost Data, RSMeans Co., USA.

Rush, R. D. (1986). *The building Systems Integration Handbook*, The American institute of Architects.

Sauter, E. (1991). "Insulated Concrete Sandwich Walls." *Exterior Wall Systems: Glass and Concrete Technology, Design and Construction, ASTM STP 1034*, B. Donaldson, Ed., ASTM, 170-186.

Schweitzer, S. (1978). "A possible average weather year on Israel's coastal plain for solar system simulation." *Solar Energy*, 21, 511-515.

Seem J. E., and Braun, J. E. (1992). "The impact of personal environmental control on building energy use." *ASHRAE Transactions,* Vol. 98(1), 903-925.

Sheridan, N. R., Bullock, K.J., and Duffie J. A. (1967). "Study of solar processes by analog computer." *Solar Energy*, 11, 69-76.

Simmonds, P., Holst, S., Reuss, S., and Gaw, W. (2000). "Using radiant cooled floors to condition large spaces and maintain comfort conditions." *ASHRAE Transactions*, Vol. 106(1), 695-701.

Simmonds, P. (1994). "Control strategies for combined heating and cooling radiant systems." *ASHRAE Transactions*, Vol. 100(1), 1031-1039.

Simmonds, P. (1993). "Thermal comfort and optimal energy use." *ASHRAE Transactions*, Vol. 99(1), 1037-1048.

Simmonds, P. (1991). "The utilization and optimization of a building's thermal inertia in minimizing the overall energy use." *ASHRAE Transactions*, Vol. 97(2), 1031-1042.

Smith, C. (1993). "System performance." *Active Solar Systems*, MIT Press, 465-509.

Spence, W. P. (1998). *Construction Methods, Materials, and Techniques*, Delmar Publishers, NY.

Stein B., and Reynolds J. (2000). *Mechanical and Electrical Equipment for Buildings*, John Wiley and Sons.

Suman, P. (2003). Programming a control strategy for a low temperature solar collector system.

Tabor, H. (1958). "Radiation, convection, and conduction coefficients in solar collectors." Bulletin of the Research Council of Israel, 6C, 155.

York, D. A., and Tucker, E.F., (1980). DOE-2 reference manual. Los Alamos, NM, Los Alamos scientific laboratory.

Younger, M. S. (1979). *Handbook of Linear Regression*, Library of Congress, California.

Walpole, R., and Myers, R. (1985). *Probability and Statistics for Engineers and Scientists*, Macmillan, NY.